



KIT SCIENTIFIC REPORTS 7625

Proceedings of the International Workshops ABC-Salt (II) and HiTAC 2011

Marcus Altmaier, Christiane Bube, Bernhard Kienzler,
Volker Metz, Donald T. Reed (Eds.)

Marcus Altmaier, Christiane Bube, Bernhard Kienzler, Volker Metz,
Donald T. Reed (Eds.)

Proceedings of the International Workshops ABC-Salt (II) and HiTAC 2011

Karlsruhe Institute of Technology
KIT SCIENTIFIC REPORTS 7625

Proceedings of the International Workshops ABC-Salt (II) and HiTAC 2011

edited by
Marcus Altmaier
Christiane Bube
Bernhard Kienzler
Volker Metz
Donald T. Reed

Report-Nr. KIT-SR 7625

Impressum

Karlsruher Institut für Technologie (KIT)
KIT Scientific Publishing
Straße am Forum 2
D-76131 Karlsruhe
www.ksp.kit.edu

KIT – Universität des Landes Baden-Württemberg und
nationales Forschungszentrum in der Helmholtz-Gemeinschaft



Diese Veröffentlichung ist im Internet unter folgender Creative Commons-Lizenz
publiziert: <http://creativecommons.org/licenses/by-nc-nd/3.0/de/>

KIT Scientific Publishing 2012
Print on Demand

ISSN 1869-9669
ISBN 978-3-86644-912-1

In November 2011 the Institute for Nuclear Waste Disposal at the Karlsruhe Institute of Technology organized two workshops on topics of high importance to the safe disposal of nuclear waste, ABC-Salt(II) and HiTAC. The safe disposal of long-lived nuclear waste is one of the main challenges associated with nuclear energy production today. A thorough understanding of actinide geochemical processes and their quantification are required as building blocks of the nuclear waste disposal safety case. As a consequence of many dedicated research activities, a detailed scientific understanding of fundamental processes controlling the behavior of radionuclides in aqueous systems has been established. The performance and safety of a repository based on analysis of pertinent scenarios can thus be assessed based upon scientific evidence and laws of nature.

The need for international exchange and scientific discussions on actinide chemistry, in the context of nuclear waste disposal, has long been realized and is reflected in international research activities, multilateral cooperation agreements and well-established scientific conferences like Migration, Actinides or Plutonium-Futures. As these large international conferences serve as a general forum to present new scientific results and trends, only very few workshops so far have specifically targeted actinide brine chemistry or high temperature aqueous chemistry. KIT-INE organized ABC-Salt (II) together with LANL-CO and also took the initiative to organize the HiTAC workshop. The proceedings of the ABC-Salt (II) and HiTAC workshops summarize recent research on actinide and brine chemistry relevant to waste disposal in rock-salt formations and the aqueous chemistry at the elevated temperature conditions expected in high level waste scenarios. The two successful workshops highlighted new scientific studies, offered room to discuss specific research activities and finally strengthened ties within the international scientific research community.

I would like to express my thanks to the respective organizing committees and especially acknowledge the financial support for the workshops. ABC-Salt (II) was supported by the Federal Ministry of Economics and Technology (BMWi, Germany), the Department of Energy Waste Isolation Pilot Plant (DOE/WIPP, USA). HiTAC was supported by the Federal Ministry of Economics and Technology (BMWi, Germany).

Prof. Horst Geckeis, head of KIT-INE

Table of Contents

PART I.....	3
OVERVIEW OF THE ABC-SALT (II) WORKSHOP	5
SUMMARY OF THE ABC-SALT (II) WORKSHOP	7
PROGRAM.....	13
Oral contributions	13
Poster presentation.....	15
ABSTRACTS OF ORAL CONTRIBUTIONS.....	17
List of contributions.....	19
POSTER ABSTRACTS	63
List of poster contributions	65
WORKSHOP PARTICIPANTS.....	109
PART II.....	115
OVERVIEW OF THE HITAC WORKSHOP.....	117
SUMMARY OF THE HITAC WORKSHOP	119
PROGRAM.....	125
Oral contributions	125
Poster presentation.....	127
ABSTRACTS OF ORAL CONTRIBUTIONS.....	129
List of contributions.....	131
POSTER ABSTRACTS	149
List of contributions.....	151
WORKSHOP PARTICIPANTS.....	181



PART I

2nd International workshop

on

Actinide Brine Chemistry in a Salt-Based Repository - ABC-Salt (II) -

Karlsruhe, Germany

November 7 - 8, 2011



Waste Isolation Pilot Plant
www.wipp.energy.gov

Organisation

Organizers

*Karlsruhe Institute of Technology (KIT)
Institute for Nuclear Waste Disposal (INE)
Karlsruhe, Germany*

*Los Alamos National Laboratory (LANL)
Earth and Environmental Sciences Division (EES12)
Carlsbad Operations
Carlsbad, New Mexico, United States of America*

Sponsors

*Federal Ministry of Economics and Technology (BMWi), Germany
Department of Energy Waste Isolation Pilot Plant (DOE/WIPP), United States of America*

Organizing Committee

Marcus Altmaier, Christiane Bube, Volker Metz
*Karlsruhe Institute of Technology (KIT), Institute for Nuclear Waste Disposal (INE)
PO-Box 3640, 76021 Karlsruhe, Germany*

Donald T. Reed

*Los Alamos National Laboratory (LANL), Earth and Environmental Sciences Division (EES12), Carlsbad
Operations, 1400 University Drive, Carlsbad, NM 88220, United States of America*

Contact, e-mail: *marcus.altmaier@kit.edu, volker.metz@kit.edu, dreed@lanl.gov*

Acknowledgements

We gratefully acknowledge Angelika Aurich, Elke Bohnert, Elke Lukas, Bernhard Kienzler, Stefanie Krieger, Andrej Skerencak, Hieronymus Sobiesiak and Denise Wedemeyer for their administrative and technical support.

OVERVIEW OF THE ABC-SALT (II) WORKSHOP

Among the geological formations discussed as suitable hosts for nuclear waste disposal – crystalline rocks, clay and rock salt - salt offers several unique features. Most importantly, it is known that salt, due to its self-sealing properties, leads to conditions that clearly favor the complete isolation of waste for the long-term disposal of radioactive waste in dry conditions. In the huge majority of scenarios, the nuclear waste will be imbedded in a dry salt matrix without any significant mobilization of radioactivity. This situation is a markedly different than waste disposal in crystalline or clay rocks, where groundwater saturation is expected. The actinide and brine chemistry discussed within the ABC-Salt workshop is relevant for low probability repository failure scenarios, when water intrusion into a salt-based repository cannot be excluded. The potential for radionuclide mobilization in the unlikely event of water intrusion and the subsequent interaction of concentrated salt brine solutions with the waste needs to be understood and predicted in detail as this would be a key mobilization pathway of radionuclides into the environment. Performance assessment calculations that account for this low-probability scenario will require input from geochemistry and actinide chemistry to support reliable model calculations and long-term safety predictions. The behavior of radionuclides in salt brines is not only relevant for salt-based repositories but also for potential nuclear waste repositories in some other deep geological formations. At a depth of several hundred meters, argillaceous and crystalline formation waters are Na⁺/Cl⁻ type solutions. Formation waters with elevated ionic strength occur for instance in Ordovician shales in the Canadian Shield and Cretaceous argillites in Northern Germany.

The ABC-Salt (II) workshop on actinide brine chemistry in Karlsruhe followed the first ABC-Salt workshop held in 2010 in Carlsbad, New Mexico, USA. Both ABC-Salt workshops were co-organized by the Karlsruhe Institute of Technology, Institute for Nuclear Waste Disposal (KIT-INE) and the Los Alamos National Laboratory, Carlsbad Office (LANL-CO). Although centered on a German - US American initiative, ABC-Salt (II) explicitly solicited and encouraged participation from outside these countries. Strong participation from several European and Asian countries together with many participants from Germany and the US confirmed the importance of this workshop and highlighted the significance that the topic of actinide and brine (geo)chemistry has reached on an international level.

ABC-Salt brought together the scientific community working on high ionic-strength aqueous systems and the experts involved in implementing aqueous geochemistry in salt-based repository projects. The aim of the workshop was to present new scientific investigations and discuss advanced approaches to establish a better understanding of the aqueous geochemistry and radiochemistry required to predict the long-term safety of a salt-based nuclear waste repository. ABC-Salt (II) thus served as a very successful and timely platform for the exchange of new scientific results, the discussion of current topics in the field, the identification of needed future research activities and the promotion of scientific exchange on actinide brine chemistry within the international community.

SUMMARY OF THE ABC-SALT (II) WORKSHOP

ABC-Salt (II) highlighted that our present knowledge of actinide brine chemistry in saline systems has reached a remarkably high standard that allows the assessment of relevant processes potentially affecting radionuclide mobilization. Predictions of the long-term performance of a salt-based nuclear waste repository are supported by our detailed understanding of many of the relevant fundamental chemical processes. The ABC-Salt(II) workshop was mainly organized around oral contributions but also received significant input from the presented posters. The workshop sessions were divided into four main sections, including overview talks on current repository projects, geochemistry and microbial processes in saline systems, actinide chemistry in brines (in particular actinide solubility, complex formation and sorption processes) and thermodynamic databases / geochemical modeling.

Several institutions participating in ABC-Salt (II) have expressed their ongoing interest and commitment to scientific research on actinide brine chemistry. A need for increased international exchange and cooperation that goes beyond the current bilateral nature of the research activities on actinide brine chemistry was expressed. Potential cooperation could range from the discussion of geochemical aspects of nuclear disposal projects and concepts, to advanced model development and thermodynamic database work. It also may extend to joint experimental research activities and exchange of scientific personnel. Given the rather small international scientific community working on actinide brine chemistry topics, the desire to cooperate on an international level was strongly emphasized. International cooperation is considered highly important, to optimize the available scientific knowledge and expertise but also to more efficiently utilize the limited financial and technical resources available. In this context, it was considered essential to have funding tools available to promote the exchange of young researchers in this field to develop and maintain competence in the field of actinide and brine chemistry. The possibility of non-European Union partner institutions entering European research projects as associated groups, as was successfully implemented in the European FP7 ReCosy and FIRST-Nuclides projects, was also indicated as a favorable option for continued scientific exchange on specific topics of mutual interest.

The importance of geochemistry for safety analyses was discussed in the context of the current US and German situations. The WIPP project was presented as an example of the successful implementation of actinide and brine chemistry in performance assessment calculations. Moreover, specific technical examples from modeling exercises were given. Regarding the Asse II site in Germany, the present decision to completely retrieve the waste was discussed. The status of the German project to provide a Preliminary Safety Assessment for Gorleben was given along with a description of the needed contributions from actinide chemistry to make a robust estimation of source term concentrations. The need for advanced computational tools to perform more comprehensive model calculations in performance assessment was also highlighted.

The thermodynamic databases supplying fundamental input parameters for geochemical model calculations were also discussed. The need to use the advanced Pitzer approach for ionic-strength corrections and calculation of activity coefficients in saline systems (typically $I > 4 \text{ mol (kg H}_2\text{O)}^{-1}$) is generally accepted. The discussion was mainly centered on two projects dedicated to establishing comprehensive Pitzer-consistent database. Both the representatives of the German THEREDA consortium and the partners from LANL-CO and Sandia National Laboratory responsible for the WIPP thermodynamic database indicated a strong interest in increased interactions. As a direct application of data will not be possible in most cases due to problems arising from data consistency issues, it would be most beneficial to discuss the need for closing existing data gaps and reducing overall uncertainties both in terms of the thermodynamic data and the completeness of chemical models. The recent initiative to establish a “Salt Club” within the framework of the NEA was briefly outlined and very well-received and supported by the audience. There is clearly a strong interest in the ABC-Salt participants to integrate actinide and brine chemistry into this newly emerging organizational platform.

Detailed scientific knowledge on the processes influencing the specific geochemical boundary conditions controlling actinide chemistry in aqueous systems is critical for predicting repository safety. Geochemical constraints on the expected brine composition, redox controlling processes, expected pH conditions, formation of secondary mineral phases or limitation of the free carbonate concentration in solution are directly affecting radionuclide chemistry and the radionuclide source term. The session on fundamental geochemistry in saline systems therefore received much attention.

In discussions on exactly which Sorel-type magnesium-hydroxychloride phase is most relevant for site specific long-term predictions, it was stressed that the present understanding is sufficient to predict the relevant processes buffering pH conditions in salt-based repositories and calculate the respective pH conditions. Carbonate retention processes and pH buffering controlled by magnesium-hydroxy-chloro-carbonate phases in MgCl_2 dominated solution were similarly discussed. The relevance of using adequate models for predicting the behavior of iron under the relevant geochemical boundary conditions was addressed. Iron is present in huge amounts as part of the emplaced waste canisters and construction materials and strongly affects geochemical processes. Steel corrosion will control hydrogen production, overall redox conditions and the formation of secondary iron mineral phases relevant as host phases for actinide retention.

Considering the case of radium, a precise understanding of solubility control and speciation is also relevant for applications outside the nuclear waste disposal community since thermodynamic descriptions of radium chemistry are needed to assess various Technologically Enhanced Naturally Occurring Radioactive Materials. For example evaporation ponds for the management of residues solutions, containing high levels of radium may be found in the industries of geothermal energy production, oil and gas production, coal mining (settling ponds), water treatment plants, uranium and other metals mining (typically in the in-situ leaching technique)

and niobium industries (settling ponds). Any pond can potentially leak and contaminate groundwater and salts precipitating in these ponds may pose a potential radiological health concern.

Several contributions focused on the need to investigate the potential impact of microbial effects on actinide chemistry and repository safety in rock salt. As a first important step, the characterization of the main microbial communities present is required. This was exemplified within the presentation of work performed within the WIPP project, with further details on the relevance of microbial systems being added from ongoing German research studies. An interest in initiating studies to compare microbial communities isolated from different sites was expressed.

The core of the ABC-Salt (II) workshop was the discussion of recent studies on actinide chemistry in brines. This is reflected by the several scientific talks and the many poster contributions. Several studies have stressed the need to establish robust solubility limits and thermodynamic descriptions for actinide solubility and speciation. Examples were presented for Np(V) solubility in NaCl and CaCl₂ systems from recent studies. It was argued that there is a general need to couple fundamental studies on actinide solubility in pure salt solutions and site specific investigations under complex brine compositions to check the applicability of predictions drawn from simplified systems and check the potential relevance of minor brine components. The impact of overall redox conditions on the expected actinide oxidation state distribution also received much attention. Redox transformations of radionuclides will in many cases define their chemical behavior and hence directly affect source term estimations. The approach taken within WIPP performance assessment to define the predominant actinide oxidation states under consideration by expert opinion was discussed and considered conservative. Regardless of this convincing pragmatic approach to constrain redox effects, several research projects gave specific examples from research that was focused on deriving more precise chemical models and more quantitative evidence to assess redox processes on a molecular level. Sorption processes are known to promote significant radionuclide retention, thus leading to an important limitation on the amounts of radionuclides potentially mobilized from a repository over a given timescale. Sorption effects have been investigated in much detail for many low ionic-strength systems. Sorption effects are also known to reduce radionuclide concentrations in salt brine systems, but so far no comprehensive investigation of sorption processes and no mechanistic understanding of sorption at high ionic-strength conditions are available. In addition to the empirical experimental evidence from site-specific studies where sorption effects determined the effective radionuclide concentrations present in solution, new and more fundamental studies under simplified experimental conditions are required. This is also needed to extend low ionic-strength modeling approaches to salt brine conditions.

Organic ligands can be present in a salt-based repository as part of the emplaced waste inventory or by degradation of organic material, e.g. cellulose. The potential impact of these complexing organic ligands at high ionic-strength is therefore a relevant aspect of actinide brine chemistry. Given that actinide-organic

interactions are known to exist and influence actinide solubility, an adequate thermodynamic description is only available in a few cases. The additional question of how competing metal cations like Fe, Pb, Al, Mg, or Ca will influence the availability of free organic ligand concentrations for actinide complexation reactions in many cases remains unclear.

Recent research activities were focused on assessing the impact of borate on actinide solubility and speciation, especially for the trivalent actinides. Although there is experimental evidence of specific An(III)-borate complexation, the effect of borate complexation reactions on the respective actinide solubility is expected to be rather small. While work on actinide-borate complexation is continuing, a conservative estimate of the potential effect of borate on the actinide source term would argue for rather insignificant effects compared to overall uncertainties in solubility. Apart from the experimental studies on actinide borate interactions, it was argued that a comprehensive thermodynamic description will require more precise descriptions of the borate speciation scheme.

The relevance and quantitative description of the role of actinide eigencolloids, especially in the Th(IV) system, also has received much attention. The WIPP approach of using colloid enhancement parameters to define the total dissolved actinide concentration in the source term for performance assessment calculations was discussed. There was also a discussion of the recently reported crystalline Pu nanoclusters prepared under strongly acidic media and their proposed relevance for geochemical condition in the context of nuclear waste disposal. Even though there is wide-ranging experimental evidence on the importance of colloidal species in actinide solubility studies, there was no final consensus reached on how to account for colloidal species in high ionic-strength systems.

Throughout the many oral presentations and posters presented at ABC-Salt (II), the importance of using advanced spectroscopic tools for deriving a detailed understanding of the chemical reactions on a molecular level was apparent. It was emphasized that the accuracy and reliability of many geochemical predictions are directly linked to the accuracy of the underlying experimental data, the quality of chemical model development and the thermodynamic parameterization subsequently derived. Consequently, the continued development and availability of advanced speciation techniques is considered a topic of vital importance to the scientific community working on actinide brine chemistry. As examples for new experimental techniques potentially applicable to the investigation of saline systems, the use of ultra-microelectrodes for redox measurements, GEO-PET analysis and High Resolution X-ray Adsorption Spectroscopy to investigate actinide speciation were presented at ABC-Salt (II).

A number of topics that are specific to the permanent disposal of heat-producing high-level radioactive waste (HLW) in a salt repository were not explicitly addressed in the ABC-salt (II) workshop. For HLW, where spent nuclear fuel and temperatures that are significantly higher than ambient may be present, a description of

temperature effects on actinide brine chemistry is needed. Other specific effects like spent nuclear fuel corrosion, behavior of vitrified waste and radiolytic processes are likewise required. While high-level waste topics were not yet explicitly addressed within the ABC-Salt workshops and elevated temperature conditions were separately covered within the HiTAC workshop, it was recognized that it would be beneficial to include these topics in future ABC-Salt workshops to allow for a more comprehensive picture.

It was consensus at ABC-Salt (II), that the workshop was an important event to demonstrate and discuss the present state-of-art on several aspects of actinide brine (geo)chemistry. It was also emphasized by the participants actually involved in current repository programs that scientific research and expertise on actinide and brine (geo)chemistry is essential to support repository safety analysis for scenarios where salt brine systems are expected. It was specifically argued by several participants that there is both a strong desire from the involved scientist and an actual need to further develop the international exchange and scientific cooperation on this important topic with the ABC-Salt workshops having established a very useful international platform. Sharing this conviction, KIT-INE and LANL-CO have agreed to continue their joint initiative and plan to organize a third ABC-Salt (III) workshop in the USA in 2013 in cooperation with the respective project agencies involved.

PROGRAM

Oral contributions

Session 1: Overview / introductory talks

- *H. Geckeis*. Research at KIT-INE related to nuclear waste disposal in salinar host rocks.
- *A. van Luik*. WIPP Update and Proposed Salt-Chemistry Studies.
- *D.T. Reed*. WIPP Two-Year Investigation Focus and Underground Tests.
- *S. Köster*. Activities on nuclear waste disposal research coordinated by Federal Ministry of Economics and Technology (BMWi).

Session 2: Modelling, databases and safety analysis

- *C. Leigh*. Geochemical modeling for the WIPP.
- *G. Bracke*. Preliminary Safety Analysis Gorleben.
- *A. Wolfsberg*. Simulating subsurface radionuclide migration: Process-level considerations and high performance computing directions.
- *H. Moog*. THEREDA – Thermodynamic Reference Database.

Session 3: Biogeochemistry in saline systems

- *D. Freyer*. Sorel cement as geotechnical barrier in salt formations.
- *C. Bube*. Thermodynamics of long-term metastable magnesium (chloro) hydroxo carbonates at 25 °C.
- *G. Roselle*. Gas Generation due to Anoxic Corrosion of Steel and Lead in Na-Cl ± Mg Dominated Brines.
- *Y. Rosenberg*. Thermodynamic properties of the Na-Ra-Cl-SO₄-H₂O system - Estimating Pitzer Parameters for RaCl₂.
- *J. Swanson*. An Overview of Research on Microbial Interactions in the Waste Isolation Pilot Plant.
- *A. Geissler*. Microorganisms in potential nuclear waste disposal host rocks.
- *M. Perdicakis*. Can we use ultramicroelectrodes to perform electrochemistry in brines ?

Session 4: Actinide chemistry in brines

- *X. Gaona*. Redox chemistry of Np(V/VI) under hyperalkaline conditions: aqueous speciation, solubility and chemical analogies with Pu.
- *D.T. Reed*. Actinide Speciation and Oxidation-state Distribution in the WIPP.

- *N. Finck*. Trivalent cations retention upon brucite precipitation.
- *V. Petrov*. Pentavalent neptunium solubility and solid phase transformation at high ionic strengths.
- *D. Fellhauer*. Solubility and speciation of Np in dilute to concentrated CaCl₂ solutions under different redox conditions.
- *V. Metz*. Interactions of U(VI) with cement alteration products at high ionic strength.
- *T. Rabung*. Trivalent Metal Ion Sorption under Saline Conditions.
- *P. Thakur*. Actinides Complexation by Organic Ligands as a function of temperature and high ionic strength.
- *H. Rojo*. Complexation of Nd(III)/Cm(III) and Np(IV) with Gluconate in dilute to concentrated alkaline NaCl and CaCl₂ solutions.

Session 5: Radionuclide source term / international programs

- *B. Kienzler*. Preliminary Safety Analysis Gorleben (vSG): Source Term for Radionuclides.
- *G. Buckau*. Basis and status of EURATOM Waste Management Research.

Poster presentation

The following posters were presented during the Workshop:

- *B. Kienzler*. FIRST-Nuclides, Fast / Instant Release of Safety Relevant Radionuclides from Spent Nuclear Fuel.
- *G. Bracke*. Preliminary Safety Analysis Gorleben.
- *M. Altmaier, X. Gaona, D. Fellhauer, G. Buckau*. Recosy Intercomparison exercise on redox determination methods – final report on main conclusions and recommendations.
- *J. Kulenkampff, F. Enzmann, M. Gründig, M. Wolff, H. Lippold, J. Lippmann-Pipke*. Direct observation of preferential transport pathways in salt rocks by means of GeoPET.
- *C. Marquardt, N. Banik, M. Bouby, T. Schäfer, H. Geckeis*. Radionuclides in natural clay rock and saline systems - activities at INE in the frame of a BMWi project.
- *P. Thakur*. An overview of environmental monitoring of the WIPP site.
- *E. Krawczyk-Bärsch, T. Arnold*. Approach to study the influence of extremophiles on the migration behavior of radionuclides.
- *D.A. Ams, J.S. Swanson, J.E.S. Szymanowski, J.B. Fein, M. Richmann, D.T. Reed*. Neptunium (V) Adsorption to a Halophilic Bacterium: Surface Complexation Modeling in High Ionic Strength Systems.
- *M. Bouby, H. Geckeis, G. Buckau*. Ionic strength and complexation induced humic acid agglomeration study.
- *K. Rozov*. Synthesis, characterization and stabilities of Mg-Fe(II)-Al-Cl containing layered double hydroxides (LDHs).
- *Y.O. Rosenberg, V. Metz, J. Ganor*. Ra-Ba Co-precipitation in a Large Scale Evaporitic System.
- *G. Roselle*. Iron-Based Waste Packages as Engineered Barriers in a Salt Repository.
- *Y.-L. Xiong*. Experimental Determination of Thermodynamic Properties of $\text{PbC}_2\text{O}_4(\text{aq})$.
- *J.-H. Jang, Y.-L. Xiong, M.B. Nemer*. Solubility of $\text{FeC}_2\text{O}_4 \cdot 2\text{H}_2\text{O}$ in MgCl_2 and NaCl Solutions.
- *Y.-L. Xiong, L. Kirkes, T. Westfall, T. Olivas*. Experimental Determination of Solubilities of Sodium Tetraborate (Borax) in NaCl Solutions to High Ionic Strengths, and Thermodynamic Model for the $\text{Na-B(OH)}_3\text{-Cl-SO}_4$ System.
- *X. Gaona*. Formation and equilibrium conditions of An(III,IV,V,VI)-eigencolloids in dilute to concentrated NaCl , CaCl_2 and MgCl_2 solutions.
- *D.C. Sassani, C. Leigh*. The Models for the Colloid Source Term at WIPP.

- *T. Kobayashi, E. Yalcintas, M. Altmaier.* Solubility of $\text{TcO}_2(\text{s}) \cdot x\text{H}_2\text{O}$ in dilute to concentrated NaCl, CaCl_2 , and BaCl_2 solutions.
- *E. Yalcintas, T. Kobayashi, M. Altmaier, H. Geckeis.* Redox Behavior of the Tc(VII)/Tc(IV) Couple in Dilute to Concentrated NaCl Solutions.
- *P. Lindqvist-Reis.* Spectroscopic Evidence of Ion-Association in Aqueous Ln^{3+} and An^{3+} Perchlorate Solutions at Low Water Activity.
- *D. Reed, D. Ams, J.-F. Lucchini, M. Borkowski, M.K. Richmann, H. Khaing, J. Swanson.* Actinide Interactions in WIPP Brine.
- *M. Borkowski, M. Richmann, S. Kalanke, D.T. Reed.* Borate Chemistry and Interaction with Actinides in High Ionic Strength Solutions at Moderate pH.
- *K. Hinz, M. Altmaier, T. Rabung, H. Geckeis.* An(III) Borate complexation.
- *S. Kalanke.* Complexation of Neptunium (V) with Borate.
- *H. Rojo, X. Gaona, Th. Rabung, M. Garcia, T. Missana, M. Altmaier.* An(III) and An(IV) complexation with gluconate in dilute to concentrated solutions.
- *B. Kienzler, N. Finck, M. Plaschke, Th. Rabung, J. Rothe, D. Schild.* Cs and U Retention in Cement during Long-Term Corrosion Tests in Salt Brines.
- *M. Rothmeier, V. Petrov, T. Rabung, J. Lützenkirchen, N. Finck, M. Altmaier.* Surface charging of (oxyhydr)oxide minerals to high ionic strength.
- *T. Vitova, M.A. Denecke, N. Finck, J. Göttlicher, B. Kienzler, J. Rothe.* High-resolution X-ray absorption spectroscopy of U in cemented waste form.

ABSTRACTS OF ORAL CONTRIBUTIONS

List of contributions

WIPP Update and Proposed Salt-Chemistry Studies <i>A. van Luik</i>	21
WIPP Two-Year Investigation Focus and Underground Tests <i>R. Patterson and D.T. Reed</i>	23
Preliminary Safety Analysis Gorleben <i>G. Bracke</i>	25
THEREDA – Thermodynamic Reference Database <i>H. C. Moog</i>	27
Sorel cement as geotechnical barrier in salt formations <i>D. Freyer</i>	29
Thermodynamics of long-term metastable magnesium (chloro) hydroxo carbonates at 25°C <i>C. Bube, M. Altmaier, V. Metz, V. Neck, D. Schild, B. Kienzler</i>	31
Gas Generation due to Anoxic Corrosion of Steel and Lead in Na-Cl ± Mg Dominated Brines <i>G. T. Roselle</i>	33
Thermodynamic Properties of the Na-Ra-Cl-SO ₄ -H ₂ O System- Estimating Pitzer Parameters for RaCl ₂ <i>Y. O. Rosenberg, V. Metz and J. Ganor</i>	35
An Overview of Research on Microbial Interactions in the Waste Isolation Pilot Plant <i>J. Swanson, D. Ams, K. Simmons, H. Khaing, D.T. Reed</i>	37
Microorganisms in potential nuclear waste disposal host rocks <i>A. Geissler, H. Moll, V. Bachvarova, L. Lütke, S. Selenska-Pobell, G. Bernhard</i>	39
Can we use ultramicroelectrodes to perform electrochemistry in brines ? <i>M. Perdicakis, A. Chebil, M. Etienne</i>	41
Redox chemistry of Np(V/VI) under hyperalkaline conditions: aqueous speciation, solubility and chemical analogies with Pu <i>X. Gaona, D. Fellhauer, K. Dardenne, J. Rothe, M. Altmaier</i>	43
Actinide Speciation and Oxidation-state Distribution in the WIPP <i>D.T. Reed, M. Borkowski, M. Richmann, J.-F. Lucchini, J. Swanson and D. Ams</i>	45
Trivalent cations retention upon brucite precipitation <i>N. Finck, K. Dardenne</i>	47
Solubility and speciation of Np in dilute to concentrated CaCl ₂ solutions under different redox conditions <i>D. Fellhauer, M. Altmaier, V. Neck, J. Runke, J. Lützenkirchen, X. Gaona, Th. Fanghänel</i>	49

Interactions of U(VI) with cement alteration products at high ionic strength <i>V. Metz, C. Bube, D. Schild, M. Lagos, E. Bohnert, K. Garbev, M. Altmaier, B. Kienzler</i>	51
Trivalent Metal Ion Sorption under Saline Conditions <i>Th. Rabung, A. Schnurr, V. Petrov, J. Lützenkirchen, H. Geckeis</i>	53
Actinides Complexation by Organic Ligands as a function of temperature and high ionic strength <i>P. Thakur and G.P. Mulholland</i>	55
Complexation of Nd(III)/Cm(III) and Np(IV) with Gluconate in dilute to concentrated alkaline NaCl and CaCl ₂ solutions <i>H. Rojo, X. Gaona, Th. Rabung, M. Garcia, T. Missana, M. Altmaier</i>	57
Preliminary Safety Analysis Gorleben (vSG): Source Term for Radionuclides <i>B. Kienzler</i>	59
Basis and Status of EURATOM Waste Management Research <i>G. Buckau</i>	61

WIPP Update and Proposed Salt-Chemistry Studies

Abraham van Luik

United States Department of Energy, Carlsbad Field Office, 4021 National Parks Highway, Carlsbad NM 88220, USA
email: abraham.vanluik@wipp.ws

The successful 12 years of operations at the Waste Isolation Pilot Plant (WIPP) in New Mexico (see Figure 1) were illustrated with shipment numbers, emplaced waste statistics, descriptions of the waste and how it is placed into the repository for final disposal. The reason the WIPP site was selected was highlighted as being based on National Academy of Sciences recommendations regarding the use of salt as a host rock, in 1957, namely: 1) stable geology (~250 million years), 2) lack of water, 3) easy to mine, 4) self-healing fractures, 5) salt “creep” will encapsulate the waste, and 6) high thermal conductivity. Key achievements for the WIPP repository include:

- 12+ years of safe operation
- 10,026 shipments received
- ~78,086 cubic meters of TRU waste emplaced
- 12,000,000 loaded miles
- ~7 waste panels mined in the underground
- 21 storage sites cleaned of legacy TRU waste
- 0 releases to the environment
- 0 contaminated WIPP personnel
- 24 years as the New Mexico mine operator of the year



Fig. 1: Waste Isolation Pilot Plant (view of surface facilities) has operated for 12+ years as a repository for transuranic waste in a bedded salt formation

Proposed plans for future “heater-test” studies at WIPP were also outlined (see Figure 2). The purpose of these studies is to determine the feasibility of placing heat-emitting wastes into a salt body similar to the one at

WIPP. These studies, if and when funded, would, in addition to rock mechanics issues, also address the following chemistry-related issues: 1) measuring the thermodynamic properties of brines and minerals at elevated temperatures, 2) studying repository interactions with waste container and constituent materials, 3) measuring the effect of elevated temperature and ionizing radiation on brine chemistry, 4) measuring the effect of temperature on radionuclide solubility in brine, and 5) measuring radionuclide oxidation distribution and redox control at elevated temperatures.

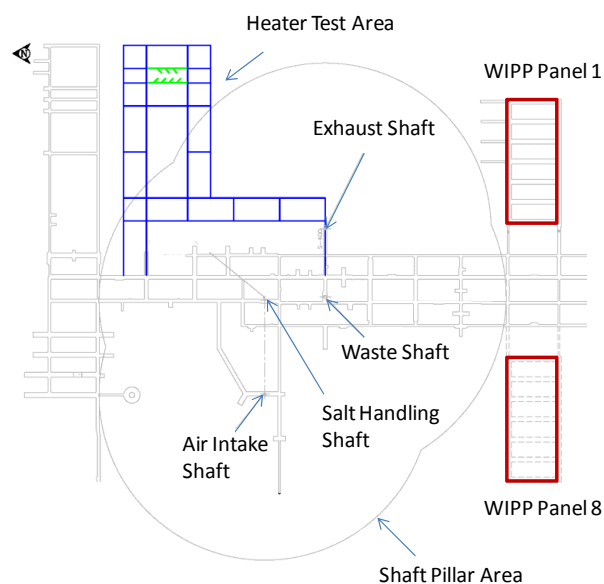


Fig. 2: Salt disposal investigations test area (blue outline) in the WIPP underground (note WIPP panels 1 and 8 in the far right). The test area is located east of the salt handling and exhaust shafts to stay clear of WIPP operations.

WIPP Two-Year Investigation Focus and Underground Tests

Russ Patterson¹ and Donald Reed²

¹ United States Department of Energy, Carlsbad Field Office, 4021 National Parks Highway, Carlsbad NM 88220, USA

² Los Alamos National Laboratory, Earth & Environmental Sciences Division, Carlsbad Operations, Actinide Chemistry & Repository Science Program, 1400 University Drive/Carlsbad, NM 88220, USA
email: dreed@lanl.gov

INTRODUCTION

The Waste Isolation Pilot Plant (WIPP) transuranic repository remains a cornerstone of the U.S. Department of Energy's (DOE) nuclear waste management effort. Waste disposal operations began at the WIPP on March 26, 1999 but a requirement of the repository license is that the WIPP needs to be recertified every five years for its disposal operations. The WIPP received its second recertification in November 2010 and we are now in the third recertification cycle that is scheduled for 2014. An updated license application is scheduled to be provided to the Environmental Protection Agency (EPA), who is the regulator of the WIPP site, in March of 2013.

A two-year program plan of WIPP-specific experiments and model updates was put into effect to prepare for the 2014 recertification. Research by the Los Alamos Actinide Chemistry and Repository Science team and Sandia National Laboratories Chemistry Program is underway to support parameter and model updates identified in the plan. The goal of this program is to improve the robustness of the current WIPP model [1, 2] and quantify the conservatism in the current assumptions that form the basis of the safety case.

Additionally, tests to support future and expanded operations in a salt-based repository are proposed. Thermo-mechanical experiments are under consideration to be performed in the testing area of the WIPP underground. Some chemistry and actinide chemistry studies to support these experiments are also proposed.

DESCRIPTION OF THE WORK

The research and model changes identified in the two year program plan are performed under a DOE-approved quality assurance program plan. This research is conducted at the Carlsbad Environmental Monitoring and Research Center (Los Alamos) or the Chemistry Labs (Sandia) in Carlsbad New Mexico where the WIPP is located. Research to support proposed changes will be used to support changes that are incorporated into the WIPP model after review and approval/concurrence by the EPA. A peer-review may be required in this process by the EPA depending on the extent and nature of the changes proposed.

EXPECTED RESULTS

WIPP 2-year Program Plan Emphasis

The program plan for the third WIPP recertification was initiated a year ago and will be completed by the end of calendar year 2012. The need for a peer review will be decided in February 2012 and conducted, if needed, in the fall of 2012. With or without a peer review, the data cut-off for the 2014 recertification application is January 2013.

The technical focus of the changes outlined in the WIPP program plan are not completely defined but are expected to include the following:

- Shift aqueous speciation modelling from the FMT code to the EQ3/6 code
- Shift to a model-supported variable-pH brine chemistry model from a “bracketing” approach
- Update and improve the Pitzer data base in the current WIPP model:
 - Fe, borate (see Figure 1), organic ligand complexation
 - Thorium (+4) actinide model and solubility in brine

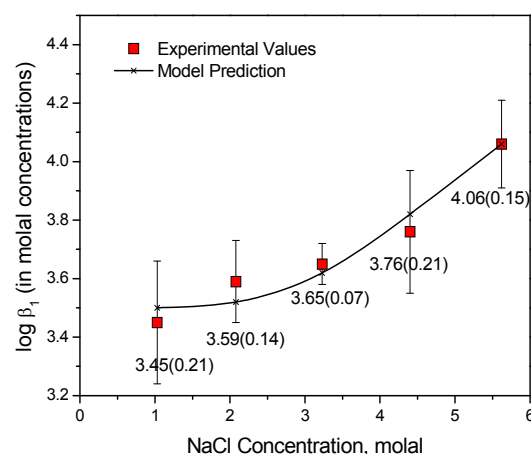


Fig. 1: Effect of ionic strength on $\log \beta_1$ for the complexation of borate with Nd^{3+} (analog for +3 actinides). Pitzer parameters generated as a fit to these data can be used to model this complexation reaction.

- Actinide colloid enhancement factors (bio-colloids, intrinsic colloids and inorganic colloids)

- Further Pu(V/VI) and Am(V) reduction studies (microbial and Fe(II/0) reactions)
- U(VI) solubility studies with carbonate that support the current 1 mM solubility assumption
- Solubility of organic ligands in WIPP brine
- Iron-induced gas generation rates based on WIPP-specific corrosion rates

This research will be documented in a series of reports and publication during the upcoming year or so and form the basis of proposed changes submitted to the EPA.

Proposed Salt Disposal Investigation Experiments

The goal of the proposed salt disposal investigation experiments is to perform integrated thermal, mechanical, hydrologic and geochemical tests in a newly excavated experimental station in the WIPP underground. This excavation was approved by the EPA regulator and is already underway. A schematic of the proposed experimental configuration is shown in Figure 2. The overall timeframe for these experiments is multiple years with post-test forensics to establish the effects of heating on salt closure, porosity, and water movement/content planned.

The use of salt for high-level waste (HLW) disposal also requires some additional studies in brine and actinide chemistry to account for the low-probability brine-intrusion scenarios as will likely be required by a regulator of the HLW repository. Much of the current WIPP model and experience can be used to support the safety case for a thermally heated repository in salt but there are some data gaps. The most important of these, across the range of temperature of interest, are expected to include:

- 1) Thermodynamic data for brine and actinide chemistry reactions
- 2) Waste package interactions at variable to high ionic strength
- 3) Radiolysis effects on brine and actinides in brine systems
- 4) Radionuclide solubilities as a function of temperature
- 5) Redox effects and reactions as a function of temperature

It is also anticipated that a combination of strategically-selected experimental results, extrapolations from existing room temperature data, and confirmatory experiments will be used to fill these gaps in the

development of potential HLW applications for a salt-based repository.

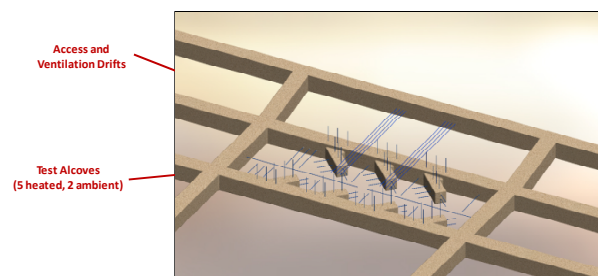


Fig. 2: Topview of proposed field tests in the WIPP underground experimental area. The array of alcoves (~7 proposed) will be configured with instrumentation holes to collect needed data in real time.

REFERENCES

1. DOE, "Title 40 CFR Part 1991 Compliance Certification Application for the Waste Isolation Pilot Plant, DOE/CAO-2009." DOE Carlsbad Field Office, Carlsbad, NM, 2009.
2. DOE, "Title 40 CFR Part 1991 Subparts B and C Compliance Recertification Application 2009, Appendix SOTERM." DOE Carlsbad Field Office, Carlsbad, NM, 2009.

Preliminary Safety Analysis Gorleben

Guido Bracke

*Department of Final Disposal, GRS mbH, Schwertnergasse 1, 50667 Cologne, Germany
email: guido.bracke@grs.de*

INTRODUCTION

In Germany, the Gorleben salt dome has been discussed as a possible site for a repository for heat-generating radioactive waste since the 1970s. Since then, scientists have been exploring the salt dome both above and below ground, carrying out various studies and experiments.

The safety requirements governing the final disposal of heat-generating radioactive waste [1] has the objective to protect man and environment. Unreasonable burdens and obligation for future generations shall be avoided. The main safety principles are the concentration of the radioactive and other pollutants in an isolating rock zone. The risk by released radioactive substances shall be negligible to risks associated with natural radiation exposure. No intervention or maintenance work shall be required during the post-closure phase. The retrieval / recovering of the waste shall be possible.

Based on these requirements the tasks and objectives of the preliminary safety analysis of Gorleben are to give a synthesis and comprehensible assessment of the findings obtained so far, whether a safe repository at the Gorleben site would be possible and which conditions may apply [2]. An important objective is to identify the needs for research and exploration.

The study will be reviewed by a team of international experts, whether the study and its results are in line with the international state of the art in science and technology.

STRUCTURE OF THE PRELIMINARY SAFETY ANALYSIS GORLEBEN

The preliminary safety analysis Gorleben is composed of various working packages, their central package being the analysis of long-term safety.

Therefore, work packages include the

- description of the geological site
- predictions of its geological evolution over the next million years,
- waste that could presumably be emplaced in a repository at the Gorleben site,
- safety and demonstration concept for the Gorleben site
- design of a repository concept

The long-term safety analysis will model the radiological consequences to provide information on the question whether and how the waste could be confined safely at Gorleben by a combination of geological

barriers (e.g. the salt rock, the surrounding overburden) and geotechnical barriers (e.g. the sealing of shafts and drifts).

Therefore, work packages include

- a compilation of a database of features, events and processes to derive scenarios
- the analysis of scenarios of repository evolution with characterization of their likelihood
- application of specific simulation software to verify the confinement and to analyse possible radiological consequences of scenarios.

Additional work packages include

- an optimization of repository designs
- operational safety
- human intrusion scenarios

The findings will be subject of a concluding synthesis, assessment and recommendations.

Several project partners are involved in the study. GRS is responsible for the scientific-technical as well as administrative organisation of the project. GRS is working on the major parts of the work packages itself.

CURRENT STATUS OF THE PROJECT

The concept for safety has to consider:

Operational phase:

- Technical barriers against release of radionuclides
- Warranty of undercriticality
- Emplacement working homewards
- Minimization of impact of accidents
- ...

Post-closure phase:

- Safe containment of the waste and its containers
- Minimization / limitation of fluid flow
- Retardation of radionuclide transport
- Warranty of undercriticality
- ...

The demonstration of compliance shall show the operational safety, integrity of the geological barriers and geotechnical sealings, undercriticality and the complete or safe containment of radionuclides.

A radiological hazard index (RHI) has been defined. Complete isolation is given, if the RHI = 0 and there is no release of radionuclides from the isolating rock zone. A proof of safe confinement is possible, if the diffusive or advective transport of radionuclides from the isolating rock zone leads to a RHI < 1. Additional criteria (dilution in overlying rock) may be applied to comply with a safe confinement. The repository is not feasible, if all criteria are missed.

THEREDA – Thermodynamic Reference DatabaseHelge C. Moog¹¹*Gesellschaft für Anlagen- und Reaktorsicherheit (GRS), Theodor-Heuss-Str. 4, 38122 Braunschweig, Germany
email: helge.moog@grs.de***INTRODUCTION**

Thermodynamic equilibrium calculations are used to estimate the maximum likely solubility of hazardous contaminants such as radio nuclides in aqueous solutions. Various databases existed in Germany to conduct such calculations, which were only poorly comparable.

Further, due to the long term character of activities related to the safe disposal of radioactive waste, a method was missing, to store thermodynamic data in a way that ensures internal consistency, that allows for easy access, and allows for an easy application in thermodynamic equilibrium calculation with some of the most popular codes.

To meet this demand a project was launched in 2006 to create a common, mutually agreed and web-based thermodynamic reference database. The database is run by the following institutions:

- GRS: Gesellschaft für Anlagen- und Reaktorsicherheit mbH, Abteilung Prozessanalyse, Theodor-Heuss-Straße 4, D-38122 Braunschweig, Germany
- KIT-INE: Karlsruhe Institute of Technology, Institute for Nuclear Waste Disposal, P.O. Box 3640, D-76021 Karlsruhe, Germany
- HZDR-IRC: Helmholtz-Zentrum Dresden-Rossendorf, Institute of Radiochemistry, Bautzner Landstraße 400, D-01328 Dresden, Germany
- TU-BAF: Technische Universität Bergakademie Freiberg, Fakultät für Chemie und Physik, Institut für Anorganische Chemie, Leipziger Straße 29, 09596 Freiberg, Germany
- AF-Consult: AF-Consult Switzerland AG, Täfernstraße 26, CH-5405 Baden, Switzerland

DESCRIPTION OF THE WORK

At the beginning the members of THEREDA agreed upon quality objectives:

- Transparency: all data should be traceable to a publicly available reference.
- Consistency: all data should be stored in a way which ensures internal consistency, also when independent data are modified.
- Comprehensiveness: the database should cover the whole range of possible applications with regard to safety assessments for nuclear disposal

sites. Where data are missing, appropriate estimates should be added.

- Uncertainties: wherever possible, uncertainties of data were to be captured.
- Data assessment: the referenced source, the data quality and the way in which every particular datum was derived should be captured in terms of pre-defined identifiers. Thus, data of poor quality and estimates, which were added to meet the objective "comprehensiveness", are marked accordingly for the user.

Criteria for the quality of thermodynamic data were largely adopted from the NEA-database. However, additional provisions had to be met for the inclusion Pitzer parameters.

To store the data a PostgreSQL-databank was created, running on an Apache web server. It can be accessed with php-based interface modules. JOOMLA! was installed as content management system which serves as intranet to the THEREDA-members and as access point for external users for the download of data and documentations.

The developed data structure is quite flexible. An arbitrary number of interaction models, such as Pitzer or SIT can be added. This can also be done for non-ideal solid phases and for the (non-ideal) gas phase.

Parameter files are created on the basis of element selection by members of THEREDA. Supported formats are:

- PHREEQC
- EQ3/6, Versions 7.2 and 8.0a (planned)
- CHEMAPP
- Geochemist's Workbench

In addition data can also be downloaded in a JSON-format intended to encourage external users to create own programs to import data from THEREDA. However, at the time being, external users have access to ready-to-use parameter files only, which are not dynamically create from element selection and which are archived.

To ensure the quality of released parameter files, benchmark calculations are performed and documented. The objective is not only to ensure the correctness of the calculations, but also to compare the results obtained with the different supported codes.

RESULTS

The contributing institutions have captured their data in the databank. Elements considered are:

- System of oceanic salts: H, O, Na, K, Mg, Ca, Cl, S, C
- Hydrated cement phases: Si, Al
- Actinides, fission- and activation products: Pa, Th, U, Np, Pu, Am, Cm, Rb, Sr, Tc, Cs, Sm, Nd, Ra

Data were entered for gaseous and aqueous species as well as solid phases. These data also include Pitzer and SIT interaction coefficients.

However, most of the captured data are still disclosed from the public. They are going to be released in discrete steps. The first release appeared in June 2011. It contained the system of oceanic salts, apart from carbon. It was contributed by TU-BAF. Depending on the particular system, calculations are possible for elevated temperatures up to 393.15 K. For the development of this data set, all relevant data from the literature were completely evaluated, including those published later than 1984, when the famous paper from Harvey, Möller and Weare appeared (Harvie et al 1984). Upon fitting of experimental data to polynomials in terms of temperature caution was applied to remain consistent with Pitzer parameters from Harvey et al. (1984); however, small numerical discrepancies between calculations performed with the THEREDA-database and that from Harvey et al. (1984) remain.

Outlook

At present, releases are prepared for the following elemental subsystems:

- H, O, Na, K, Mg, Ca, Cl, SO₄, C, Si, Al at 298.15 K: hydrated cement phases. Data for hydrated cement phase are contributed by AF Colenco. Data for carbonates and CO₂(g) are contributed by TU-BAF.
- H, O, Na, K, Mg, Ca, Cl, Am(III), Nd(III), Cm(III) at 298.15 K. Data for Am(III), Nd(III), and Cm(III) are contributed by KIT-INE.

These new data sets are consistent with the first release, which in fact is part of the new ones.

Other activities include the development of a web-based graphical user-interface, designed to facilitate THEREDA-members in developing and refining the database. Completion of revision 1.0 is due by end of January 2012.

Acknowledgements

This project is jointly funded by the Federal Ministry of Education and Research (BMBF) (GRS: 02C1426/02C1628, FZD: 02C1436, TU-BAF: 02C1446), the Federal Ministry of Economics and Technology (BMWi) (FZK/KIT: 02E10126/02E1067, FZD: 02E10136, GRS: 02E10146, TU-BAF:

02E10709), and the Federal Office for Radiation Protection (BfS) with funds from the Federal Ministry for the Environment, Nature Conservation and Nuclear Safety (BMU).

REFERENCES

1. Charles E Harvie†, Nancy Möller, John H Weare (1984): The prediction of mineral solubilities in natural waters: The Na-K-Mg-Ca-H-Cl-SO₄-OH-HCO₃-CO₃-CO₂-H₂O system to high ionic strengths at 25°C, *Geochimica et Cosmochimica Acta*, **48**, Pages 723-751 (1984).

Sorel cement as geotechnical barrier in salt formations

Daniela Freyer

*TU Bergakademie Freiberg, Institut für Anorganische Chemie, Germany
email: Daniela.freyer@chemie.tu-freiberg.de*

Sorel cement (magnesia cement) is formed by reaction of caustic magnesium oxide with concentrated magnesium chloride solution. The so formed binder phases in the system MgO – MgCl₂ – H₂O are basic magnesium salt hydrates [x Mg(OH)₂ · y MgCl₂ · z H₂O]. The material is used for many years as barrier construction material in salt formations, since, particularly in the potash mining the magnesia cement is stable towards salts and their solutions. The common binder phases are 3 Mg(OH)₂ · 1 MgCl₂ · 8 H₂O (3-1-8 phase) and/or 5 Mg(OH)₂ · 1 MgCl₂ · 8 H₂O (5-1-8 phase).

For the evaluation of the chemical long term stability of a magnesia cement or concrete the solubility data of the phases in presence of salt solutions of appropriate salt formations must be considered.

The solubility data in the system Mg(OH)₂-MgCl₂-H₂O at room temperature indicate that in contact with MgCl₂ solution (above 1 mol/kg H₂O) the 3-1-8 phase is thermodynamically stable [1-3].

The situation has to be proved also for salt solutions of rock salt formations. Relevant formations of the german Zechstein such as the Leine- or Stassfurt-sequences contain beside halite (main component) also anhydrite, polyhalite and carnallite. In appropriate equilibrium solutions magnesium contents of 1 to 4 mol MgCl₂ / kg H₂O can be reached in the sodium chloride saturated solutions. From recently completed solubility investigations in the system NaCl-Mg(OH)₂-MgCl₂-H₂O [3] result, that 3-1-8 phase is stable above 0.5 mol MgCl₂ / kg H₂O. At lower MgCl₂ concentrations brucite is the stable phase. The intermediate formation of 5-1-8 phase can be observed especially at lower MgCl₂ concentrations (0.3 - 2 molal). The transformation in the stable 3-1-8 phase requires a long time (weeks – years), may be the reason of the statement of Xiong et al. [4], that the 5-1-8 phase is the stable phase at appropriate concentrations.

Investigations of magnesia cement or concrete material in contact with salt solutions confirm the phase behavior. Magnesia cement or concrete consisting of 5-1-8 phase deforms or expands after or during salt solution contact caused by formation of the stable 3-1-8 phase from the metastable 5-1-8 phase. In case of restraint by salt ground the crystallization of 3-1-8 phase from 5-1-8 phase by expansion should not be possible - a compaction of the material or encapsulation of 3-1-8 by 5-1-8 phase should be the consequence. After such a confirmation of integrity, magnesia cement formulation independent from the binder phases (3-1-8 or 5-1-8) could be used.

By these results sorel cement is qualified as a long term stable material for geotechnical barriers in salt formations beside the positive effect to reduce the radionuclide solubilities by slightly alkaline pH value of the material.

REFERENCES

1. D'Ans J., Busse W., Freund H.-E., „Über basische Magnesiumchloride“, Kali u. Steinsalz 8 (1955) 3 – 7.
2. Altmaier M., Metz V., Neck V., Müller R., Fanghänel Th., “Solid-liquid equilibria of Mg(OH)₂(cr) and Mg₂(OH)₃Cl·4H₂O(cr) in the system Mg-Na-H-OH-Cl-H₂O at 25°C”, Geochim. Cosmochim Acta 2003, **67**, 3595-3601.
3. Oestreich M., Freyer D., Neck V., Altmaier M., Bube Ch., Metz V., Voigt W., „Solid-liquid equilibria in the system Mg(OH)₂-MgCl₂-H₂O at 25°C and 40°C and NaCl-Mg(OH)₂-MgCl₂-H₂O at 25°C”, in preparation.
4. Xiong Y., Deng H., Nemer M., Johnsen S., “Experimental determination of the solubility constant for magnesium chloride hydroxide hydrate (Mg₃Cl(OH)₄ · 4 H₂O, phase 5) at room temperature, and its importance to nuclear waste isolation in geological repositories in salt formations”, Geochim. Cosmochim. Acta 2010, **74**, 4605-4611.

Thermodynamics of long-term metastable magnesium (chloro) hydroxo carbonates at 25°C

C. Bube, M. Altmaier, V. Metz, V. Neck[†], D. Schild, B. Kienzler

Karlsruhe Institute of Technology, Institut für Nukleare Entsorgung, P.O. Box 3640, 76021 Karlsruhe, Germany
email: christiane.bube@kit.edu

INTRODUCTION

Mg(OH)₂-based materials are used as backfill and buffer materials in low-/intermediate level waste repositories in rock salt. Due to interactions with Mg(OH)₂-based materials, the geochemical milieu in such repositories is buffered at a weakly alkaline pH and low pCO₂. These conditions are favourable in terms of low radionuclide solubilities. It is known that magnesite (MgCO₃(s)) is the thermodynamically stable carbonate solid phase in the system Mg-Cl-HCO₃-CO₃-H-OH-H₂O at room temperature. Due to the kinetically inhibited formation of magnesite, pCO₂ and pH in this system are controlled for a considerable time span by the formation of long-term metastable magnesium hydroxo (chloro) carbonates, e.g. hydromagnesite, Mg₅(CO₃)₄(OH)₂·4H₂O(s), and chlorartinite, Mg₂(OH)CO₃Cl·3H₂O(s).

Determining the geochemical conditions, in particular pH and pCO₂, is of fundamental importance for long-term safety assessments of radioactive waste repositories.

DESCRIPTION OF THE WORK

This study aims at determining the phase transition between the two metastable Mg-carbonate phases, hydromagnesite and chlorartinite, and deriving a stability constant for chlorartinite. Batch experiments are conducted in Ar glove boxes by adding 0.05 molar (M) Na₂CO₃ to MgCl₂-solutions (0.25 M to 4.5 M) and monitoring pH_c (-log(c_{H+})) for more than 3 years. Different analytical methods (Raman spectroscopy, XRD, SEM-EDS, XPS) are applied to analyze the respective precipitates.

The equilibrium constant of chlorartinite is calculated based on the equilibrium at phase transition between hydromagnesite and chlorartinite.

First, the equation of the two equilibrium constants of hydromagnesite and chlorartinite is solved for the HCO₃⁻-activity:

$$\{HCO_3^-\} = \frac{K_{HM}^0 \cdot \{H^+\}^6}{\{Mg^{2+}\}^5 \cdot a_{H_2O}^6}$$

and

$$\{HCO_3^-\} = \frac{K_{CA}^0 \cdot \{H^+\}^2}{\{Mg^{2+}\}^2 \cdot \{Cl^-\} \cdot a_{H_2O}^4}$$

with K_{HM}⁰ and K_{CA}⁰ being the equilibrium constants for hydromagnesite and chlorartinite.

At phase equilibrium and corresponding HCO₃⁻-activity, the resulting equations can be set equal and solved for the equilibrium constant of chlorartinite K_{CA}⁰. This constant is then calculated using the equilibrium solution composition from the experimental observations, activity coefficients calculated with The Geochemist's Workbench[®] [1] based on the thermodynamic dataset of Harvie et al. [2] and literature data for the constant of hydromagnesite [3,4] (mean value of both sources is used).

RESULTS

With different analytical methods, it is confirmed that hydromagnesite is formed as long-term metastable phase in the solutions of MgCl₂-concentrations below 2.5 M, while chlorartinite is formed in solutions with MgCl₂-concentrations higher than 2.8 M (see Raman μ-spectrometric results in Fig.1).

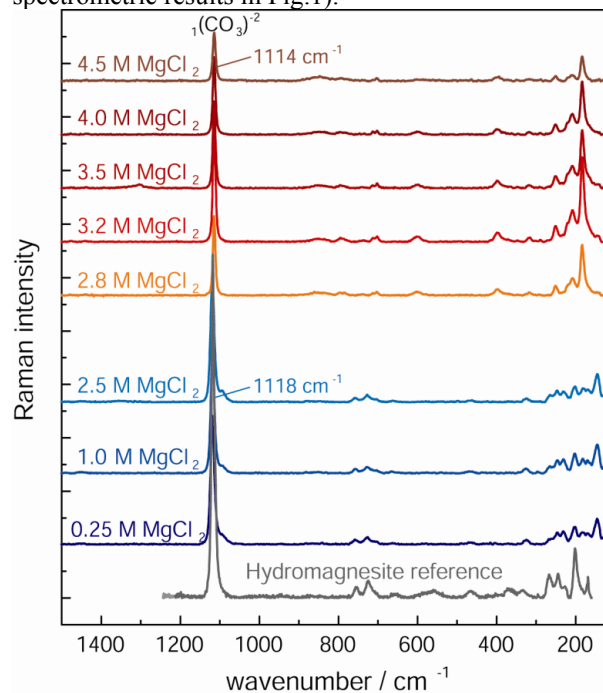


Fig. 1: Results of the Raman spectroscopic analysis of the precipitated phases. Spectra of samples with MgCl₂-concentration <2.8 M match with the hydromagnesite reference, while spectra of samples with higher MgCl₂-concentrations show different characteristics, especially at lower wave numbers.

The SEM analysis of a precipitate sampled from the 2.8 M MgCl₂ solution reveals a morphology that seems to be an intermediate between the plate-like structure of

hydromagnesite and the needle-like structure of chlorartinite. The equilibrium constant of chlorartinite has therefore been calculated for phase transition at a MgCl_2 -concentration of 2.8 M. The error that has been assigned to the constant results from the unknown exact location of the phase transition (between 2.5 M and 3.2 M MgCl_2) and the large uncertainty of the equilibrium constant of hydromagnesite. The equilibrium constant of chlorartinite is calculated as $\log K_{\text{CA}} = 13.15 \pm 0.36$ for the reaction equation $\text{Mg}_2(\text{OH})\text{CO}_3\text{Cl}\cdot 3\text{H}_2\text{O}(\text{s}) + 2 \text{H}^+ \leftrightarrow 2 \text{Mg}^{2+} + \text{HCO}_3^- + \text{Cl}^- + 4 \text{H}_2\text{O}(\text{l})$.

CONCLUSIONS

The phase transition between hydromagnesite and chlorartinite has been identified with different analytical methods. The equilibrium constant for chlorartinite, which is derived from the phase transition observed in the experiments, enables a comprehensive thermodynamic description of the Mg-Cl- HCO_3 - CO_3 -H-OH- H_2O system at room temperature (see Fig. 2). The provided data allows for an improved thermodynamic description of the system relevant for nuclear waste disposal in rock salt.

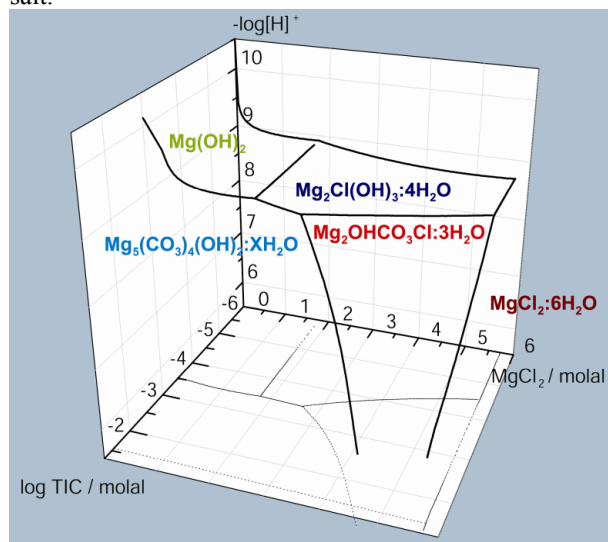


Fig. 2: Phase diagram of the stable and long-term metastable phases in the system Mg-Cl- HCO_3 - CO_3 -H-OH- H_2O system at room temperature ($\text{MgCO}_3(\text{s})$ formation suppressed).

REFERENCES

1. C.M. BETHKE et al., “The Geochemist’s Workbench”, University of Illinois, Urbana (2009).
2. C.F. HARVIE et al., “The prediction of mineral solubilities in natural waters: The Na-K-Mg-Ca-H-Cl- SO_4 -OH- HCO_3 - CO_2 - H_2O system to high ionic strengths at 25°C”, *Geochim. Cosmochim. Acta*, **48**, 723-751 (1984).
3. E. KÖNIGSBERGER et al., “Low-temperature thermodynamic model for the system Na_2CO_3 - MgCO_3 - CaCO_3 - H_2O ”, *Geochim. Cosmochim. Acta*, **63**, 3105-3119 (1999).
4. R.A. ROBIE et al., “Thermodynamic properties of minerals and related substances at 298.15 K and 1 Bar (10^5 Pascals) pressure and at higher temperatures”, *U.S. Geol. Survey Bull.*, **2131** (1995).

Gas Generation due to Anoxic Corrosion of Steel and Lead in Na-Cl ± Mg Dominated Brines

Gregory T. Roselle

*Sandia National Laboratories, Carlsbad Defense Waste Management Programs,
4100 National Parks Highway, Carlsbad, NM 88220, USA
email: gtrosel@sandia.gov*

INTRODUCTION

The Waste Isolation Pilot Plant (WIPP) is a deep geologic repository developed by the U.S. Department of Energy for the disposal of transuranic radioactive waste in bedded salt (Permian Salado Fm.). In order to minimize radionuclide release from the repository it is desirable to maintain actinide elements such as Pu, Am, U, and Np in their least-soluble form (i.e., low oxidation states). Post-closure conditions in the WIPP will control the speciation and solubilities of radioelements in the waste. Microbially-produced CO₂ from cellulosic, plastic and rubber materials in the waste may acidify any brine present and increase the actinide solubilities. Thus, the DOE replaces MgO in the repository to buffer f_{CO_2} and pH within ranges favoring lower actinide solubilities. Large quantities of low-C steel and Pb present in the WIPP may also consume CO₂. Steel corrosion has been identified as a major gas generation (H₂) in the WIPP repository [1]. Lead corrosion also has the potential to generate H₂. Gas production is of interest to the WIPP because it will affect room closure and chemistry ([2],[3]).

DESCRIPTION OF THE WORK

The objective of this work is to determine: (a) the extent to which steel and Pb consume CO₂ via the formation of carbonates or other phases, potentially supporting MgO in CO₂ sequestration; and (b) determining hydrogen gas generation rates based on measured corrosion rates. In these experiments steel and Pb coupons are immersed in brines under WIPP-relevant conditions using a continuous gas flow-through system. The experimental apparatus maintains the following conditions: P_{O₂} < 5 ppm; temperature of 26 °C; relative humidity at 78 ± 10 %; and a range of CO₂ partial pressure (P_{CO₂}) values (0, 350, 1500 and 3500 ppm, balance N₂). Four high-ionic-strength-brines are used: Generic Weep Brine (GWB), a Na-Mg-Cl dominated brine associated with the Salado Fm.; Energy Research and Development Administration WIPP Well 6 (ERDA-6), a predominately Na-Cl brine; GWB with organic ligands (EDTA, acetate, citrate, and oxalate); and ERDA-6 with the same organic ligands.

RESULTS

Interim results from a series of multiyear experiments will be presented. Steel coupons show formation of several phases dependent on the P_{CO₂}. Scanning Electron Microscope (SEM) analysis with Energy

Dispersive Spectroscopy (EDS) shows the presence of a green Fe (±Mg)-chlorohydroxide phase (green rust?) at P_{CO₂} values <1500 ppm. At higher P_{CO₂} the dominant corrosion product is a Fe-Mg-Ca hydroxycarbonate phase. Lead coupons show no corrosion products at lower P_{CO₂} values but significant formation of a Pb-Ca hydroxycarbonate phase at P_{CO₂} > 350 ppm.

Multiple cleaning cycles were used to remove all corrosion products from the coupons, which were then weighed to determine corrosive mass loss. These data are used to calculate average corrosion rates for each experimental condition. The data show that steel corrosion rates are a strong function of P_{CO₂} for all brine types (Figure 1). ERDA-6 brines appear to be more corrosive than GWB brines. Corrosion rates for Pb coupons show no consistent trend as a function of P_{CO₂} or brine type.

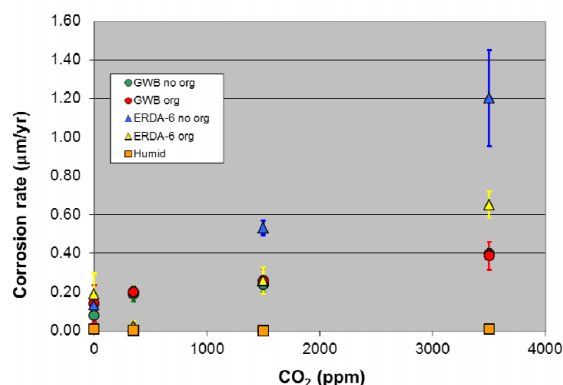
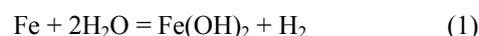
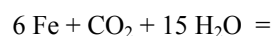


Fig. 1: Average corrosion rates for steel coupons in the various brines plotted as a function of the atmospheric CO₂ concentration. Data are from the 6 month experiments. Bars indicate one standard deviation for the average corrosion rates.

The rate of H₂ gas generation will depend on the corrosion rate and the type of corrosion products formed. Based on SEM observations of the experiments, possible anoxic corrosion products of steel in the absence of CO₂ are (Fe,Mg)(OH)₂ via the reaction:



In the presence of microbially-produced CO₂ steel corrosion can proceed via the reactions:





The anoxic corrosion of Pb could also result in H₂ gas generation via the formation of PbO in the CO₂-free environments and PbCO₃ in the presence of CO₂:



These reactions can be used in conjunction with the experimentally determined corrosion rates to estimate H₂ gas generation rates due to steel and lead corrosion. Preliminary estimates indicate that the corrosion rates observed in the current experiments may be significantly lower than those currently used in the WIPP Performance Assessment Model.

REFERENCES

1. BRUSH, L.H., "Systems Priority Method – Iteration 2 Baseline Position Paper: Gas Generation in the Waste Isolation Pilot Plant" Sandia National Laboratories, Albuquerque, NM (1995).
2. BUTCHER, B.M., "Preliminary Evaluation of Potential Engineered Barrier Modifications for the Waste Isolation Pilot Plant (WIPP)" *SAND89-3095*, Sandia National Laboratories, Albuquerque, NM (1990).
3. BRUSH, L.H., "Test Plan for Laboratory and Modeling Studies of Repository and Radionuclide Chemistry for the Waste Isolation Pilot Plant" *SAND90-0266*, Sandia National Laboratories, Albuquerque, NM (1990).

ACKNOWLEDGEMENT

This research is funded by WIPP programs administered by the Office of Environmental Management (EM) of the U.S Department of Energy. Sandia National Laboratories is a multi-program laboratory managed and operated by Sandia Corporation, a wholly owned subsidiary of Lockheed Martin Corporation, for the U.S. Department of Energy's National Nuclear Security Administration under contract DE-AC04-94AL85000.

Thermodynamic Properties of the Na-Ra-Cl-SO₄-H₂O System- Estimating Pitzer Parameters for RaCl₂Y. O. Rosenberg¹, V. Metz² and J. Ganor¹¹ *Department of Geological and Environmental Sciences, Ben-Gurion University of the Negev, P.O.B 653, Beer Sheva 84105, Israel
email: yoavoved@gmail.com*² *Institute for Nuclear Waste Disposal (INE), Karlsruhe Institute of Technology, P.O.B. 3640, 76021 Karlsruhe, Germany***INTRODUCTION**

²²⁶Ra is a critical radionuclide with respect to the long-term safety of radioactive waste disposal. Hence, the fate of radium in deep bedrock repositories has been deserved special attention in safety case studies for potential high level waste repositories, e.g., in Sweden and Switzerland [e.g., 1, 2]. Radium solubility might be extensively controlled by co-precipitation with barite (BaSO₄), i.e., the formation of a (Ra,Ba)SO₄ solid solution [3 and references therein]. The similar ionic radii of Ra²⁺ and Ba²⁺, electronegativities, electronic configuration and the identical crystallographic structure of pure RaSO₄ and barite [4] make barite an almost ideal host mineral for Ra. As a result there is a growing interest to understand how (Ra,Ba)SO₄ solid solution may control Ra solubility with respect to long-term safety issues of nuclear-waste disposal [5].

In saline environments the activity coefficient of aqueous ions ($\gamma_{i^{v+}}$) may significantly deviate from unity. Pitzer parameters for RaCl₂ interaction are needed for the calculation of $\gamma_{\text{Ra}^{2+}}$. However, due to radioactivity safety issues, no experimental data for the fit of such parameters exists. As a general approach, it is common to assume that for similar ions (e.g., Ra²⁺ and Ba²⁺) the activity coefficients are roughly equal [4, 6]. While for relatively dilute solutions this approximation may be valid, it may not be the case in high ionic strength solutions [7].

The purpose of this study is to examine the limitation of the assumption that $\gamma_{\text{Ra}^{2+}}/\gamma_{\text{Ba}^{2+}} = 1$ by estimating the RaCl₂ Pitzer parameters from linear regression with hydrated cation radii, and to calculate $\gamma_{\text{Ra}^{2+}}$ as a function of NaCl concentration.

DESCRIPTION OF THE WORK

The use of the Pitzer formalism requires a set of interaction parameters, which account for each cation-anion pair ($\beta^{(0)}$, $\beta^{(1)}$, $\beta^{(2)}$ and C^ϕ), for each cation-cation and anion-anion pair (θ), and for each cation-cation-anion and anion-anion-cation triplet (ψ). These parameters are used to calculate the osmotic coefficient of the solution and the conventional activity coefficients for any individual ion using virial expansion equations.

The second virial coefficient (calculated by $\beta^{(0)}$, $\beta^{(1)}$ and, for 2-2 interactions, $\beta^{(2)}$) represents a weighed mean of the short range (repulsive and attractive) electrostatic forces between pairs of ions [8]. Pitzer and

Mayorga [8] discussed the dependence of $\beta^{(0)}$ and $\beta^{(1)}$ on the sum of radii of opposite charge ions ($R_+ + R_-$) and a second dependence on the absolute magnitude of the difference between these radii $|R_+ - R_-|$. Therefore, it was decided to explore how known Pitzer parameters depend on the radii of the cations.

To this end Pitzer parameters for the MCl₂ and MBr₂ (M = Mg²⁺, Ca²⁺, Sr²⁺ and Ba²⁺) and the ionic radii of M²⁺ (in coordination numbers CN = 6, 8, 10 and 12) from the literature were critically reviewed [9].

RESULTS

The trend between the MCl₂ Pitzer parameters and ionic radii of CN 8 are presented in Fig.1. Although linear correlation of $\beta^{(1)}$ and C^ϕ is poor in Fig. 1b-c (solid line, $0.5 < R^2 < 0.8$), an obvious trend with ionic radii is observed both for MCl₂. Similar results were found for the MBr₂ binary interaction parameters and for the MCl₂ with with CN 12 [9].

If one examines Fig. 1b-c, it can be argued that the values of Sr²⁺ are outliers; omitting these values significantly improves the correlation between $\beta^{(1)}$ and C^ϕ parameters and the ionic radii (dashed lines, Fig. 1). The RaCl₂ Pitzer parameters estimated using Sr²⁺ in the regression have no significant preference over the assumption $\gamma_{\text{Ra}^{2+}}/\gamma_{\text{Ba}^{2+}} = 1$, since the estimated parameters are very similar to the BaCl₂ parameters. As the aim of this study is to examine the limitation of this assumption, we preferred to omit Sr²⁺ from the regression in order to represent the strict case; i.e. the maximum deviation of RaCl₂ Pitzer parameters from BaCl₂ parameters (open rectangles, Fig. 1).

Following this procedure the average value of the RaCl₂ parameters were estimated according to the linear correlation with ionic radii of CN 8 and 12. The calculation of $\gamma_{\text{Ra}^{2+}}/\gamma_{\text{Ba}^{2+}}$ conducted with these parameters is presented in Fig. 2. Despite the uncertainty in the calculation, the ratio is still significantly lower than 1 (horizontal line which represents RaCl₂ parameters equal to BaCl₂ parameters).

Ra and Ba co-precipitation was studied in evaporation batch experiments [3]. Numerical simulation of the experiments showed that the effective partition coefficient is predicted more accurately with the RaCl₂ parameters than when assuming that $\gamma_{\text{Ra}^{2+}}/\gamma_{\text{Ba}^{2+}}=1$ (Fig. 3).

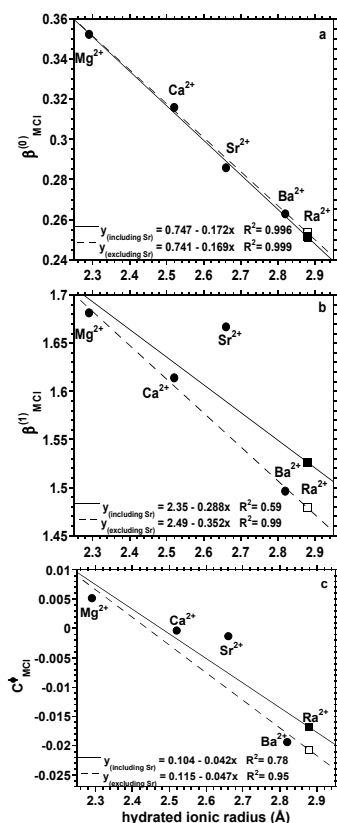


Fig. 1: Linear regressions between binary interaction parameters of: a) $\beta_{MCl}^{(0)}$, b) $\beta_{MCl}^{(1)}$ and c) C_{MCl}^{ϕ} and hydrated radii of CN 8. In the regression of the solid line $M^{2+} = Mg^{2+}, Ca^{2+}, Sr^{2+}$ and Ba^{2+} while that of the dashed line exclude Sr^{2+} . Close and open rectangles correspond to extrapolated $RaCl_2$ parameters with regressions that include and exclude Sr^{2+} respectively.

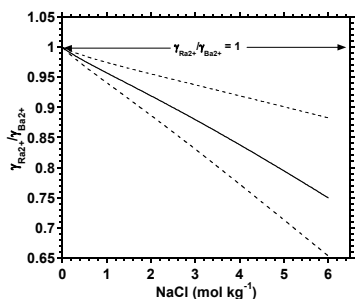


Fig. 2: Activity coefficient ratio (solid line), $\gamma_{Ra^{2+}}/\gamma_{Ba^{2+}}$, as a function of ionic strength as calculated with the average of the $RaCl_2$ parameters estimated with CN 8 and CN 12. Uncertainty envelope (dashed line) corresponds to ± 1 standard deviation of the mentioned average).

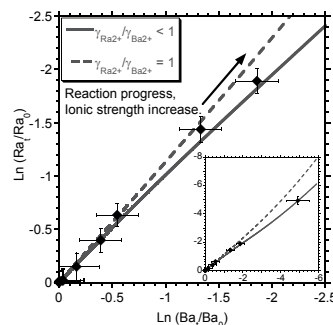


Fig. 3: Ln-Ln plot showing the results of a numerical model (lines) and experimental results (closed circles). The model was run with the assumption that $\gamma_{Ra^{2+}}/\gamma_{Ba^{2+}} = 1$ (dashed line) and using the estimated Pitzer parameters of $RaCl_2$ (solid line). The increasing difference between the models is attributed to the increase in ionic strength due to evaporation, which lowers the ratio $\gamma_{Ra^{2+}}/\gamma_{Ba^{2+}}$.

REFERENCES

- Grandia, F., et al., *Assessment of the radium-barium co-precipitation and its potential influence on the solubility of Ra in the near-field*. SKB TR-08-07. 2008: Svensk Kärnbränslehantering AB, Stockholm.
- Berner, U., et al., *Radium solubilities from SF/HLW wastes using solid solution and co-precipitation models*. 2002, Paul Scherrer Institute: Villigen, Switzerland, Internal Report TM-44-02-04.
- Rosenberg, Y.O., et al., Co-precipitation of radium in high ionic strength systems: 2. Kinetic and ionic strength effects. *Geochimica et Cosmochimica Acta*, **75**(19): p. 5403-5422. (2011).
- Zhu, C., Coprecipitation in the Barite isostructural family: 1. Binary mixing properties. *Geochimica et Cosmochimica Acta*, **68**(16): p. 3327-3337. (2004).
- Bosbach, D., Solid-solution formation and the long-term safety of nuclear-waste disposal, in *EMU notes in mineralogy*, M. Prieto and H. Stoll, Editors. 2010, European Mineralogical Union and the Mineralogical Society of Great Britain & Ireland: London. p. 345-376.
- Langmuir, D., et al., The geochemistry of Ca, Sr, Ba and Ra sulfates in some deep brines from the Palo Duro Basin, Texas. *Geochimica et Cosmochimica Acta*, **49**(11): p. 2423-2432. (1985).
- Langmuir, D., et al., The Thermodynamic Properties of Radium. *Geochimica et Cosmochimica Acta*, **49**(7): p. 1593-1601. (1985).
- Pitzer, K.S., et al., Thermodynamics of electrolytes. II. Activity and osmotic coefficients for strong electrolytes with one or both ions univalent. *The Journal of Physical Chemistry*, **77**(19): p. 2300-2308. (1973).
- Rosenberg, Y.O., et al., Co-precipitation of radium in high ionic strength systems: 1. Thermodynamic Properties of the Na-Ra-Cl-SO₄-H₂O System-Estimating Pitzer Parameters for $RaCl_2$. *Geochimica et Cosmochimica Acta*, **75**(19): p. 5389-5402. (2011).

An Overview of Research on Microbial Interactions in the Waste Isolation Pilot Plant

Julie Swanson, David Ams, Karen Simmons, Hnin Khaing, Donald Reed

*Los Alamos National Laboratory, Earth & Environmental Sciences Division, Carlsbad Operations,
Actinide Chemistry & Repository Science Program, 1400 University Drive/Carlsbad, NM 88220, USA
jsswanson@lanl.gov*

INTRODUCTION

Microorganisms in a nuclear waste repository can affect actinide solubility by changing the redox environment, adsorbing actinides, degrading or generating complexants, or by changing actinide oxidation states [1,2]. While research on the microbiology of subsurface igneous and clay repositories has made many advances, there are fewer data available on the microbial effects in salt-based repositories, such as the Waste Isolation Pilot Plant (WIPP) in Southeastern New Mexico. Microorganisms that grow in hypersaline systems may not be as metabolically versatile or active as those found in subsurface soils or groundwaters [3,4], and extrapolations of their interactions with emplaced waste cannot be easily made from data obtained with organisms at other repositories. This research is being conducted to gain a more realistic understanding of the potential effects of WIPP-indigenous organisms on repository performance.

DESCRIPTION OF THE WORK

The goals of this work are manifold: 1) to characterize the microbial ecology of the Salado formation and surrounding groundwaters in order to predict the metabolic capability of indigenous populations, 2) to investigate the potential degradation of emplaced organic waste components, such as complexing agents and cellulose, 3) to measure the sorption of actinides onto WIPP-relevant microorganisms, and 4) to determine if metal/actinide bioreduction occurs at the high ionic strength expected in the repository.

RESULTS

Microbial characterization

Clone libraries constructed from bacterial and archaeal 16S and eukaryotic 18S rRNA-encoding genes reflect a low-diversity community (see Figure 1). At higher salt concentrations (> 2.5 M), haloarchaea, such as *Halobacterium* sp., *Halorubrum*-like sp., *Halopelagica* sp., and *Natronomonas*-like sp. dominate the community structure. Similar organisms have been retrieved from other subsurface halite formations in the US and Europe, suggesting that findings from this research may be useful to other salt-based repositories. At lower salt concentrations (2.5 M), *Bacteria* (*Limnobacte* sp., *Pelomona* sp., and *Nesterenkonia* sp.) were detected along with two archaeal sequences (*Halobacterium noricense* and a *Halorubrum*-like sp.).

Fungi (*Coniothyrium* sp., *Cladosporium* sp., *Engyodontium* sp.) also appeared in incubations at 2.5 M NaCl; these were likely introduced into the WIPP from above-ground. Anaerobic enrichment incubations are also underway.

Organic complexing agent degradation and solubility

Acetate and citrate were readily degraded aerobically by a mixed culture of haloarchaea cultivated from halite, but only after oxalate had precipitated from solution (see Figure 2) [5]. Oxalate was weakly degraded by an organism previously isolated from WIPP halite, but its disappearance was mainly due to its low solubility. Acetate was also degraded by a halophilic bacterium in dilute brines. Degradation experiments under nitrate-reducing conditions are also underway. The potential for cellulose degradation is being investigated using the fungal and actinomycetal cultures isolated from halite.

Bioreduction of metals/actinides

Iron solubility in brines is a limiting factor in its reduction by halotolerant/halophilic bacteria, and haloarchaea have not been shown to reduce metals. In incubations of lower ionic strength (~1.5 M) groundwaters from the WIPP site, the precipitation of metal sulfides was noted. XANES analysis showed both iron(II) and (III) oxidation states in these precipitates. As both iron-reducing and sulfate-reducing bacteria were detected in these incubations, it is likely that both direct and indirect (via sulfide) reduction of iron occurred. In groundwater and halite incubations at higher ionic strength, iron is also reduced abiotically, albeit at a slower rate.

Biosorption

Adsorption of Np (V) onto a Gram-negative, halophilic bacterium in 4 M NaClO₄ was enhanced relative to adsorption in 2 M NaClO₄ over the majority of the pH range evaluated (see Figure 3) [6]. This was apparently due to the effect of increasing aqueous ion activity coefficients at high ionic strength. Sorption studies using a Gram-positive halophilic bacterium and a haloarchaeon isolated from WIPP environs are underway.

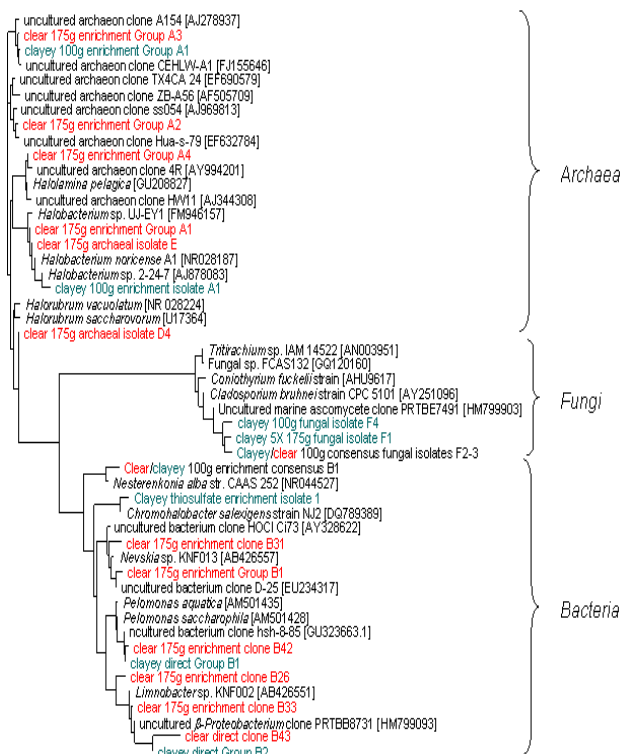


Fig. 1: Phylogenetic tree showing the relatedness of small subunit rRNA gene-encoding sequences retrieved from samples of clear (red) and clayey (green) halite incubated in either 100 or 175g NaCl. Reference sequences included.

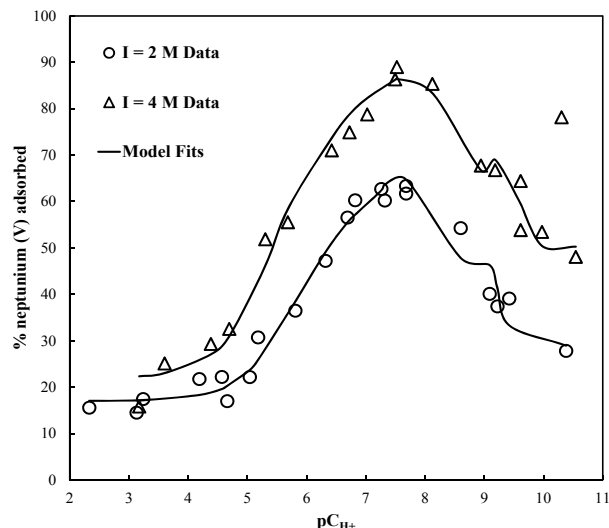


Fig. 3: Sorption of Np (V) onto *Chromohalobacter* sp. in 2 M and 4 M perchlorate.

REFERENCES

- [1] MCCABE A, “The Potential Significance of Microbial Activity in Radioactive Waste Disposal”, *Experientia*, **46**, 779-787 (1990).
- [2] PEDERSEN K, “Microorganisms and Their Influence on Radionuclide Migration in Igneous Rock Environments”, *Journal of Nuclear and Radiochemical Sciences*, **6**, 11-15 (2005).
- [3] OREN A, “Thermodynamic Limits to Microbial Life at High Salt Concentrations”, *Environmental Microbiology*, **13**, 1908-1923 (2011).
- [4] VREELAND RH, et al., “Distribution and diversity of halophilic bacteria in a subsurface salt formation”, *Extremophiles*, **2**, 321-331.
- [5] SWANSON, J et al., “Degradation of Organic Complexing Agents by Halophilic Microorganisms in Brines” accepted in *Geomicrobiology Journal* (2011).
- [6] AMS, D et al., “The Effect of High Ionic Strength on Neptunium (V) Adsorption to a Halophilic Bacterium” accepted in *Geochimica et Cosmochimica Acta* (2011).

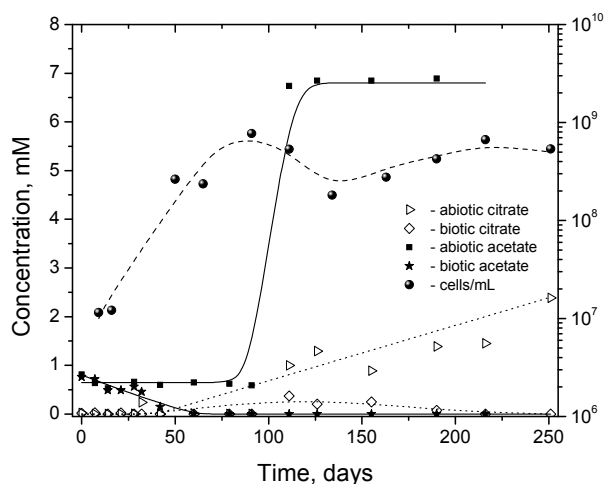


Fig. 2: Degradation of acetate and citrate in high Mg²⁺ brine by a mixed culture of haloarchaea, as evidenced by the increase in abiotic concentrations, but not in biotic, after oxalate disappearance.

Microorganisms in potential nuclear waste disposal host rocks

Andrea Geissler, Henry Moll, Velina Bachvarova, Laura Lütke,
Sonja Selenska-Pobell, Gert Bernhard

Helmholtz-Zentrum Dresden-Rossendorf, Institute of Radiochemistry, Germany
email: a.geissler@hzdr.de

INTRODUCTION

Microorganisms can exist even in extreme environments and interact in different ways with actinides /1/. So far, little is known about the influence of microorganisms on the migration of actinides after an accidental release from a nuclear waste repository. For this reason it is important to know what microorganisms exist in potential nuclear waste disposal host rocks (as for example clay and salt) and to investigate interactions of the present microorganisms with actinides.

DESCRIPTION OF THE WORK

It will be presented how the bacterial diversity in a Opalinus Clay sample from the Mont Terri Rock Laboratory, Switzerland was investigated by the use of culture-independent and -dependent methods. The interactions of bacterial clay isolates with actinides will be discussed by taking the system curium(III)-*Sporomusa* sp. as an example. Finally, there will be an overview given about future investigations in salt.

RESULTS

By the use of culture-independent methods, total DNA was recovered from an unperturbed opalinus clay sample and an unexpectedly variety of bacterial groups was found /2/. The bacterial community was predominated by representatives of *Firmicutes*, *Betaproteobacteria*, and *Bacteroidetes*. All isolates cultivated from the opalinus clay sample in R2A medium under anaerobic conditions where affiliated with *Firmicutes* /3/. The 16S rRNA genes of the isolates affiliated with *Sporomusa* sp. belong to the class *Negativicutes* and the family *Veillonellaceae*. The interaction between soluble species of curium(III) and *Sporomusa* cells was studied at trace curium(III) concentrations (0.3 µM) using time-resolved laser-induced fluorescence spectroscopy (TRLFS) /4/. The biosorption studies showed strong interactions between curium(III) and the cells already at low biomass concentrations of 10 mg_{dry weight}/L between pH 3 and 8. Extraction studies with 0.01 M EDTA solution have shown that 30% of curium(III) was strongly/irreversibly bound on *Sporomusa* cells. The majority of curium(III) is bound via biosorption by surface functional groups of the cell envelope. Two Cm³⁺-*Sporomusa* species could be identified from the luminescence emission spectra,

R–O–PO₃H–Cm²⁺ and R–COO–Cm²⁺, having peak maxima at 599.7 and 602.2 nm, respectively. In summary, an strong interaction over a broad pH (1.5 → 8) and biomass concentration range (0.01–200 mg_{dry weight}/L) and an pH dependent curium(III) coordination on functional groups of the cell envelope was observed.

In the second part, there will be given some information about *Halophiles* in general and the future investigations on microbial diversity in salt.

ACKNOWLEDGEMENTS

This work was funded by BMWi under contract number 02E10618. The authors are indebted to the U.S. Department of Energy, Office of Basic Energy Sciences, for the use of ²⁴⁸Cm via the transplutonium element production facilities at Oak Ridge National Laboratory; ²⁴⁸Cm was made available as part of collaboration between HZDR and the Lawrence Berkeley National Laboratory (LBNL).

REFERENCES

1. Lloyd, J. R., Macaskie, L. E.: "Biochemical basis of microbe-radionuclide interactions". *Interactions of Microorganisms with Radionuclides*, eds Keith-Roach, M. J., Livens, F. R. Elsevier Science Ltd., 313-342 (2002).
2. Bachvarova, V., Selenska-Pobell, S.: "Fast and reliable bacterial diversity assay of Opalinus clay samples collected from the Mont Terri underground laboratory". *Annual report Institute of Radiochemistry, Helmholtz-Zentrum Dresden-Rossendorf*, 30, (2010).
3. Bachvarova V. et al.: "Bacterial isolates cultured under anaerobic conditions from an opalinus clay sample from the Mont Terri Rock laboratory". *Annual report Institute of Radiochemistry, Helmholtz-Zentrum Dresden-Rossendorf*, 18, (2009).
4. Moll, H. et al.: "Speciation of curium(III) bound by bacteria found in rocks considered for nuclear waste disposals". In: Presented at the 13th International Conference MIGRATION'11, Abstracts, Beijing, China, September 2011, pp. 144-145.

Can we use ultramicroelectrodes to perform electrochemistry in brines ?

Michel Perdicakis, Asma Chebil, Mathieu Etienne

*Laboratoire de Chimie Physique et Microbiologie pour l'Environnement,
UMR 7564, Nancy-Université - CNRS, 405 rue de Vandœuvre, 54602 Villers-lès-Nancy Cedex, France
email: perdi@lcpme.cnrs-nancy.fr*

INTRODUCTION

Electrodes in the micrometric range are called ultramicroelectrodes (UMEs) or simply microelectrodes according to the particular origin of electrochemists. These electrodes present several advantages towards the traditional ones because of their small size. In addition to the applications that exploit this very small size for detection or production of species in restricted volumes or for Scanning ElectroChemical Microscopy (SECM) experiments, other specific applications of UMEs are based on their intrinsic characteristics: reduced ohmic drop, reduced time constants and steady state diffusional currents without the necessity of forced convection [1].

In the framework of the RECO-SY project of the Euratom Community (see Acknowledgements), we tried to make use of the higher sensitivity of UMEs to measure very low concentrations of redox indicators in concentrated NaCl solutions. The goal was to determine redox potentials in brines by monitoring voltammetrically the concentrations of the reduced and oxidized forms of a redox indicator added to the solution beforehand. These attempts completely failed. Actually, as it is shown in the example relative to oxygen solutions in Fig. 1, the voltammetric response of UMEs –that perfectly work in diluted media or pure water– becomes completely meaningless once immersed in NaCl brines.

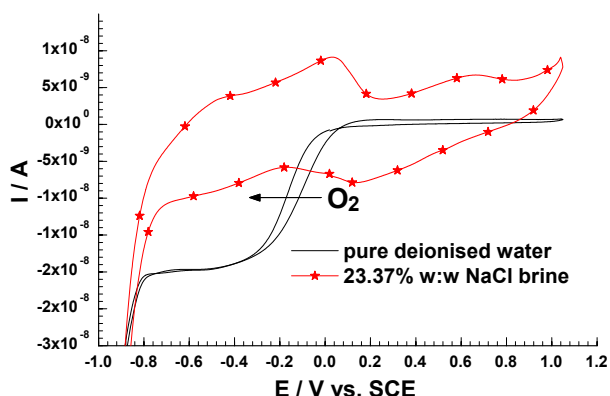


Fig. 1: Cyclic voltammograms at a 50µm platinum UME for aerated pure deionized water and aerated 23.37% w:w NaCl brine. Scan rate 5mV/s.

The purpose of this work was to find the reasons why UMEs do not work in brines whereas traditional millimetric electrodes are working satisfactorily and, if possible, to build UMEs that are compatible with these highly concentrated media.

DESCRIPTION OF THE WORK

We tested nine platinum UMEs having diameters ranging between 10 and 50µm in NaCl solutions whose concentration varied from 5.84 to 29.22% w:w. The UMEs used were either commercial or homemade, and their insulating body was formed of various glasses (Pyrex, soft glass, quartz, quartz suprasil...) or polymeric resins (epoxy, polyester, PTFE).

For convenience, dissolved oxygen was used as the main electroactive species but several experiments were also carried out with the model species ferrocene dimethanol.

The results achieved with the different UMEs were compared with those obtained using a routine 2mm diameter platinum rotating disc electrode. The disk electrode shroud was fabricated from PTFE.

RESULTS

The voltammetric response of the platinum UMEs that we tested strongly depends on the nature of the insulating material used to make the body of the electrodes. And the more concentrated the solution is, the more the resulting voltammetric signal is distorted. This distortion is particularly noticeable during the reverse scans (Fig. 2).

The UMEs that the insulating part is made of "quartz-suprasil" are the less affected by the brines. However, the fabrication of such an electrode is quite difficult because the melting point of platinum (1772°C) and the softening point of quartz-suprasil (~1600°C) are relatively close. The use of platinum wires insulated with PTFE is an interesting alternative but there are problems with their mechanical behaviour and then with polishing. We classified the UMEs as a function of the insulating materials in the following order, from least to most resistant: quartz fiber < epoxy, softglass < polyester, Pyrex < quartz-suprasil, PTFE.

The distortions of voltammograms that are observed when the UMEs are immersed in brines are linked with phenomena occurring at the metal / insulating material interface. The same phenomena must occur when millimetric electrodes are used, but they are not detected because of the much higher distance between this interface and the main surface area of the platinum disc. Actually, "...for disks of large radius, the contribution from the disk edge is small at times of electrochemical interest; however, as the electrode radius decreases, the relative importance of this source

of flux increases..." [2] therefore the mass transport parallel to the electrode surface come into play.

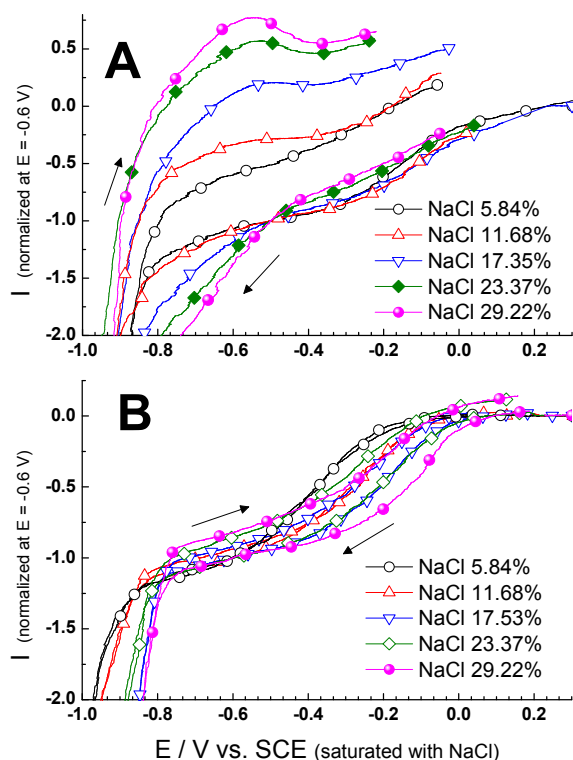


Fig. 2: Influence of the NaCl concentration on the voltammograms shape recorded for aerated brines with: (A) a 25 μ m UME prepared from *Thomas Recording* quartz-platinum-tungsten raw fiber for SECM use, (B) a 50 μ m platinum UME homemade of "quartz-suprasil" from *Heraeus*. Scan rate 5mV/s.

We suggested two hypotheses to explain these experimental results:

i) the corrosion of the insulating material, caused by the concentrated NaCl solutions, releases electroactive species that are responsible for the deformation of the voltammetric curves. It is this assumption that has motivated the fabrication of UMEs made of platinum wire shrouded with extremely pure quartz glass.

and/or

ii) Brines preferentially attack the insulating material close to the platinum disk. Therefore, crevices are created at the insulating material / platinum interface. Inside these crevices, the mixing of the brine with the species released by the insulating material leads to the formation of a new and extremely concentrated medium or a gel where specific electrochemical reactions take place and produce signals that are superimposed to the voltammetric response of oxygen.

Experiments are planned in order to confirm the validity of these assumptions.

ACKNOWLEDGEMENTS

The research leading to these results has received funding from the European Union's European Atomic Energy Community's (Euratom) Seventh Framework Programme FP7/2007-2011 under grant agreement n° 212287 (RECOZY project <http://www.recozy.eu>).

The authors wish to thank Dr. Kay Schuster from the Institute of Photonic Technology (Jena, Germany) and Dr. Philippe Roy from the XLIM Research Institute (University of Limoges, France) who kindly provided us with quartz Suprasil capillaries for the UMEs construction.

REFERENCES

1. CHRISTIAN AMATORE, "Electrochemistry at Ultra-microelectrodes" in: I. Rubinstein (Ed.), *Physical Electrochemistry*, Marcel Dekker, Inc. New York, Page 131-208 (1995).
2. JAMES B. FLANAGAN et al., "Digital Simulation of Edge Effects at Planar Disk Electrodes" *J. Amer. Chem. Soc.*, **77**, Page 1051-1055 (1973).

Redox chemistry of Np(V/VI) under hyperalkaline conditions: aqueous speciation, solubility and chemical analogies with Pu

X. Gaona¹, D. Fellhauer^{2,3}, K. Dardenne¹, J. Rothe¹, M. Altmaier¹

¹*Institut für Nukleare Entsorgung, Karlsruher Institut für Technologie (KIT-INE), Germany
xavier.gaona@kit.edu*

²*European Commission, Joint Research Centre, Institute for Transuranium Elements, European Commission*

³*Institut für Physikalische Chemie, Universität Heidelberg, Heidelberg, Germany*

INTRODUCTION

The redox chemistry of the Np(V/VI) couple under alkaline conditions remains largely unknown. In the aqueous phase, the formation of hexavalent anionic species (e.g. $\text{NpO}_2(\text{OH})_3^-$ and $\text{NpO}_2(\text{OH})_4^{2-}$) has been proposed, although no thermodynamic data are currently selected in the NEA reviews [1]. The same thermodynamic data gap applies to Pu(VI), for which only first and second hydrolysis products ($\log^*\beta_{1,1}$ and $\log^*\beta_{1,2}$) are currently selected by the NEA. In analogy to U(VI), the precipitation of Na- and Ca-neptunates and plutonates is also expected. The formation of these aqueous species and solid compounds may significantly limit the stability field of Np(V) and Pu(IV) in cementitious and saline environments, and therefore deserves further attention.

DESCRIPTION OF THE WORK

Aqueous speciation of the Np(V/VI) redox couple in hyperalkaline conditions was investigated in tetramethylammonium hydroxide (TMA-OH) solutions, in order to limit the precipitation of solid phases and maintain Np in solution for EXAFS/XANES analysis. Carbonate concentration (as impurity of TMA-OH) was $2\text{--}3 \times 10^{-3}$ M. The $-\log[\text{H}^+]$ of the samples prepared ranged between 9 and 14, whereas redox conditions were defined by the absence or presence of NaClO (5×10^{-3} M and 5×10^{-2} M) as oxidizing agent. The initial concentration of Np(V) in all samples was $\sim 2 \times 10^{-3}$ M.

Solubility experiments were performed to determine the thermodynamic properties of Np(VI) aqueous species and solid compounds forming in dilute to concentrated alkaline NaCl solutions. A Np(VI) stock solution (with ~ 200 mg of ^{237}Np) was prepared by electrolysis of Np(V) in HCl, and precipitated at $-\log[\text{H}^+] = 12$ in NaCl 2.5 M. After two months of equilibration, the resulting solid phase was distributed in 5 experimental series of increasing I (0.1 M, 0.5 M, 1.0 M, 2.5 M and 5.0 M NaCl), with $7 \leq -\log[\text{H}^+] \leq 14$. Oxidizing conditions ensuring the stability of Np(VI) were achieved with 5×10^{-3} M NaClO in each sample. The aqueous concentration of Np was measured after 10 kD ultrafiltration by liquid scintillation counting (LSC). Solid phase was characterized by XRD, chemical analysis, SEM-EDS and XANES/EXAFS.

A Pu(VI) stock solution (with ~ 100 mg of ^{242}Pu) was prepared by electrolysis of Pu(IV) in HClO_4 .

Analogously to Np(VI) solubility experiments, the Pu(VI) stock solution was neutralized with an alkaline solution aiming at $-\log[\text{H}^+] = 12$ in NaCl 2.5 M. Despite the expected large oversaturation with respect to $\text{PuO}_2(\text{OH})_2 \cdot \text{H}_2\text{O}(\text{cr})$, and eventually a Na-plutonate, no solid phase was precipitated (even after 9 months of equilibration time). Supernatant solution (~ 5 mM Pu(VI)) was characterized by UV-vis and XANES/EXAFS.

RESULTS

UV-vis spectra obtained from the supernatant in TMA-OH solutions and in absence of NaClO showed very clear Np(V) features, identified as NpO_2^+ , $\text{NpO}_2(\text{CO}_3)^-$ and $(\text{NpO}_2)_x(\text{OH})_y(\text{CO}_3)_z^{x-y-2z}$. XANES of these samples confirmed the predominance of Np(V). No UV features were observed within $800 \text{ nm} \leq \lambda \leq 1300 \text{ nm}$ for samples with NaClO, even though Np(VI) is expected to occur. This different behaviour could be explained by the lower Np concentration in some of the samples, but is also indicative of the possible formation of centrosymmetric Np(VI) species (i.e. $\text{NpO}_2(\text{OH})_4^{2-}$) with lower absorptivity coefficients. XANES of this second set of samples confirmed the predominance of Np(VI), in accordance with reference spectra obtained by in-situ electrolysis of a Np solution.

XRD, chemical analysis, SEM-EDS and EXAFS characterization of the solid phases considered for the Np(VI) solubility experiments indicated the prevalence in all systems ($0.1 \text{ M} \leq I \leq 5.0 \text{ M}$) of a neptunate-like structure with a Na:Np ratio 1:1, likely $\text{Na}_2\text{Np}_2\text{O}_7 \cdot x\text{H}_2\text{O}$. EXAFS further indicated the predominance of a distorted structure, where Np-O_{ax} and Np-O_{eq} distances were longer and shorter, respectively, than in usual neptunyl moieties. In all cases, solubility curves obtained showed three different regions (see Fig. 1): region a. $6 \leq -\log[\text{H}^+] \leq 8\text{--}9$, showing a steep decrease in the solubility with a (still undefined) slope < 2 ; region b. $8\text{--}9 \leq -\log[\text{H}^+] \leq 10\text{--}11$, with a nearly pH-independent [Np], and region c. $10\text{--}11 \leq -\log[\text{H}^+] \leq 13\text{--}14$, showing an increase in the solubility with a well-defined slope of 1. Regions b and c agree very well with observations previously reported for U(VI) under similar experimental conditions. Given the stoichiometry of the solid phase and considering the analogies with U(VI), the following equilibrium reactions can be proposed for regions b and c, respectively: $\text{NaNpO}_2\text{O}(\text{OH})(\text{cr}) + \text{H}_2\text{O} \Leftrightarrow \text{Na}^+ + \text{NpO}_2(\text{OH})_3^-$ and

$\text{NaNpO}_2\text{O}(\text{OH})(\text{cr}) + 2\text{H}_2\text{O} \Leftrightarrow \text{Na}^+ + \text{NpO}_2(\text{OH})_4^{2-} + \text{H}^+$. The equilibrium reaction controlling Np(VI) solubility in region a remains undefined, although it is suspected that reduction to Np(V) may have occurred. In the following, thermodynamic modelling of Np(VI) solubility data will be completed considering both SIT and Pitzer approaches.

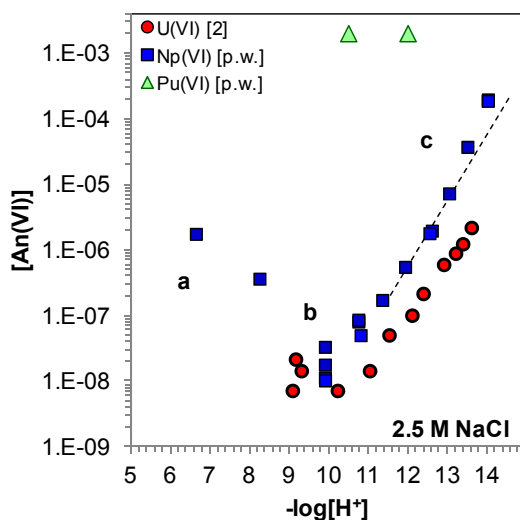


Fig. 1: Solubility data obtained in this work for Np(VI) and Pu(VI) in alkaline NaCl solutions (only 2.5 M data shown). Solubility data obtained in [2] under similar experimental conditions for U(VI) included for the sake of comparison.

Despite the large oversaturation expected with respect to $\text{PuO}_2(\text{OH})_2 \cdot \text{H}_2\text{O}(\text{cr})$ (and eventually $\text{Na}_2\text{Pu}_2\text{O}_7 \cdot x\text{H}_2\text{O}$), no Pu(VI) solid phase formation occurred in the alkaline 2.5 M NaCl solutions after 9 months (see Fig. 1). Evaluation of the XANES data collected for the aqueous sample confirmed the predominance of Pu(VI) aqueous species, according with reference spectra published elsewhere [3]. Furthermore, Pu–O_{ax} and Pu–O_{eq} distances consistent with Pu(VI) resulted from the fitting of EXAFS data ($1.78 \pm 0.02 \text{ \AA}$ and $2.29 \pm 0.03 \text{ \AA}$, respectively). A more distant shell fitted at $3.77 \pm 0.05 \text{ \AA}$ was unequivocally assigned to a Pu–backscattering atom. These results indicate the formation and stability of Pu(VI) polymers or *eigen-colloids*. If confirmed a thermodynamic equilibrium, these species will need to be characterized and considered in the already very complex picture of plutonium redox chemistry [4]. These results also stress that the rule of chemical analogies for An of the same redox state might be jeopardized, or hindered by strong kinetic effects in the case of Pu(VI).

REFERENCES

1. Guillaumont, R. et al., “Chemical Thermodynamics 5. Update on the Chemical Thermodynamics of Uranium, Neptunium, Plutonium, Americium and Technetium” NEA OECD, Elsevier (2003).
2. Altmaier, M. et al., “Solubility of U(VI) in NaCl and MgCl₂ solution” *Proceedings of the Migration Conference* (2003).
3. Brendebach, B. et al., “X-ray absorption spectroscopic study of trivalent and tetravalent actinides in solution at varying pH values” *Radiochimica Acta*, **97**, 701–708 (2009).
4. Neck, V. et al., “Solubility and redox reactions of Pu(IV) hydrous oxide: Evidence for the formation of PuO_{2+x}(s, hyd)” *Radiochimica Acta*, **95**, 193–207 (2007).

Actinide Speciation and Oxidation-state Distribution in the WIPP

Donald Reed, Marian Borkowski, Michael Richmann, Jean-Francois Lucchini, Juliet Swanson and David Ams

*Los Alamos National Laboratory, Earth & Environmental Sciences Division, Carlsbad Operations,
Actinide Chemistry & Repository Science Program, 1400 University Drive/Carlsbad, NM 88220, USA
email: dreed@lanl.gov*

INTRODUCTION

The Waste Isolation Pilot Plant (WIPP) transuranic repository remains a cornerstone of the U.S. Department of Energy's (DOE) nuclear waste management effort. Waste disposal operations began at the WIPP on March 26, 1999 but a requirement of the repository license is that the WIPP needs to be recertified every five years for its disposal operations. The WIPP has just received its second recertification in November 2010. Research by the Los Alamos Actinide Chemistry and Repository Science team [1-4] that is centered on the speciation of key actinides under WIPP-specific conditions to improve the robustness of current models and quantify the conservatism in the current assumptions being made is continuing.

The overall ranking of actinides, from the perspective of potential contribution to release from the WIPP, is: Pu ~ Am > U >> Th and Np. The calculated oxidation-state-specific actinide solubilities over the past recertifications are tabulated in Table 1.

Table 1. Oxidation-state-specific solubility of actinides in Salado (high magnesium) and Castile (high sodium chloride) brines				
	Brine	PAVT 1999	PABC 2004	PABC 2009
An(III)	Salado	1.2×10^{-7}	3.9×10^{-7}	1.7×10^{-6}
An(III)	Castile	1.3×10^{-8}	2.9×10^{-7}	1.5×10^{-6}
An(IV)	Salado	1.3×10^{-8}	5.6×10^{-8}	5.6×10^{-8}
An(IV)	Castile	4.1×10^{-9}	6.8×10^{-8}	6.8×10^{-8}

DESCRIPTION OF THE WORK

Recently, our research emphasis has been on WIPP-specific systems in the following areas: 1) colloidal fraction of +3 and +4 actinides looking at analog and plutonium systems, 2) redox distribution of plutonium under highly reducing iron-rich brine systems, and 3) the characterization and key interactions of halophilic microorganisms indigenous to the WIPP site. These investigations were performed under anoxic conditions, at 25 ± 3 °C, in simulated WIPP brines (GWB and ERDA-6), and over multiple years. The data obtained extend past understanding of WIPP-specific actinide chemistry to brine systems that more closely simulate the expected environment in the WIPP.

RESULTS

Colloidal Fraction of Dissolved Actinides in the WIPP

In the current WIPP PA approach, most of the dissolved mobile actinide concentrations in solution are colloidal in nature. These colloids impact actinide release in the low-probability dissolved brine release events. The colloidal fraction of actinides and analogs is established by a combination of sequential filtration (down to ~7 nm) and by ultracentrifugation (up to 130,000 rpm, Beckman ultracentrifuge). The results obtained in our long-term thorium solubility studies are shown in Fig. 1. These data indicate a relatively small colloidal effect (a factor of 2 or less) which is somewhat less than reported in the literature [5] for shorter-term experiments. Similarly small effects were observed for long-term plutonium and neodymium solubility studies. These data, together, show a relatively small tendency to form intrinsic colloids in the high ionic strength brines expected in the WIPP.

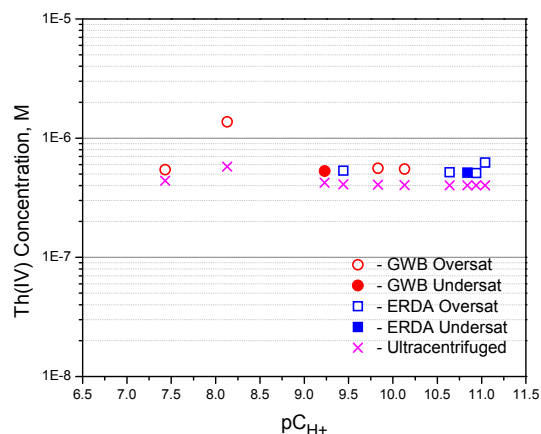


Fig. 1: Concentration of thorium in brine showing the effects of ultracentrifugation on the measured solution concentration

Oxidation-State Distribution of Plutonium under Highly Reducing Conditions

Plutonium experiments were also performed in GWB and ERDA-6 brine in the presence of reduced iron (Fe coupon, Fe powder, and Fe_3O_4) at pH ~ 9. Under these conditions the plutonium, initially present as Pu(VI) was reduced to Pu(IV) consistent with results previously reported [4]. XANES analysis of the collected iron corrosion products and coupon surfaces indicated that the predominant oxidation state

associated with the iron phases was also Pu(IV). The measured solution concentrations were in the 10^{-8} to 10^{-9} M range. The presence of carbonate up to the 10 mM concentration investigated did not significantly affect the solubility of the plutonium. At longer times however, a conversion of Pu(IV) to predominantly Pu(III) was noted (see Fig. 2). These results suggest a more significant role for Pu(III) under WIPP-related conditions and led to a correspondingly enhance solubility (by a factor of ~ 10). These data, however, do not reflect the potential effects of radiolysis associated with the more WIPP-relevant Pu-239 isotope (as used in earlier studies [4] where only Pu(IV) was noted), and do not account for the potential effects of organic complexation which tend to stabilize Pu(IV) relative to Pu(III). In total, these results support and confirm the performance assessment assumption that both Pu(III) and Pu(IV) contribute to the solubility of plutonium in the WIPP.

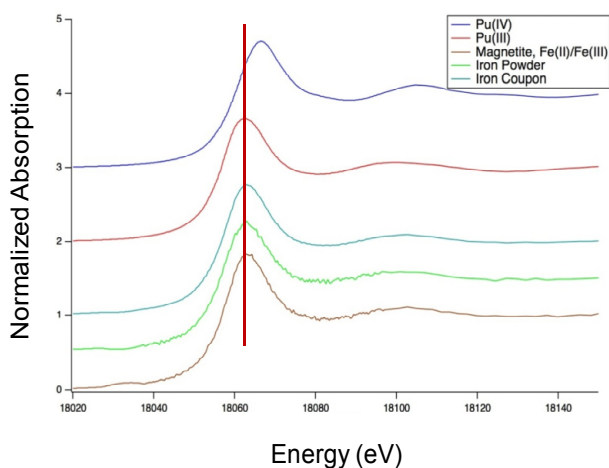


Fig. 2: XANES analysis of long-term plutonium experiments in the presence of excess reduced iron (XANES performed by Jeff Terry and Dan Olive – Illinois Institute of Technology at the Argonne Advanced Photon Source)

Characterization and Interaction of WIPP-Indigenous Microorganisms

Cultivation-dependent and independent methods are being used to characterize the microorganisms present in the WIPP. The community comprises mostly haloarchaea (including *Halobacterium*, *Halorubrum*-like, and *Natronomonas* spp.), although some halophilic bacteria have been detected on the surface of the mine walls (*Halomonas* sp.). A mixed haloarchaeal culture enriched from the halite was capable of degrading organic ligands present in the waste under aerobic conditions, and anaerobic studies are underway. Bioreduction of iron was observed in a co-culture of *Pontibacillus* sp. and *Haloferax* sp. enriched from briny groundwater at the repository. The reacted medium, in turn, caused the reduction of neptunium. Biosorption of actinides and other metals to bacteria isolated from WIPP groundwaters are also being investigated and appears to be dependent upon ionic strength (note Ams

et al., abstract in this compilation). These results underscore the potentially important effects that microbial activity may have on actinide speciation and solubility in waste repositories.

References

- [1] LUCCHINI, JF et al., “Solubility of Nd^{3+} and UO_2^{2+} in WIPP brine as oxidation-state invariant analogs for plutonium,” *Journal of Alloys and Compounds*, Volumes 444-445 (2007) 506-511.
- [2] BORKOWSKI, M et al., “Complexation of Nd(III) with Tetraborate Ion and Its Effect on Actinide(III) Solubility in WIPP Brine.” *Radiochim. Acta*, 98, 1-6 (2010).
- [3] BORKOWSKI, M et al., “Actinide (III) Solubility in WIPP Brine: Data Summary and Recommendations.” Report LA-14360. Los Alamos National Laboratory. September 2009. LA-UR 09-03222.
- [4] REED, DT et al., “Reduction of Plutonium (VI) in Brine under Subsurface Conditions.” *Radiochim. Acta*, 94 (2006) 591-597.
- [5] ALTMAIER, M et al., “Solubility and Colloid formation of Th(IV) in concentrated NaCl and MgCl_2 Solutions.” *Radiochimica Acta*, vol. 92: 537-43 (2004).

Trivalent cations retention upon brucite precipitation

Nicolas Finck*, Kathy Dardenne

¹*Institute for Nuclear Waste Disposal (INE), Karlsruhe Institute of Technology (KIT), P.O. Box 3640, D-76344 Eggenstein-Leopoldshafen (Germany).*

* email: Nicolas.finck@kit.edu

INTRODUCTION

The Asse salt mine was used as test site for the disposal of radioactive waste in Germany. It is anticipated that MgCl_2 -rich brine will enter the emplacement rooms and react with the cemented wastes. Investigations were carried out to select the adequate backfill material [1]. Geochemical modeling lead to the conclusion that a brucite-based backfill material would be best suited: it will control the pH and the concentration of dissolved inorganic carbon within ranges that are favorable with respect to actinide solubility. In case ground water may come into contact with the waste matrix, radionuclide (RN) will be released upon corrosion. The migration of RN out of the repository will be retarded by interaction of the dissolved species with the backfill material. Investigations on the RN, and in particular the trivalent actinides, retention by incorporation in the structure of brucite ($\text{Mg}(\text{OH})_2$) are rather scarce. This study presents results obtained for brucite precipitated in the presence of trivalent cations.

DESCRIPTION OF THE WORK

Brucite was precipitated in the presence of trivalent cations with increasing size [2]: Lu (0.86 Å), Y (0.90 Å) and Am (0.98 Å). Prior to further analysis, the samples were characterized by X-ray diffraction (XRD). Data were collected with a Bruker D8 Advance diffractometer (Cu K_α radiation) equipped with a Sol-X detector. The phase identification was performed with the EVA software (Bruker) and the Rietveld refinement with the TOPAS 4.2 software (Bruker). The local chemical environment of the trivalent cation was probed by extended X-ray absorption fine structure (EXAFS) spectroscopy. Polarized EXAFS (pEXAFS) data were collected for oriented samples considering several angles (α) between the electric field of the X-ray beam and the brucite layer plane: 10, 35, 55 and 80° [3]. In a polarized EXAFS experiment, neighboring shells can be probed selectively. For $\alpha = 0^\circ$, the contribution from in-plane neighbors is enhanced and the out-of-plane contribution is extinguished. At 90°, the contribution from in-plane neighbors is extinguished and enhanced for out-of-plane shells. At $\alpha = 35^\circ$, polarized and conventional powder EXAFS data are identical. Data were collected at the INE-Beamline for actinide research at ANKA [4].

RESULTS

Brucite precipitated in the presence of Lu (LuCopBru [5]), Y (YCopBru) or Am (AmCopBru) had the same structure as the undoped brucite according to the respective diffractogram (Fig 1). No other phase could be detected, meaning that the cations are structurally bound to brucite. Interestingly, the peak corresponding to the (001) plane for all doped brucite had markedly higher intensity compared to brucite [6]. This effect can be attributed to the metal ion, which has higher atomic number as Mg and thus increased scattering power. Consequently, the trivalent metal ion is very likely structurally associated with this plane. This is further supported by the Rietveld refinement of all samples. The data were nicely fit considering that part of Mg is substituted by the metal ion: Mg:Lu = 295:1, Mg:Y = 1000:1 and Mg:Am = 1250:1 (molar ratios). This result strongly suggests a homovalent Mg substitution for the metal ion. No significant change in the unit cell parameters upon substitution for the metal ion could be evidenced.

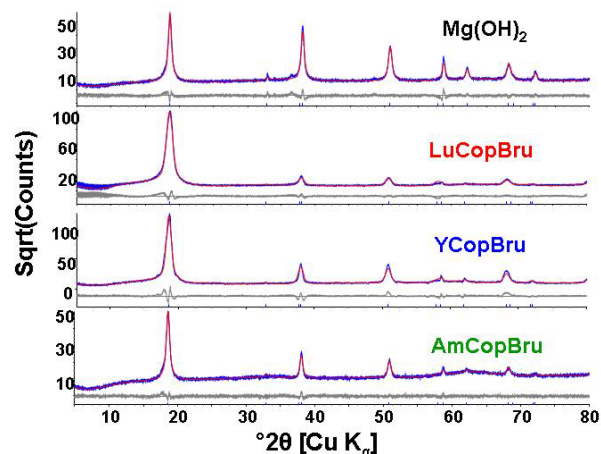


Fig. 1: Experimental diffractograms (blue) and fit results from Rietveld refinement (red) for all samples. The difference curve is shown in grey.

The pEXAFS spectra collected for LuCopBru and YCopBru showed a clear angular dependence (Fig. 2). The amplitude decreased with increasing angle and the position of the maxima was shifted for YCopBru. This result clearly hints a structural association to brucite, and that the metal ion is located in an anisotropic environment.

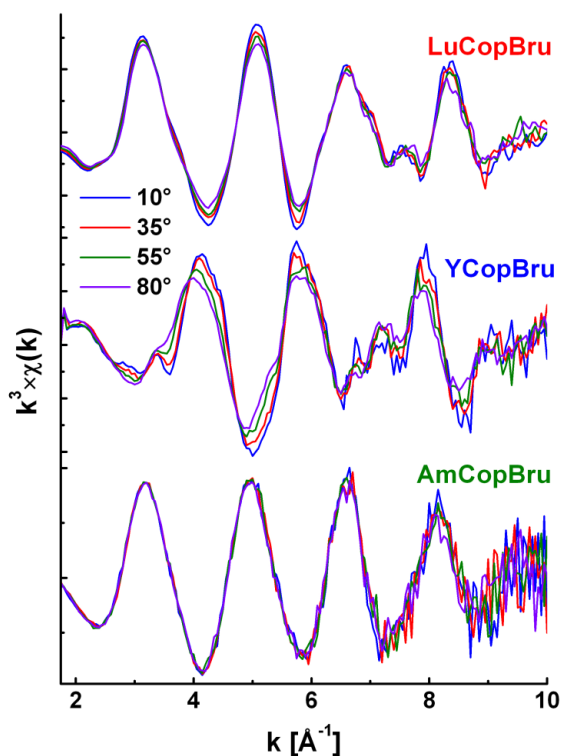


Fig. 2: pEXAFS spectra collected for LuCopBru, YCopBru and AmCopBru.

The data for LuCopBru were nicely fit considering a single O shell located at 2.26 Å and a next nearest Mg shell at 3.29 Å. The apparent coordination number for both shells decreased for increasing angle, hinting an in-plane orientation of the Mg shell. Brucite is made of Mg octahedra sharing edges ($d(\text{Mg}-\text{O}) = 2.10$ Å, $d(\text{O}-\text{O}) = 2.78$ Å, $d(\text{Mg}-\text{Mg}) = 3.14$ Å [6]). Considering edge sharing between Mg and Lu polyhedra, the distance from Lu to Mg can be considered as the sum of the distance from Mg and from Lu to the middle shared edge. The calculated bond length (3.35 Å) is very close to the experimental value. Furthermore, the experimental Lu–Mg bond length matches the sum of two neighboring Mg atoms and the difference in ionic radii ($3.14 + 0.14 = 3.28$ Å). Consequently, Lu very likely substitutes Mg at brucite octahedral site [5]. The data for YCopBru were fit considering two O shells (located at 2.24 and 2.40 Å) and two Mg shells (located at 3.29 and 3.50 Å). Considering that Y and Mg polyhedra share edges and both Y–O bond lengths, the calculated interatomic distances are 3.32 and 3.53 Å, matching the experimental values. Consequently, Y and Mg polyhedra very likely share edges. The shortest distance can be explained by Y substituting Mg at an octahedral site. For the longest, two hypotheses could possibly account for the results: Y is either surface bound to brucite and/or Y is located at an octahedral site and the Mg shell is pushed away, in-plane, from its regular position.

The data for AmCopBru showed almost no polarization dependence. Accordingly, the fit results displayed only a low angular dependence. The data were fit considering a single O shell at 2.43 Å and next nearest Mg shells at 3.22 and 3.44 Å. The longest bond length corresponds to the sum of $d(\text{Mg}-\text{Mg})$ in brucite and the difference in ionic radii: $3.14 + 0.26 = 3.40$ Å. Consequently, Y and Mg polyhedra may share edges. The shortest Y–Mg bond length may best be explained by face sharing between the polyhedra. In that case, the Am polyhedron must be oriented out-of-plane. In this configuration, the possible angular effect is weakened. Finally, the sum of the contributions due to Am located in several distinct environments seriously weakens the potential angular effect. The interpretation is difficult and the data do not allow locating exactly Am with respect to the brucite structure: Am could be incorporated in the structure and/or surface sorbed.

The results show that the smallest Lu and Y can be incorporated in brucite upon precipitation. In contrast, the data do not allow concluding about incorporation for Am. Consequently, the substitution is very likely governed by crystal chemistry. With regard to the disposal of nuclear waste, further investigations will enclose the stability of such samples.

REFERENCES

1. V. Metz et al., Geochemically derived non-gaseous radionuclide source term for the Asse salt mine – assessment for the use of a $\text{Mg}(\text{OH})_2$ -based backfill material. *Radiochim. Acta*, **92**, 819–825 (2004).
2. R.D. Shannon, Revised effective ionic radii and systematic studies of interatomic distances in halides and chalcogenides. *Acta Cryst. A*, **32**, 751–767 (1976).
3. A. Manceau et al., Polarized EXAFS, distance-valence least-square modeling (DVLS), and quantitative texture analysis approaches to the structural refinement of Garfield nontronite. *Phys. Chem. Minerals*, **25**, 347–365 (1998).
4. K. Dardenne et al., New developments at the INE-Beamline for actinide research at ANKA, *J. Phys.: Conf. Ser.*, **190**, 012037 (2009).
5. N. Finck et al., Sites of Lu(III) sorbed to and coprecipitated with hectorite. *Environ. Sci. Technol.*, **43**, 8807–8812 (2009).
6. M. Catti et al., Static compression and H disorder in brucite, $\text{Mg}(\text{OH})_2$, to 11 GPa: a powder neutron diffraction study. *Phys. Chem. Minerals*, **22**, 200–206 (1997).

Solubility and speciation of Np in dilute to concentrated CaCl₂ solutions under different redox conditionsD. Fellhauer^{1,2}, M. Altmaier³, V. Neck³, J. Runke^{2,3}, J. Lützenkirchen³, X. Gaona³, Th. Fanghänel^{1,2}¹ European Commission, JRC, Institute for Transuranium Elements, Karlsruhe, Germany
David.Fellhauer@ec.europa.eu² Heidelberg University, Institute of Physical Chemistry, Heidelberg, Germany³ Karlsruhe Institute of Technology, Institut für Nukleare Entsorgung, Karlsruhe, Germany**INTRODUCTION**

For reliable safety assessment of nuclear waste in a salt-based repository a thorough understanding of the aquatic chemistry and thermodynamics of actinides in concentrated chloride systems is required. In the case of water intrusion actinides might come in contact with CaCl₂ solutions. CaCl₂ brines can form due to corrosion processes of cementitious waste in concentrated MgCl₂ solutions, given that certain stoichiometric requirements are fulfilled.

Recent studies on the solubility of tri-, tetra- and hexavalent actinides in alkaline CaCl₂ solution revealed that Ca²⁺ strongly affects both aqueous speciation and solid phase composition of actinides (1-5). For An(IV) (An = Th, Np, Pu) and Cm(III) the formation of hitherto unknown ternary Ca-An-OH complexes was observed leading to an enhanced An solubility in alkaline CaCl₂ solutions. The impact of Ca²⁺ on the solid phase stoichiometry is obvious from investigations with U(VI) in 0.02 to 4.0 M CaCl₂ (5) where a transformation of the initial metaschoepite phase (UO₃·2H₂O(cr)) into calcium diuranate (CaU₂O₇·3H₂O(cr)) were described for pH_c > 8. The solubility of the ternary Ca containing phase is orders of magnitude lower compared to the Ca-free binary phase under the same alkaline geochemical conditions.

In this contribution, the results of our recent investigations of the aqueous speciation and solubility behaviour of Np(IV)- and Np(V)-hydroxide phases in alkaline CaCl₂ solution are discussed.

DESCRIPTION OF THE WORK

Experiments were conducted at room temperature (22 ± 2°C) under Ar atmosphere. Appropriate amounts of corresponding Np(IV) or Np(V) hydroxide phases (1 – 5 mg Np^{IV}O₂(am,hyd) or Ca_{0.5}Np^VO₂(OH)₂·1.3H₂O(s) or CaNp^VO₂(OH)_{2.6}Cl_{0.4}(s)·2.2H₂O(s)) were suspended in 10 – 30 ml 0.25 to 4.5 M CaCl₂ solution and investigated as independent batch samples. For the Np(IV) experiments, reducing conditions were adjusted by additions of 10⁻³ M Na₂S₂O₄ or ca. 30 mg Fe powder. The aqueous phase of the samples were analysed for pH_c (= -log [H⁺]), redox potential E_h (combination electrodes) and Np concentration (LSC after 10kD ultrafiltration) as function of time. Aqueous Np(V) speciation was determined by UV-Vis-NIR, XANES and EXAFS). Solid phases were characterized by different methods e.g. XRD, quantitative chemical analysis, DTA, XANES, EXAFS and SEM-EDS.

Experimental solubility data were evaluated by the specific ion interaction theory (SIT) or Pitzer approach.

RESULTS

a) Np(IV): The experimental solubility data of NpO₂(am,hyd) in alkaline 0.25 to 4.5 M CaCl₂ solutions are displayed in figure 1. In 0.25 and 1.0 M CaCl₂ the Np(IV) concentrations measured after ultrafiltration were at or below the detection limit (log [Np(IV)] = -8.3) – similar to literature data for Np(IV) obtained in NaCl and NaClO₄ media.

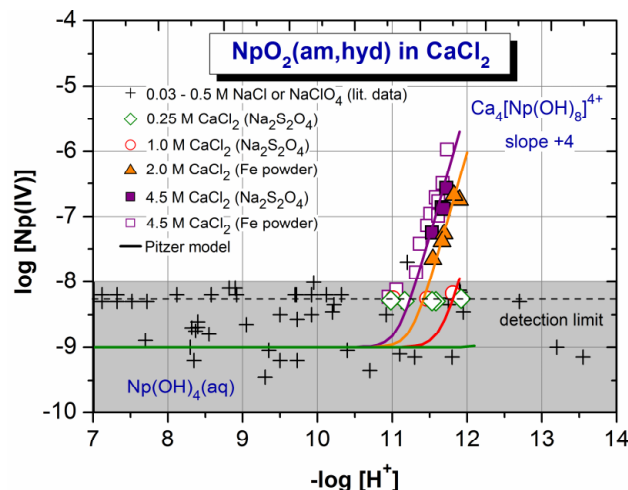
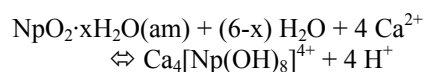


Fig. 1: Experimental solubility and Pitzer model for NpO₂(am,hyd) in alkaline 0.25 to 4.5 M CaCl₂ solutions.

In 2.0 and 4.5 M CaCl₂ and for pH_c = 11 - 12, however, a steep increase of the solubility is observed with a maximum value of 10⁻⁶ M (in 4.5 M CaCl₂ at pH_c = 11.8); the solubility curve shows a defined dependence on Ca²⁺ concentration and pH_c (slope +4 for log [Np(IV)] vs. pH_c). The same behaviour was observed previously (1) for ThO₂(am,hyd) in CaCl₂ solution in analogous experiments where the predominant aqueous species for pH_c > 11 could be identified by EXAFS as ternary complex Ca₄[Th(OH)₈]⁴⁺ (2). We therefore assume that for Np(IV) the analogue ternary Np(IV) complex (Ca₄[Np(OH)₈]⁴⁺) is responsible for the enhanced solubility observed in alkaline CaCl₂ solution:



The equilibrium constants for Np(IV) were evaluated by both the SIT and Pitzer models. Systematic trends in the complex formation constants log *β° (which is defined

by the equilibrium $4 \text{Ca}^{2+} + \text{An}^{4+} + 8 \text{H}_2\text{O} \Leftrightarrow 4 \text{H}^+ + \text{Ca}_4[\text{An}(\text{OH})_8]^{4+}$ for An = Th(IV), Np(IV) and Pu(IV) allow the estimation of the complex formation constant for U(IV) from the correlation with the ionic radii $r_{\text{An}^{4+}}$.

b) Np(V): For the Np(V) experiments, about 250 mg of freshly precipitated greenish $\text{NpO}_2\text{OH}(\text{am})$ were equilibrated in 2.0 M CaCl_2 at $\text{pH}_c = 11.6$. After 5 month, the initial solid phase had transformed into a greyish solid. The transformation product was carefully analyzed, its stoichiometry is $\text{CaNpO}_2(\text{OH})_{2.6}\text{Cl}_{0.4}(\text{s}) \cdot 2.2\text{H}_2\text{O}(\text{s})$. Equilibration of the grey material under less alkaline conditions (0.25 – 2 M CaCl_2 , pH_c 8 – 10) leads to a fast transformation into a reddish solid phase with a chemical formula of $\text{Ca}_{0.5}\text{NpO}_2(\text{OH})_2 \cdot 1.3\text{H}_2\text{O}(\text{s})$.

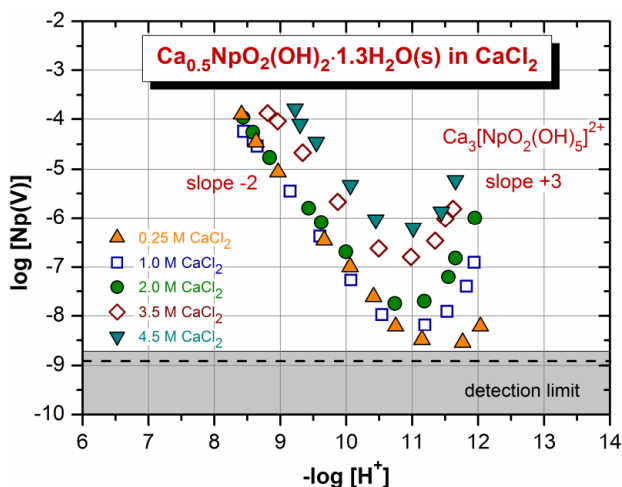
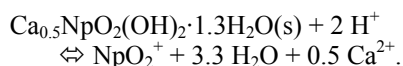


Fig. 2: Experimental solubility data for the reddish solid phase $\text{Ca}_{0.5}\text{Np}^{\text{V}}\text{O}_2(\text{OH})_2 \cdot 1.3\text{H}_2\text{O}(\text{s})$ in alkaline 0.25-4.5 M CaCl_2 solutions.

The solubility of both ternary Ca-Np(V)-OH phases was studied in 0.25 – 4.5 M CaCl_2 at pH_c 8 – 12. Under the same conditions, the solubility of the reddish solid is lower in all cases indicating that the grey phase is only meta-stable. The results obtained for the (more) stable reddish solid phase are discussed in the following.

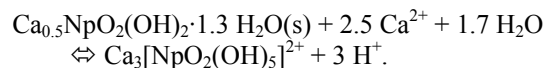
The solubility data for $\text{Ca}_{0.5}\text{NpO}_2(\text{OH})_2 \cdot 1.3\text{H}_2\text{O}(\text{s})$ are displayed in figure 2. Between $\text{pH}_c = 8$ and 10 a systematic decrease of the Np(V) concentration with a slope of -2 is observed as expected for the equilibrium



The predominance of the NpO_2^+ ion in this pH_c range was confirmed by UV-Vis-NIR spectroscopy up to 2.0 M CaCl_2 (the NpO_2^+ cation has a characteristic NIR band at 980.2 nm). In 3.5 and 4.5 M CaCl_2 , a shift of the NIR-band to higher values (983 nm in 3.5 M and 985 nm in 4.5 M CaCl_2) is observed. This indicates that the predominant Np(V) species for highly concentrated CaCl_2 solutions at this pH must rather be formulated as (inner-sphere) $\text{NpO}_2^+ \cdot \text{Cl}^-$ or even ternary Ca-NpO₂⁺-Cl⁻ complex (EXAFS of an aqueous sample containing 5 mM Np(V) in 4.5 M CaCl_2 / pH_c 3 confirms the

presence of a Cl and Ca shell at 1.8 Å and 3.5 Å, respectively).

For $[\text{CaCl}_2] \geq 1.0 \text{ M}$ and $\text{pH}_c > 11$, the solubility clearly increases with well-defined slope +3 pointing to the formation of a ternary Ca-Np(V)-OH complex with five hydroxo ligands. Based on the results from thermodynamic SIT evaluation, the corresponding equilibrium is best described by assuming three Ca^{2+} ions for the ternary complex:



The formation of a ternary Ca-Np(V)-OH complex in alkaline CaCl_2 solution was confirmed by EXAFS.

REFERENCES

1. M. ALTMAIER et al., "Solubility of Zr(IV), Th(IV) and Pu(IV) hydrous oxides in CaCl_2 solutions and the formation of ternary Ca-M(IV)-OH complexes" *Radiochim. Acta*, **96**, 541-550 (2008).
2. B. BRENDENBACH et al., "EXAFS Study of Aqueous Zr^{IV} and Th^{IV} Complexes in Alkaline CaCl_2 Solutions: $\text{Ca}_3[\text{Zr}(\text{OH})_6]^{4+}$ and $\text{Ca}_4[\text{Th}(\text{OH})_8]^{4+}$ " *Inorg. Chem.*, **46**, 6804-6810 (2007).
3. T. RABUNG et al., "A TRLFS study of Cm(III) hydroxide complexes in alkaline CaCl_2 solutions" *Radiochim. Acta*, **96**, 551-559 (2008).
4. D. FELLHAUER et al., "Solubility of tetravalent actinides in alkaline CaCl_2 solutions and formation of $\text{Ca}_4[\text{An}(\text{OH})_8]^{4+}$ complexes: A study of Np(IV) and Pu(IV) under reducing conditions and the systematic trend in the An(IV) series" *Radiochim. Acta*, **98**, 541-548 (2010).
5. M. ALTMAIER et al., "Solubility of U(VI) and formation of $\text{CaU}_2\text{O}_7 \cdot 3\text{H}_2\text{O}(\text{cr})$ in alkaline CaCl_2 solutions", Migration 2005, book of abstracts.

Interactions of U(VI) with cement alteration products at high ionic strength

V. Metz¹, C. Bube¹, D. Schild¹, M. Lagos¹, E. Bohnert¹, K. Garbev²,
M. Altmaier¹ and B. Kienzler¹

Karlsruhe Institute of Technology (KIT), ¹Institut für Nukleare Entsorgung (INE) and ²Institut für Technische Chemie (ITC-TAB), P.O. Box 3640, D-76021 Karlsruhe, Germany
email: volker.metz@kit.edu

INTRODUCTION

Retention of actinides in the near field is crucial for the safety of long-term disposal of radioactive waste in deep geological formations. Ordinary Portland cement (OPC) is used as matrix material for solidification of low / intermediate active waste. In order to study the near-field processes relevant to a low/intermediate level waste (L/ILW) repository in rock salt, experiments are conducted with simulated full-scale cemented waste products and laboratory scale samples. The evolution of the measured concentration of major solution components, dissolved uranium and the secondary solid phases, are compared to geochemical equilibrium calculations.

MATERIALS AND METHODS

On the laboratory-scale, systems with different ratios of cement to MgCl₂-rich brine are studied to gain understanding of the corrosion progress ($0.01 \leq m/V \leq 1.0$ kg cement (L solution)⁻¹). Static full-scale experiments are conducted with 336 kg of cemented waste form simulates doped with 1020 g U_{nat}. The U-doped OPC monoliths #33 and #34 were exposed to 135 liters of MgCl₂-rich brine. Details on the initial compositions of the LLW simulates and the sampling are given by Kienzler et al. (2000). Thermodynamic equilibrium calculations were done with “The Geochemist’s workbench” (GWB) software package (Bethke and Yeakel, 2009) using the Pitzer approach (Pitzer, 1973) to calculate activities of aqueous species in the highly saline solutions. The thermodynamic database was based on data of Harvie et al. (1984), which has been extended for Si (Reardon, 1992) and Al aqueous species (Hummel et al., 2002) and Pitzer parameters reported by Reardon (1988; 1990). Thermodynamic data for Uranium species and solid phases was taken from the current KIT-INE database.

RESULTS AND DISCUSSION

The results of the thermodynamic simulations are in good agreement with the measured concentrations of major solution components and the pH in equilibrated laboratory scale and full-scale experiments. In the laboratory experiments with a low amount of cement compared to the available solution ($m/V < 0.2$), pH_m (i.e. $-\log m_{H^+}$) is found to be in the range of ~8.5-9. This corresponds to the calculated pH_m, which is controlled by the formation of Mg-oxychloride (Fig. 1). The

results are found to be in agreement with those of the full-scale experiments of a low water (W) to cement (C) ratio ($W/C < 0.4$) and/or within the first years of the experiments. In the systems with a higher ratio of cement to brine, Mg in the solutions is observed to be significantly exchanged against Ca from the solid phase. The reactions lead to an increase in the measured pH_m to values between 11 and 12 at ratios of $m/V > 0.5$ kg cement (kg H₂O)⁻¹. These high pH_m values correspond to the results of the full-scale experiments after ~15 years for simulated cement monoliths having $W/C > 0.4$.

The observed changes in solution composition from a near neutral MgCl₂- to an alkaline CaCl₂-dominated solution strongly affect the U(VI) concentration. In the case of samples #33 and #34, after 4-5 years, U concentration was ~10⁻⁷ molal, followed by a decrease to concentrations in the range of 2·10⁻⁹ - 2·10⁻⁸ molal after 8 years. The increase in pH_{exp} after 8 to 13.6 years is accompanied by increasing U concentrations.

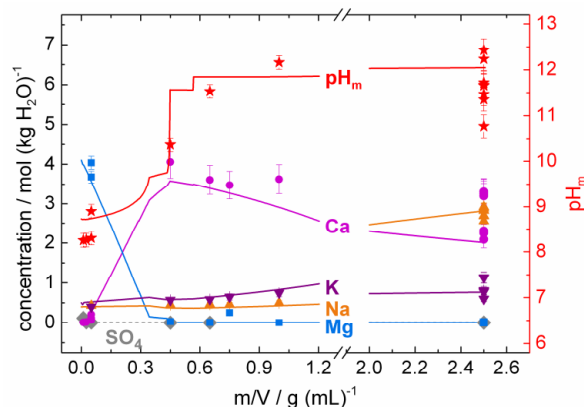


Fig. 1: Cement corrosion in MgCl₂-rich brine; symbols denote experimental data points, lines denote calculated concentrations and pH_m values.

Considering the high inventory of uranium in the waste product, the low concentrations in the aqueous phase indicate that the uranium concentration is controlled by solubility phenomena. Taking into account the evolution of the solution composition in the full-scale experiments, U solubilities were calculated with respect to relevant U(VI) phases. Since measured Si concentrations were below the detection limit (i.e. 1·10⁻³ molal), U concentration in equilibrium with uranophane could be calculated only for the minimum and maximum expected Si concentrations of the last sampling, i.e. 5·10⁻⁶, to 1·10⁻³ molal. For Si concentrations between 5·10⁻⁶ and ~10⁻⁴ molal,

measured U concentrations are in agreement with the calculated concentrations for uranophane as solubility-limiting phase. Within error, calculated U concentrations using Ca-diuranate and Na-diuranate as solubility-controlling phases were in agreement with the experimental results over the full pH range (Fig. 2).

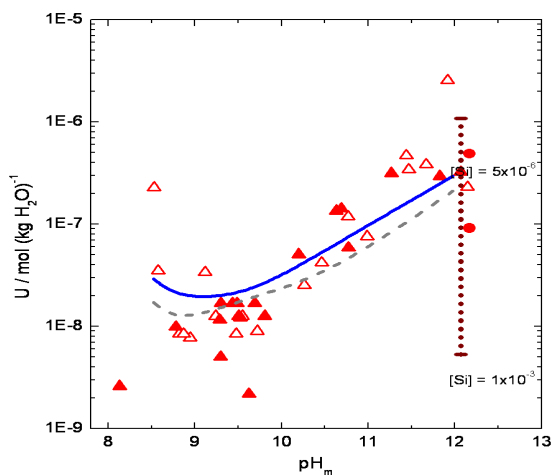


Fig. 2: Concentrations of dissolved U as function of pH_m measured over 4 to 21.4 years in full-scale experiments (#33 and #34). Triangles denote experimental data; lines depict thermodynamic solubility calculations for equilibrium with Ca-diuranate (solid line), Na-diuranate (dashed line), uranophane (vertical dotted line).

Kienzler et al. (2010) conclude from XANES, TRIFS and XRD measurements that a crystalline uranophane-like phase is present in the altered monolith #33, possibly in addition to other U(VI)-bearing phases. They mention that precipitation of diuranates would be expected under the highly alkaline conditions of the cementation process. As a continuation of their work, additional methods are used in this study to further identify U-bearing solid phases in the corroded monolith.

Using Raman spectrometry, the molecular structures of amorphous U rich aggregates with a size of 20 μm or larger were analyzed in solid samples drilled from the corroded cement monolith #33. Spectra of the studied aggregates resembled considerably. The spectra of the aggregates were compared to Raman spectra of U(VI) minerals obtained from the RRUFF database (<http://rruff.info/>) and from powder samples of uranophane, Ca-diuranate and Na-diuranate. Spectra of the U rich phases were in good agreement with the spectrum of Ca-diuranate and showed distinct similarities with that of Na-diuranate (Bube et al., 2011). Raman spectra of the U rich aggregates differed considerably from those of other U(VI) oxyhydroxides, hydroxides, silicates and carbonates, in particular those of schoepite, soddyite and uranophane.

Thermodynamic calculations support that U concentrations in equilibrium with diuranates as well as

uranophane are in the range of the measured concentrations. Yet, aqueous U concentration in equilibrium with uranophane as the solubility-limiting phase cannot be confirmed unambiguously because measured aqueous Si concentrations are below the detection limit. The conclusion of Kienzler et al. (2010) regarding a coexistence of two (or more) U(VI) phases in the corroded monoliths is in agreement with the results of the present study. Heterogeneous U distribution in the altered monolith #33 and results of Kienzler et al. (2010) lead to the assumption that dissolved U achieves local equilibria with amorphous diuranate-like and/or crystalline uranophane-like phases at different positions within μ -scale heterogeneities of the cemented waste simulate.

ACKNOWLEDGMENTS

The research leading to these results has been financially supported in part from the German Federal Office for Radiation Protection (BfS) within the projects “Analyse der Eigenschaften von simulierten, zementierten 1:1 Gebinden und ihres Phasenbestandes nach 20 Jahren Auslaugung in Salzlösungen” and “Studie zur Abschätzung der standortspezifischen Pu- und Am-Rückhaltung (SchachanlageASSE II)”.

REFERENCES

- BETHKE, C.M. and Yeakel, S. 2009 The Geochemist's Workbench. University of Illinois, Urbana, USA.
- BUBE, C., Metz, V., Schild, D., Lagos, M., Bohnert, E., Garbev, K., Altmaier, M., Kienzler, B. (2011) Interactions of U(VI) with cement alteration products in highly saline solutions. 1st International Symposium on Cement-based Materials for Nuclear Waste, NUWCEM 2011, October 2011, Avignon, France.
- HARVIE, C.E., Møller, N. and Weare, J.H. (1984) *Geochimica et Cosmochimica Acta* 48, 723-751.
- HUMMEL, W., Berner, U. and Curti, E. 2002 Nagra/PSI chemical thermodynamic data base 01/01. Universal Publishers, Parkland, Florida, USA.
- KIENZLER, B., Metz, V., Brendebach, B., Finck, N., Plaschke, M., Rabung, T., and Schild, D. (2010) *Radiochimica Acta* 98, 675-684.
- KIENZLER, B., Vejmelka, P., Herbert, H.J., Meyer, H. and Althenhein-Haese, C. (2000) *Nuclear Technology* 129, 101-118.
- PITZER, K.S. (1973) *Journal of Physical Chemistry* 77, 268-277.
- REARDON, E.J. (1988) *Journal of Physical Chemistry* 92, 6426-6431.
- REARDON, E.J. (1990) *Cement and Concrete Research* 20, 175-192.
- REARDON, E.J. (1992) *Waste Management* 12, 221-239.

Trivalent Metal Ion Sorption under Saline Conditions

Th. Rabung¹, A. Schnurr¹, V. Petrov², J. Lützenkirchen¹, H. Geckeis¹

¹ *Institut für Nukleare Entsorgung, Karlsruhe Institute of Technology, Hermann-von-Helmholtz-Platz 1, 76344 Eggenstein-Leopoldshafen, Germany
email: thomas.rabung@kit.edu*

² *Lomonosov Moscow State University, Leninskie Gory Main Building, 119992 Moscow, Russia*

INTRODUCTION

Sorption processes on mineral surfaces play an important role in the retardation behaviour of radionuclides and have to be considered in performance assessment calculations. In the past, a huge number of experimental studies have been performed to quantify and to understand sorption processes and to describe them with surface complexation models. However, almost all experimental data are restricted to low ionic strength conditions and a large gap exists for experimental data at ionic strength > 1 M. Saline conditions are not restricted to solutions relevant to rock salt formations as e.g. in the Waste Isolation Pilot Plant (WIPP) in the USA and the Gorleben, Morsleben and Asse sites in Germany. Elevated salt concentrations up to 6.5 M are also found in sedimentary rocks which are currently under investigation within nuclear waste disposal programs [1, 2]. At present it is completely unclear, whether existing sorption data and sorption model approaches can be applied to saline conditions.

DESCRIPTION OF THE WORK

In the present work, experiments have been performed with quartz as a model mineral phase and illite (illite de Puy) and Na-montmorillonite (Na-SWy-2) as representative clay minerals. In all cases sorption of Eu(III) radiolabelled with ¹⁵²Eu was studied in batch experiments, where ionic strength was varied up to 5 M NaCl. Solid/liquid ratios were 10 g/l in case of experiments with quartz and 2 g/L in case of clay minerals. Metal ion concentrations were at $1-2 \times 10^{-7}$ M. Experiments with Cm(III) and the time resolved laser fluorescence spectroscopy (TRLFS) are directed to obtain detailed information on the metal ion speciation at the mineral surfaces as a function of ionic strength.

RESULTS

In all systems we observed a clear shift of the sorption edges to higher pHc ($\text{pHc} = -\log[\text{H}^+]$) and in general a decreasing sorption with increasing ionic strength (Fig.1). The degree of sorption is clearly stronger for the clay minerals and notably for Na-montmorillonite. While for quartz only inner-sphere surface complexation is expected for Eu(III), outer sphere sorption at low pH must be considered for clay minerals. Competition of Na(I) with Eu(III) for the

cation exchange sites is responsible for the strong sorption decrease with increasing ionic strength conditions. At higher NaCl concentrations a similar decreasing trend for the Eu(III) sorption is found as for quartz.

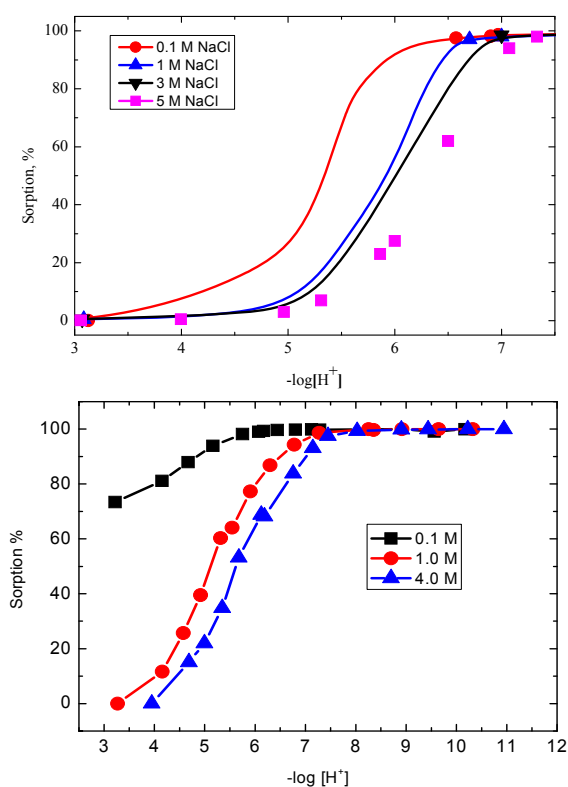


Fig. 1: Eu(III) sorption onto quartz (above) and onto Na-montmorillonite (down) at different ionic strengths.

Eu(III) sorption to clay minerals under variable ionic strength conditions was calculated by taking a well established non-electrostatic sorption model, but developed and tested so far only for lower ionic strength conditions (2SPNE/CE, Bradbury and Baeyens [3]). The Pitzer formalism was used to calculate activity coefficients for aqueous species. We assumed in our calculations that the nature of the Eu(III) surface species does not vary at different ionic strength conditions. Furthermore, the applied model does not consider the formation of Na^+ inner-sphere surface complexes, and no electrostatic correction term is included for surface species. Model calculations for different ionic strengths yield fair agreement with the experimental data and reproduce the observed trend. This finding suggests that

the shift in sorption edges with increasing ionic strength is basically due to a variation of ion activities and a concomitant change in aqueous metal ion speciation.

TRLFS experiments with Cm(III) indicate no significant differences for sorbed inner-sphere Cm(III) complexes at low and high ionic strength conditions. Emission peak positions and lifetimes are quite comparable. This spectroscopic finding confirms model assumptions mentioned above. Our preliminary study indicates that the non-electrostatic 2SPNE/CE model can be applied to predict sorption of trivalent actinide ions also for elevated ionic strength conditions at least in NaCl dominated solutions. More detailed TRLFS measurements are planned and experiments will be extended to MgCl₂ and CaCl₂ rich brines to study their influence on metal ion sorption.

ACKNOWLEDGEMENT

We are grateful to M. Marques from the Labor für Entsorgung (LES) of the Paul-Scherrer-Institute (PSI), Switzerland for providing the purified illite de Puy and Na-SWy-2.

REFERENCES

1. Laboratory for Waste Management, Nuclear Energy and Safety Research Department, Paul Scherrer Institute (PSI), Progress Report 2010.
2. Vilks, P., "Sorption in saline waters – State-of-Science Review", Nuclear Waste Management Organization, Toronto, Ontario, Technical Report NWMO TR-2009-18 (2009).
3. Bradbury, M.H., Baeyens, B., "Sorption modelling in illite Part I: Titration measurements and the sorption of Ni, Co, Eu and Sn", *Geochim. Cosmochim. Acta*, 73, 990-1003 (2009).

Actinides Complexation by Organic Ligands as a function of temperature and high ionic strength

P. Thakur and G.P. Mulholland

*Carlsbad Environmental Monitoring & Research Center,
1400 University Drive, Carlsbad, New Mexico 88220
email: pthakur@cemrc.org*

INTRODUCTION

The Waste Isolation Pilot Plant (WIPP) located in the remote Chihuahuan desert of southeastern New Mexico near Carlsbad is a transuranic (TRU) waste repository operated by the U.S. Department of Energy (DOE). The repository is currently storing defense-related TRU wastes in the Salado Formation, a bedded salt formation approximately 655 m (2150 ft.) below the surface of the Earth. The safe management and disposal of nuclear wastes have stimulated significant interest in the study of coordination chemistry of actinides with organic ligands that are expected in the WIPP wastes. Some of the organic ligands contained in nuclear wastes have a strong binding ability for actinides and their presence could result in significant increase in the solubility of actinides in brine and, hence their migration from a repository to the environment. Therefore detailed understanding of their thermodynamics is important for the long-term performance assessment of the repository. Unfortunately, much of the currently available data on complexation between these ligands and actinides were obtained at $I < 1.0$ M and it is difficult to extrapolate such data to the high ionic strengths typical of the wastes. In addition of providing stability constant values of actinides with these ligands over a range of ionic strengths, the data obtained from the experimental work will be used to calculate the Pitzer parameters to evaluate activity coefficients for the actinide interactions with other components of the brine. Once complete, the results of this study will provide an improved model for the solution thermodynamics in the WIPP repository and could be useful in the high level waste.

DESCRIPTION OF THE WORK

This study reports the stability constants and the thermodynamic parameters of the trivalent actinides (Am^{3+} , Cm^{3+} and Eu^{3+}) as a function of temperature and high ionic strength with selected organic (EDTA, oxalate, citrate). These ligands are part of the TRU waste, which are being emplaced in the WIPP (Waste Isolation Pilot Plant). In this study, a solvent extraction method at tracer level was used to measure the stability constants with these organic ligands as a function of ionic strength. The complexation thermodynamics were determined by the temperature dependence of the stability constants at $I = 6.60$ m NaClO_4 .

RESULTS

EDTA forms only 1:1 complex with these actinides while Cit and Ox form both 1:1 and 1:2 complexes. The increase in temperature greatly enhances the formation of these complexes. The complexation enthalpy is endothermic at $I = 6.60$ m NaClO_4 , in contrast to the exothermic enthalpy values usually observed for these complexes at lower ionic strength. The stability constant values of Am^{3+} , Cm^{3+} and Eu^{3+} with Ox at different temperature are listed in Table 1 and thermodynamic parameters for the formation of $\text{M}(\text{Ox})^+$ and $\text{M}(\text{Ox})_2^-$ in 6.0 m (NaClO_4) are listed in Table 2 along with the thermodynamic data of the analogous dicarboxylic ligands.

REFERENCES

1. CHOPPIN, G.R. et al., Correlation between Ligand Coordination Number and the Shift of the ${}^7\text{F}_0 - {}^5\text{D}_0$ Transition Frequency in Europium (III) Complex, *Inorg. Chem.*, **36**, 249 (1997).
2. KIMURA, T. et al., Luminescence study on determination of the hydration number of $\text{Cm}(\text{III})$, *J. Alloys & Compd.*, **213/214**, 313-317 (1994).

Table 1. Stability constants of Am³⁺, Cm³⁺ and Eu³⁺ with Ox (log β₁₀₁) and (log β₁₀₂) at I = 6.60m (NaClO₄), T= 0-60°C.

<i>Am-Ox</i>	<i>0°C</i>	<i>25°C</i>	<i>45°C</i>	<i>60°C</i>
log β ₁₀₁	5.18±0.08	5.37±0.09	5.65±0.08	5.85±0.09
log β ₁₀₂	8.52±0.08	9.04±0.09	9.21±0.11	9.41±0.11
Cm-Ox				
log β ₁₀₁	5.09±0.08	5.34±0.08	5.58±0.09	5.82±0.10
log β ₁₀₂	8.49±0.09	8.61±0.08	8.98±0.10	9.44±0.10
Eu-Ox				
log β ₁₀₁	4.72±0.07	5.03±0.08	5.33±0.09	5.49±0.08
log β ₁₀₂	8.54±0.01	8.93±0.09	9.30±0.11	9.50±0.11

Table 2. Thermodynamics of complexation of Am³⁺, Cm³⁺ and Eu³⁺ with aliphatic dicarboxylate ligands at 25°C.

	I, m (NaClO ₄)	ΔG ₁₀₁ kJ·mol ⁻¹	ΔH ₁₀₁ kJ·mol ⁻¹	ΔS ₁₀₁ J·K ⁻¹ ·mol ⁻¹
Am-oxalate	6.60	-30.53±0.60	19.3±4.7	167±12
Cm-oxalate	6.60	-30.36±0.58	20.6±3.5	171±14
Eu-oxalate	6.60	-28.60±0.52	22.5±4.5	171±11
Eu-oxalate	1.0	-30.30±0.17	13.6±2.5	147±8.0
Eu-malonate	1.0	-26.36±0.06	13.5±0.09	134±1.2
Eu-succinate	1.0	-20.20±0.15	12.2±0.15	109±1.2
Eu-glutarate	1.0	-18.40±0.15	13.5±0.09	107±1.2
Eu-adipate	1.0	-17.50±0.15	10.5±0.15	94±1.2

Table 3. Stability constants of Am³⁺, Cm³⁺ and Eu³⁺ -EDTA complexation in NaClO₄ media at 25°C.

I, m, NaClO ₄	Am ³⁺	Cm ³⁺	Eu ³⁺
0.10	17.45±0.11	17.09±0.12	17.35±0.13
0.30	16.78±0.12	16.62±0.12	16.73±0.12
0.51	16.34±0.13	16.54±0.13	16.68±0.12
1.03	15.89±0.12	15.67±0.12	15.78±0.13
2.18	14.12±0.12	14.34±0.11	14.52±0.12
3.44	13.89±0.13	13.90±0.12	14.04±0.11
4.92	14.45±0.13	14.54±0.13	14.61±0.12
6.60	15.88±0.12	16.06±0.12	15.76±0.12

Complexation of Nd(III)/Cm(III) and Np(IV) with Gluconate in dilute to concentrated alkaline NaCl and CaCl₂ solutions

H. Rojo¹, X. Gaona², Th. Rabung², M. Garcia¹, T. Missana¹, M. Altmaier²

¹CIEMAT, Research Centre for Energy, Environment and Technology, Madrid, Spain
email: mdelhenar.rojo@ciemat.es

²Institut für Nukleare Entsorgung, Karlsruhe Institute of Technology (KIT-INE), Karlsruhe, Germany

INTRODUCTION

Radionuclide sorption and solubility in cementitious and saline systems can be affected by the presence of organic ligands. Gluconic acid (GLU) is a poly-hydroxycarboxylic acid expected in repositories for low and intermediate-level radioactive waste (LILW) as component of cementitious materials. The formation of very stable An(III/IV)–GLU complexes has been reported in the literature [1–3]. In the case of An(IV), the stability of these complexes can be further increased in the presence of Ca²⁺, where ternary Ca–An(IV)–GLU have been reported to form in the case of Th. To the date, all studies available in the literature have focussed on low ionic strengths and low Ca²⁺ concentrations. In CaCl₂–rich brines, the formation of highly stable Ca–GLU complexes may outcompete with Ca–An(III/IV)–GLU complexes.

This study aims at assessing the solubility and aqueous speciation of Nd(III)/Cm(III) and Np(IV) in the presence of GLU and dilute to concentrated NaCl and CaCl₂ solutions, with the final goal of building up comprehensive thermodynamic and activity models for Na/Ca–Nd(III)/Cm(III)–GLU and Ca–Np(IV)–GLU under alkaline conditions. This research should provide a sound basis to interpret An(III/IV) behaviour in cementitious and saline–cementitious systems in presence of GLU.

DESCRIPTION OF THE WORK

All experiments were carried out in Ar-gloveboxes. Solubility experiments of Nd(III) were conducted with Nd(OH)₃(am) as solid phase. Samples were prepared with NaCl (0.1 M and 5.0 M) and CaCl₂ (0.25 M and 3.5 M) as background electrolytes. Gluconate concentration ranged between 10⁻⁶ M and 10⁻² M. Parallel experimental series were prepared at constant $-\log[H^+]$ (~12) and varying [GLU], and constant [GLU] (10⁻³ M) and varying $-\log[H^+]$. Solid phases were characterized by XRD before and after equilibration with GLU solutions to assess the possible formation of new Nd–GLU and/or Ca–GLU phases. TOC analyses were conducted over a set of representative samples in NaCl and CaCl₂ solutions to quantify the total concentration of GLU in solution and therefore assess the possible loss of material through sorption or precipitation processes.

TRLFS measurements were performed with ~10⁻⁷ Cm(III) per sample, with 0.1 M ≤ [NaCl] ≤ 2.5 M or

0.1 M ≤ [CaCl₂] ≤ 3.5 M as background electrolytes. In the systems with NaCl as background electrolyte, two different concentration levels of Ca²⁺ were considered: 10⁻² M and 10⁻³ M. The initial concentration of GLU in all samples (10⁻⁶ M) was increased to 3×10⁻³ M by step-wise additions. After each GLU addition, samples were equilibrated for 1 day before TRLFS measurement. The sorption of the Cm–complexes on the cuvette surface was tested for t ≤ 5 days.

Np(IV) was obtained by chemical reduction of a Np(V) stock solution with Na₂S₂O₄ 0.05 M at pH = 8. The resulting solution was brought to pH = 12, where a quantitative precipitation of NpO₂(am,hyd) was achieved within 2 days. The resulting solid phase was divided in different series with 0.1 M ≤ [CaCl₂] ≤ 3.5 M as background electrolyte. GLU concentration ranged between 10⁻⁶ M and 10⁻² M. LSC analysis of the samples was carried out after the 10 kD ultrafiltration of the aqueous phase.

RESULTS

Nd(OH)₃(am) solubility in NaCl/CaCl₂ solutions and presence of GLU

The solubility of Nd(OH)₃(am) remained unaffected by GLU in NaCl solutions 0.1 M and 5.0 M. XRD and TOC analyses confirmed that no new solid phases (Nd–GLU or Ca–GLU) were forming and that all GLU remained in solution in the conditions of the experiment. On the other hand, solubility of Nd(OH)₃(am) in 0.25 M CaCl₂ solutions was clearly increased by GLU under hyperalkaline conditions (Fig. 1). The species forming are pH-dependent (figure not shown), and unequivocally involve the participation of Ca²⁺. In contrast to observations at low CaCl₂ concentrations, solubility experiments with 3.5 M CaCl₂ as background electrolyte showed no significant effect of GLU for concentrations ≤ 10⁻³M. Under analogous experimental conditions but absence of GLU, the formation of very stable Ca–Nd(III)–GLU complexes have been reported in the literature [4–5]. These species are likely able to outcompete the formation of complexes of Nd(III) with GLU.

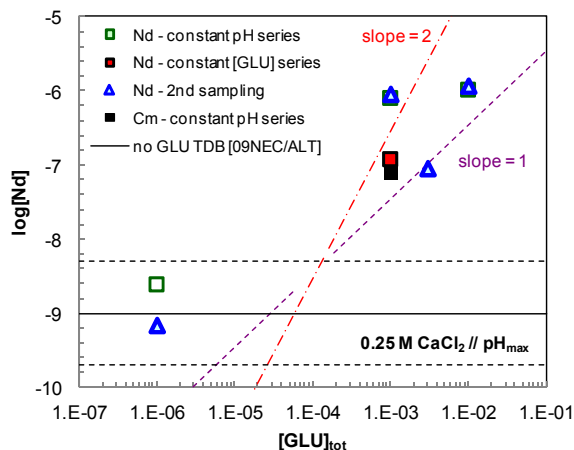


Fig. 1: Solubility of $\text{Nd}(\text{OH})_3(\text{am})$ and $\text{Cm}(\text{OH})_3(\text{am})$ in 0.25 M CaCl_2 as background electrolyte under increasing $[\text{GLU}]$. The pH of the solution was fixed in all cases at $\text{pH}_{\text{max}} \sim 12$.

TRLFS of Cm(III) in NaCl/CaCl₂ solutions and presence of GLU

Preliminary results of TRLFS experiments indicate the formation of 2–3 species in NaCl systems and $10^{-3} \text{ M} \leq [\text{Ca}] \leq 10^{-2} \text{ M}$. The comparison of experimental series under same experimental conditions but different $[\text{Ca}^{2+}]$ confirms the key role of Ca^{2+} in the process of Cm–GLU complex formation, with the likely formation of a complex with Ca:GLU 1:1.

Two to three Ca–Cm–GLU species were identified in 0.1 M and 0.25 M CaCl_2 solutions. The effect of GLU was significantly decreased in 1.0 M and 3.5 M CaCl_2 solutions, where the formation of Ca–Cm–GLU species was only observed at significantly higher GLU concentrations. Further data analysis of all spectra is on-going to properly identify the complexes forming and accordingly propose a speciation scheme in agreement with Nd(III) solubility data.

NpO₂(am,hyd) solubility in CaCl₂ solutions and presence of GLU

Fig. 2 shows that GLU has a significant effect on $\text{NpO}_2(\text{am,hyd})$ solubility in CaCl_2 solutions. The increase in the solubility is stronger at higher concentrations of Ca^{2+} , very likely because of the formation of ternary complexes analogous to those described in the literature for Th(IV) ($\text{CaAn}(\text{IV})(\text{OH})_4\text{GLU}_2(\text{aq})$) [1].

The system seems to reach a saturation level at $[\text{Np}] \sim 10^{-5.5}$, independently of $[\text{CaCl}_2]$. This observation could be explained by the formation of a $\text{Np}(\text{IV})\text{--GLU}$; this hypothesis is to be confirmed by further characterization of the solid phase by XRD, SEM–EDS and XANES/EXAFS techniques.

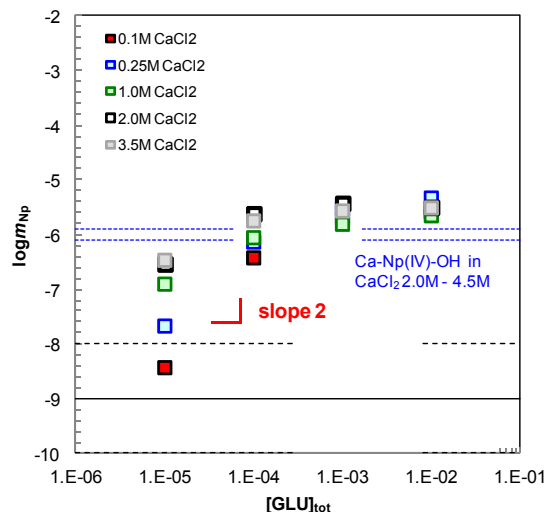


Fig. 2: Solubility of $\text{NpO}_2(\text{am,hyd})$ in $0.1 \text{ M} \leq [\text{CaCl}_2] \leq 3.5 \text{ M}$ and increasing $[\text{GLU}]$. The pH of the solution was fixed in all cases at $\text{pH}_{\text{max}} \sim 12$. Dashed lines in blue corresponding to $[\text{Np}]$ expected in 2.0 M and 4.5 M due to the formation of Ca–Np(IV)–OH species [6].

REFERENCES

1. J. Tits et al., “The effect of isosaccharinic acid and gluconic acid on the retention of Eu(III), Am(III) and Th(IV) by calcite”, *Applied Geochemistry*, **20**, 2082–2096 (2005).
2. X. Gaona et al., “Review of the complexation of tetravalent actinides by ISA and gluconate under alkaline to hyperalkaline conditions”, *Journal of Contaminant Hydrology*, **102**, 217–227 (2008).
3. E. Colàs et al., “Solubility of $\text{ThO}_2 \cdot x\text{H}_2\text{O}(\text{am})$ in the presence of gluconate”, *Radiochimica Acta*, **99**, 269–273 (2011).
4. V. Neck et al., “Thermodynamics of trivalent actinides and neodymium in NaCl, MgCl_2 , and CaCl_2 solutions: Solubility, hydrolysis, and ternary Ca–M(III)–OH complexes”, *Pure and Applied Chemistry*, **81**, 1555–1568 (2009).
5. Th. Rabung et al., “A TRLFS study of Cm(III) hydroxide complexes in alkaline CaCl_2 solutions”, *Radiochimica Acta*, **96**, 551–559 (2008).
6. D. Fellhauer et al., “Solubility of tetravalent actinides in alkaline CaCl_2 solutions and formation of $\text{Ca}_4[\text{An}(\text{OH})_8]^{4+}$ complexes: A study of Np(IV) and Pu(IV) under reducing conditions and the systematic trend in the An(IV) series”, *Radiochimica Acta*, **98**, 541–548 (2010).

Preliminary Safety Analysis Gorleben (vSG): Source Term for Radionuclides

B. Kienzler

*Institut für Nukleare Entsorgung, Karlsruhe Institute of Technology (KIT-INE), Karlsruhe, Germany
email: Bernhard.Kienzler@kit.edu***INTRODUCTION**

The preliminary safety analysis Gorleben project (VSG) started in 2010 with the aim of providing a realistic estimate whether and under which circumstances the Gorleben site (Germany) is suitable for a potential high-level waste repository. Within the scope of the VSG, an optimized disposal concept is developed. Based on this concept, a radionuclide source term is provided and further research requirements are identified.

DESCRIPTION OF THE WORK

Deriving a radionuclide source term is one of the central issues for assessing the radionuclide release from a potential repository. Within the VSG project, it is the task of the Institute for Nuclear Waste Disposal (INE) to provide a radionuclide source term for the given boundary conditions (e.g. waste inventory, canisters, backfill, host rock). The basis for the source term is assessing the geochemical conditions, which may evolve in the near-field of the wastes. This includes composition and pH of the intruding solutions, interaction with near-field materials and redox conditions. Kinetic and thermodynamic approaches are compiled that describe the radionuclide mobilization from different waste types (spent fuel, vitrified wastes, compacted hulls and end pieces). Finally, maximum radionuclide concentrations are given as an upper limit of the radioactive element concentrations that may evolve under the expected boundary conditions and further research topics are identified.

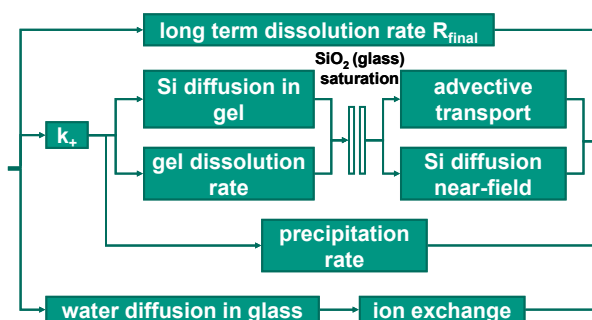
RESULTS**Geochemical conditions**

Two types of intruding solutions were considered as boundary cases: saturated NaCl solution and MgCl₂-rich solution. Reducing conditions will be provided due to the consumption of oxygen by the corrosion of steel canisters and subsequent anoxic steel corrosion with formation of H₂ gas. Carbonate-free conditions are assumed.

Kinetic and thermodynamic approaches for RN mobilization*Vitrified wastes*

In total, 3729 stainless-steel canisters with vitrified high-level wastes from reprocessing need to be disposed in Germany. The glass matrix serves as a kinetic barrier with respect to easily soluble elements (e.g. Cs) and colloids and as a geochemical barrier which retains mobilized radionuclides by the formation of secondary

phase precipitates. The glass corrosion mechanisms can be described with a model developed by Grambow [1] (Fig. 1). The short-term dissolution rate depends on the saturation of the solution with respect to SiO₂(aq), the formation of a gel layer, which reduces diffusion and the ion exchange between solution and glass matrix. Once the solution is saturated with SiO₂(aq), the



dissolution is dominated by a long-term dissolution rate.

Fig. 1: Schematic illustration of the glass corrosion mechanisms [1].

Spent Nuclear Fuel

Approximately 11000 t of spent nuclear fuel from power reactors need to be considered for final disposal in Germany. Mobilization of radionuclides can be differentiated into two fractions: The fast, so-called “instant release fraction” (IRF) and the release from the matrix, which is dominated by radiolytically controlled matrix dissolution processes. Main contribution to the IRF comes from radionuclides at gaps and fractures. The complex structure of spent nuclear fuel and, thus, the IRF strongly depend on reactor operation, burn-up and temperature ramps (see Fig. 2).

Maximum radionuclide concentrations

Based on experimental data, maximum radionuclide concentrations are derived for the two boundary solutions (5M NaCl and 4.5 M MgCl₂) and two pH values, pH 6 and pH 9 (see Tab. 1). Radionuclide solubilities tend to decrease from the slightly acidic region (pH~6) to alkaline pH values around 9. In addition, actinides have lower solubilities in their lower oxidation states under reducing conditions.

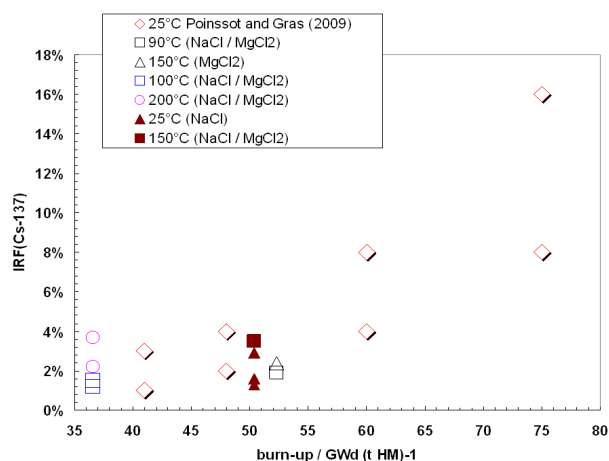


Fig. 2: Instant release fraction of different burn-up spent nuclear fuels in dilute solutions [2] and chloride-rich solutions at different temperatures [3].

CONCLUSIONS

In general, it is favorable to keep reducing conditions in the repository due to the lower solubilities of radionuclides. In addition, it is recommended to use suitable backfill materials to buffer the pH around 9

(e.g. Mg-based Sorel cements) in order to keep maximum radionuclide concentrations low.

Further recommendations for research and development are to enhance the understanding of temperature effects on radionuclide solubilities (including speciation and Pitzer parameters) and release processes from SNF.

Sorption processes in rock salt and on backfill and canister corrosion products also require improved understanding.

REFERENCES

1. B. GRAMBOW, "Beschreibung der kinetischen Barrierenwirkung von HAW-Glas im integrierten Nahfeldmodell", FZK-INE 015/97 (1998).
2. L. JOHNSON et al., "Spent fuel radionuclide source-term model for assessing spent fuel performance in geological disposal. Part I: Assessment of the instant release fraction", *J Nucl. Mat.*, **346**, 56-65 (2005).
3. A. LOIDA et al., "Abgebrannter LWR-Kernbrennstoff: Auslaugverhalten und Freisetzung von Radionukliden", FZK-INE 009/99 (1999).
4. B. KIENZLER et al., "Radionuclide Source Term for HLW Glass, Spent Nuclear Fuel, and Compacted Hulls and End Pieces (CSD-C Waste)", *to be published*.

Tab. 1: Solubility controlled element concentrations in the relevant pH range [4].

	5 M NaCl pH _m 6, (M)	5 M NaCl pH _m 9, (M)	4.5 M MgCl ₂ pH _m 6, (M)	4.5 M MgCl ₂ pH _m 9 (M)
Am(III)	>10 ⁻¹	10 ⁻⁵	>10 ⁻¹	10 ^{-4.5}
Th(IV)	10 ⁻⁶	10 ⁻⁶	10 ⁻⁶	10 ⁻⁶
U(IV)	10 ⁻⁶	10 ⁻⁶	10 ⁻⁶	10 ⁻⁶
U(VI)	10 ^{-4.5}	10 ^{-6.5}	>10 ⁻²	10 ^{-5.5}
Np(IV)	10 ^{-6.5}	10 ^{-6.5}	10 ^{-6.5}	10 ^{-6.5}
Np(V)	>10 ⁻¹	10 ^{-3.5}	>10 ⁻¹	10 ⁻³
Pu(III)	>10 ⁻⁴	10 ⁻⁸	>10 ^{-2.5}	10 ⁻⁸
Pu(IV)	10 ⁻⁸	10 ⁻⁸	10 ⁻⁸	10 ⁻⁸
Pu(V)	10 ^{-5.5}	10 ⁻⁸	10 ^{-5.5}	10 ⁻⁸
Zr(IV)	10 ⁻⁶	10 ⁻⁶	10 ⁻⁶	10 ⁻⁶
Tc(IV)	10 ⁻⁶	10 ⁻⁶	10 ⁻⁶	10 ⁻⁶
Tc(VII)	>10 ⁻¹	>10 ⁻¹	>10 ⁻¹	>10 ⁻¹
Se	solubility not estimated			

Basis and Status of EURATOM Waste Management Research

Gunnar Buckau

*European Commission, Joint Research Centre – Institute for Transuranium Elements, P.O. Box 2340, 76125 Karlsruhe, Germany
email: gunnar.buckau@ec.europa.eu*

INTRODUCTION

Nuclear waste disposal research is promoted on a European Union level by different programmes and activities. The legal basis is the EURATOM treaty, signed 25 March 1957 in Rom as one of the two founding treaties of what has become the European Union. Key actors for implementation of such research programmes and associated nuclear waste disposal activities are Directorate General “Research and Innovation (DG RTD), DG Energy and Transport (DG ENER), DG Joint Research Centre, Institute for Transuranium Elements (DG JRC-ITU) and the “Implementing Geological Disposal Technology Platform (IGD-TP). Some key aspects of the roles and contributions by these key actors are presented and discussed below. Exhaustive information including a complete spectrum of their respective activities can be found on their respective homepages¹.

JRC-ITU

The JRC-ITU is implementing a research programme directly funded by the European Commissions budget (“Direct Action”). The programme is focussing on the key competence of the JRC-ITU, namely instrumentation, techniques, expertise and operating license for the investigation of spent fuel and high-level material and waste. One of the key questions around the safety assessment and long-term prediction for the disposal of spent fuel is the rate of oxidative dissolution of the spent fuel matrix when potentially coming in contact with water in a distant future. Based on this, the JRC-ITU direct action is focussing on the several different aspects and fundamental mechanistic questions around the oxidative dissolution of the spent fuel matrix under repository conditions. Another part of the activities deal with long-term storage evolution of spent fuel, a key question for several of the present national spent fuel management strategies, as well as retrievability and especially recoverability repository concepts.

DG RTD

The DG RTD is managing and “indirect action” programme. In this case, the programme is implemented through funding of projects, open to participation within the EU, complemented by the different levels of possible participation of associated states and beyond. Cooperation beyond the EU and associated states are,

for example recent emphasis and specific support for joint implementation of EURATOM and Chinese projects, and encouragement of involvement of organizations taking part in the recently broadened US programme. The indirect actions are based on annual calls with different types of instruments in order to meet different objectives and creating different structures. These instruments include RD&D projects, networks, sharing of infrastructure, various types of support activities as well as actions for assessing the present situation and planning future activities. There are presently about ten projects operating in the area of radioactive waste disposal, dealing with detailed investigations of mechanistic process understanding, large underground technical development, verification and demonstration projects, improvement of the safety assessment analysis, and finally socio-political issues around the governance of repository projects.

DG ENER

A recent activity lead by the DG ENER was negotiation with the Member States and conclusion of the new “Waste Directive” (European directive on the safe and responsible management of spent fuel and radioactive waste). The Directive was published 22 August 2011 and will enter into force 22 August 2013. A key provision for the individual Member States within the Directive is the requirement to establish and implement a corresponding national programme. This national programme needs to be notified to the Commission (DG ENER) at the latest 23 August 2015. With the same deadline, the first implementation progress report by the respective Member States needs to be submitted to DG ENER, followed by updates on a bi-annual basis. The Commission (DG ENER with support of the JRC-ITU) will assess the notified national programmes and the progress reports and, if necessary request additional information or actions. The practical implementation of the Directive could benefit considerably from the future EURATOM RD&D programme, including information management, and training and education.

IGD-TP

The IGD-TP is primarily a focal point for interests in implementing nuclear waste disposal. As developed and published in its Vision Report and Strategic Research Agenda (SRA) for implementing the vision, however, it also covers a broader spectrum of interests. Presently, the deployment plan is being established, describing the practical implementation in the form of activities and projects. The IGD-TP will have a progressively important role for the indirect action programme. The

¹ <http://ec.europa.eu/energy>;
<http://ec.europa.eu/research>; <http://itu.jrc.ec.europa.eu>;
<http://www.igdtp.eu>

Exchange Forum (EF) organized on an annual basis presently is the key event for getting informed. Starting next year, the EF will be extended by one day and have a more detailed discussion of the investigation programme and programme planning. In the future, bi-annual scientific-technical conferences and information management activities will complement the extended EF and further support the documentation, dissemination and communication around the European activities in this field.

These IGD-TP EF, and bi-annual EURATOM disposal programme conferences and the associated proceedings, will be the key sources for getting informed and involved in the future programme.

POSTER ABSTRACTS

List of poster contributions

Fast / Instant release of safety relevant radionuclides from spent nuclear fuel (FIRST-Nuclides) <i>B. Kienzler, V. Metz, V. Montoya</i>	67
Recosy Intercomparison exercise on redox determination methods – final report on main conclusions and recommendations <i>M. Altmaier, X. Gaona, D. Fellhauer, G. Buckau</i>	69
Direct observation of preferential transport pathways in salt rocks by means of GeoPET <i>J. Kulenkampff, F. Enzmann, M. Gründig, M. Wolf, H. Lippold, J. Lippmann-Pipke</i>	71
Neptunium (V) Adsorption to a Halophilic Bacterium: Surface Complexation Modeling in High Ionic Strength Systems <i>D. A. Ams, J. S. Swanson, J. E. S. Szymanowski, J. B. Fein, M. Richmann, D. T. Reed</i>	73
Ionic strength and complexation induced humic acid agglomeration study <i>M. Bouby, H. Geckeis, G. Buckau</i>	75
Synthesis, characterization and stabilities of Mg-Fe(II)-Al-Cl containing layered double hydroxides (LDHs) <i>K. Rozov, H. Curtius, D. Bosbach</i>	77
Ra-Ba Co-precipitation in a Large Scale Evaporitic System <i>Y. O. Rosenberg, V. Metz, J. Ganor</i>	79
Iron-Based Waste Packages as Engineered Barriers in a Salt Repository <i>G. T. Roselle and C. D. Leigh</i>	81
Solubility of Ferrous Oxalate Dihydrate in Magnesium Chloride and Sodium Chloride Solution <i>J.-H. Jang, M. B. Nemer, Y.-L. Xiong</i>	83
Experimental Determination of Solubilities of Sodium Tetraborate (Borax) in NaCl Solutions to High Ionic Strengths, and Thermodynamic Model for the Na-B(OH) ₃ -Cl-SO ₄ System <i>Y.-L. Xiong, L. Kirkes, T. Westfall, and T. Olivas</i>	85
Formation and equilibrium conditions of An(III,IV,V,VI)- <i>eigencolloids</i> in dilute to concentrated NaCl, CaCl ₂ and MgCl ₂ solutions <i>X. Gaona, V. Neck[†], M. Altmaier</i>	87
The Models for the Colloid Source Term at WIPP <i>D. C. Sassani and C. D. Leigh</i>	89
Solubility of TcO ₂ (s)·xH ₂ O in dilute to concentrated NaCl, CaCl ₂ , and BaCl ₂ solutions <i>T. Kobayashi, E. Yalcintas, M. Altmaier</i>	91
Redox Behavior of the Tc(VII)/Tc(IV) Couple in Dilute to Concentrated NaCl Solutions <i>E. Yalcintas, T. Kobayashi, M. Altmaier, H. Geckeis</i>	93

Spectroscopic Evidence of Ion-Association in Aqueous Ln ³⁺ and An ³⁺ Perchlorate Solutions at Low Water Activity <i>P. Lindqvist-Reis, B. Schimmelpfennig, R. Klenze</i>	95
Actinide Interactions in WIPP Brine <i>D.T. Reed, D. Ams, J.-F. Lucchini, M. Borkowski, M.K. Richmann, H. Khaing, J. Swanson</i>	97
Borate Chemistry and Interaction with Actinides in High Ionic Strength Solutions at Moderate pH <i>M. Borkowski, M. Richmann, S. Kalanke, D. Reed</i>	99
Complexation of Nd(III)/Cm(III) with borate in dilute to concentrated alkaline NaCl and CaCl ₂ solutions <i>K. Hinz, M. A. Altmaier, Th. Rabung, H. Geckeis</i>	101
Complexation of Neptunium (V) with Borate <i>S. Kalanke, D. Reed, M. Richmann, M Borkowski, K. Mengel</i>	103
Cs and U Retention in Cement during Long-Term Corrosion Tests in Salt Brines <i>B. Kienzler, N. Finck, M. Plaschke, Th. Rabung, J. Rothe</i>	105
High-resolution X-ray absorption spectroscopy of U in cemented waste form <i>T. Vitova, M. A. Denecke, N. Finck, J. Göttlicher, B. Kienzler, J. Rothe</i>	107

FAST / INSTANT RELEASE OF SAFETY RELEVANT RADIONUCLIDES FROM SPENT NUCLEAR FUEL (FIRST-Nuclides)

Bernhard Kienzler¹, Volker Metz¹, Vanessa Montoya²

¹ Karlsruhe Institute of Technology, Institut für Nukleare Entsorgung, Karlsruhe, Germany

email: bernhard.kienzler@kit.edu

² Amphos 21, Barcelona, Spain

INTRODUCTION

The EURATOM FP7 Collaborative Project “Fast / Instant Release of Safety Relevant Radionuclides from Spent Nuclear Fuel (CP FIRST-Nuclides)” contributes to the progress towards implementing of geological disposal in line with the Vision Report and the Strategic Research Agenda (SRA) of the “Implementing Geological Disposal – Technology Platform (IGD-TP)”. The key topic “waste forms and their behaviour“ where the FIRST-Nuclides project is included, deals with understanding the behaviour of various wastes in geological repositories, in particular, high burn-up spent uranium oxide (UO₂) fuels. This waste type represents the source for the release of radionuclides after loss of the disposed canister integrity. For safety analysis, the time-dependent release of radionuclides from spent high burn-up UO₂ fuel is required. The first release consists of radionuclides (1) in gaseous form, and (2) those radionuclides showing a high solubility in groundwater.

Some important nuclides undergo only marginal retention on their way to the biosphere. In present safety analyses, these radionuclides have a significant contribution to dose to man. The basis for the calculated significant dose contribution is a simplified description of the release function. It is expected that a realistic release function results in lower peak dose rates, and thus contributes to acceptance of nuclear waste disposal.

The CP is accepted under EC FP7-Fission-2011 ”Research activities in support of implementation of geological disposal”. It started in January 2012 and has a duration of 36 months.

OBJECTIVES OF FIRST-Nuclides

With respect to the fast / instant release of radionuclides (RN) from spent nuclear fuel elements under deep underground repository conditions, a series of questions are still open. These questions concern key input data to safety analysis, such as “instant release fraction (IRF)” values of iodine, chlorine, carbon and selenium that are still largely unknown. The elements I, C, Cl and Se tend to form anionic species. Such anions are hardly chemically retained in the repository barrier system and may thus significantly contribute to the dose to man. Moreover, ¹⁴C may be present as carbide reacting with water forming mobile hydrophilic organic species.

Consortium

The project is implemented by a consortium with 10 partners from 7 EURATOM Signatory States (KIT (DE), AMPHOS21(ES), FZ JÜLICH(DE), PSI(CH), SCK·CEN(BE), CNRS(FR), CTM(ES), AEKI(HU), STUDSVIK(SE), and the EC Joint Research Center Institute for Transuranium Elements. The project is coordinated by KIT. The Coordination Team consists of KIT and AMPHOS21 which are responsible for project management, knowledge management, documentation, dissemination and training. Workpackage leaders head the individual workpackages and are members of the Executive Group.

Associated Groups (AG) participate in the project at their own costs with specific research and technological development (RTD) contributions or particular information exchange functions. Several organisations from France, Finland, USA (3) and UK contribute in this way. A group of implementation and regulatory oriented organizations are participating as an “End-User Group”. This group has a number of functions, such as: i) ensuring that end-user interests are reflected in the project work, ii) reporting, dissemination and communication, iii) providing for review of the project work and scientific-technical outcome, and iv) participating in assessment and discussion of the project outcome with respect to the potential impact on the Safety Case.

STRUCTURE OF THE COLLABORATIVE PROJECT

The CP is organized in several workpackages (WP). WP 1: Samples and tools. This WP deals with the selection, characterization and preparation of materials and set-up of tools.

Limited irradiated fuel material is available where the initial enrichment and irradiation history, etc. is known and where data can be used and published without restrictions. As a first step, fuel characterisation data are collected, revealing several categories of information: (i) essential information representing the minimum data required and information that should be available for the fuel chosen for the study, (ii) parameters and data which are not directly measured, but are derived from calculations, and (iii) supplemental information referring to characteristics that may be needed depending on the studies to be performed. Fission gas release (FGR) is determined and

samples prepared for investigations of structural defects.

WP 2 “Gas release and rim and grain boundary diffusion” and WP 3 “Dissolution based release” cover the experimental determination of fission gases release, rim and grain boundary diffusion processes and the dissolution based fast/instant radionuclide release. These investigations include the determination of the chemical form of released radionuclides, fission gases, ¹³⁵Cs, ¹²⁹I, ¹⁴C compounds, ⁷⁹Se, ⁹⁹Tc and ¹²⁶Sn. Moreover, the gap and grain boundary inventories are determined and the dependence of the fast/instant release on i) the UO₂ fuel and the respective manufacturing process, ii) the evolution of higher burn-up and burn-up history, iii) the linear power and fuel temperature history, ramping processes, and iv) storage time are assessed.

WP 3 aims at the quantification of the fast/instant radionuclide release by leaching experiments in the aquatic phase considering the fuel characteristics, burn-up and burn-up history, and the characteristics of the samples under investigations. Differences are expected with respect to the presence or absence of cladding, to the application of fuel fragments from different radial positions of fuel pellets and to the specific fuel, and burn-up characteristics (see WP 1). The instantly released elements, including their isotopic composition and chemical form, if possible, are measured in the gas phase and in the leaching solution. The investigations are complemented by micro-scale investigations on the oxidation state and coordination environments of the relevant radionuclides as well as on the crystallographic structure by using synchrotron radiation techniques.

WP 4 “Modelling” deals with modelling of migration/retention processes of fission products in the spent fuel structure. A series of codes have been developed which integrate neutronics, burn-up, fuel and fuel rod mechanical and thermal-hydraulic calculations.

The modelling work within FIRST-Nuclides helps to clarify which geometric scales dominate the fast/instant release. Special attention is attributed to model the fission product migration along the grain boundaries, the effects of fractures in the pellets and of holes/fractures in the cladding. Emphasis is given to provide more realistic relationships between FGR and release of iodine, caesium and other radionuclides in the relevant burn-up ranges by modelling the release of gaseous and non-gaseous fission products. Other modelling aims concern the speciation of ¹⁴C and rare fission / activation products after cooling to disposal conditions, the migration of gaseous and non-gaseous fission products in the microstructures of spent fuel pellets (grains, grain boundaries, gas bubbles or pores), the development of improved models to predict the FGR and release of non gaseous fission products on the fuel rod scale.

Modelling also supports the experimental set-up/designs by assessing concentration/activity limits for the elements under investigation. It also contributes to

the up-scaling from the analytical and modelling micro-scale to the experimental bulk observations and to the release on a fuel-rod scale.

WP 5 is responsible for the knowledge management, the state-of-the-art report, the general reporting, keeping the documentation up-date, and all dissemination and training measures. The state-of-the-art report addresses the specific topics of the respective workpackages. It compares previously investigated samples with material used in the present project; it describes the experimental determination procedures of fission gases release on the basis of published and grey literature as well as results from rim and grain boundary diffusion experiments. The project aims on making available all results generated to any interested party. The dissemination of scientific-technical results through reviewed publications is encouraged. Reflecting previous experiences, the persons involved in driving the scientific-technical program have a keen interest in publishing their results in prominent peer reviewed journals.

ACKNOWLEDGEMENT

The research leading to these results has received funding from the European Atomic Energy Community's Seventh Framework Programme (FP7/2007-2011) under grant agreement No. 295722 (FIRST-Nuclides).

CONTACTS

bernhard.kienzler@KIT.EDU
Vanessa.Montoya@amphos21.com

Recosy Intercomparison exercise on redox determination methods – final report on main conclusions and recommendations

M. Altmaier¹, X. Gaona¹, D. Fellhauer^{1,2}, G. Buckau^{1,2}

¹Karlsruhe Institute of Technology, Institut für Nukleare Entsorgung, P.O. Box 3640, 76021 Karlsruhe, Germany

²EC Joint Research Centre, Institute for Transuranium Elements, P.O. Box 2340, 76125 Karlsruhe, Germany

Redox processes play an important role in defining the aqueous chemistry of redox sensitive actinide elements like plutonium, neptunium and uranium. In order to assess the chemical behavior of these elements in the context of nuclear waste disposal but also for more general studies in actinide chemistry, it is necessary to predict and quantify the impact of redox conditions on the solution chemistry. The reliable measurement of redox potentials in solution therefore is a matter of highest importance for many scientific applications and research fields.

In this contribution, the outcome of the ReCosy Intercomparison Exercise (ICE) on redox determination methods is presented. The ICE exercise was conducted within the EURATOM FP7 Collaborative Project “Redox phenomena controlling systems” (CP ReCosy) and was hosted by the “Institut für Nukleare Entsorgung” (“Institute for Nuclear Waste Disposal”), Karlsruhe Institute of Technology (KIT-INE). More than 40 scientists working on different topics related to redox chemistry from 20 ReCosy partner organisations and associated groups contributed to ReCosy ICE, thus providing a broad scientific basis for ICE. The objectives of the ReCosy ICE were to compare different redox determination methods in order to

- (i) identify critical redox determination issues,
- (ii) provide the basis for more confidence in redox determinations for the individual groups, and
- (iii) identify future activities that could contribute to further progress in the confidence in determination of the redox state of nuclear waste disposal Safety Case relevant systems and conditions.

The intercomparison was based upon different redox determination methods, i.e. static electrodes (platinum, gold glassy carbon, single/combined electrodes), dynamic electrochemical measurements, amperometric measurements, optodes (optical fibres with oxygen sensitive tips) and thermodynamic calculations based on chemical composition and physicochemical properties (such as pH, ionic strength and temperature). For this purpose, a wide set of samples was used with three different types of origin and properties, namely

- (a) simple samples with well defined composition,
- (b) natural samples under near-natural conditions,
- (c) samples with microbial cultures.

Following the joint evaluation and critical discussion of ICE, the final report on ReCosy ICE has been published in 2010 as a joint effort of all ReCosy ICE participants. The final outcome of ReCosy ICE is available as a report from the authors and can be downloaded via the ReCosy website www.recosy.eu or at: <http://digbib.ubka.uni-karlsruhe.de/volltexte/1000021898>.

The main conclusion of ReCosy ICE is that the redox state of an aqueous system can be determined by the existing experimental techniques, although the degree of confidence strongly depends of the kind of aqueous system investigated and the degree of optimisation of the experimental equipment and handling protocols. In how far the available experimental accuracy and precision is sufficient to adequately characterise the sample must be assessed in each single case and cannot be generalised. As observed in the ReCosy ICE, some samples show clusters of readings from different groups and electrodes used. These samples are artificial, with high redox buffer content, with pH buffered and in the pH neutral to acidic range. Natural samples show very large differences between the different groups, electrodes and handling protocols. A predictive capability based on any of such measurements alone is considered rather uncertain. The ReCosy ICE has not yet provided the basis for identification of different processes responsible for the large drift and large differences in redox readings.

Based upon the outcome of ReCosy ICE and the joint data evaluation and interpretation, the partners of ReCosy ICE have agreed on several recommendations. ReCosy ICE was using the presently available experimental and conceptual approaches to compare and evaluate various aspects related to redox measurement and redox data interpretation, aiming at defining the current state-of-the-art. In this respect, ReCosy ICE has compiled a list of recommendations regarding redox measurements. Important outcomes are:

- It is strongly recommended to use a combination of several experimental approaches to identify and assess systematic errors as there is no single “best method” to determine the redox state of a given system. This is especially true for the analysis of (intrinsically highly complex) real systems. Ideally, it is recommended to use different sensor materials and complement potentiometric measurements with thermodynamic model calculations based upon the distribution of redox couples.

- The use of a “quality assurance” protocol for Eh measurements is advisable.
- The use of non-conventional approaches (optodes, amperometry, ...) can help to clarify the redox state and could also be used to complement conventional measurements whenever possible.
- The problems arising from electronics of the instrumentation are generally minor compared to “chemical” interferences affecting redox measurements.
- It is recommended to consider that dilution experiments with redox buffers indicate that there is a “critical minimum concentration” of redox active species to allow measurement of meaningful pe values with combined electrodes.
- Development of advanced tools for long-term redox monitoring, relevant for the robust (experimental) assessment of main performance indicators in post-closure scenarios.

For further information on ReCosy ICE, please visit the project web page www.recosy.eu or contact marcus.altmaier@kit.edu.

Acknowledgement: The research leading to these results has received funding from the European Union's European Atomic Energy Community's (Euratom) Seventh Framework Programme FP7/2007-2011 under grant agreement no. FP7-212287 (ReCosy Project).

Further recommendations concerning sampling and handling, better equilibration of samples, stirring or non-stirring during measurements, drift and surface effects on the sensor, pe-pH measurements and thermodynamic modelling of redox processes have been derived and are reported in the final ReCosy ICE report.

In addition, several topics have been identified within ReCosy ICE beyond the present state-of-the-art that may provide significant input for future research activities related to redox state determination. The main arguments again concern the central question of how the redox state of a system is defined, and what consequences result for redox state determinations? Individual questions related to this overall context are concerning:

- New approaches to identify and quantify the reasons for the observed long-term drift on measurements in a comprehensive multi-step approach.
- Better understanding of the alteration processes at the electrode surface, caused by sorption of ions, colloids or organics on the sensor material, or partial oxidation (PtO formation) and consecutive surface coating of the sensor.
- Work towards the further optimisation of cleaning protocols for electrode surfaces.
- Improve alternative techniques to complement conventional potentiometric measurements. None of the non-conventional techniques used in ReCosy ICE at present can be used for routine analysis under reducing conditions.
- Systematic assessment of temperature effects or ionic strength effects on redox related processes and redox measurements.

Direct observation of preferential transport pathways in salt rocks by means of GeoPET

Johannes Kulenkampff¹, Frieder Enzmann², Marion Gründig¹, Martin Wolf^{1,2}, Holger Lippold¹, Johanna Lippmann-Pipke¹

¹ *Helmholtz-Zentrum Dresden-Rossendorf e. V. Permoserstraße 15, 04318 Leipzig
email: johannes.kulenkampff@hzdr.de*

² *Mainz University, J.-J.-Becherweg 21, 55128 Mainz*

INTRODUCTION

Migration of radionuclides out of a salt-based repository requires transport pathways, where substances propagate by molecular diffusion or even pressure-driven advection. Diffusion coefficients and permeability, being very low in most intact saline rocks, are likely to increase considerably under geomechanical stress, inevitably occurring for instance in the excavation damage zone. Observation and evaluation of transport processes in such heterogeneously structured materials are most demanding, because they likely occur in either extremely localized, macroscopic but rare fractures or in dispersed, mostly indiscernible but still connected microscopic voids.

Applying salt solutions labelled with radionuclides we are able to observe such processes directly and - presumably for the first time with due resolution and sensitivity – with our GeoPET method. The same processes are studied with Lattice-Boltzmann flow simulations on μ CT-based images of the same samples. This strategy contrasts the common use of computer simulations based on a priori material parameters, and allows for the matching of flow simulation results in “real structures” with real time flow monitoring in the same samples. Here we report on results obtained from a number of drill cores from the ancient Stassfurt salt mine and its overburden, including aged backfill material, which has been analysed in the framework of our joint research project, funded by the Federal Ministry of Education and Research (BMBF) (Wolf et al., 2010).

DESCRIPTION OF THE WORK

Cores from saline rock formations (rock salt, and anhydrite) and their overburden (Buntsandstein) have been recovered from drill holes in Stassfurt. Sections of 10-20 cm length of these cores (diameter 10 cm) have been moulded in epoxy for injection experiments. Prior to the injection experiments, high-resolution CT-images were made.

The salt solutions were injected through the end planes. After preconditioning, a pulse of radiolabelled solution was injected. In general, ¹²⁴I is applied, with a decay time of 4.2 days, allowing observation periods up to 3 weeks.

The propagation of the radiotracers is observed by sequential scanning with a high-resolution positron-emission tomography (PET-) scanner (ClearPET from

Raytest, Straubenhardt). Thus, spatiotemporal data sets of tracer concentration distributions during the propagation through the geological samples are acquired (GeoPET-method).

These datasets are a basis for the direct experimental derivation of advanced transport parameters, like effective volume, effective internal surface area, and localization properties of the process (as preferential flow). The data also serves as basis for enhanced process comprehension and for verification of model codes: One example is the successful overlay of the simulated tracer transport in connected voids as derived from segmented CT-images, which is derived with a Lattice-Boltzmann (LBM)-Code (Fraunhofer GeoDict), with direct experimental PET-observations of the tracer transport in the identical sample (Wolf et al. 2011).

RESULTS

GeoPET is a beneficial method for spatiotemporal migration studies in heterogeneous, geological materials, because it is currently the only non-destructive laboratory method for investigating the fate of highly diluted chemical species (tracers) in space and time (Kulenkampff et al. 2008). Two characteristic types of tracer propagation processes have been identified in salt rocks. The first type results in a diffuse tracer distribution inside the material while significant tracer concentrations are observed only in the inlet and outlet gaps. We assume the tracer propagates in micro fissures, where the size of the voids is below the resolution of the μ CT (20 μ m) (Fig. 1) and the PET-voxel (~ 1 mm³) integrated activity is close to background. The second type of propagation realises in highly localized flow along preferential pathways in fractured rocks (Fig.2). Here we were able to reproduce the evolution of the tracer propagation with LBM simulations (Fig. 3). This type of preferential flow is crucial for interactions between components of the fluids and solids: Only an extremely small, effective portion of the internal surface is affected by interactions like adsorption, dissolution and precipitation. Thus, high local tracer velocities could occur, which may exceed mean transport rates - as derived from bulk permeability measurements - by orders of magnitude.

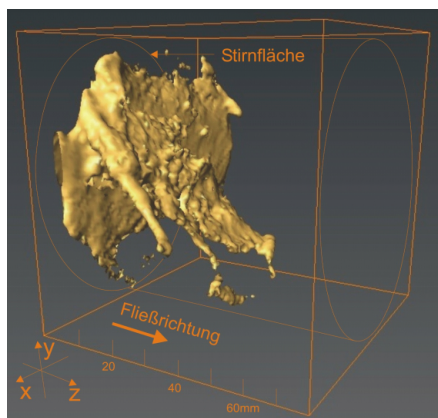


Fig. 1

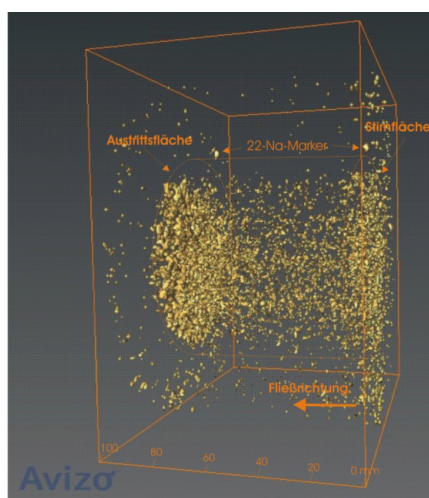


Fig. 2

Figures

Fig. 1: Isosurface of activity, 9.25 h after start of tracer pulse, showing highly localized propagation pathways. (Lower Buntsandstein, Flow rate 0.02 ml/min, 15% of effective pore volume filled)

Fig. 2: Isosurface of activity, 48.8 h after start of tracer pulse, showing diffuse propagation. (Anhydrite, Flow rate 0.08 ml/min, 82% of effective pore volume filled)

Fig. 3: Combined CT-LBM and PET datasets. From top to bottom: 1) CT-image, 2) computed tracer distribution after 6.2 h injection period (CT-based LBM), 3) PET-image after 6.2 h injection period. The bright blue boxes outline the identical volume area.

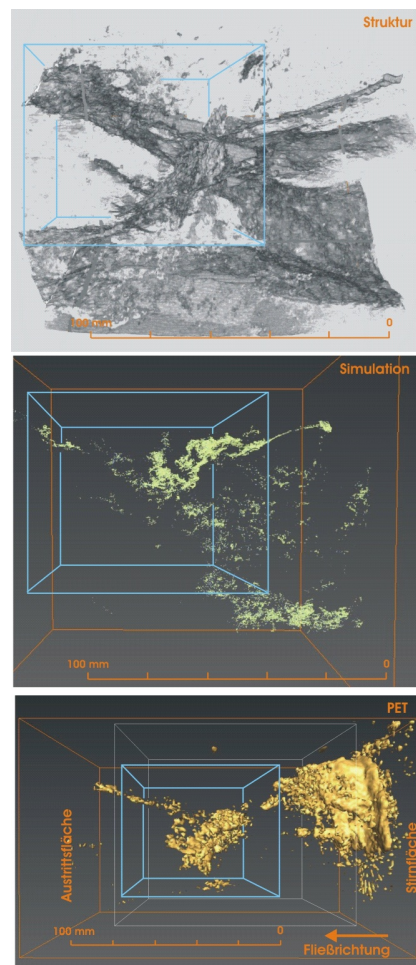


Fig. 3

REFERENCES

1. KULENKAMPFF et al., "Evaluation of Positron-Emission-Tomography for visualization of migration processes in geomaterials". Phys. Chem. Earth 33, 937-942, 2008.
2. WOLF et al., "3D-Visualisierung und Quantifizierung von Fluidströmungen in Salinargestein mittels Positronen-Emissions-Tomographie". Exkursionsführer und Veröffentlichungen der Deutschen Gesellschaft für Geowissenschaften, Heft 244, Page 200-212, 2010.
3. WOLF et al., "Combined 3D high-resolution PET and CT measurements with lattice Boltzmann simulations of fluid flow in heterogeneous material". Geophysical Research Abstracts, Vol. 13, EGU2011-10669, 2011.

Neptunium (V) Adsorption to a Halophilic Bacterium: Surface Complexation Modeling in High Ionic Strength Systems

D. A. Ams¹, J. S. Swanson¹, J. E. S. Szymanowski², J. B. Fein², M. Richmann¹, and D. T. Reed¹

¹*Los Alamos National Laboratory, Earth & Environmental Sciences Division, Carlsbad Operations, Actinide Chemistry & Repository Science Program, 1400 University Drive/Carlsbad, NM 88220, USA
email: dams@lanl.gov*

²*Department of Civil Engineering and Geological Sciences, University of Notre Dame, Notre Dame, IN 46556*

INTRODUCTION

Neptunium is one of the most important actinides for consideration in the long-term storage of nuclear waste. The fate and transport of neptunium in the environment may be influenced by a variety of factors including adsorption onto bacterial surfaces. Metal adsorption to bacterial surfaces ties the mobility of the metal to the mobility of the bacteria. Although presumed to be weakly interactive in the environment, substantial pH-dependent adsorption of the neptunyl ion to the surface of non-halophilic bacteria under low ionic strength conditions ($I < 0.5$ M) was observed [1-4].

To date, Gorman-Lewis et al. [2] performed the only study evaluating the effect of ionic strength on the adsorption of Np(V) to a bacterial surface; showing a decrease in Np(V) adsorption to the non-halophilic gram-positive bacterium *Bacillus subtilis* with increasing ionic strength over the range of 0.001 to 0.5 M. However, evaluation of the potential effects of ionic strength conditions greater than 0.5 M is critical for understanding the fate and transport characteristics of neptunium in high ionic strength aqueous natural environments, such as in the vicinity of salt-based nuclear waste repositories and high ionic-strength groundwater at DOE sites. To date, no study has evaluated the pH and ionic strength dependency on the adsorption of any actinide to halotolerant and halophilic microorganisms under high ionic strength conditions.

DESCRIPTION OF THE WORK

In this study, the adsorption of Np(V) was evaluated at high ionic strength using a halophilic bacterium isolated from a briny groundwater near the Waste Isolation Pilot Plant (WIPP) in southeast New Mexico. Np(V) adsorption was measured as a function of pH and ionic strength. Surface complexation modeling was adapted to include the effects of high ionic strength and was applied to bacterial titration and Np(V) adsorption data. The modeling was used to calculate the number of types, concentrations, and deprotonation constants of bacterial surface functional groups, as well as Np(V) binding constants for the discrete sites on the bacterial surface. Surface complexation model results yield thermodynamically-based constants that may be applied to more complex conditions that differ significantly from the experimental conditions investigated. Thus, the modeling results of this study can be included in geochemical speciation models to aid in the prediction

of Np(V) fate and transport behavior in high ionic strength environmental conditions where halotolerant and halophilic microorganisms are present.

RESULTS

Bacterial Potentiometric Titration Experiments

Each replicate titration was modeled without correcting for bulk aqueous ion activity or surface electric field effects to determine the number of types of discrete proton active sites required to account for the observed proton buffering capacity, as well as the deprotonation constant (K_a) and site concentration for each site type. Models invoking four surface sites provide the best fits to each replicate titration. The four site model fit to representative titration curves at 2 and 4 M ionic strength are shown in Figure 1. The four site model provides an excellent fit to the experimental data throughout the entire pC_{H^+} range evaluated. The averaged deprotonation constant and site concentration values calculated for each discrete surface site at each ionic strength are presented in Table 1.

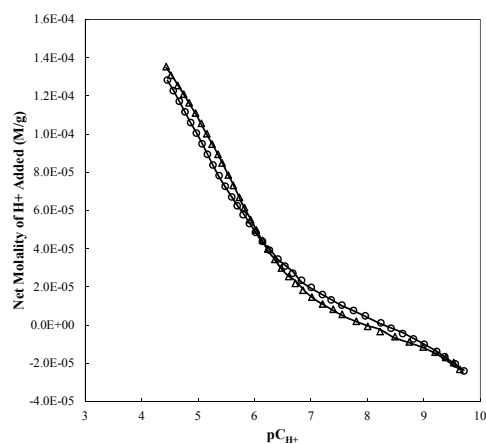


Fig. 1: Best-fit calculated 4-site surface complexation model curves (solid curves) to representative potentiometric titration data of *Chromohalobacter* sp. in 2 (open circles) and 4 (open triangles) M NaClO₄

Table 1. Average^a calculated concentrations and deprotonation constants for functional groups on the cell wall surface of *Chromohalobacter* sp.

	[site] ^b	std. dev. ^c	pK _a ^d	std. dev. ^c
I = 2 M				
L1	1.04 X 10 ⁻⁴	2.77 X 10 ⁻⁵	4.81	0.07
L2	4.43 X 10 ⁻⁵	1.03 X 10 ⁻⁵	6.01	0.13
L3	2.24 X 10 ⁻⁵	8.05 X 10 ⁻⁶	7.53	0.08
L4	3.60 X 10 ⁻⁵	1.62 X 10 ⁻⁵	9.53	0.25
I = 4 M				
L1	5.65 X 10 ⁻⁵	1.05 X 10 ⁻⁵	4.86	0.18
L2	7.38 X 10 ⁻⁵	1.15 X 10 ⁻⁵	5.92	0.12
L3	2.24 X 10 ⁻⁵	8.05 X 10 ⁻⁶	7.50	0.26
L4	4.09 X 10 ⁻⁵	2.06 X 10 ⁻⁵	9.47	0.56

(a) average of results from all replicate acid and base titration models

(b) moles of sites per gram wet weight of bacteria

(c) standard deviation of results from all replicate acid and base titration models

(d) calculated with FITEQL based on equation 6,

$$K_a = [R-L_n^{x-1}]a_{H^+} / [R-L_nH^x]$$

The shapes and positions of the bacterial titration curves in 2 and 4 M NaClO₄ are in agreement, within experimental uncertainty (Figure 1), indicating that the effect of ionic strength on proton adsorption/desorption to the bacterial surface is negligible over this range of ionic strength.

Further, previous titrations of non-halophilic gram-positive and gram-negative bacteria show a similar extent of buffering in these pC_{H+} ranges indicating that the halophilic bacteria used in this study exhibits similar protonation/deprotonation behavior as common non-halophilic soil bacteria.

Np(V) Adsorption and Desorption Experiments

The results of the pC_{H+} dependent adsorption experiments at 2 and 4 M ionic strength are presented in Figure 2. Neptunium (V) exhibits a significant adsorption affinity for the cell wall of *Chromohalobacter* sp. over the entire pC_{H+} range for both ionic strength conditions evaluated, but the observed extent of adsorption is highly dependent on both ionic strength and pC_{H+}. The sorption curve for the 4 M NaClO₄ condition is similar in shape to the 2 M ionic strength curve but the magnitude of adsorption is significantly greater under the high ionic strength condition.

The pC_{H+} dependent adsorption data were modeled by testing likely reaction stoichiometries involving the adsorption of neptunium aqueous species (neptunyl: NpO₂⁺, hydroxyl: NpO₂OH⁰, NpO₂(OH)₂⁻, and carbonate: NpO₂CO₃⁻, NpO₂(CO₃)₂³⁻, NpO₂(CO₃)₃⁵⁻) to the four bacterial surface sites determined from bacteria titration modeling (Table 1).

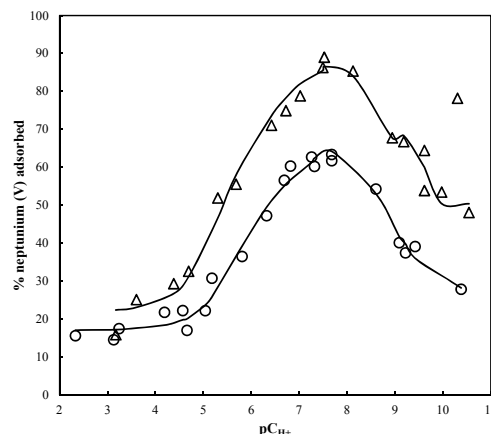


Fig 2: Experimental data for neptunium (V) adsorption onto *Chromohalobacter* sp. in 2 (open circles) and 4 (open triangles) M NaClO₄. Solid curves represent calculated surface complexation models.

The reaction stoichiometries and corresponding Np(V) binding constants that provide the best model fit to the data are presented in Table 2.

Table 2. Calculated Neptunium(V) Binding Constants

	Reaction	log K ^a	
		I = 2 M	I = 4 M
1	NpO ₂ ⁺ + R-L ₄ ^x ↔ R-L ₄ NpO ₂ ^{x+1}	3.01 ± 0.1	3.04 ± 0.1
2	NpO ₂ ⁺ + R-L ₂ ^{x-1} ↔ R-L ₂ NpO ₂ ^x	3.71 ± 0.1	3.86 ± 0.1
3	NpO ₂ ⁺ + R-L ₃ ^{x-1} ↔ R-L ₃ NpO ₂ ^x	4.11 ± 0.1	4.91 ± 0.2
4	NpO ₂ CO ₃ ⁻ + R-L ₃ ^{x-1} ↔ R-L ₃ NpO ₂ CO ₃ ^{x-2}	8.32 ± 0.1	8.71 ± 0.1
5	NpO ₂ (CO ₃) ₂ ³⁻ + R-L ₄ ^{x-1} ↔ R-L ₄ NpO ₂ (CO ₃) ₂ ^{x-4}	10.89 ± 0.1	11.86 ± 0.1
6	NpO ₂ (CO ₃) ₃ ⁵⁻ + R-L ₄ ^{x-1} ↔ R-L ₄ NpO ₂ (CO ₃) ₃ ^{x-6}	11.86 ± 0.1	12.73 ± 0.1

(a) calculated with FITEQL based on the following equation,

$$K = [R-L_nNp(V)^{m+x-1}] / a_{Np(V)m} [R-L_n^{x-1}]$$

REFERENCES

- [1] SONGKASIRI, W et al., "Bio-sorption of neptunium(V) by *Pseudomonas fluorescens*." *Radiochim. Acta* **90**, 785-789. (2002)
- [2] GORMAN-LEWIS, D et al., "Experimental study of neptunyl adsorption onto *Bacillus subtilis*." *Geochim. Cosmochim. Acta* **69** (20), 4837-4844. (2005)
- [3] LUK'YANOVA, EA et al., "Sorption of radionuclides by microorganisms from a deep repository of liquid low-level waste." *Radiochem.* **50** (1), 85-90. (2008)
- [4] DEO, RP et al., "Surface complexation of neptunium(V) onto whole cells and cell components of *Shewanella alga*: modeling and experimental study." *Environ. Sci. Technol.* **44** (13), 4930-4935. (2010)

Ionic strength and complexation induced humic acid agglomeration study

Muriel Bouby¹, Horst Geckeis¹, Gunnar Buckau^{1,2}

¹Karlsruher Institut für Technologie-Campus Nord (KIT-CN), Institut für Nukleare Entsorgung (INE), Postfach 3640, D-76021 Karlsruhe, Germany
email: muriel.bouby@kit.edu

²Present Address: European Commission, JRC, Institute for Transuranium Elements, Postfach 2340, D-76125 Karlsruhe, Germany

INTRODUCTION

Dissolved humic substances can influence significantly or even dominate the chemical form of actinides (An) and their mobility in natural aquatic systems [1-4]. To predict the long term safety of a salt-based nuclear waste repository, the behaviour of the organic matter (amongst with the humic substances) has to be examined under these specific conditions (high ionic strength media) and more particularly how/if these media affect the metal cations binding. The fact that HA agglomerates/flocculates/separates upon metal ion complexation, protonation and salting out/high ionic strength is well established and is related to the inventory of anionic proton exchanging functional groups in HA. The impact of the metal induced HA agglomeration on the kinetic stability of the metal-humate complexes needs better understanding and calls for further investigations.

DESCRIPTION OF THE WORK

The aim of this preliminary study is to get insight into the ionic strength and complexation induced humic acid agglomeration process. For this purpose, the ionic strength (IS) is varied between 0.01 and 3.0 mol/L NaClO₄, the humic acid (HA) concentration between 10 mg/L and 1.3 g/L and the metal ion HA sites loading from 50 up to 99.99 % according to [5]. The pH is kept at 6.05 ± 0.1. After standard laboratory centrifugation, the batch samples are analyzed with UV-Vis. and ICP-MS for the supernatant HA and Eu(III) concentrations.

RESULTS

The UV-Vis. detection of the supernatants after centrifugation of the batch samples evidences the agglomeration process only when the loss of HA becomes significant. The UV-Vis. spectra showing the impact of IS for three different HA concentrations are presented in Figure 1. The HA remain stable in solution up to an IS of 1 mol/L NaClO₄. Contrary to this, at 3 mol/L NaClO₄, part of the HA is removed from the solution by centrifugation.

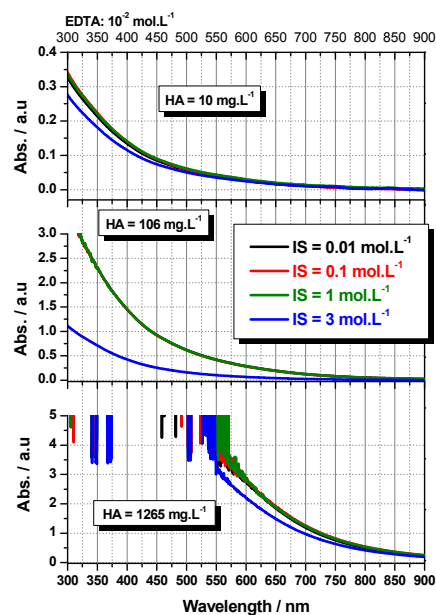


Fig. 1: IS effect as observed on the HA UV-Vis. spectra for different initial [HA] at pH 6.05 ± 0.1. The measurements are performed with the supernatants of the HA solutions obtained after centrifugation in contact with EDTA 10⁻² mol/L. Mean of three replicates, reference subtracted.

The UV-Vis. spectra recorded for different degrees of HA loading by Eu(III) for three different HA concentrations and at four IS illustrate the combined effect of the metal ion loading and the ionic strength (as seen exemplarily for IS = 3 mol/L in Figure 2). The Eu concentrations determined in the supernatant solutions by ICP-MS are consistent with the UV-Vis. data. Interestingly, the gradual HA loading seems to be correlated with an increase of the Eu fraction associated with the flocculates. Further investigations are on-going to examine the dissociation behavior of the metal ion being bound inside the agglomerates and more precisely if the dissociation is inhibited at least partly.

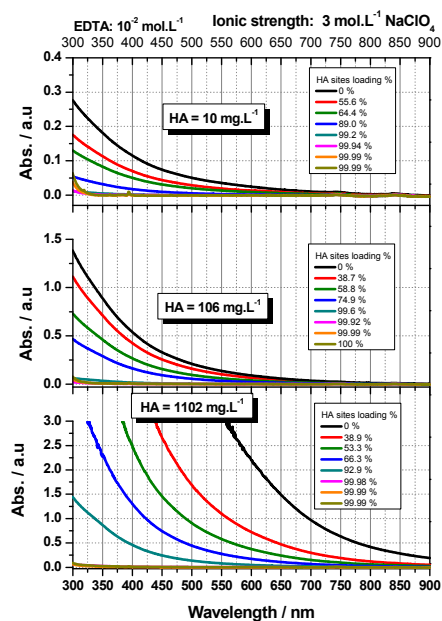


Fig 2: HA UV-Vis. spectra at $\text{pH } 6.05 \pm 0.1$, $\text{IS} = 3 \text{ mol/L NaClO}_4$ for different initial $[\text{HA}]$ and Eu loadings. The measurements are performed with the supernatants of the HA solutions obtained after centrifugation in contact with $\text{EDTA } 10^{-2} \text{ mol/L}$. Mean of three replicates, reference subtracted.

REFERENCES

1. KIM J.-I. et al., "Complexation of Am(III) with humic acids of different origins" *Radiochim. Acta*, **52**, Page 49-55 (1991).
2. CHOPPIN G.R., "The role of natural organics in radionuclide migration in natural aquifer systems" *Radiochim. Acta*, **58**, Page 113-120 (1992).
3. MOULIN V. et al., "Fate of actinides in the presence of humic substances under conditions relevant to nuclear waste disposal" *Appl. Geochem.*, **10**, Page 573-580 (1995).
4. MacCARTHY J.F. et al., "Mobilization of transuranic radionuclides from disposal trenches by natural organic matter" *J. Contam. Hydrology*, **30**, Page 49-77 (1998).
5. KIM J.-I., "Complexation of metal ions with humic acid: Metal ion charge neutralization model" *Radiochim. Acta*, **73**, Page 5-10 (1996).

Synthesis, characterization and stabilities of Mg-Fe(II)-Al-Cl containing layered double hydroxides (LDHs)

K.Rozov*, H. Curtius, D. Bosbach

*Forschungszentrum Jülich GmbH, Institut für Energie- und Klimaforschung, IEK-6***email: k.rozov@fz-juelich.de*

Layered double hydroxides phases (LDHs) are of interest to environmental geochemistry because of their ability to retain hazardous and radioactive cations and anions. In the present work an extensive and detailed investigation of hydrotalcite-Mg₃Al(OH)₈Cl·nH₂O - pyroaurite Fe(II)₃Al(OH)₈Cl·nH₂O substances was performed because hydrotalcite and iron-containing LDHs are characteristic secondary phase components when research reactor fuel reacts with highly-concentrated salt brines under repository relevant conditions of disposed nuclear fuel elements [1].

Hydrotalcite-pyroaurite solid solution series (Mg_{1-x}Fe(II)_x)₃Al₁Cl₁·nH₂O with variable $xFe_{\text{solid}} = Fe^{2+}/(Fe^{2+}+Mg^{2+})$ iron mole fractions were studied in co-precipitation experiments at T = 25, 40, 45, 50, 55 and 60 °C and pH = 10.00 ± 0.05. The compositions of the solids and reaction solutions were determined using ICP-OES, EDX (Mg, Al, Fe) and TGA techniques (Cl, OH, H₂O). Powder X-ray diffraction was applied for phase identification and determination of unit-cell parameters $a_o = b_o$ and c_o from Bragg evaluation. Syntheses products containing $xFe_{\text{solid}} > 0.13$ display additional X-ray patterns attributed to the mixture of iron oxides and hydroxides. On the other side, precipitates with $0 \leq xFe_{\text{solid}} \leq 0.13$ show only X-ray reflexes typical for pure LDH compositions. Moreover, in this case unit-cell parameters $a_o = b_o$ as a function of xFe_{solid} follow Vegard's law [2] corroborating the existence of a continuous solid solution series.

Infrared (IR) spectroscopic measurements were applied to investigate the interlayer composition, particularly to check that the interlayer space contains only chloride-ions and structural water. Obtained IR spectra clearly show strong hydroxyl (3482 cm⁻¹) and water (1636 cm⁻¹) stretching and bending bands. However, the presence of trace quantities of CO₃²⁻-groups in the interlayer space was detected by observation of the very weak adsorption band at 1376 cm⁻¹. The presence of carbonate we explained by preparation of samples for IR analyses when LDH powders were mixed with KBr phase not under an inert gas atmosphere, and due to the very strong affinity of LDHs for CO₃²⁻-anion [3].

TGA data demonstrated the temperatures at which interlayer H₂O molecules and Cl⁻-anions are lost, and at which temperatures dehydroxylation of brucite-like layer occurs. Based on the detailed analyses of TGA curves we established that the increase of xFe_{solid} does not result in a visible change of the thermal stability of hydrotalcite-pyroaurite solids. Based on chemical analyses of both the solids and the reaction solutions after syntheses, preliminary Gibbs free energies of formation have been estimated using Gibbs free energy minimization software GEM-Selektor [4] with implemented thermodynamic database [5]. Values of G_f^o for Cl-bearing hydrotalcite (-3619.04 ± 15.27 kJ/mol) and pyroaurite (-2703.61 ± 191.93 kJ/mol) were found at 298.15 K. The comparison of our estimate with G_f^o value -3746.90±11.00 kJ/mol for CO₃²⁻-bearing hydrotalcite [6] denotes the effect of intercalated anion on the aqueous solubilities of LDH when Cl-containing solids have to be more soluble than CO₃-bearing substances. Estimation of the standard molar entropy of the hydrotalcite end-member by applying Helgeson's methods and using results of co-precipitation experiments at variable temperatures let us to conclude that derivation of more precise S_f^o values would require calorimetric measurements.

Acknowledgements:

We wish to thank G.Kaiser – for her inestimable support in the laboratory; A.Neumann – for his excellent support with powder XRD analyses and interpretation of X-ray diffraction patterns;

References:

- [1]. H.Curtius, G.Kaiser, Z.Paparigas, B.Hansen, A.Neumann, M.Klinkenberg, E.Müller, H.Brücher, D.Bosbach, *Wechselwirkung mobilisierter Radionuklide mit sekundären Phasen in endlagerrelevanten Formationswässern*. Berichte des Forschungszentrums Jülich; 4333, ISSN 0944-2952.
- [2]. Danton, A.R. and N.W. Ashcroft, *Vegard's law*. Physical Review A (Atomic, Molecular, and Optical Physics), 1991. **13**(6): p. 3161-3164.

[3]. Curtius, H., K. Ufer, and K. Dardenne, *Preparation and characterization of Zr-IV containing Mg-Al-Cl layered double hydroxide*. *Radiochimica Acta*, 2009. **97**(8): p. 423-428.

[4]. Kulik, D., *GEM-Selektor. Research package for thermodynamic modelling of aquatic (geo)chemical systems by Gibbs Energy Minimization (GEM)*. <http://gems.web.psi.ch>.

[5]. Hummel, W., et al., *Nagra/PSI chemical thermodynamic data base 01/01*. *Radiochimica Acta*, 2002. **90**(9-11): p. 805-813.

[6]. Rozov, K., et al., *Solubility and thermodynamic properties of carbonate-bearing hydrotalcite-pyroaurite solid solutions with 3:1 Mg/(Al+Fe) mole ratio*. *Clays and Clay Minerals*, 2011. **59**(3): p. 215-232.

Ra-Ba Co-precipitation in a Large Scale Evaporitic System

Y. O. Rosenberg¹, V. Metz² and J. Ganor¹

¹ Department of Geological and Environmental Sciences, Ben-Gurion University of the Negev, P.O.B 653, Beer Sheva 84105, Israel.

email: yoavoved@gmail.com

² Institute for Nuclear Waste Disposal (INE), Karlsruhe Institute of Technology, P.O.B. 3640, 76021 Karlsruhe, Germany.

INTRODUCTION

The removal of radium during co-precipitation with barite (BaSO₄) (i.e., the precipitation of a (Ra,Ba)SO₄ solid solution) was extensively studied in laboratory experiments at different temperature and salinities [1-4]. The similar ionic radii, electronegativities and electronic configuration of Ra²⁺ and Ba²⁺ and the identical crystallographic structure of pure RaSO₄ and barite [5] make barite an almost ideal host mineral for Ra.

²²⁶Ra is a critical radionuclide with respect to the long-term safety of radioactive waste disposal (half-life of 1600 years). Hence, the fate of radium in deep bedrock repositories has been deserved special attention in safety case studies for potential high level waste repositories in Sweden and Switzerland [e.g., 6, 7]. As a result there is a growing interest in the radio-geochemistry community to understand how (Ra,Ba)SO₄ solid solution may control Ra solubility with respect to long-term safety issues of nuclear-waste disposal [8].

Due to the importance of the (Ra,Ba)SO₄ solid solution, ample studies investigated it on the laboratory scale (see references above). The dynamic of natural environment pose a degree of uncertainty when interpreting solid solution reactions based on field observations. Despite it, the approach closest to the natural environment is the deduction of empirical relation from field studies [9].

The aim of this study is to quantitatively understand the precipitation of a (Ra,Ba)SO₄ solid solution in the field. To this end the evaporation of reject brine enriched with Ra in a field system was studied. In light of the field system dynamics (i.e., changing temperature, evaporation rates, salinity and mineral precipitation rates), constrains can be made to the extent by which the (Ra,Ba)SO₄ solid solution is affected by these factors.

DESCRIPTION OF THE WORK

The co-precipitation of Ra²⁺ with barite was studied in a large scale field system, comprising 6 sequential evaporation ponds, having a total volume of 3.25·10⁵ m³, in which a rejected brine of a desalination plant is evaporated. The non-evaporated brine has an ionic strength of 0.7 m, ²²⁶Ra concentration of 12 Bq kg⁻¹, and it is oversaturated with respect to gypsum, celestite and barite. Upon its evaporation the

ionic strength increases up to 12 m, and a total amount of ~ 4·10⁶ kg year⁻¹ of sulphate minerals precipitates.

Two field campaigns, winter and summer, were carried out to sample the evaporitic system. The ponds water level was monitored by the plant operators on a weekly – monthly basis by measuring the water surface from a constant point on the ponds edge. Using the ponds dimensions, the mass of water at each pond was estimated. At each campaign brine and salt samples were collected and analyzed for their chemical composition and ²²⁶Ra content.

Calculations

Precipitation rate (mol sec⁻¹) of barite was calculated by assuming a steady state at each pond and that barite precipitation is the only sink of Ba according to:

$$(1) \quad Rate_{barite,n} = F_{in,n} \cdot [Ba]_{in,n} - F_{out,n} \cdot [Ba]_{pond,n}$$

where $[i]$ represents concentration (mol kg_{H₂O}⁻¹) of element i in pond n . $F_{in,n}$ and $F_{out,n}$ are the water inflow and outflow fluxes (kg_{H₂O} sec⁻¹) calculated according to the change in conservative ions ($C = Mg, K$ and Li):

$$(2) \quad F_{out,n} = F_{in,n} \cdot [C]_{in,n} / [C]_{pond,n}$$

Using a constant concentration-based partition coefficient for Ra in barite ($K'_{D,barite}$) in all of the ponds, [²²⁶Ra]_{pond,n} can be predicted as:

$$(3) \quad [{}^{226}Ra]_{pond,n} = \frac{F_{in,n} \cdot [{}^{226}Ra]_{in,n}}{F_{out,n} + Rate_{Ba,n} \cdot K'_{D,barite} / [Ba]_{pond,n}}$$

RESULTS

Using Eq. (3) the concentrations of ²²⁶Ra at steady state in each pond are predicted. This calculation relies on the derived $F_{in,n}$, $F_{out,n}$ and $Rate_{Ba,n}$ (Eqs. (1) and (2)), the measured $[Ba]_{pond,n}$ concentrations, and initially assumes a constant value for $K'_{D,barite}$ in all of the ponds regardless their ionic strength and barite precipitation rates. Only the initial measured [²²⁶Ra] concentration of the non-evaporated brine is included in the calculation for the prediction of [²²⁶Ra]_{pond,1} in pond 1; thereafter, the inflow [²²⁶Ra]_{in,2} of the next pond is set equal to the predicted value of the preceding pond.

Figure 1 presents the predicted values of [²²⁶Ra]_{pond,n} vs. the measured [²²⁶Ra] concentrations for the two field campaigns and under two assumptions: 1. $K'_{D,barite} = 1.04$ (closed symbols) as derived from laboratory experiments conducted with the same brine [4], and 2. $K'_{D,barite} = 1.8$ (open symbols) as derived from laboratory experiments by Doerner and Hoskins [1]. Generally the predicted values of [²²⁶Ra]_{pond,n} agrees

well with the measured values when considering the effective partition coefficient derived by Rosenberg et al. [4] (i.e., most of the values fall on the 1:1 dashed line). Moreover, as evaporation proceeds, the predicted values of $[^{226}\text{Ra}]_{\text{pond},n}$ using $K'_{D,\text{barite}} = 1.8$ over estimate the removal of Ra by co-precipitation. Before the final stages of evaporation (i.e., away from the origin, Fig. 1), measured $[^{226}\text{Ra}]_{\text{pond}}$ concentrations are 200-300% higher than the values predicted with $K'_{D,\text{barite}} = 1.8$.

The decrease in $K'_{D,\text{barite}}$ is due to kinetic and ionic strength effects on (Ra,Ba)SO₄ co-precipitation [4]. Note that the convergence of the open symbols toward the origin is due to the fact that the present study deals with a terminal system; that is, almost all of the water is evaporated at the end of the system, forcing the solutes to precipitate. As the value of $K'_{D,\text{barite}}$ decreases, more Ra remains in the solution. As long as the precipitation potential of barite is not exhausted all the Ra will be practically removed. However, in an alternative scenario where the precipitation of barite is brought to a halt (i.e., thermodynamic equilibrium or kinetic inhibition), remaining Ra concentrations can be significantly higher than expected when kinetic and ionic strength effects are disregarded.

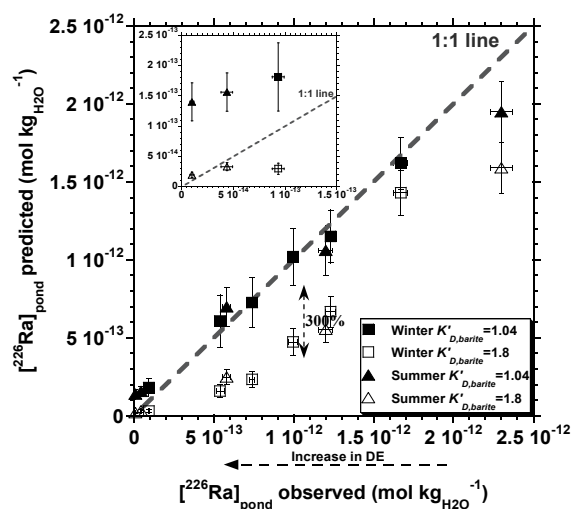


Fig. 1: Predicted ^{226}Ra concentrations vs. observed ^{226}Ra concentrations during winter (■, □) and summer (▲, △) campaigns. Ra concentrations were predicted using a partition model for Ra-Ba co-precipitation (Eq. (3)) in two scenarios: 1. $K'_{D,\text{barite}} = 1.04$ among all ponds (closed symbols); 2. $K'_{D,\text{barite}} = 1.8$ among all ponds (open symbols).

REFERENCES

1. Doerner, H.A., et al., Co-Precipitation of Radium and Barium Sulfates. *Journal of American Chemical Society*, **47**: p. 662-675. (1925).
2. Gordon, L., et al., Coprecipitation of Radium with Barium Sulfate. *Analytical Chemistry*, **29**(1): p. 34-37. (1957).
3. Marques, B.E., La Précipitation Fractionnée du Sulfate de Baryum Radifère. *Comptes rendus hebdomadaires des séances de l'Académie des sciences*, **198**: p. 1765-1767. (1934).
4. Rosenberg, Y.O., et al., Co-precipitation of radium in high ionic strength systems: 2. Kinetic and ionic strength effects. *Geochimica et Cosmochimica Acta*, **75**(19): p. 5403-5422. (2011).
5. Zhu, C., Coprecipitation in the Barite isostructural family: 1. Binary mixing properties. *Geochimica et Cosmochimica Acta*, **68**(16): p. 3327-3337. (2004).
6. Grandia, F., et al., *Assessment of the radium-barium co-precipitation and its potential influence on the solubility of Ra in the near-field*. SKB TR-08-07. 2008: Svensk Kärnbränslehantering AB, Stockholm.
7. Berner, U., et al., *Radium solubilities from SF/HLW wastes using solid solution and co-precipitation models*. 2002, Paul Scherrer Institute: Villigen, Switzerland, Internal Report TM-44-02-04.
8. Bosbach, D., Solid-solution formation and the long-term safety of nuclear-waste disposal, in *EMU notes in mineralogy*, M. Prieto and H. Stoll, Editors. 2010, European Mineralogical Union and the Mineralogical Society of Great Britain & Ireland: London. p. 345-376.
9. Böttcher, M.E., et al., Metal-ion partitioning during low-temperature precipitation and dissolution of anhydrous carbonates and sulphates, in *EMU notes in mineralogy*, M. Prieto and H. Stoll, Editors. 2010, European Mineralogical Union and the Mineralogical Society of Great Britain & Ireland: London. p. 139-188.

Iron-Based Waste Packages as Engineered Barriers in a Salt Repository

Gregory T. Roselle and Christi D. Leigh

*Sandia National Laboratories, Carlsbad Defense Waste Management Programs Group,
4100 National Parks Highway, Carlsbad, NM 88220, USA
email: gtrosel@sandia.gov*

INTRODUCTION

Deep geologic disposal of radioactive waste relies on multiple barriers whose function is to enhance the isolation of the waste from the environment. These barriers include both natural geologic barriers and engineered barrier systems. An effective engineered barrier system design includes both physical isolation and chemical containment. Numerous types of engineered barrier systems have been used and/or proposed world-wide. These barriers usually consist of a variety of sub-systems within a repository framework such as: the waste form, waste containers, buffers, backfill and seals/plugs.

The use of waste containers as part of an engineered barrier system typically involves the design of a container that is resistant to corrosion and thereby acts as a physical barrier to waste release. For example, the Swedish fuel disposal program (SKB) has proposed using a copper canister to encapsulate spent nuclear fuel. The canister is designed to withstand corrosion and any mechanical forces caused by movements in the rock. The Yucca Mountain Nuclear Waste Repository also proposed the use of a corrosion resistant outer canister as an engineered barrier. However, in this case the outer canisters were to be made of corrosion-resistant steel (alloy 22).

In contrast to these repository designs, the Waste Isolation Pilot Plant (WIPP) operated by the U.S. Department of Energy (DOE) emplaces waste in 208 liter (55-gal) low-C-steel drums (or other low-C-steel waste containers) in the repository that are not resistant to corrosion. In fact, the DOE does not take credit for containment of TRU waste by the waste containers. Nevertheless, the low-C-steel waste containers play an important role in impeding the movement of radionuclides through the near-field of the repository. This abstract explores the idea of using corrosion-allowable steel containers as engineered barriers.

WASTE ISOLATION PILOT PLANT

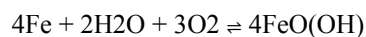
The Waste Isolation Pilot Plant (WIPP) is a deep geologic repository developed by the U.S. Department of Energy (DOE) for the disposal of defense-related transuranic waste. The WIPP is located in southeastern New Mexico at a depth of 655 m, within the bedded salts of the Permian Salado Formation. Waste emplaced in the WIPP is encapsulated primarily in 208 liter (55 gallon) drums composed of low carbon steel. The US DOE takes no credit for the waste containers as

engineered barriers. The only engineered barrier considered in WIPP is the MgO emplaced with the waste, which acts as a CO₂ and pH buffer. Even though no credit is taken for the corrosion of the steel containers as an engineered barrier, it does play an important role in minimizing radionuclide release.

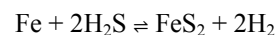
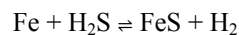
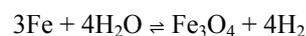
BEHAVIOR OF Fe-BASE WASTE PACKAGES IN WIPP

Closure of WIPP disposal rooms will begin to crush the drums (and other waste containers) about 10-15 years after emplacement. After repository closure, if brine enters the repository, low-C-steel waste containers will corrode. The corrosion of metals (particularly iron) in the WIPP (both in the waste and the waste containers) will quickly deplete the O₂ in the repository leading to anoxic conditions. Anoxic corrosion will be controlled by the availability of water (in brine) at the metal surface, as well as the internal atmosphere within the WIPP.

Oxic corrosion. (corrosion of steels via aqueous or gaseous free molecular O₂)



Anoxic corrosion. (corrosion of low-C steels without free molecular O₂)



Brine Availability. Where will the brine come from after the WIPP is filled and the panel closures are installed?

- Possible seepage into the repository from the disturbed rock zone (DRZ) around the repository. Total brine content of the Salado

Fm. typically 1-2 wt %, but can be up to 3 wt %

- Approximately 1.5% H₂O in the waste
- Possible seepage down the shafts from overlying formations
- Possible human intrusion (from inadvertent drilling) through the repository and into a brine reservoir in the underlying Castile formation

Many WIPP scientists and engineers argue that the quantities of brine predicted to enter the repository are overstated (typically for the sake of regulatory conservatism).

Gas Generation (H₂). According to probabilistic performance-assessment (PA) calculations carried out by the WIPP Project, anoxic corrosion of low-C steels could produce enough H₂ to increase the pressure in the repository to lithostatic (~150 atm). Any additional H₂ production initiates fracturing, or reopens preexisting fractures, in the repository-level anhydrite marker beds and clay seams. When this happens, PA predicts that H₂ migrates into the marker beds just above the repository.

EFFECTS OF METAL CORROSION IN THE WIPP

Metals in the form of low-carbon steel and lead are present within the waste itself, as well as the containers used to hold the waste. The current inventory predicts that 9.2×10^8 mol of Fe will be present in the waste and its containers. Anoxic corrosion of the low-C steel waste plays several significant roles in determining the nature of the environment within the WIPP following closure.

Near-field chemical conditions: Anoxic corrosion will result in strongly reducing conditions that are at or even below the lower stability limit of H₂O on an Eh-pH diagram (see below). In fact, f_{O_2} is so low that H₂O is unstable in the WIPP and H₂O is reduced to H₂ by low-C steels.

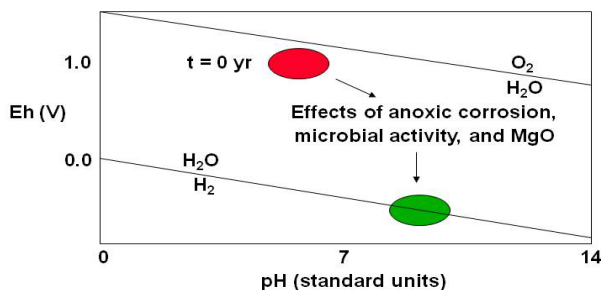


Fig. 1: Expected Eh vs. pH development of the WIPP near field chemical conditions.

Effects of reducing conditions on radioelement mobility: Radionuclides that can speciate in more than one oxidation state, but are less mobile when they occur in their lower or lowest oxidation states, would be reduced and thus immobilized under the strong reducing conditions produced by anoxic corrosion of metal in the repository. Examples include: U, Np, Pu, and Am in the TRU waste in the WIPP and Se, Tc, U, Np, Pu, and Am in spent fuel or high-level waste in a bedded or domal salt repository

ADVANTAGES OF CORROSION-ALLOWANCE STEEL AS ENGINEERED BARRIER

- Corrosion-allowance, Fe-base materials are inexpensive relative to corrosion-resistant materials
- Characterization of the behavior of corrosion-allowance materials is relatively straightforward
- Corrosion-allowance, Fe-base materials can create strongly reducing near-field conditions
- Corrosion-allowance, Fe-base materials will produce large quantities of corrosion products that will likely be very effective sorbers of radionuclides.

The function of an engineered barrier that is typically applied to waste containers is related to the physical containment of radionuclides. However, reducing the potential for radioelement transport by engineering the environment's chemistry can also create an effective barrier. A corrosion-allowance waste package can perform essentially two engineered barrier functions, one as an operational and near-term physical containment barrier and another as a long-term corrosion-produced chemical barrier. Moving from the concept of a corrosion-resistant waste package that is engineered to not react with the local environment to one that enhances containment by active environmentally-induced corrosion is a large shift from the traditional concept of engineering a barrier. In either case, the goal is to prevent or substantially delay the movement of water or radionuclides to the accessible environment, as well as reducing uncertainties in modeling performance of the disposal system.

ACKNOWLEDGEMENT

This research is funded by WIPP programs administered by the Office of Environmental Management (EM) of the U.S Department of Energy. Sandia National Laboratories is a multi-program laboratory managed and operated by Sandia Corporation, a wholly owned subsidiary of Lockheed Martin Corporation, for the U.S. Department of Energy's National Nuclear Security Administration under contract DE-AC04-94AL85000.

Solubility of Ferrous Oxalate Dihydrate in Magnesium Chloride and Sodium Chloride Solution

Je-Hun Jang, Martin B. Nemer, and Yong-Liang Xiong

*Sandia National Laboratories¹
 Carlsbad Programs Group
 4100 National Parks Highway
 Carlsbad, NM 88220, U.S.A.
 jjang@sandia.gov*

INTRODUCTION

Oxalate ($C_2O_4^{2-}$) combines with various divalent metal ions to form sparingly soluble minerals such as $CaC_2O_4 \cdot H_2O$ (Whewellite), $CaC_2O_4 \cdot 2H_2O$ (Weddellite), $MgC_2O_4 \cdot 2H_2O$ (Glushinskite), $MnC_2O_4 \cdot 2H_2O$ (Lindbergite), and $FeC_2O_4 \cdot 2H_2O$ (Humboldtine). These minerals are typically found at the lichen-rock interfaces, and sometimes serve as indicators of active chemical weathering driven by oxalate-producing microorganisms. At the Waste Isolation Pilot Plant (WIPP) near Carlsbad, New Mexico, U.S.A., oxalate is present as a waste component, and a significant amount of iron is present in the form of steel waste canisters. Oxalate can solubilize actinides by forming aqueous complexes, increasing their mobility. A favorable removal mechanism for oxalate is its precipitation with benign cations. Under the reducing conditions present at WIPP after closure, it is possible that ferrous oxalate dihydrate ($FeC_2O_4 \cdot 2H_2O$, humboldtine) could form if oxalate is available after the formation of whewellite. A limited number of literature articles have dealt with the solubility product for $FeC_2O_4 \cdot 2H_2O$. To determine the solubility product for $FeC_2O_4 \cdot 2H_2O$, we examined the dissolution of $FeC_2O_4 \cdot 2H_2O$ by measuring the concentration of dissolved ferrous iron ($[Fe(II)]_{diss}$) with the Ferrozine method in $MgCl_2$ and $NaCl$ solutions of incremental concentrations. Some reactors took more than 400 days to achieve apparent equilibrium in terms of $[Fe(II)]_{diss}$. Higher $[Fe(II)]_{diss}$ was observed in $MgCl_2$ and $NaCl$ solutions of higher concentration. At comparable ionic strengths, the $[Fe(II)]_{diss}$ in $MgCl_2$ solution was higher than in $NaCl$ solution. In $MgCl_2$ solution, phenomena such as (i) a color change in reactors of lower solid-to-liquid ratio and (ii) a higher $[Fe(II)]_{diss}$ in reactors of higher solid-to-liquid ratio were observed, which could indicate the presence of reaction(s) other than simple dissolution of $FeC_2O_4 \cdot 2H_2O$. Further chemical and theoretical analyses are in progress and will be presented in the meeting together with conclusions.

¹ Sandia National Laboratories is a multi-program laboratory operated by Sandia Corporation, a wholly owned subsidiary of Lockheed Martin Corporation, for the U.S. Department of Energy's National Nuclear Security Administration under contract DE-AC04-94AL85000.

Experimental Determination of Solubilities of Sodium Tetraborate (Borax) in NaCl Solutions to High Ionic Strengths, and Thermodynamic Model for the Na-B(OH)₃-Cl-SO₄ System

Yongliang Xiong¹, Leslie Kirkes¹, Terry Westfall¹, and Taya Olivas¹

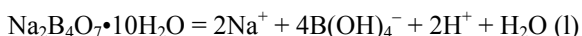
¹ Sandia National Laboratories (SNL), Carlsbad Programs Group, 4100 National Parks Highway, Carlsbad, NM 88220, USA
email:yxiong@sandia.gov

INTRODUCTION

Recent experimental studies have suggested that borate could potentially complex with Nd(III), an analog to Am(III) [1]. Therefore, a comprehensive thermodynamic model involving interactions of borate with major ions in brines is needed to accurately describe the contributions of borate to the solubility of Am(III) in brines in salt formations, as they contain significant concentrations of borate.

DESCRIPTION OF THE WORK

In this study, solubility experiments on sodium tetraborate (Na₂B₄O₇·10H₂O, borax) are conducted in NaCl solutions up to 5.0 m at room temperature (22.5 ± 1.5 °C). In combination with solubility data of sodium tetraborate in Na₂SO₄ solutions from literature, the solubility constant (log *K*) for sodium tetraborate regarding the following reaction,



is determined as -24.88 ± 0.10 °C based on the Pitzer model. In addition, the lambda parameter ($\lambda_{\text{NaB}(\text{OH})_4(\text{aq}), \text{Na}^+}$) for the interaction between NaB(OH)₄(aq) and Na⁺ is evaluated as 0.09192. It is also discovered that it is necessary to revise $\theta_{\text{B}(\text{OH})_4^-, \text{SO}_4^{2-}}$ of the Felmy and Weare (1986) [2] model and include $\Psi_{\text{B}(\text{OH})_4^-, \text{SO}_4^{2-}, \text{Na}^+}$ in order to accurately model solubility of sodium tetraborate in Na₂SO₄ medium. The revised $\theta_{\text{B}(\text{OH})_4^-, \text{SO}_4^{2-}}$ is 0.1697 in comparison with the value of -0.012 in the Felmy and Weare (1986) model, and $\Psi_{\text{B}(\text{OH})_4^-, \text{SO}_4^{2-}, \text{Na}^+}$ is 0.096.

RESULTS

The model developed in this study, which incorporates NaB(OH)₄(aq) $\Psi_{\text{B}(\text{OH})_4^-, \text{SO}_4^{2-}, \text{Na}^+}$ and revised values for log *K* for sodium tetraborate and for $\theta_{\text{B}(\text{OH})_4^-, \text{SO}_4^{2-}}$, can precisely model solubility of sodium tetraborate to high

ionic strengths. The comparison of the current model with that of Felmy and Weare (1986) demonstrates that there is a significant improvement associated with the current model in predicting solubilities of sodium tetraborate in both NaCl and Na₂SO₄ media. The current model is also validated by comparison of model predicted solubilities of sodium tetraborate in the mixtures of NaCl + Na₂SO₄ to ionic strengths of 8.0 m with independent experimental values from the literature. The validation test indicates that the differences between solubilities predicted by the current model and experimental solubilities are less than 0.05 m with an error less than 30% (Figure 1). In comparison, the differences between solubilities predicted by the Felmy and Weare (1986) model and experimental solubilities are generally higher than 0.05 m, and can be as high as 0.17 m with an error up to 150%.

ACKNOWLEDGEMENTS

Sandia National Laboratories is a multiprogram laboratory operated by Sandia Corporation, a wholly owned subsidiary of Lockheed Martin Corporation, for the United States Department of Energy's National Nuclear Security Administration under Contract DE-AC04-94AL85000. This research is funded by WIPP programs administered by the Office of Environmental Management (EM) of the U.S Department of Energy.

Formation and equilibrium conditions of An(III,IV,V,VI)-*eigencolloids* in dilute to concentrated NaCl, CaCl₂ and MgCl₂ solutions

X. Gaona, V. Neck[†], M. Altmaier

*Institut für Nukleare Entsorgung, Karlsruher Institut für Technologie (KIT-INE), Germany
xavier.gaona@kit.edu*

INTRODUCTION

The behaviour of actinides under repository conditions is closely related to the redox state in which An are present. The NEA thermodynamic data books [1,2] provide a very accurate review and data selection for the most relevant redox states of An solid compounds and aqueous species, the latter accounting only for monomeric (or small oligomeric) species.

The formation of An-*eigencolloids* (or colloids intrinsically formed by actinides) has been documented for An(IV) [3,4]. Systematic experimental observations in the near-neutral to strongly alkaline pH range from under- and over-saturation solubility experiments show [An(IV)] ~ 100 times higher than those predicted by thermodynamic calculations, when no or insufficient phase separation is performed. This observation is valid for NaCl, NaClO₄ or MgCl₂ and a wide range of I (0.1M to 7.5M), and highlights the relevant role that An(IV)-*eigencolloids* may play in the source term and near-field processes of a repository.

DESCRIPTION OF THE WORK

In this work, new experimental efforts were dedicated to assess the possible formation of An(III)-, An(V)- and An(VI)-*eigencolloids*. Undersaturation solubility experiments conducted with Nd(OH)₃(am,hyd) resulted in [Nd] ~ 100 to 1000 times higher than those predicted by thermodynamic calculations for $-\log[H^+] > 10$, when no phase separation was considered. Centrifugation of the supernatant at 4000 g for 10 minutes decreased this concentration to values only slightly higher than those obtained by ultrafiltration or ultracentrifugation, indicating that An(III)-*eigencolloids* may form but do not show the high relevance observed for An(IV).

Undersaturation solubility experiments conducted with NpO₂OH(am,hyd) for $9 \leq -\log[H^+] \leq 14$ and $0.1M \leq I \leq 5M$ (for both NaCl and NaClO₄) led to the same Np concentration with (10kD ultrafiltration) or without a separation step, therefore confirming the absence of An(V)-*eigencolloids*, even at concentration levels of 10⁻⁷ M.

A well-characterized Na₂U₂O₇·H₂O(cr) solid phase was used to assess the formation of U(VI)-*eigencolloids*. When performing undersaturation solubility experiments for $9.5 \leq -\log[H^+] \leq 13.5$ and no phase separation, [U(VI)] ~ 100 times higher than thermodynamic predictions were determined for both I = 0.5M NaCl and I = 5M NaCl. Centrifugation of the supernatant at 4000 g for 10 minutes, however,

decreased U(VI) concentration to levels defined by monomeric UO₂(OH)₃⁻ and UO₂(OH)₄²⁻. These results highlight the importance of An(IV)- compared to An(III)-*eigencolloids*, as well as the absence of solubility enhancement by An(V,VI)-*eigencolloid* formation.

Ongoing studies to assess An(IV)-*eigencolloids* involvement in thermodynamic equilibrium reactions focus on ²³²Th-²²⁸Th isotopic distribution in ThO₂·xH₂O (undersaturation) solubility experiments in alkaline conditions. These results will be discussed in combination with the tendency of actinides to hydrolyze (An(V) < An(III) < An(VI) < An(IV)), its possible relationship with *eigencolloid* formation and the relevance of the latter for the safety assessment of actinides.

REFERENCES

1. Guillaumont, R. et al., "Chemical Thermodynamics 5. Update on the Chemical Thermodynamics of Uranium, Neptunium, Plutonium, Americium and Technetium" NEA OECD, Elsevier (2003).
2. Rand, M.H. et al. "Chemical Thermodynamics 11: Chemical Thermodynamics of Thorium". NEA OECD, Elsevier (2009).
3. Altmaier, M. et al. "Solubility and colloid formation of Th(IV) in concentrated NaCl and MgCl₂ solution" *Radiochimica Acta*, **92**, 537-543 (2004).
4. Neck, V. et al. "Solubility of plutonium hydroxides/hydrous oxides under reducing conditions and in the presence of oxygen" *C. R. Chimie*, **10**, 959-977 (2007).

The Models for the Colloid Source Term at WIPP

David C. Sassani¹ and Christi D. Leigh²

¹Sandia National Laboratories, P.O. Box 5800, MS 0736, Albuquerque, NM 87185-0736, USA
email: dsassan@sandia.gov

²Sandia National Laboratories, Carlsbad Defense Waste Management Programs Group,
4100 National Parks Highway, Carlsbad, NM 88220, USA

INTRODUCTION

The Waste Isolation Pilot Plant (WIPP) is a U.S. Department of Energy (DOE) repository in southeast New Mexico (Carlsbad, NM) for Defense transuranic (TRU) waste. The WIPP was initially certified in May 1998 and opened operations in March 1999¹. Since then, it has received a first recertification in April 2006 and a second recertification in November 2010.

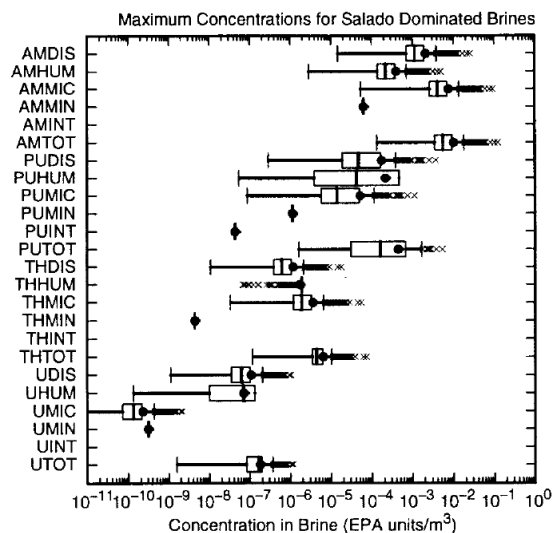
The disposal facility is located in the Salado Fm., which is a Permian bedded-salt formation. The Salado Fm. consists mostly (90 - 95 wt %) of salt that is nearly pure halite (NaCl). The formation also includes clay seams and “marker beds” with anhydrite (CaSO₄), gypsum (CaSO₄·2H₂O), magnesite (MgCO₃), polyhalite (K₂MgCa₂(SO₄)₄·2H₂O), and clays. Fluid exists within the Salado as intergranular (grain-boundary) brine, intragranular brine (fluid inclusions) with an average total brine content of ~1-2 wt % (ranging up to ~3 wt %).

The WIPP disposal facility is located at a depth of 655 m (2150 ft) below surface and has been constructed with multiple panels of disposal rooms. The WIPP waste is comprised typically of equipment/disposables associated with weapons production. Though the WIPP waste consists mainly of contact-handled (CH) waste, the inventory also contains some remote handled (RH) waste.

DESCRIPTION OF THE WORK

The WIPP compliance certification application (CCA) performance assessment (PA) source term model includes dissolved radionuclides constrained by solubility limits of actinide phases and actinides associated with a variety of colloid types². The four colloid types included within the WIPP CCA are actinide intrinsic colloids (i.e., Pu eigencolloids), mineral fragment colloids, humic substance colloids, and microbial colloids (these last three types each attach U, Pu, Np, Th, and Am). The CCA results show that colloidal actinides contributed substantially to calculated Am, Pu, and Th releases (Figure 1)³.

The parameter constraints used to implement the colloid representations within the WIPP PA have changed very little in the compliance recertification applications submitted in 2004⁴ and 2009⁵. As such, Table SOTERM-25 of Appendix SOTERM-2009⁵ shows that, for the median parameter values, releases are dominated generally by colloidal species.



TRI-6342-5151-0

Fig. 1: Elemental concentrations (EPA units/m³) in Salado brines for Am, Pu, Th, and U as dissolved (DIS) and colloidal forms: humic substance (HUM); microbial (MIC); mineral fragment (MIN); or intrinsic (INT); and totals (TOT)³.

RESULTS

Investigations into the models for colloids at WIPP⁶ are evaluating more recent literature data and concepts together with completed and ongoing targeted experimental work at both Sandia National Laboratories and Los Alamos National Laboratory. These studies are working towards answering regulatory questions regarding potential additional colloids species for consideration (e.g., Th intrinsic colloids^{7, 8}) and to identify updated parameter values that would constrain apparent model conservatism.

Such conservations include (a) fully populating the mineral fragment and humic substances colloids surfaces with *each* of the actinides considered (i.e., no competition for sites) and (b) choosing values of actinide-humic substance complexation constants at solution compositions (e.g., pH of ~6 and no reaction with the MgO engineered barrier) that maximize the binding of radionuclides to these colloids. Reparameterization will facilitate sensitivity studies for quantifying conservatism in the colloid models, and can even provide the detailed bases for updated baseline PA models.

For example, by accounting for flocculation of humic substance colloids in WIPP relevant brines

reacted with MgO (Figure 2)^{9,10}, the reparameterization of the humic-substance colloid model would provide a representation that is more relevant to the expected WIPP conditions. Specifically, the resulting pH above 9 would mean that actinide-humic complexation constants would be expected to be far lower than those used (at pH of 6) and the expected concentration of humic substances under WIPP relevant conditions would be adjusted to zero.

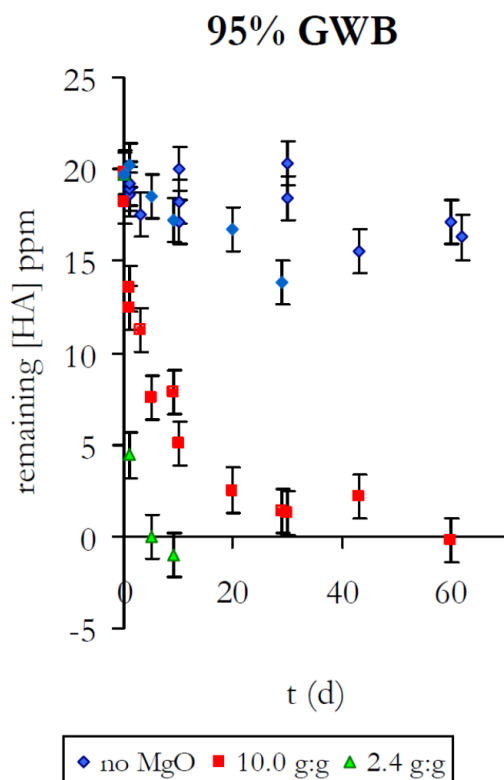


Fig. 2: Example of Humic Acid coagulation over time (d–days) with and without Premier MgO (g:g– grams liquid per grams solid) in WIPP Generic Weep Brine (GWB)⁹.

REFERENCES

- MORA, C. J., “Sandia and the Waste Isolation Pilot Plant 1974 - 1999” SAND99-1482, (1999).
- U.S. DOE, “Title 40 CFR Part 191 Compliance Certification Application for the Waste Isolation Pilot Plant” Vol. 1 21. DOE/CAO-1996-2184. Carlsbad, NM: U.S. Department of Energy Carlsbad Area Office (1996).
- HELTON J. C., Bean, J. E., Berglund, J. W., Davis, F. J., Economy, K., Garner, J. W., Johnson, J. D., MacKinnon, R. J., Miller, J., O’Brien, D. G., Ramsey, J. L., Schreiber, J. D., Shinta, A., Smith, L. N., Stoelzel, D. M., Stockman, C., and Vaughn, P., “Uncertainty and Sensitivity Analysis Results Obtained in the 1996 Performance Assessment for the Waste Isolation Pilot Plant” (see Figure 11.1.1) Sandia Report SAND98-0365 (1999).
- U.S. DOE, “Title 40 CFR 191 Parts B and C Compliance Recertification Application for the Waste Isolation Pilot Plant” 10 vols. DOE/WIPP-04-3231. Carlsbad, NM: U.S. Department of Energy Carlsbad Field Office (2004).
- U.S. DOE, “Title 40 CFR Part 191 Subparts B and C Compliance Recertification Application for the Waste Isolation Pilot Plant” DOE/WIPP-09-3424. Carlsbad, NM: U.S. Department of Energy Carlsbad Field Office (2009).
- SASSANI, D. C., “Analysis Plan for Evaluating Constraints on Colloid Parameters in the WIPP Repository”, Sandia National Laboratories Waste Isolation Pilot Plant AP-152, (2011).
- ALTMAYER, M., V. Neck, and T. Fanghänel, “Solubility and Colloid Formation of Th(IV) in Concentrated NaCl and MgCl₂ Solution,” *Radiochimica Acta*, Vol. 92, no. 9-11, page 537-543 (2004).
- XIONG, Y.L., L.H. Brush, J.W. Garner, and J.J. Long “Responses to Three EPA Comments Pertaining to Comparisons of Measured and Predicted Dissolved and Colloidal Th(IV) and Am(III) Concentrations” Analysis Report May 4, 2010, Carlsbad, NM: Sandia National Laboratories, ERMS 553409 (2010).
- WALL, N.A. and S.A. Mathews, “Humic acids in the WIPP”, Presentation for 2003 Radiochemistry Conference, Carlsbad, NM, July 14-16, 2003, SAND2003-1683P, (2003).
- WALL, N.A. and S.A. Mathews, “Sustainability of humic acids in the presence of magnesium oxide.” *Applied Geochemistry*, No. 9, 20, page 1704-1713 (2005).

Sandia National Laboratories is a multi-program laboratory managed and operated by Sandia Corporation, a wholly owned subsidiary of Lockheed Martin Corporation, for the U.S. Department of Energy’s National Nuclear Security Administration under contract DE-AC04-94AL85000. This research is funded by WIPP programs administered by the Office of Environmental Management (EM) of the U.S. Department of Energy.

Solubility of $\text{TcO}_2(\text{s}) \cdot x\text{H}_2\text{O}$ in dilute to concentrated NaCl , CaCl_2 , and BaCl_2 solutionsT. Kobayashi¹, E. Yalcintas¹, M. Altmaier¹¹ Karlsruhe Institute of Technology, Institut für Nukleare Entsorgung, P. O. Box 3640, 76021 Karlsruhe, Germany, taishi.kobayashi@kit.edu**INTRODUCTION**

Safety assessment for nuclear waste repositories in rock salt requires a reliable prediction of radionuclide solubility limits in relevant high saline system. ⁹⁹Tc in radioactive waste is one of the fission products of ²³⁵U and ²³⁹Pu and has a long half life ($2.1 \cdot 10^5$ y). Under reducing conditions, Tc exists in tetravalent oxidation state [1], and the migration behaviour primarily depends on the solubility of Tc(IV) oxide. Although several literature data on the solubility of Tc(IV) oxide have reported and reviewed [1-4], they are mostly limited in dilute aqueous systems. Hess et al. investigated the solubility of $\text{TcO}_2(\text{s}) \cdot x\text{H}_2\text{O}$ in dilute to concentrated NaCl solution [4] in acidic and neutral pH region, and Tc(IV)-Cl complex and compounds has been proposed under the conditions of high Cl concentration. However, little is known in alkaline pH region and no solubility data have been reported in other brine system.

The present study mainly focuses on the Tc(IV) solubility in CaCl_2 solutions, since the corrosion of an excess amount of cementitious waste forms in MgCl_2 brines leads to CaCl_2 -dominated solutions. Recent studies have revealed that tetravalent actinide (An(IV)) forms ternary Ca-An(IV)-OH complexes in CaCl_2 solutions [5,6]. For the performance assessment of waste disposal, it is highly important to evaluate a possible impact of Ca complex formation on the Tc(IV) solubility.

In this study, the solubility of $\text{TcO}_2(\text{s}) \cdot x\text{H}_2\text{O}$ in dilute to concentrated NaCl, CaCl_2 , and BaCl_2 solutions is investigated under neutral and alkaline pH conditions. $\text{TcO}_2(\text{s}) \cdot x\text{H}_2\text{O}$ is preliminarily prepared from Tc(VII) stock solution by electrochemical reduction and by the reduction with $\text{Na}_2\text{S}_2\text{O}_4$. The solid phase is then placed into the sample solutions and the solubility is determined after aging periods. For comparison, sample solutions are also prepared by oversaturation approach, where the initial Tc(VII) is directly reduced to obtain Tc(IV) solubility by adding $\text{Na}_2\text{S}_2\text{O}_4$ and Sn(II).

EXPERIMENTAL

In the undersaturation method, the solids precipitated by three different methods; (1) $\text{TcO}_2(\text{s}) \cdot x\text{H}_2\text{O}$ directly precipitated from 2 mM TcO_4^- by electrochemical reduction, (2) $\text{TcO}_2(\text{s}) \cdot x\text{H}_2\text{O}$ directly precipitated from 1 mM TcO_4^- by adding $\text{Na}_2\text{S}_2\text{O}_4$, (3) 0.1 mM TcO_4^- reduced electrochemically to obtain $\text{Tc(IV)Cl}_5 \cdot \text{H}_2\text{O}$ in 1 M HCl and $\text{TcO}_2(\text{s}) \cdot x\text{H}_2\text{O}$ precipitated by adding NaOH. All these solid phases were separated by

centrifugation and washed with 1 mM $\text{Na}_2\text{S}_2\text{O}_4$ and $\text{CaCl}_2/\text{Ca(OH)}_2$ several times. The suspension of $\text{TcO}_2(\text{s}) \cdot x\text{H}_2\text{O}$ was placed into the sample solutions of 0.5, 1.0, 2.0, and 4.5 M $\text{CaCl}_2/\text{Ca(OH)}_2$ containing 1 mM $\text{Na}_2\text{S}_2\text{O}_4$ to keep the reducing condition. The sample solutions in NaCl/NaOH and $\text{BaCl}_2/\text{Ba(OH)}_2$ were also prepared in a similar method. In the oversaturation method, aliquots of TcO_4^- stock solution were added to the sample solutions which were pre-equilibrated with $\text{Na}_2\text{S}_2\text{O}_4$ and Sn(II) at given pHs. All solid phase and sample preparations were performed in an Ar glove box.

After given periods, hydrogen ion concentrations (pH_c) and redox potential (E_h) were determined with combination pH electrodes (type ROSS, Orion) and Pt combination electrode with Ag/AgCl reference system (Metrohm). After filtration through 10kD ultrafiltration membranes (Pall Life Sciences), Tc concentration was determined by liquid scintillation counting (LSC) with TriCarb 2500TR/AB instrument (Cammerra-Packard). The detection limit for ⁹⁹Tc is approximately 10^{-8} M. In order to investigate the Tc oxidation state, the solvent extraction technique was used. After the filtration, sample solutions were contacted to chloroform containing 1 mM tetraphenylphosphonium chloride (TPPC) (Aldrich) to extract TcO_4^- to the organic phase.

RESULTS**1. Tc(IV) solubility in 0.1 M NaCl/NaOH solution**

The solubility prepared by method (3) increased with an increasing pH_c in the range of $\text{pH}_c > 11$, suggesting the formation of anionic hydrolysis species such as TcO(OH)_3^- proposed in the literature [3]. The solubility data by undersaturation method agrees well with the values by oversaturation method, where initial 10^{-5} M TcO_4^- was reduced by Sn(II) [7]. When the solid phase was prepared by adding $\text{Na}_2\text{S}_2\text{O}_4$ (method (2)), the obtained values are almost constant at $10^{-7.2}$ M at $\text{pH}_c > 11$, due to the possible contribution of colloids or residual Tc(VII). In our recent study, the Tc(VII) reduction kinetics in $\text{Na}_2\text{S}_2\text{O}_4$ solution was found to be much slower than in Sn(II) [7].

2. Tc(IV) solubility in 0.5 - 4.5 M $\text{CaCl}_2/\text{Ca(OH)}_2$ solution by undersaturation method

The solubility of $\text{TcO}_2(\text{s}) \cdot x\text{H}_2\text{O}$ in 1.0 M $\text{CaCl}_2/\text{Ca(OH)}_2$ prepared by direct electrochemical reduction (method (1)) are similar to the solubility in 0.1 M NaCl/NaOH (method (3)). No significant effect in $\text{CaCl}_2/\text{Ca(OH)}_2$ was observed. When the solid phase was prepared by $\text{Na}_2\text{S}_2\text{O}_4$ reduction (method (2)), the

obtained values are constant at $10^{-7.2}$ M at $\text{pH}_c > 10$, which is similar to the case in 0.1 M NaCl/NaOH (method (2)).

The solubility data in 0.5, 1.0, 2.0 and 4.5 M $\text{CaCl}_2/\text{Ca}(\text{OH})_2$ solutions are compared in Fig. 1. The solid phases were prepared by the electrochemical reduction. After the aging period more than 7 months, although the data in 2.0 and 4.5 M $\text{CaCl}_2/\text{Ca}(\text{OH})_2$ are slightly higher than the data in 0.5 and 1.0 M, no significant effect due to the Ca-Tc(IV)-OH complex formation is confirmed.

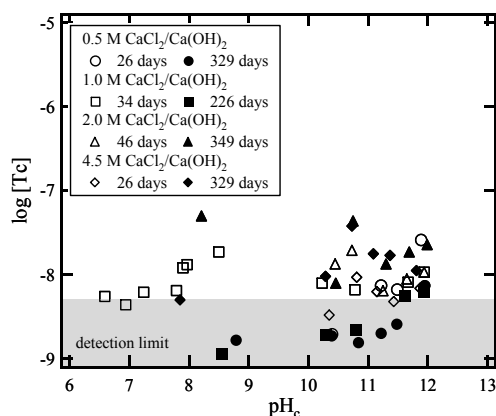


Fig. 1 Solubility of $\text{TcO}_2(\text{s}) \cdot x\text{H}_2\text{O}$ in 0.5 – 4.5 M $\text{CaCl}_2/\text{Ca}(\text{OH})_2$ obtained after the filtration through 10 kD membranes. The solid phases were preliminarily prepared by electrochemical reduction and placed into the sample solutions. The maximum pH_c in the system is 12.

3. Tc(IV) solubility in 0.5 - 4.5 M $\text{CaCl}_2/\text{Ca}(\text{OH})_2$ solution by oversaturation method

When the sample solutions were prepared directly from TcO_4^- by adding $\text{Na}_2\text{S}_2\text{O}_4$ or $\text{Sn}(\text{II})$, it was observed that the steady state was established after several weeks. The values from oversaturation approach in 0.5 – 4.5 M $\text{CaCl}_2/\text{Ca}(\text{OH})_2$ are much higher than the values from undersaturation approach shown in Fig 1, while rapid decrease of initial Tc concentrations was observed in the oversaturation solubility experiment in 0.1 M NaCl/NaOH. In the oxidation state analysis by solvent extraction method, less than 10 % of Tc in the solution extracted to the organic phase, indicating the limited contribution of TcO_4^- . The observed E_h values, which are much lower than the stability field of TcO_4^- , also support the results of the extraction experiment.

From the oversaturation approach in $\text{CaCl}_2/\text{Ca}(\text{OH})_2$, it may need more time to reach an equilibrium with macroscopic amount of solid phase, and colloids may exist as rather stable state, contributing the measured solubility data. For further investigation of the Tc(IV) solubility, the characterization of the solid phase is needed both in oversaturation and undersaturation experiments.

4. Tc(IV) solubility in 0.1 and 1.0 M $\text{BaCl}_2/\text{Ba}(\text{OH})_2$ solution

$\text{BaCl}_2/\text{Ba}(\text{OH})_2$ system is considered to be an analogous to $\text{CaCl}_2/\text{Ca}(\text{OH})_2$ system and has higher maximum $\text{pH}_c \sim 13$. The solubility in 0.1 and 1.0 M $\text{BaCl}_2/\text{Ba}(\text{OH})_2$ was obtained up to pH_c 13. No significant difference was observed compared to the values in 0.1 M NaCl/NaOH system even at high pH region.

CONCLUSION

The solubility of $\text{TcO}_2(\text{s}) \cdot x\text{H}_2\text{O}$ in NaCl/NaOH, $\text{CaCl}_2/\text{Ca}(\text{OH})_2$, and $\text{BaCl}_2/\text{Ba}(\text{OH})_2$ was investigated from undersaturation and oversaturation approaches. The solubility of $\text{TcO}_2(\text{s}) \cdot x\text{H}_2\text{O}$ in 0.5 – 4.5 M $\text{CaCl}_2/\text{Ca}(\text{OH})_2$ solutions showed similar values to the solubility in 0.1 M NaCl/NaOH solutions, suggesting no significant effect of Ca-Tc(IV)-OH complex formation. Higher solubility data in the oversaturation method may arise from the possible contribution of the colloids. The solid phase analysis is planned for further investigation of the Tc(IV) solubility in saline systems.

REFERENCES

1. Rard J. et al., *Chemical Thermodynamics of Technetium*, Elsevier, Amsterdam (1999).
2. Mayer R. et al., "Solubilities of Tc(IV) Oxides, *Radiochim. Acta*, **55**, 11-18 (1991).
3. Eriksen T. et al., "The solubility of $\text{TcO}_2 \cdot n\text{H}_2\text{O}$ in Neutral to Alkaline Solutions under Constant p_{CO_2} ", *Radiochim. Acta*, **58/59**, 67-70 (1992).
4. Hess N. et al., "Thermodynamic Model for the Solubility of $\text{TcO}_2 \cdot x\text{H}_2\text{O}(\text{am})$ in the Aqueous Tc(IV) – $\text{Na}^+ - \text{Cl}^- - \text{H}^+ - \text{OH}^- - \text{H}_2\text{O}$ System, *J. Solution Chem.*, **33**, 199-226 (2004).
5. Fellhauer D. et al., "Solubility of tetravalent actinides in alkaline CaCl_2 solutions and formation of $\text{Ca}_4[\text{An}(\text{OH})_8]^{4+}$ complexes: A study of Np(IV) and Pu(IV) under reducing conditions and the systematic trend in the An(IV) series", *Radiochim. Acta*, **98**, 541-548 (2010).
6. Altmaier M. et al., "Solubility of Zr(IV), Th(IV) and Pu(IV) hydrous oxides in alkaline CaCl_2 solution and the formation of ternary Ca-M(IV)-OH complexes", *Radiochim. Acta*, **96**, 541-550 (2008).
7. Kobayashi T. et al., "Redox behaviour of the Tc(VII)/Tc(IV) couple in diluted NaCl solution in various reducing systems"; Proceedings for 7th international symposium on Technetium and Rhenium, to be published.

Redox Behavior of the Tc(VII)/Tc(IV) Couple in Dilute to Concentrated NaCl Solutions

E. Yalcintas, T. Kobayashi, M. Altmaier, H. Geckeis

*Karlsruhe Institute of Technology, Institut für Nukleare Entsorgung, P.O. Box 3640, 76021 Karlsruhe, Germany
ezgi.yalcintas@kit.edu***INTRODUCTION**

For the long-term performance assessment of nuclear waste repositories, predictions of radionuclide solubility limits are of high importance. Due to its high abundance in nuclear waste and long half-life ($^{99}\text{Tc} \sim 211\,000\text{ a}$), technetium is an element of high relevance for nuclear waste disposal. A robust assessment of Tc reduction-oxidation (redox) processes is required, as they control Tc geochemistry and solubility in aqueous systems and influence the migration behavior of technetium in the environment. For nuclear waste disposal in rock salt formations (WIPP, Gorleben), technetium redox process and Tc(IV) solubility in highly saline NaCl, MgCl_2 and CaCl_2 brines need to be investigated.

In aqueous geological systems, Tc will be either present in Tc(VII) or Tc(IV) oxidation state [1]. The heptavalent TcO_4^- pertechnetate anion, is the most stable species under non-reducing conditions and highly soluble. On the other hand, sparingly soluble tetravalent hydrous oxide ($\text{TcO}_2 \cdot x\text{H}_2\text{O}$) is formed by Tc(VII) reduction [1] and can be described as



The redox behavior of the Tc(VII)/Tc(IV) couple has been investigated in many reducing aqueous systems [2-6]. For instance, Cui et al. observed that the reduction of Tc(VII) to Tc(IV) by Fe(II)(aq) was kinetically hindered while precipitated Fe(II) and sorbed Fe(II) on the vessel walls rapidly reduced Tc(VII) [2]. The redox behaviour of Tc(VII) by Fe(II)(aq) was also investigated at pH 6-8 [3] and in acidic solutions with different experimental parameters such as Fe(II)(aq) concentration [4]. $\text{Na}_2\text{S}_2\text{O}_4$ and Sn(II) were also used as reducing chemicals in solubility experiments due to the fast and complete reduction of Tc(VII) [5,6]. Recently, the applicability of thermo-dynamics to explain redox behaviour of Tc(VII) with E_h -pH diagrams was shown for dilute systems using various kind of homogenous and heterogeneous reducing chemicals [7]. The understanding of Tc redox behaviour is currently rather restricted to dilute aqueous systems as very little experimental data and, to our knowledge, no systematic studies have been performed in concentrated salt brine media.

In the present study, the redox behaviour and transformation of the Tc(VII)/Tc(IV) couple was investigated in 0.1 M, 0.5 M and 5.0 M NaCl solutions. Several reducing chemicals in homogenous aqueous systems (hydroquinone, methylene blue, $\text{Na}_2\text{S}_2\text{O}_4$, SnCl_2), and heterogeneous suspensions (like Fe(II)/Fe(III) or Fe powder systems) were investigated. The

results are systematised according to the E_h /pH conditions in solution to predict Tc redox behaviour in high saline systems. Furthermore, data are compared with thermodynamic calculations and predictions.

EXPERIMENTAL

The samples were prepared at different ionic strength conditions in NaCl (0.5 M and 5.0 M) with additions of 1mM $\text{Na}_2\text{S}_2\text{O}_4$, 1mM SnCl_2 , 3mM hydroquinone (HQ), 0.1mM Methylene blue (MB), 1mM/0.1mM Fe(II)/Fe(III) and 1mg/ 15ml Fe powder. The pH values were adjusted by HCl and NaOH of same ionic strength and the initial Tc(VII) concentration set to $[\text{TcO}_4^-] = 10^{-5}\text{ M}$ by addition of NaTcO_4 stock solutions to the pre-equilibrated solutions. Hydrogen ion concentrations (pH_c) were determined using a combination glass electrode (type ROSS, Orion). The values of $\text{pH}_c = \text{pH}_{\text{exp}} + A$ were obtained from the operational "measured" pH_{exp} values using empirical corrections factors. The redox potentials were measured with a Pt-combination electrode (Metrohm) using a Ag/AgCl reference. The measured values were converted to E_h versus the standard hydrogen electrode by correction for the potential of the Ag/AgCl reference electrode (+208 mV for 3 M KCl junction electrolyte). No corrections for high ionic strength conditions were applied. After 10 kD (2-3 nm) ultrafiltration, the Tc concentration in the filtrate was determined by Liquid Scintillation Counting (Quantulus, Perkin Elmer).

RESULTS

In the $\text{Na}_2\text{S}_2\text{O}_4$ system, the Tc concentration in 0.5 M and 5.0 M NaCl decreased from the initial 10^{-5} M Tc(VII) concentration level, indicating the reduction of Tc(VII) and precipitation of a Tc(IV) solid phase (see fig. 1a). At higher pH_c , the Tc concentration increases with increasing pH_c similar to the case in 0.1 M NaCl, suggesting the formation of anionic $\text{TcO}(\text{OH})_3^-$ species as proposed in literature[8]. In the SnCl_2 system, reduction of Tc(VII) is observed in neutral and alkaline pH regions as shown in fig. 1b. In the acidic pH range, different Tc concentrations are observed in 0.1 to 5.0 M NaCl. In order to confirm the redox behaviour under this condition, experiments with longer equilibrium time are needed. In Fe(II)/Fe(III) solutions including Fe precipitates, Tc concentration rapidly decreased to the detection limit at $\text{pH}_c > 6$, while no reduction took place at acidic pH conditions (fig. 1c).

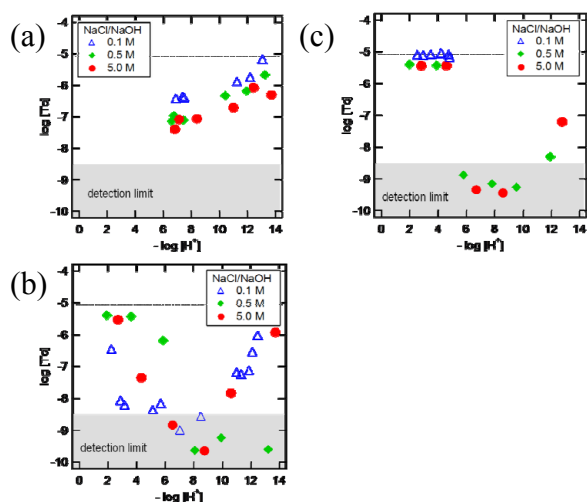


Fig. 1: Redox behavior in 0.1 M, 0.5 M and 5.0 M NaCl in (a) $\text{Na}_2\text{S}_2\text{O}_4$, (b) SnCl_2 , and (c) Fe(II)/Fe(III) systems after 3 days equilibration time.

Fig. 2 shows the observed Tc redox behaviour in 0.5 M and 5.0 M NaCl plotted within a E_h -pH diagram. Samples in which no reduction is observed are plotted as filled symbols; samples in which the initial TcO_4^- was partly or completely reduced are plotted as open symbols. In the Fe powder system, reduction was only observed at neutral pH conditions. No reduction was observed in the hydroquinone and methylene blue systems after 3 days. The results in 0.5 M and 5.0 M are comparable to that in 0.1 M [5], and hint that the high ionic strength does not significantly affect Tc(VII) redox behavior.

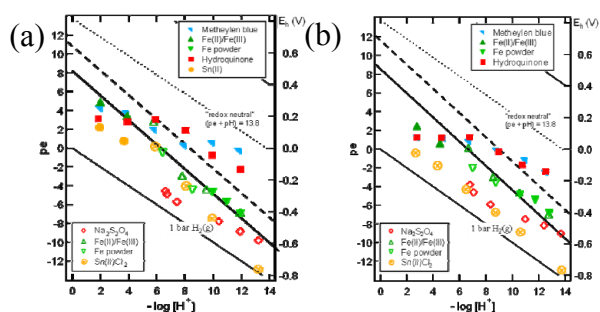


Fig. 2: Redox behavior of Tc(VII) in (a) 0.5 M NaCl and (b) 5.0 M NaCl solutions. Open symbols indicate reduced Tc(IV), filled symbols not reduced Tc(VII). Solid lines represent the experimental borderline for Tc(VII) reduction, the broken Tc(VII)/Tc(IV) transition lines are calculated from NEA-TDB [1] and corrected by the SIT.

In the neutral and alkaline pH region, similar experimental borderlines for the reduction of Tc(VII) region are observed in 0.5 M and 5.0 M NaCl solutions (as shown in fig. 2). The calculated equilibrium lines following [1] for $(\text{TcO}_4^- + 4\text{H}^+ + 3\text{e}^- \rightleftharpoons \text{TcO}_2 \cdot x\text{H}_2\text{O(s)} + (2-x)\text{H}_2\text{O})$ at the respective ionic strength condition are also shown. The experimental borderlines are slightly lower than the calculated lines, which has also

been observed in 0.1 M NaCl. In the acidic pH range, a specific behaviour is observed, and the borderline for the reduction does not fully agree with the experimental data such as in HQ and Fe(II)/Fe(III) system.

For improved quantitative data analysis and predictions on Tc redox behaviour in salt brines, experiments with longer aging time and subsequent oxidation state analysis are needed. In addition, a systematic evaluation of redox measurement in salt brines needs to be performed, similar to the approach established for measuring proton concentrations (pH_c) in salt brines. This work is part of an ongoing comprehensive study at KIT-INE to investigate Tc redox chemistry and Tc(IV) solubility in dilute to concentrated NaCl, MgCl_2 and CaCl_2 solutions under redox neutral and alkaline conditions.

REFERENCES

1. Rard et al., "Chemical Thermodynamics of Technetium, In: Chemical Thermodynamics" (Eds.: Sandino M.C.A. and Östholms E.) **Vol.3**. Elsevier, North Holland, Amsterdam (1999).
2. Cui et al., "Reduction of Pertechnetate by Ferrous Iron in Solution: Influence of Sorbed and Precipitated Fe(II)" *Environ. Sci. Technol.*, **30**, 2259-2262 (1996).
3. Zachara et al., "Reduction of pertechnetate [Tc(VII)] by aqueous Fe(II) and the nature of solid phase redox products" *Geochimica et Cosmochimica Acta*, **71**, 2137-2157 (2007).
4. Ben Said et al., "A novel approach to the Oxidation Potential of the Tc(VII)/Tc(IV) Couple in Hydrochloric Acid Medium through the Reduction of TcO_4^- by Fe^{2+} Ion" *Radiochim. Acta.*, **83**, 195-203 (1998).
5. Hess N. et al., "Thermodynamic Model for the Solubility of $\text{TcO}_2 \cdot x\text{H}_2\text{O(am)}$ in the Aqueous Tc(IV) – $\text{Na}^+ - \text{Cl}^- - \text{H}^+ - \text{OH}^- - \text{H}_2\text{O}$ System", *J. Solution Chem.*, **33**, 199-226 (2004).
6. Warwick et al., "The solubility of technetium (IV) at high pH", *Radiochim. Acta.*, **95**, 709-716, 2007.
7. Kobayashi et al., "Systematic Evaluation of Tc(VII)/Tc(IV) Redox Processes in 0.1 M NaCl Solutions" *3rd Annual Workshop Proceedings*.
8. Eriksen T. et al., "The solubility of $\text{TcO}_2 \cdot n\text{H}_2\text{O}$ in Neutral to Alkaline Solutions under Constant p_{CO_2} ", *Radiochim. Acta*, **58/59**, 67-70 (1992).

Spectroscopic Evidence of Ion-Association in Aqueous Ln³⁺ and An³⁺ Perchlorate Solutions at Low Water Activity

Patric Lindqvist-Reis, Bernd Schimmelpfennig, Reinhardt Klenze

Institute for Nuclear Waste Disposal, Karlsruhe Institute of Technology, P.O. Box 3640, 76021, Karlsruhe, Germany
patric.lindqvist@kit.edu

INTRODUCTION

It is well known that the luminescence lifetime of Eu³⁺ in aqueous solution decreases with increasing concentration of perchloric acid, though the cause of this *quenching* has been a matter of some controversy, because it opposes the fact that perchlorate ions cannot quench the excited state lifetime the way water molecules do by coupling with OH vibrational overtones. Tanaka et al. explained the shorter lifetime of Eu³⁺ by an increase of its hydration number,^[1] whereas Breen et al. reasoned that perchlorate ions in the second hydration sphere weaken the hydrogen bonding to the water molecules of the inner-sphere and thus influence their OH-vibrational manifolds, which would give rise to an increase of the energy transfer efficiency.^[2] Our work supports the latter view for Eu³⁺ and Cm³⁺; in addition, it provides evidence for solvent-shared ion pairs (SIPs; M³⁺-OH₂...OClO₃⁻) and contact ion pairs (CIPs; M³⁺-OClO₃⁻...OH₂) in aqueous solutions at low water activity. Here, we present some key results on this topic. The results are obtained by time-resolved laser fluorescence spectroscopy (TRLFS) and supporting density functional theory (DFT). Eu³⁺(⁵D₀) and Cm³⁺(⁶D_{7/2}) emission spectra and the corresponding decay rates (k_{obs}) are recorded as a function of concentration of perchloric acid. It is informative to express the acid concentration as mol fraction to water, $R = [\text{H}_2\text{O}]/[\text{HClO}_4]$. In these experiments, we identify three concentration regions. Region **A**, where “free ions”, 2SIP, and SIP are the main species, covers the low perchloric acid concentration up to ~3 M ($R \sim 15$), region **B** (mostly SIP) from ~3 M to ~8 M ($15 < R < 4$), and region **C** (mixtures of SIP and CIP) from ~8 M to ~12 M ($4 < R < 2.2$).

DESCRIPTION OF THE WORK

Details for the TRLFS and VSBS setup are given in [3]. All DFT calculations were performed with TUBOMOLE at the RI-DFT level using the BP86-functional and TZVP-quality basis sets for all atoms; f-in-core (Stuttgart type) pseudopotential was used for curium; for details, see [4].

RESULTS

TRLFS. The emission decay rates (k_{obs}) of Eu³⁺(⁵D₀) and Cm³⁺(⁶D_{7/2}) increase gradually with the addition of acid in region **A**. With further addition in region **B** the increase of

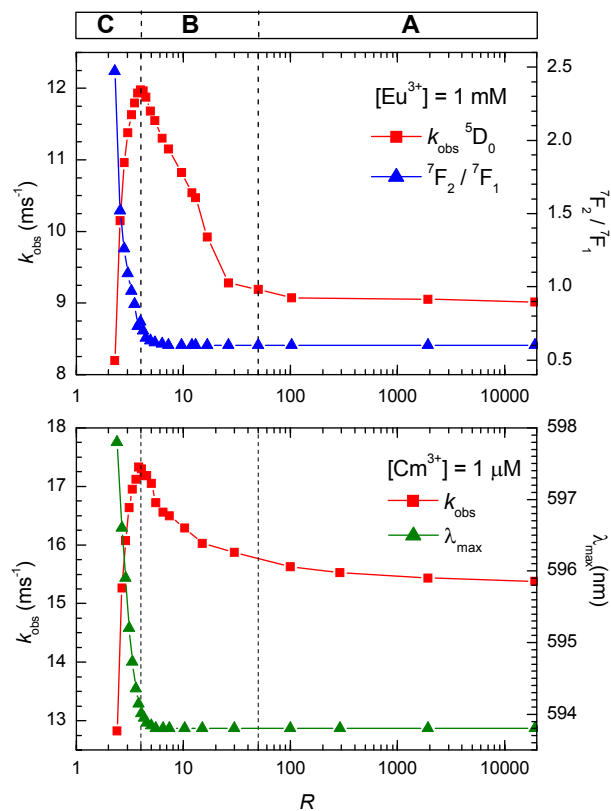


Fig. 1: (Top) Emission decay rate constants (k_{obs}) and the integrated intensity ratio of ${}^7F_2/{}^7F_1$ of the ${}^5D_0 \rightarrow {}^7F_1$ transitions for 1 mM Eu³⁺(aq) as a function of R . (Bottom) k_{obs} and peak maximum λ_{max} of the ${}^6D_{7/2} \rightarrow {}^8S_{7/2}$ transition for 1 μ M Cm³⁺(aq).

the decay rate accelerates, even though the corresponding spectra remain unchanged. At higher acidities in region **C**, the decay rate decreases sharply. This, on the other hand, is accompanied by a redshift of the curium spectra and an increase of the hypersensitive (7F_2) band of the europium spectra (Fig. 1).

The increase of k_{obs} with increasing perchlorate acid concentration in region **B** is most likely due to formation of SIPs. This may be understood by considering that fact that, while perchlorate ions progressively enter the second coordination spheres of the metal ions on going from free ions to 2SIP to SIP, the hydrogen bonding between water molecules in the first the first sphere and perchlorate ions in the second sphere weakens. This, in turn, gives rise to stronger OH bonds of the first shell water molecules and

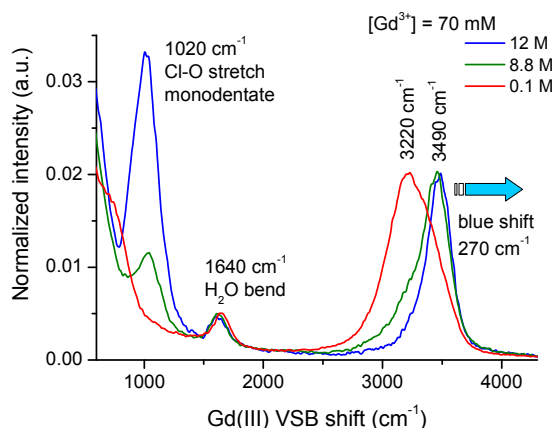


Fig. 2: VSBs associated with the ${}^6P_{7/2} \rightarrow {}^8S_{7/2}$ transition of Gd^{3+} in 0.07 M $Gd(ClO_4)_3$ in 0.1 ($R = 550$), 8.8 ($R = 4.0$), and 12 ($R = 2.3$) M $HClO_4$.

hence an increase of their OH vibrational frequency (blue shift). This is most likely what causes k_{obs} to increase. On the other hand, the decrease in k_{obs} at high perchlorate ion concentration in region C, accompanied by major spectral changes, is obviously due to perchlorate ions entering the first hydration spheres to form CIPs upon replacement of two to three water ligands.

Vibronic side bands (VSBs). If one carefully looks in the region 3000–4000 cm^{-1} above (at higher wavelengths) the main electronic transitions of $Cm^{3+}(aq)$ and $Gd^{3+}(aq)$, it is possible to discern a very weak and rather broad band known as a VSB. VSBs arise due to the coupling between the electronic transition and ligand vibrational modes in the vicinity of the emitting ion. Hence, the VSB in Fig. 2 almost exclusively shows the OH stretching modes of the water molecules in the first hydration sphere, while the contributions from the second hydration sphere or the aqueous bulk are negligible. This means that one may *in situ* record the vibrational spectra of the first hydration spheres of Cm^{3+} and Gd^{3+} ions in dilute solution.

The formation of SIPs and CIPs are clearly seen in the Gd^{3+} vibronic spectrum as a Cl–O stretching band at $\sim 1020\text{ cm}^{-1}$. This band increases markedly with increasing acid concentration in region C because of CIP formation. Analogous results are found for curium. In addition, with increasing concentration of perchloric acid the stretching vibrations of the water ligands are blue-shifted with up to 270 cm^{-1} . This is a rather large shift that clearly suggests a significant increase of the O–H bond strength of these waters, and, as stated above, is due to a weakening of the hydrogen bonds between the first shell water molecules and perchlorate ions in the second sphere (Fig. 2).

DFT. In the DFT-optimized $[Cm(H_2O)_9](ClO_4)_3(aq)$ molecular cluster the first coordination sphere consists of nine water ligands arranged in a tricapped trigonal prism (the symmetry is C_3 for the whole cluster but $\sim D_{3h}$ for the CmO_9 core), whereas the second coordination sphere contains water molecules and perchlorate ions. In this SIP cluster the $Cm-OH_2\cdots OH_2$

hydrogen bond distances are shorter than those of $Cm-OH_2\cdots O_4Cl$, indicating stronger O–H bonds (and thus higher OH stretching frequency) of the inner shell waters in the latter case than in the former, which is in line with the VSB results above.

To conclude, the formation of SIPs of the type $M^{3+}-OH_2\cdots O_4Cl$ decrease the emission lifetimes of $Eu^{3+}(aq)$ and $Cm^{3+}(aq)$, while $M^{3+}-O_4Cl\cdots OH_2$ CIPs, in which up to 2-3 water ligands can be replaced by perchlorate ions in ~ 8 -12 M $HClO_4$, significantly increase their lifetimes and change their spectra. In addition, these SIPs and CIPs give rise to a significant blue-shift of the water stretching band and the appearance of Cl–O band in the vibronic spectra. DFT calculations corroborate a weakening of the H-bonds around the perchlorate ion in the SIP complex; however, the structure optimization of this large molecular cluster is on the limit for what is makeable with the current method, not so much for the rather extensive computational work but rather because of using a good starting model as not to be trapped in myriads of local minima. To avoid these problems we have started molecular dynamics simulations of large systems of $Cm(ClO_4)_3(aq)$.

REFERENCES

1. TANKA et al., “Luminescence lifetimes of aqueous europium chloride, nitrate, sulfate, and perchlorate solutions. Studies on the nature of the inner coordination sphere of the europium(III) ion”, *Inorg. Chem.*, **23**, 2044-2046, (1984).
2. BREEN et al., “Europium(III) luminescence excitation spectroscopy. Inner-sphere complexation of europium(III) by chloride, thiocyanate, and nitrate ions”, *Inorg. Chem.*, **22**, 536-540, (1983).
3. STEPERT et al., “Complexation of europium(III) by bis(dialkyltriazinyl)bipyridines in 1-octanol”, *Inorg. Chem* (DOI: 10.1021/ic202119x).
4. APOSTOLIDIS et al., “[$An(H_2O)_9$](CF_3SO_3)₃ ($An = U-Cm, Cf$): Exploring Their Stability, Structural Chemistry, and Magnetic Behavior by Experiment and Theory” *Angew. Chem. Int. Ed.*, **49**, 6343-6347 (2010).

Actinide Interactions in WIPP Brine

Donald T. Reed, David Ams, Jean-Francois Lucchini, Marian Borkowski, Michael K. Richmann,
Hnin Khaing, Juliet Swanson

*Earth and Environmental Sciences, Los Alamos National Laboratory, Carlsbad Operations, 1400 University Dr,
Carlsbad,
NM 88220, USA
email: dreed@lanl.gov*

INTRODUCTION

This overview summarizes the progress of work conducted recently by the Actinide Chemistry and Repository Science team. Reported herein are the effects of microbial activity, brine components and colloid formation on actinide solubilities and their transport in Waste Isolation Pilot Plant (WIPP).

DESCRIPTION OF THE WORK

The solubility of uranium (VI) was determined in WIPP-relevant brines (GWB and ERDA-6) as a function of pC_{H^+} and ionic strength, in the absence of carbonate [1]. These were the first WIPP-relevant data for the VI actinide oxidation state.

Studies of neptunium (V) adsorption onto halophilic bacteria surface were conducted to establish the effect of microbial fragment colloids on the transport of radionuclides in high ionic strength systems. The bacteria were titrated to measure pK_a values and concentrations of functional groups on the bacterial surface. These values were used in modeling the adsorption behavior of neptunium (V) as a function of pH.

Studies of thorium solubility in carbonate free brine were conducted from over- and under saturation to determine baseline for carbonate effect and to measure the contribution of intrinsic colloidal fraction of thorium to the total solubility. Brine solutions were equilibrated for 1.5 years, thorium steady state concentrations were measured by ICP-MS and colloidal fraction was measured using ultracentrifugation.

RESULTS

Solubility of U(VI) in WIPP brine – effect of borate in carbonate free system

In the absence of carbonate, the uranium (VI) solubilities were about 10^{-6} M in GWB brine at $pC_{H^+} \geq 7$ and about 10^{-8} - 10^{-7} M in ERDA-6 at $pC_{H^+} \geq 8$ (Fig.1). They established a uranium solubility that was 10-100 times lower than published results and in good agreement with modeling results.

In the absence of carbonate, hydrolysis was the main complexation mechanism for uranium (VI) at high ionic

strength and $pC_{H^+} \geq 7$. However, the effect of borate complexation was noticeable at $pC_{H^+} \sim 8$ -9. A significant increase of uranium in ERDA-6 solutions and a shift of pC_{H^+} to values close to the pK_a (9.02) of boric acid at $I = 5.0$ M, were observed after an addition of 5×10^{-2} M of tetraborate.

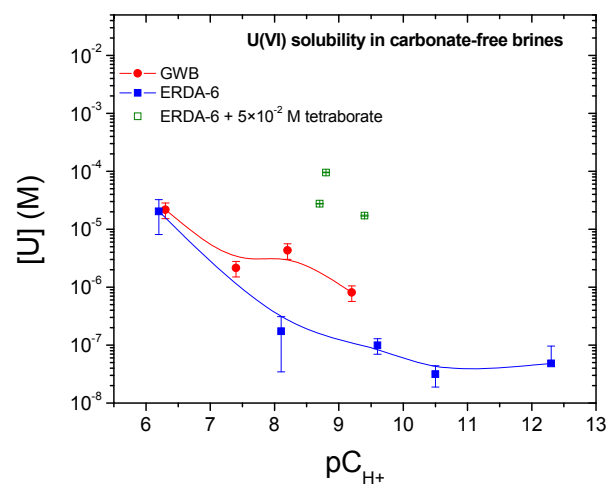


Fig. 1: Uranium (VI) solubility in carbonate-free GWB (red curve) and ERDA-6 (blue curve) versus pC_{H^+} , and effect of a 5×10^{-2} M tetraborate addition in ERDA-6 (green squares) [1].

Adsorption of Np(V) onto halophilic bacteria

This study is the first to evaluate the adsorption of neptunium (V) to the surface of a halophilic bacterium as a function of pH from approximately 2 to 10 and at ionic strengths of 2 and 4 M. This is also the first study to evaluate the effects of carbonate complexation with neptunium (V) on adsorption to whole bacterial cells under high pH conditions.

A thermodynamically-based surface complexation model was adapted to describe experimental adsorption data under high ionic strength conditions where traditional corrections for aqueous ion activity are invalid. Adsorption was significant over the entire pH range evaluated for both 2 and 4 M ionic strength conditions and was shown to be dependent on the speciation of the sites on the bacterial surface and neptunium (V) in solution. Adsorption behavior appeared to be controlled by the relatively strong electrostatic attraction of the positively charged neptunyl ion to the negatively charged bacterial surface

at pH below circum-neutral. At pH above circum-neutral, the adsorption behavior was controlled by the presence of negatively charged neptunium (V) carbonate complexes resulting in decreased, although still significant, adsorption. Adsorption in 4 M NaClO₄ was enhanced relative to adsorption in 2 M NaClO₄ over the majority of the pH range evaluated apparently due to the effect of increased aqueous ion activity at high ionic strength.

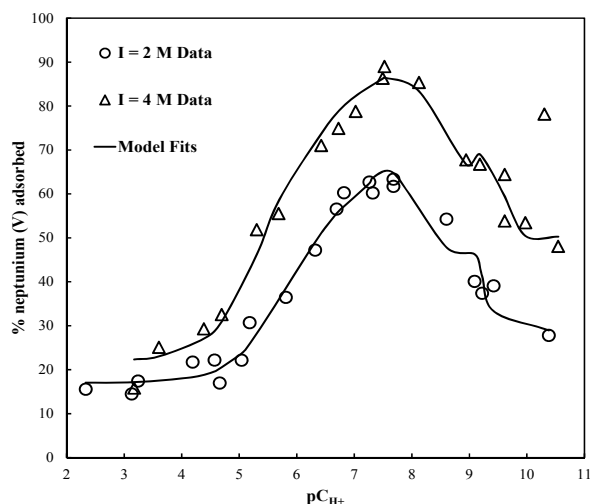


Fig. 2: Results of Np(V) adsorption studies on bacteria surface as a function of pC_{H+} for two ionic strength solutions.

On the basis of these data the following log K values were calculated and are presented in the Table below.

Table 3. Best-fitting log K values for Np(V) adsorption data sets

	I = 2 M	I = 4 M
$\text{NpO}_2^+ + \text{R-L}_4^0 \leftrightarrow \text{R-L}_4\text{NpO}_2^+$	3.01	3.04
$\text{NpO}_2^+ + \text{R-L}_2^- \leftrightarrow \text{R-L}_2\text{NpO}_2^0$	3.69	3.86
$\text{NpO}_2^+ + \text{R-L}_3^- \leftrightarrow \text{R-L}_3\text{NpO}_2^0$	4.22	4.96
$\text{NpO}_2\text{CO}_3^- + \text{R-L}_4^- \leftrightarrow \text{R-L}_4\text{NpO}_2\text{CO}_3^{2-}$	8.93	9.22
$\text{NpO}_2(\text{CO}_3)_2^{3-} + \text{R-L}_4^- \leftrightarrow \text{R-L}_4\text{NpO}_2(\text{CO}_3)_2^{4-}$	10.66	11.83
$\text{NpO}_2(\text{CO}_3)_3^{5-} + \text{R-L}_4^- \leftrightarrow \text{R-L}_4\text{NpO}_2(\text{CO}_3)_3^{6-}$	11.88	12.73

(a) R represents the bacterium to which the functional group L_n is attached.

These results can be incorporated into geochemical speciation models to aid in the prediction of neptunium (V) mobility in complex geochemical systems.

Thorium studies on solubility and colloid formation

Thorium samples at various pC_{H+} were equilibrated until steady state was achieved. Thorium solubility measured from under- and oversaturation were similar in both brines and constant for the entire investigated pC_{H+} range. The average thorium concentration was

equal to 6×10^{-7} M. This value depends on neither the pC_{H+}, nor the composition of the brine.

Solubility of Th(IV) measured in our systems were in good agreement with the concentration of colloidal and dissolved species reported in the literature in the similar experimental conditions [2] where thorium hydroxy-oxide ThO(OH)₂ was the solubility-controlling phase.

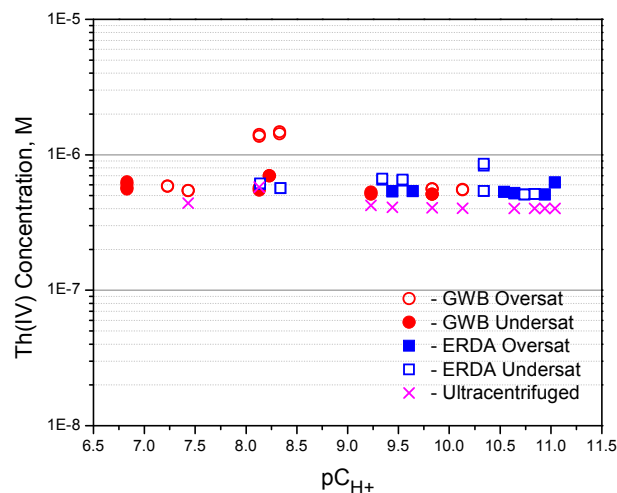


Fig. 3: Th concentrations after 1.5 years of equilibration in GWB and ERDA-6 brine and after ultracentrifugation, 2 hours @ 130 000 rpm (1 019 000 x g).

Thorium colloidal fraction was found to be about 50% of total Th concentration measured. The Th colloidal fraction reported in literature [2] was scattered ranging from 10% to 99%. Our data is located in the center of this distribution and pretty constant from sample to sample. Equilibration time in our experiment was longer than reported in the literature but this needs more work for detail clarification.

REFERENCES

- LUCCHINI et al., "Uranium (VI) Solubility in Carbonate-free WIPP Brine" *Submitted to Radiochimica Acta* (2011).
- ALTMAYER et al., "Solubility and colloid formation of Th(IV) in concentrated NaCl and MgCl₂ solution". *Radiochim Acta* **92**, 537-543 (2004).

Borate Chemistry and Interaction with Actinides in High Ionic Strength Solutions at Moderate pHMarian Borkowski¹, Mike Richmann¹, Sandra Kolanke², Donald Reed¹¹ *Los Alamos National Laboratory, Earth & Environmental Sciences Division, Carlsbad Operations, Actinide Chemistry & Repository Science Program, 1400 University Drive/Carlsbad, NM 88220, USA
email: marian@lanl.gov*² *Clausthal University, Clausthal, Germany***INTRODUCTION**

Borates in solution have many interesting properties that can be used to study their complexation with metal and actinide ions. Borate compounds, although soluble in water, are relatively transparent over a wide range in the UV-VIS-NIR and do not interfere with metal/actinide ion spectra. Naturally occurring isotopes B-10 (19.6%) and B-11 (80.4%) are NMR active. Borate oxy-anions provide a useful Raman-active probe and borate solutions are good solvents for electrochemical studies. Borates in solution also buffer pH over a wide range (6 to 12). Borate is present in Waste Isolation Pilot Plant (WIPP) brines (up to ~160 mM) and is a component of the simulated brines currently used to establish actinide solubility.

Many aspects of borate chemistry, especially in basic media, are still unknown and an important emphasis in our current studies is to investigate this chemistry and understand the specifics of its impact on the actinide systems of interest. Recently we reported that neodymium is complexed by the tetraborate ion (log K ~4) [1] and that plutonium may form even stronger complexes than that of neodymium [2]. Herein we report on further progress in our study of borate chemistry and its complexation of actinides.

DESCRIPTION OF THE WORK

Samples of sodium tetraborate and boric acid at pH ranging from 3 to 10 were prepared and an NMR study was conducted. Chemical shift versus pH was measured. Solids were also crystallized from similar solutions and analyzed by XRD to establish their structure.

The complexation of Np(V), Pu(VI) and Cm(III) with borate was investigated spectroscopically to establish the speciation and determine the formation constants.

RESULTS

Boron can link to either three oxygens to form a triangle or four oxygens to form a tetrahedron. Boric acid is a very weak acid and acts exclusively by hydroxyl-ion acceptance rather than proton donation. Titration of sodium tetraborate with hydrochloric acid indicated that tetraboric acid, although a diprotic acid, has effectively one pKa of 8.95 that is very similar to monoboric acid.

The solution chemistry of borates is a topic of current interest due to a history of conflicting reports that are

not yet totally resolved. A variety of methods unequivocally established the existence of polyborate anions in aqueous solution. Aqueous polyborate equilibria were studied by ¹¹B NMR and by Raman Spectroscopy [3]. On the basis of these data the formation constants for B(OH)₄⁻, B₃O₃(OH)₄⁻, B₄O₅(OH)₄²⁻ and B₅O₆(OH)₄⁻ were reported [3] and the distribution of the expected forms of borate as a function of pH are presented in Figure 1 for the pH range of 5-11 and a borate concentration of 0.4 M. This speciation will vary as a function of pH and the concentration of boron.

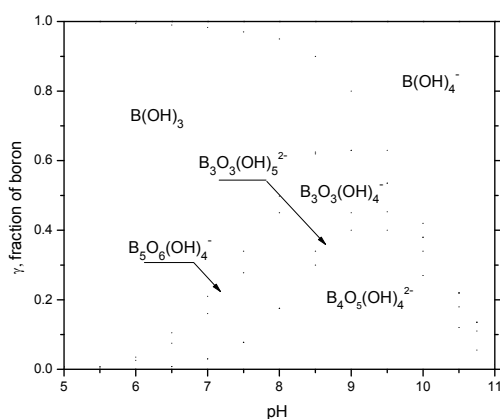


Fig. 1: Abundance of different polyborate species as a function of pH

NMR studies of sodium tetraborate and boric acid solutions are presented in Figure 2 A and B. These results confirmed our earlier observations based on XRD measurements of the solids that were crystallized from sodium tetraborate and boric acid as a function of pH. In both cases, the borate aqueous speciation depends only on the pH of the solution and not on the initial form of the borate used in solution preparation.

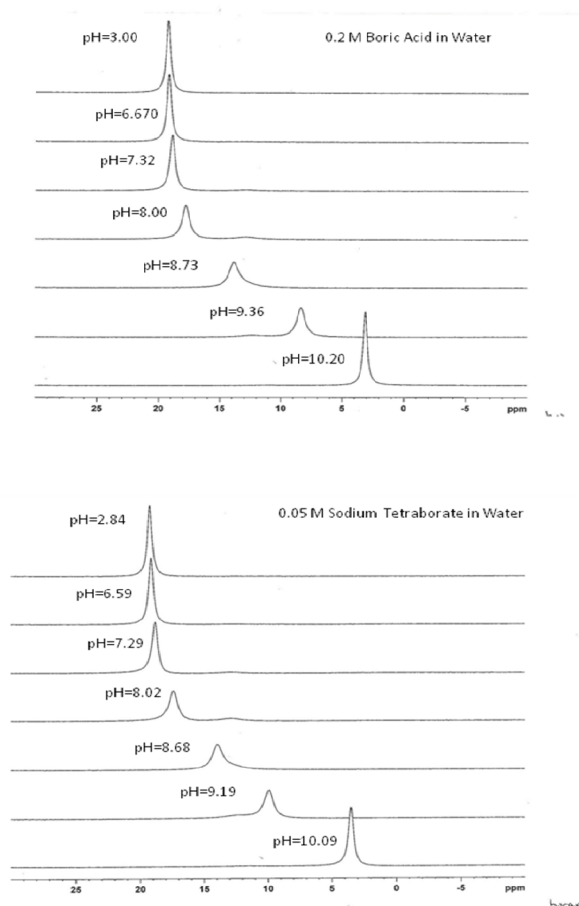


Fig. 2 A and B: Chemical shift measured in boric acid and sodium tetraborate solutions as a function of pH at 30°C.

The proposed speciation equilibration scheme for aqueous borate as a function of pH is shown in Figure 3. This sequence is a simple function of increased tetrahedral boron atom content in the polyborate molecule. Assuming that the data in Figure 1 are correct, some of the forms are only present at very low concentration and may be neglected.

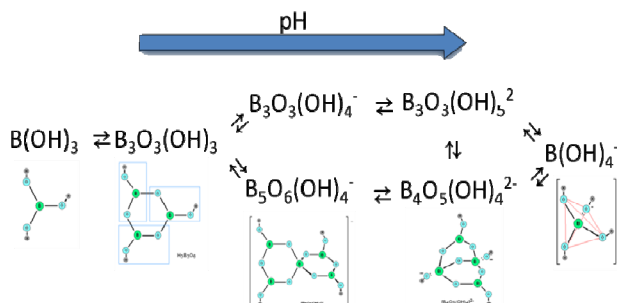


Fig. 3: Expected transition forms of borate as a function of pH.

The complexation strength of different polyborate forms may be very similar. They are unable to form a covalent bond. They can only attract cations by weak electrostatic interactions. An example of such an interaction was established spectrophotometrically for Np(V) and is presented in Figure 4.

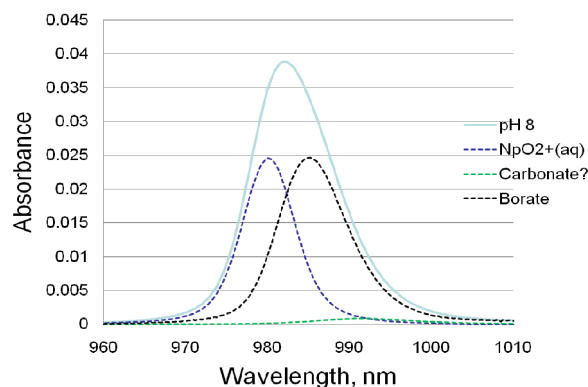


Fig. 4: Deconvoluted spectrum of Np(V) in 50 mM sodium tetraborate solution at pH=8.0

The interaction of borate with trivalent and hexavalent actinides should be much stronger and experimental data confirm this expectation. Borate can form complexes with metals in a moderately alkaline pH range. At these pH values, actinides are strongly hydrolyzed and borate ions will compete with hydrolysis. Under these conditions, as a general rule, ternary complexes will be formed. Also, at higher borate concentrations, the formation of 1:2 complexes cannot be excluded.

REFERENCES

- [1] BORKOWSKI, M et al., "Complexation of Nd(III) with tetraborate ion and its effect on actinide (III) solubility in WIPP brine" *Radiochimica Acta*, **98**, 577 (2010).
- [2] BORKOWSKI, M et al., "Borate Ion Complexation of the Lanthanides and Actinides: Implications for the WIPP Salt Geologic Repository" *Proceedings of the ACTINIDES-2009 Conference*, San Francisco, CA, (2009).
- [3] ANDERSON, JL et al., "Temperature jump rate studies of polyborate formation in aqueous boric acid", *J. Phys Chem* **68**, 1128-1132 (1964).

Complexation of Nd(III)/Cm(III) with borate in dilute to concentrated alkaline NaCl and CaCl₂ solutions

K. Hinz, M. Altmaier, Th. Rabung, H. Geckeis

Karlsruhe Institute of Technology, Institut für Nukleare Entsorgung, P.O. Box 3640, 76021 Karlsruhe, Germany
katja.hinz@kit.edu

INTRODUCTION

In order to assess the long-term performance of a nuclear waste repository it is necessary to predict the chemical behavior of actinides in aqueous solutions. In the USA (WIPP) and Germany (Gorleben) waste disposal in deep underground facilities located in rock salt formations are currently under planning or operative. In the unlikely scenario of intruding water, concentrated salt brine solutions are expected. Scientific research on aqueous actinide chemistry in brine systems is therefore a highly relevant research topic.

Boron may be present in the repository as part of the emplaced waste inventory but also can be present as part of the elements constituting the intruding water. The interaction of actinides with borate rich solutions have to be considered as they may potentially lead to mobilization and subsequent transport of actinides to the environment. Under reducing conditions, as found in a nuclear waste repository, the tri- and tetravalent actinide oxidation states are favored. A previous study has shown that the solubility of Nd(OH)₃(am) can be slightly increased by the presence of borate at pH_c ~8.6 [1]. In this framework, this study focuses on the solubility and speciation of the trivalent elements Cm(III) and Nd(III) as chemical analogs for Am(III) and Pu(III). The complexation of borate with these elements at an extended pH_c range in NaCl and CaCl₂ solutions has been investigated by solubility and TRLFS experiments.

EXPERIMENTAL

All experiments were prepared and carried out in Argon gloveboxes. Solubility experiments of Nd(III) were performed with Nd(OH)₃(am) as solid phase. Samples were prepared with NaCl (0.1 M and 5.0 M) and CaCl₂ (0.25 M and 3.5 M) as background electrolytes. Two tetraborate concentrations (1 mM and 10 mM) were added. The pH-values were adjusted by addition of HCl and NaOH/Ca(OH)₂(s) of same ionic strength and borate concentration at 7 < -log[H⁺] < 13. [H⁺] was determined by using a combination glass electrode (type Ross Orion). After 10 kd (2-3 nm) ultrafiltration the Nd concentration in the filtrate was determined by ICP-MS (Perkin Elmer).

TRLFS measurements were performed with ~10⁻⁷ M Cm(III) per sample, with 0.25/3.5 M CaCl₂ as background electrolytes and two borate concentrations (1 and 10 mM). In both systems pH_c-values 8 and 12

were investigated. Single emission spectra and fluorescence lifetimes were obtained.

RESULTS

Nd(OH)₃(am) solubility in NaCl/CaCl₂ solutions with borate

No significant increase in the solubility of Nd(OH)₃(am) in all NaCl-/CaCl₂-systems was observed compared to the solubility of Nd(OH)₃(am) under the absence of borate [2]. Borate as a complexing ligand seems not to have a significant effect on the solubility of trivalent actinides (see Fig.1) under the investigated conditions. XRD analyses showed no new Nd-borate and/or Ca/Na-borate solid phases were forming.

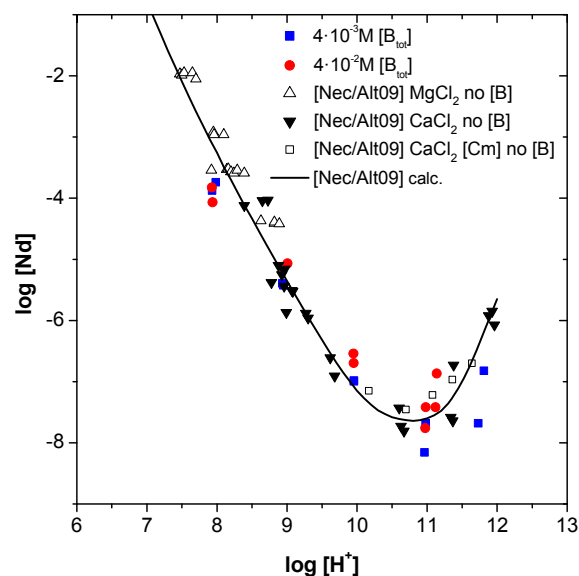


Fig. 1: Solubility of Nd(OH)₃(am) in 3.5 M CaCl₂ as background electrolyte at two tetraborate concentrations (1 und 10 mM) as function of pH_c.

TRLFS of Cm(III) in CaCl₂ solutions and presence of borate

TRLFS studies at pH_c ~8 show slight peak shifts related to Cm(III)-borate complexation (see Fig.2). At these pH_c conditions and borate concentrations, the hydrolysis of Cm(III) is competing with borate complexation. For this reason it is difficult to analyze the spectra quantitatively and separate possible borate species

spectra from pure hydrolysis spectra. At higher pH_c conditions $pH_c \sim 12$, borate complexation is clearly out-competed by the hydroxid ligand which is now present in high concentrations. The fluorescence spectra in the $CaCl_2$ -system show a very weak borate complexation in agreement with the Nd(III) solubility data.

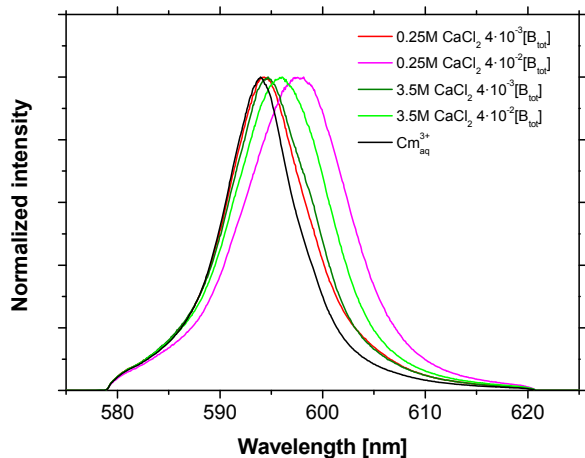


Fig. 2: Emission spectra of Cm(III) at two borate concentrations (1 and 10 mM) and two $CaCl_2$ concentrations (0.25 and 3.5 M) as background electrolyte. The $pH_c = 8$ is fixed in all cases.

Fluorescence lifetimes in the $CaCl_2$ -systems remained unaffected by borate. In the $CaCl_2$ -system mono-exponential decay can be observed contrary to the NaCl-system where biexponential decay was found. In the high alkaline pH_c region ($pH_c = 12$) the measured lifetime spectra show very similar fluorescence behavior as in the borate free system (see Fig. 3) [3].

This study has shown that an An(III) solubility enhancement related to the complexation of trivalent actinides with borate is of minor relevance for source term estimations under geochemical conditions comparable to the conditions investigated in this work. Aquatic borate species are found to be weakly coordinating ligands. Given the high uncertainties in borate speciation as well as the weak effect of borate observed in our solubility and TRLFS studies, it is possible to derive neither a chemical model nor a quantitative thermodynamic model without heavily relying on assumptions. To further derive information on the borate-actinide chemistry, studies in $MgCl_2$ solutions and studies with higher boron concentrations in NaCl or $CaCl_2$ and $MgCl_2$ are in progress.

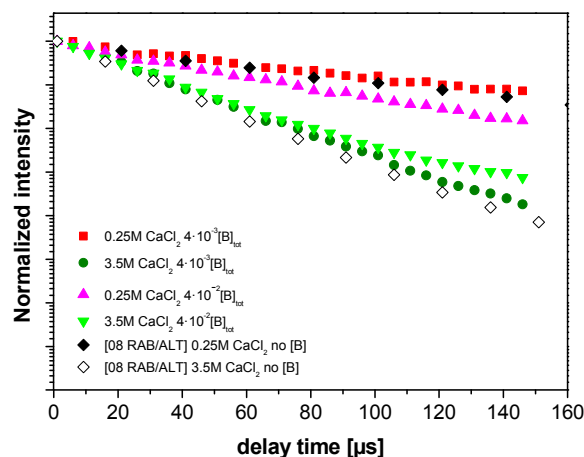


Fig. 3: Cm(III) lifetime spectra at $pH_c = 12$ at two borate concentrations (1 and 10 mM) and $CaCl_2$ as background electrolyte.

REFERENCES

- [1] M. Borkowski et al., "Complexation of Nd(III) with tetraborate ion and its effect on actinide (III) solubility in WIPP brine" *Radiochimica Acta*, **98**, 577 (2010).
- [2] V. Neck et al., "Thermodynamics of trivalent actinides and neodymium in NaCl, $MgCl_2$, and $CaCl_2$ solutions: Solubility, hydrolysis and ternary Ca-M(III)-OH complexes", *Pure and Applied Chemistry*, **81**, 1555-1568 (2009).
- [3] Th. Rabung et al., "A TRLFS study of Cm(III) hydroxide complexes in alkaline $CaCl_2$ solutions", *Radiochimica Acta*, **96**, 551-559 (2008).

Complexation of Neptunium (V) with Borate

Sandra Kalanke¹, Donald Reed², Michael Richmann²,
Marian Borkowski², Kurt Mengel¹

¹TU Clausthal, Institut für Endlagerforschung
email: ska09@tu-clausthal.de

²Earth and Environmental Science Division, Los Alamos National Laboratory, Carlsbad Operation

INTRODUCTION

The Asse salt structure in Central Germany has been exploited over 60 years for potash and halite and subsequently has been used as a national research mine for radwaste disposal. Some 100 000 m³ of low-level waste had been deposited in the Zechstein 3 (Permian) salt formation at 750 m depth. Together with the low-level waste, actinides have been deposited in low but significant proportions. In addition, inactive chemicals from reprocessing plants are present in large quantities amongst which are boric acid and organic compounds such as resins.

DESCRIPTION OF THE WORK

The complexation of Neptunium (V) with borate was investigated by using absorption spectrometry as a function of pH and ionic strength. Borate forms a 1:1 complex with neptunium that leads to a red-shift in the 980 nm Np(V) peak. This shift was used to quantify the extent of complexation present under the range of conditions investigated. Spectra obtained were deconvoluted and fit to linear combinations of the pure aqua and fully complexed spectra. These data were used to determine the formation constant and the effects of ionic strength on this constant. These studies provide needed data on the subsurface interactions and speciation of neptunium when borate is present in the groundwater or brine (e.g. ASSE and WIPP).

The main text of the introduction should appear here. Headings and subheadings should be formatted using the style given in the text.

A tab stop allows for easy indenting of the text (although the first paragraph and paragraphs that follow headings should not be indented).

RESULTS

The solution chemistry of borates is a complex system influenced by pC_{H^+} and concentration of borate. The figure right shows the relative importance of various boric acid species in a pC_{H^+} - range 5 to 11 at a boric acid concentration of 0.4 M.

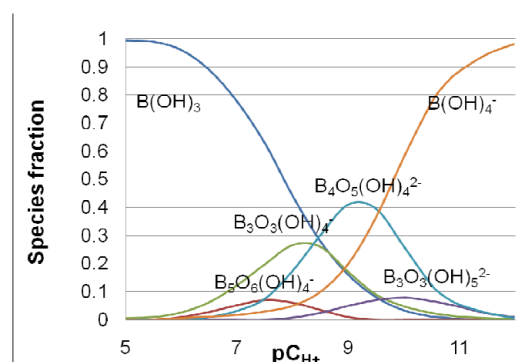


Fig. 1: pC_{H^+} -dependence of borate system

The formation of a Neptunium(V) complex with sodium tetraborate shows as well a dependence of pC_{H^+} . In a pH-range higher $pC_{H^+}=6$ the formation of the complex is visible. An isosbestic point at a wave-length of 983 nm shows the formation of only one product. With increasing $pC_{H^+} > 8$ the reaction of Neptunium(V) with carbonate overwhelm borate complexation.

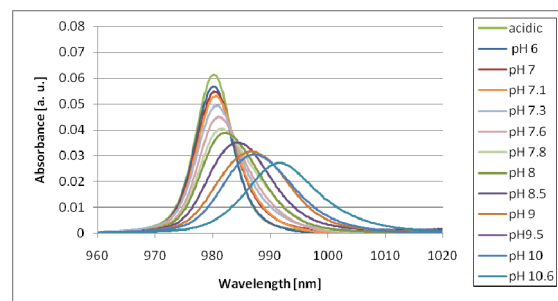


Fig. 2: pH- dependence of the formation of Neptunium(V)- complex with sodiumtetraborate

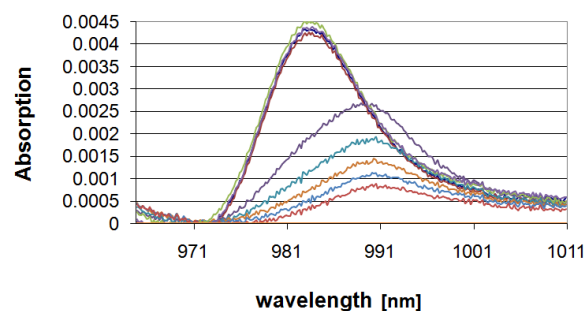


Fig. 3: Decrease of the Np(V)-borate peak at 985 nm and the arising of a band for a Np(V)-carbonate complex at 991 nm

The formation constant for the complexation of Np(V) with sodium tetraborate were measured in NaCl-solutions with concentrations of 0.1, 0.5, 1, 2, 3, 4 and 5 M as a function of tetraborate concentration. A constant $pC_{H^+}=7.6$ was chosen. The concentration of the Np(V)-borate complex was calculated by deconvolution and fitting of the obtained spectras for the free Np(V) and the complex

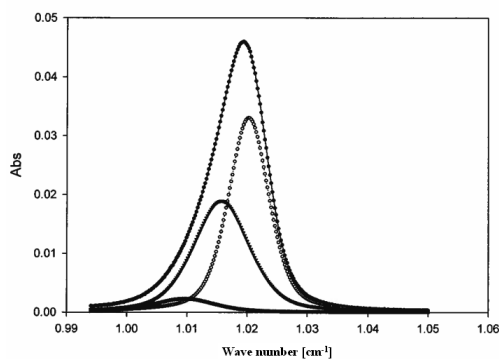


Fig. 4: Decoupled data of the Neptunium(V)-borate-complex at a pH= 7.57

The plot of Np(V) with borate stability constant vs. NaCl ionic strength is flat, similar to the plot of boric acid pKa vs. NaCl ionic strength. Logarithm of stability constant slightly decreases with ionic strength. These data will be used for Pitzer parameters and SIT parameters calculation.

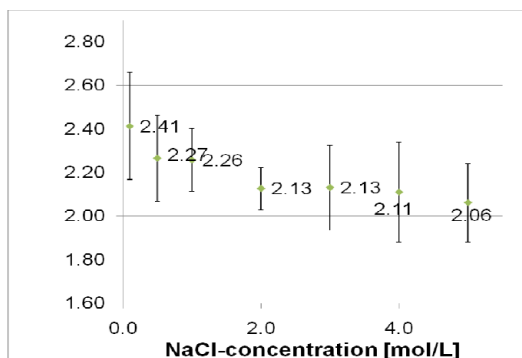


Fig. 4: The calculated formation constants as a function of ionic strength

REFERENCES

1. WOOD, G.W. et al., "An introduction to Boron: History, Sources, Uses and Chemistry" *Environmental Health Perspectives*, **102**, Supplement 7 (1994).
2. BORKOWSKI, M. et al., "Complexation of Nd(III) with tetraborate ion and its effect in actinide(III) solubility in WIPP brine" *Radiochim. Acta*, **98**, Page 1-6 (1994).

Cs and U Retention in Cement during Long-Term Corrosion Tests in Salt Brines

B. Kienzler, N. Finck, M. Plaschke, Th. Rabung, J. Rothe

Karlsruhe Institute of Technology (KIT), Institut für Nukleare Entsorgung (INE),
email: bernhard.kienzler@kit.edu

INTRODUCTION

Resistance against leaching and corrosion is considered as a main quality criterion for all kind of radioactive waste forms. In the case of cemented waste forms, the composition as well as the production process influences the leaching and corrosion behaviour and the radionuclide release/retention. Since 1979, leaching and corrosion tests have been performed using simulated full-scale cemented waste forms. The cement blocks were doped with ¹³⁷Cs, natural uranium and ²³⁷Np and have been exposed to various salt brines. The brines were sampled regularly and analysed with respect to the radionuclides, pH, and the composition of the brines.

RESULTS

Some results of the analyses of solutions with respect to the radionuclides are shown in Fig. 1 and 2.

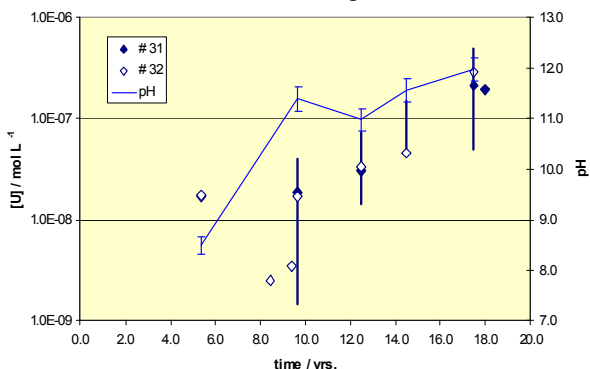


Fig. 1: Evolution of the bulk U concentration and bulk pH in saturated NaCl solution.

In Fig. 2 a comparison is shown between measured and calculated Cs release into the solution. All samples under investigation showed an ¹³⁷Cs release between 20 and 30 % in saturated NaCl solution and a release between 10 and 15% in MgCl₂ solution, if the W/C ≤ 0.32. For W/C ~ 0.4, the cemented waste forms underwent complete degradation which lead to significant increase of the surface. Consequently, the Cs release went up to more than 50%.

After 18 years, four corroded cement blocks were recovered and drill cores and abraded material were prepared. Results of various analytical methods revealed (1) the distribution of radioactivity within the cement blocks, (2) element and other component distributions, (3) the water content by thermogravimetric measurements, and the mineralogical phase

analyses by (4) X-ray powder diffraction analyses and by (5) scanning electron microscopic investigations.

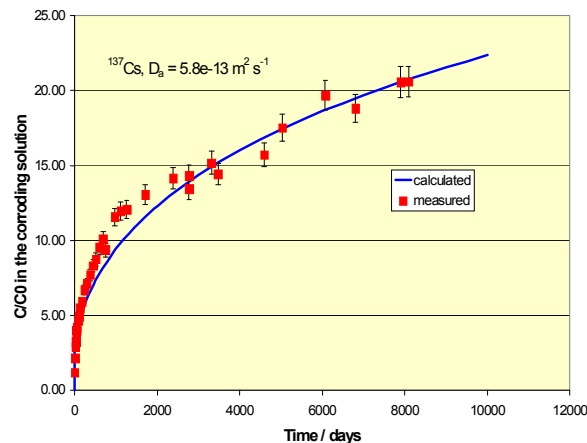


Fig.3: Modeling of the evolution of ¹³⁷Cs concentration as function of time in saturated NaCl solution.

Of high interest was the retention of U(VI). Some examples of the different analytical methods are shown. Uranium is a minor component, identification of U phases by comparison between the spectra from #31 and #33 with uranium-free materials (#30 and #28).

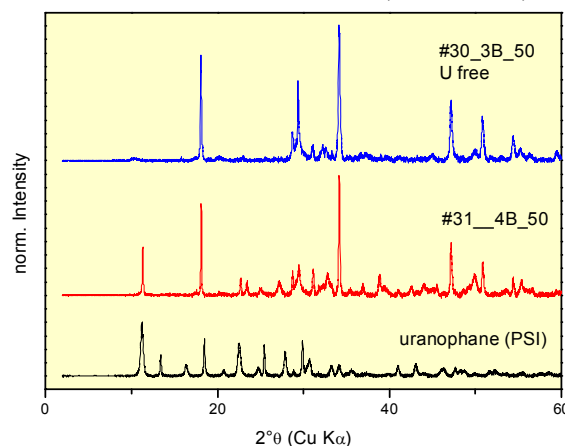


Fig 4: XRD pattern of the sample stored in NaCl solution.

In the XRD pattern of the sample which was stored in NaCl solution, following phases could be identified: Portlandite, calcite, halite, Friedel's Salt type and CSH type phases. Strong indications were found for crystalline (Ca(UO₂)₂(SiO₃OH)₂·5H₂O phase (β-uranophane).

Time resolved laser fluorescence measurements (TRLF) revealed significant signals (Fig. 5) which have been compared to reference systems.

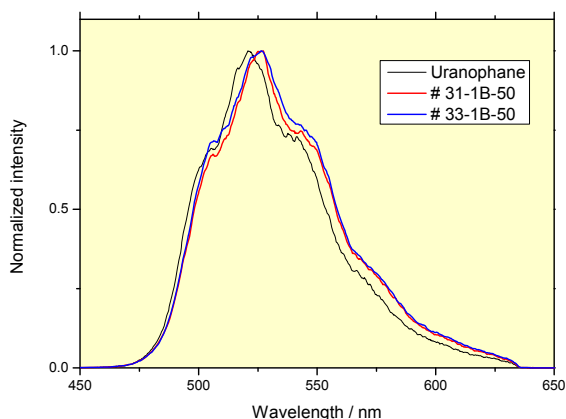


Fig 5: TRLF pattern of the sample stored in NaCl solution.

All samples show high U(VI) fluorescence intensities, long fluorescence lifetimes and similar spectra. The peak positions and fluorescence lifetimes could be interpreted by following facts: Soddyite, Ca-uranate, Na-uranate, and schoepite show no fluorescence signal at the selected wavelength and were excluded. The observed spectra and lifetime were similar to uranophane reference samples.

U L3-edge XANES spectra were compared to reference compounds UO_2 and meta-schoepite. Bond distance of axial oxygen compared well with the α -uranophane (1.82 Å). The apparent absence of coordination shells beyond the oxygen coordination shell and the U-O_{eq} distance supported the assumption of a highly distorted or asymmetric U coordination, and/or the coexistence of several U(VI) phases in the samples.

CONCLUSIONS

The main achievements of the investigations showed that in NaCl and MgCl_2 systems the **dissolved radionuclide concentrations** were $[\text{U(VI)}] \leq 5 \times 10^{-7} \text{ mol l}^{-1}$ at $9.0 \leq \text{pH} \leq 12.0$ and that the Cs release depends on porosity (W/C ratio) and degradation of cement. Investigations of the **solid material** showed a homogeneous spatial U(VI) distribution in NaCl and MgCl_2 systems after 17 to 18 yrs of leaching, whereas Cs and NO_3^- distributions showed distinguished profiles. The analyses of the **uranium solids** revealed consistent results by different methods, XRD, XANES/EXAFS, TRLFS. Soddyite, meta-schoepite could be ruled-out by XANES/EXAFS, TRLFS measurements. The results were consistent for both solutions and locations of specimen. EXAFS showed highly distorted or asymmetric U coordination, and/or the coexistence of several U(VI) phases in the samples.

Strong indications for uranophane, $(\text{Ca}(\text{UO}_2)_2(\text{SiO}_3\text{OH})_2 \cdot 5\text{H}_2\text{O})$ were observed. Other possible uranium phases such as soddyite, meta-schoepite, and di-uranate phases could not be identified by combining the results of the various experimental techniques.

Detection of single Ca_2UO_7 crystals ($\varnothing \sim 100 \mu\text{m}$) of unclear origin by Raman spectroscopy.

High-resolution X-ray absorption spectroscopy of U in cemented waste formT. Vitova¹, M. A. Denecke¹, N. Finck¹, J. Göttlicher², B. Kienzler¹, J. Rothe¹¹Karlsruhe Institut für Technologie (KIT); Institut für Nukleare Entsorgung (INE); P.O. Box 3640, D-76021 Karlsruhe, Germany

email: Tonya.Vitova@kit.edu

²Karlsruhe Institut für Technologie (KIT); Institut für Synchrotronstrahlung; P.O. Box 3640, D-76021 Karlsruhe, Germany**INTRODUCTION**

High-resolution X-ray absorption near edge structure spectroscopy (HR-XANES) applies an analyzer crystal spectrometer in Rowland geometry to alleviate energy broadening effects in conventional XANES spectra, thereby providing detailed electronic and geometric structural information. We present the advantages of HR-XANES over conventional XANES spectroscopy for a speciation investigation of U embedded in cement as a model waste form and aged under aqueous saline conditions for 20 years.

DESCRIPTION OF THE WORK

The U L₃ and U M₄ edge HR-XANES of a series of natural minerals (autunite Ca(UO₂)₂(PO₄)₂·10-12H₂O, schroekingierite NaCa₃(UO₂)(CO₃)₃(SO₄)F·10H₂O, uranophane Ca(UO₂)₂SiO₃(OH)₂·5H₂O, kasolite Pb(UO₂)SiO₄·H₂O, phurcalite Ca₂(UO₂)₃(PO₄)₂(OH)₄·4H₂O, U in fluorite CaF₂) and of U in an aged cement waste form (U_cement) [1] have been recorded. The increased information content in the high energy resolved spectra is demonstrated through comparison of the autunite and schroekingierite HR-XANES with conventional XANES spectra. The HR-XANES of the remaining natural mineral spectra are used to identify potential phases in the aged U_cement sample.

All spectra were recorded at the ID26 beamline at the European Synchrotron Radiation Facility (ESRF), Grenoble, France. The synchrotron radiation was monochromatized by a Si(311) (U L₃ edge) or Si(111) (U M₄ edge) double crystal monochromator. The experimental energy resolution was about 1.8 eV (U L₃ edge) or 0.8 eV (U M₄ edge), determined as the width of the measured quasi-elastic peak scattered by a Si wafer. The energy of the primary monochromator was scanned from 17155 to 17180 eV or from 3715 eV to 3750 eV with 0.1 eV step width across the U L₃ edge (17166 eV) and U M₄ edge (3552 eV), respectively. For each excitation energy, the fluorescence photons emitted from the sample were monochromatized by three spherically bent Ge(777) (U L₃ edge) or one Si(220) (U M₄ edge) analyzer crystals and focused on the detector (Si drift, KETEK, or avalanche photodiode, Oxford). The sample, crystal and detector were positioned on a circle (Rowland geometry) with 1 m diameter, equal to the bending radius of the crystals.

RESULTS

The spectral features of a conventional XANES spectrum are broadened mainly by instrumental effects and uncertainty in the core-hole energy correlated with the core-hole lifetime via the Heisenberg uncertainty principle. The deep core-hole in transmission mode is replaced by a shallow core-hole lifetime broadening in a fluorescence mode experiment. However, this advantage is not utilized in the latter due to the modest energy resolution of standard solid-state detectors. In HR-XANES, the solid-state detector is replaced by an analyzer crystal spectrometer (wavelength dispersion) providing overall experimental energy broadening of about 1 eV. The HR-XANES spectrum is obtained by scanning the energy of the primary beam across the absorption edge of interest while monochromatizing the emitted fluorescence emission line using the analyzer crystal spectrometer. The analyzer crystal (or crystals) are bent, in order to focus the monochromatized emission onto a detector.

Two uranium minerals, autunite and schroekingierite, are used as models to compare the structural sensitivity of the HR-XANES spectra at the U M₄ and L₃ edges. Autunite and schroekingierite have tetragonal (P4/nmm) and triclinic (P -1) crystal structures and the U atoms are both coordinated with O atoms in the first coordination sphere and with P (autunite) or C (schroekingierite) atoms in the second. In Fig. 1, the autunite and schroekingierite U L₃ edge HR-XANES spectra (a) are compared to the conventional fluorescence XANES spectra measured (b). All HR spectral features are sharper than the conventional XANES and a pre-edge is resolved. This pre-edge resonance results from transitions of 2p_{3/2} electrons to U 5f unoccupied states, as confirmed by multiple-scattering calculations performed with the FDMNES code [2]. The U M₄ HR-XANES of autunite and schroekingierite also show significant improvement in energy resolution (Fig. 1c); they exhibit fine structure not visible in the conventional fluorescence mode spectra (not shown here).

The differences between the two mineral U M₄ edge HR-XANES spectra (such as the energy shift of feature D enlarged in the inset Fig. 1c) are small compared to the large differences associated with their unlike U coordination environments observed in the U L₃ HR-XANES pre-edge features, intensity variations of the most pronounced resonance (white line: WL) and the post edge resonances (Fig. 1a). Note that these

feature differences between these two minerals are absent or not as evident in their conventional spectra (Fig. 1b).

We use the enhanced structural sensitivity of U L₃ edge HR-XANES spectra for U speciation analyses of U in the aged cement by comparison to reference mineral spectra (kasolite, phurcalite, uranophane and U incorporated in fluorite, Fig. 2a). Specifically, the areas of difference spectra resulting from subtracting the individual reference mineral normalized HR-XANES from the normalized spectrum for the U_cement sample are compared. The difference spectra are shown in Fig. 2b and their areas in Fig. 3. Note that the U_cement HR-XANES spectrum is plot two times in Fig. 2a) in order to facilitate the comparison with reference spectra. This analysis suggests that the largest similarity (signalled by the smallest area difference) is found between U_cement and phurcalite. U containing fluorite appears to be another potential U phase in the U_cement material, as the form of its difference spectrum and its area are similar to those for phurcalite. The difference spectrum for kasolite also has a small area. The largest difference in this difference area comparison is found between U_cement and uranophane. This result is in contrast to the report in [1], where uranophane was assumed to be the most probable U containing mineral phase in U_cement.

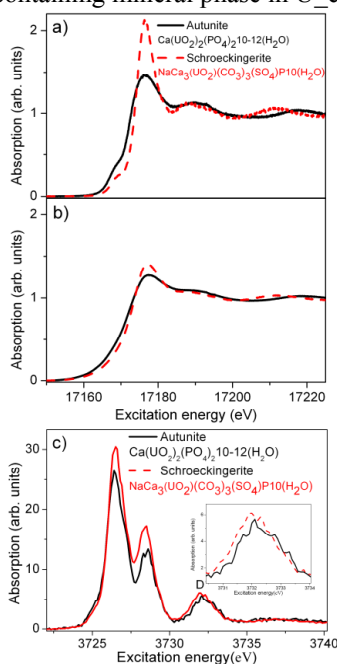


Fig. 1: HR a) and conventional b) U L₃ edge XANES and HR U M₄ edge XANES spectra c) for the natural U minerals autunite and schroëckingerite.

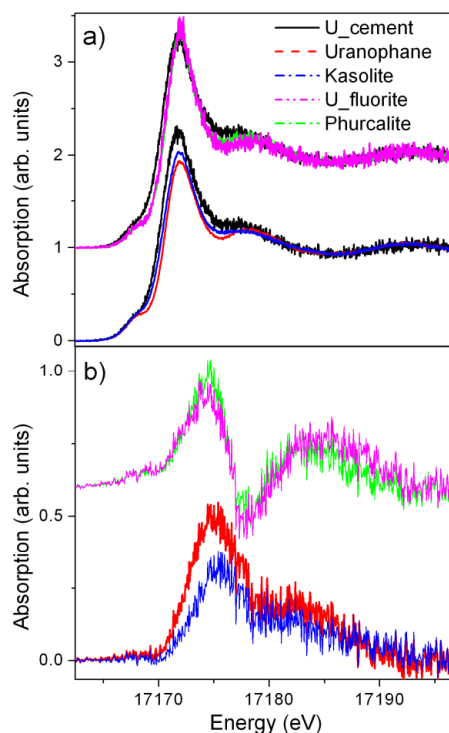


Fig. 2: U L₃ edge HR-XANES of U_cement, uranophane, kasolite, U in fluorite and phurcalite (a) and the difference spectra (b, see text for details).

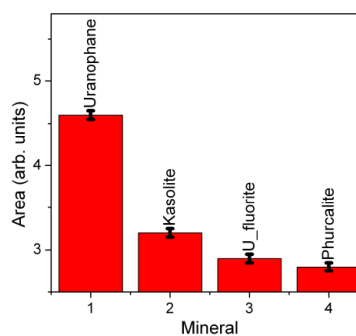


Fig. 3: The areas of the difference spectra shown in Fig. 2b.

REFERENCES

1. B. KIENZLER et al., “Chemical status of U(VI) in cemented waste forms under saline conditions”, *Radiochim. Acta*, **98**, 675–684 (2010).
2. T. VITOVA et al., “High energy resolution x-ray absorption spectroscopy study of uranium in varying valence states”, *Phys. Rev. B*, **82**, 235118 (2010).

WORKSHOP PARTICIPANTS

Margret Acker	TU Dresden, Sachgebiet Strahlenschutz	margret.acker@tu-dresden.de
Marcus Altmaier	Karlsruhe Institute of Technology (KIT), Institute for Nuclear Waste Disposal (INE)	marcus.altmaier@kit.edu
Samer Amayri	Johannes Gutenberg-Universität Mainz, Institute of Nuclear Chemistry	amayri@uni-mainz.de
Thuro Arnold	Helmholtz-Zentrum Dresden-Rossendorf, Institute of Radiochemistry	t.arnold@hzdr.de
Nidhu Banik	Karlsruhe Institute of Technology (KIT), Institute for Nuclear Waste Disposal (INE)	nidhu.banik@kit.edu
Astrid Barkleit	TU Dresden, Sachgebiet Strahlenschutz	a.barkleit@hzdr.de
Holger Bittdorf	Project Management Agency Karlsruhe (KIT-PTKA)	holger.bittdorf@kit.edu
Elke Bohnert	Karlsruhe Institute of Technology (KIT), Institute for Nuclear Waste Disposal (INE)	elke.bohnert@kit.edu
Angelika Bohnstedt	Karlsruhe Institute of Technology (KIT), Programm NUKLEAR	angelika.bohnstedt@kit.edu
Ingo Böttcher	Federal Office for Radiation Protection (BfS)	iboettcher@bfs.de
Muriel Bouby	Karlsruhe Institute of Technology (KIT), Institute for Nuclear Waste Disposal (INE)	muriel.bouby@kit.edu
Guido Bracke	Gesellschaft für Anlagen- und Reaktorsicherheit (GRS mbH)	guido.bracke@grs.de
Vinzenz Brendler	Helmholtz-Zentrum Dresden-Rossendorf, Institute of Radiochemistry	v.brendler@hzdr.de
Christiane Bube	Karlsruhe Institute of Technology (KIT), Institute for Nuclear Waste Disposal (INE)	christiane.bube@kit.edu
Gunnar Buckau	EC Joint Research Centre, Institute for Transuranium Elements (ITU)	gunnar.buckau@ec.europa.eu
Paul Carbol	EC Joint Research Centre, Institute for Transuranium Elements (ITU)	paul.carbol@ec.europa.eu
Sascha Eidner	University of Potsdam, Institute of Chemistry (Physical Chemistry)	eidner@chem.uni-potsdam.de
Thomas Fanghänel	EC Joint Research Centre, Institute for Transuranium Elements (ITU)	Thomas.FANGHAENEL@ec.europa.eu
David Fellhauer	EC Joint Research Centre, Institute for Transuranium Elements (ITU)	david.fellhauer@ec.europa.eu
Nicolas Finck	Karlsruhe Institute of Technology (KIT), Institute for Nuclear Waste Disposal (INE)	nicolas.finck@kit.edu
Heidmarie Fischer	Gesellschaft für Anlagen- und Reaktorsicherheit (GRS mbH)	heidmarie.fischer@grs.de
Bettina Franke	Landesamt für Bergbau, Energie und Geologie (LBEG)	bettina.franke@lbeg.niedersachsen.de

Daniela Freyer	TU Bergakademie Freiberg, Institut für Anorganische Chemie	Daniela.Freyer@chemie.tu-freiberg.de
Jiwchar Ganor	Ben-Gurion University of the Negev, Dept. of Geological and Environmental Sciences	ganor@bgumail.bgu.ac.il
Xavier Gaona	Karlsruhe Institute of Technology (KIT), Institute for Nuclear Waste Disposal (INE)	xavier.gaona@kit.edu
Horst Geckeis	Karlsruhe Institute of Technology (KIT), Institute for Nuclear Waste Disposal (INE)	horst.geckeis@kit.edu
Andrea Geißler	Helmholtz-Zentrum Dresden-Rossendorf, Institute of Radiochemistry	a.geissler@hzdr.de
Alix Günther	Helmholtz-Zentrum Dresden-Rossendorf, Institute of Radiochemistry	a.guenther@hzdr.de
Christina Hansmeier	Gesellschaft für Anlagen- und Reaktorsicherheit (GRS mbH)	Christina.Hansmeier@grs.de
Katja Hinz	Karlsruhe Institute of Technology (KIT), Institute for Nuclear Waste Disposal (INE)	katja.hinz@kit.edu
Sandra Kalanke	Clausthal University of Technology, Institute of Disposal Research	sandra.kalanke@tu-clausthal.de
Ralf Kautenburger	Universität des Saarlandes	r.kautenburger@mx.uni-saarland.de
Bernhard Kienzler	Karlsruhe Institute of Technology (KIT), Institute for Nuclear Waste Disposal (INE)	bernhard.kienzler@kit.edu
Reinhardt Klenze	Karlsruhe Institute of Technology (KIT), Institute for Nuclear Waste Disposal (INE)	reinhardt.klenze@kit.edu
Taishi Kobayashi	Karlsruhe Institute of Technology (KIT), Institute for Nuclear Waste Disposal (INE)	taishi.kobayashi@kit.edu
Siegfried Köster	Federal Ministry of Economics and Technology (BMWi)	siegfried.koester@bmwi.bund.de
Raymond Kowe	Nuclear Decommissioning Authority (NDA)	raymond.kowe@nda.gov.uk
Evelyn Krawczyk-Bärsch	Helmholtz-Zentrum Dresden-Rossendorf, Institute of Radiochemistry	e.krawczyk-baersch@hzdr.de
Johannes Kulenkampff	Helmholtz-Zentrum Dresden-Rossendorf, Institute of Radiochemistry, FS Leipzig	j.kulenkampff@hzdr.de
Dmitrii Kulik	Paul-Scherrer Institut (PSI)	dmitrii.kulik@psi.ch
Christi Leigh	Sandia National Laboratory, Carlsbad Office	cdleigh@sandia.gov
Patric Lindqvist-Reis	Karlsruhe Institute of Technology (KIT), Institute for Nuclear Waste Disposal (INE)	patric.lindqvist@kit.edu
Holger Lippold	Helmholtz-Zentrum Dresden-Rossendorf, Institute of Radiochemistry, FS Leipzig	h.lippold@hzdr.de
Christian Marquardt	Karlsruhe Institute of Technology (KIT), Institute for Nuclear Waste Disposal (INE)	christian.marquardt@kit.edu
Volker Metz	Karlsruhe Institute of Technology (KIT), Institute for Nuclear Waste Disposal (INE)	volker.metz@kit.edu
Henry Moll	Helmholtz-Zentrum Dresden-Rossendorf, Institute of Radiochemistry	h.moll@hzdr.de

Helge Moog	Gesellschaft für Anlagen- und Reaktorsicherheit (GRS mbH)	helge.moog@grs.de
Christina Möser	Universität des Saarlandes	c.moeser@mx.uni-saarland.de
Claude Musikas	Agence de l'OCDE pour l'Énergie Nucléaire (OECD-NEA)	musikas.claude@neuf.fr
Petra Panak	Heidelberg University, Physikalisch-Chemisches Institut	petra.panak@kit.edu
Michel Perdicakis	LCPME, Nancy University, CNRS	perdi@lcpme.cnrs-nancy.fr
Vladimir Petrov	M.V. Lomonosov Moscow State University, Chemistry Department, Radiochemistry Div.	vladimir.g.petrov@gmail.com
Thomas Pick	Niedersächsisches Ministerium für Umwelt und Klimaschutz	thomas.pick@mu.niedersachsen.de
Thomas Rabung	Karlsruhe Institute of Technology (KIT), Institute for Nuclear Waste Disposal (INE)	thomas.rabung@kit.edu
Linfeng Rao	Lawrence Berkeley National Laboratory	lrao@lbl.gov
Donald T. Reed	Los Alamos National Laboratory, Carlsbad Operations	dreed@lanl.gov
Beate Riebe	Leibniz-University Hannover, Institute for Radioecology and Radiation Protection	riebe@irs.uni-hannover.de
Maria del Henar Rojo	CIEMAT	mdelhenar.rojo@ciemat.es
Greg Roselle	Sandia National Laboratory, Carlsbad Office	gtrosel@sandia.gov
Yoav Rosenberg	Ben-Gurion University of the Negev, Dept. of Geological and Environmental Sciences	yoavoved@gmail.com
Jörg Rothe	Karlsruhe Institute of Technology (KIT), Institute for Nuclear Waste Disposal (INE)	joerg.rothe@kit.edu
Markus Rothmeier	Karlsruhe Institute of Technology (KIT), Institute for Nuclear Waste Disposal (INE)	markus.rothmeier@kit.edu
Konstantin Rozov	Forschungszentrum Jülich GmbH, Institut für Energie- und Klimaforschung	k.rozov@fz-juelich.de
Sonia Salah	Belgian Nuclear Research Center	ssalah@sckcen.be
Jonas Sander	Universität des Saarlandes	r.kautenburger@mx.uni-saarland.de
Thorsten Schäfer	Karlsruhe Institute of Technology (KIT), Institute for Nuclear Waste Disposal (INE)	thorsten.schaefer@kit.edu
Katja Schmeide	Helmholtz-Zentrum Dresden-Rossendorf, Institute of Radiochemistry	k.schmeide@hzdr.de
Juliane Schott	Helmholtz-Zentrum Dresden-Rossendorf, Institute of Radiochemistry	j.schott@hzdr.de
Holger Seher	Gesellschaft für Anlagen- und Reaktorsicherheit (GRS mbH)	holger.seher@grs.de
Andrej Skerencak	Karlsruhe Institute of Technology (KIT), Institute for Nuclear Waste Disposal (INE)	andrej.skerencak@kit.edu

Kastriot Spahiu	Svensk Kärnbränslehantering AB (SKB)	kastriot.spahiu@skb.se
Silvia Stumpf	Project Management Agency Karlsruhe (KIT-PTKA)	silvia.stumpf@kit.edu
Juliet Swanson	Los Alamos National Laboratory (LANL), Carlsbad Office	jsswanson@lanl.gov
Steffen Taut	TU Dresden, Sachgebiet Strahlenschutz	steffen.taut@tu-dresden.de
Punam Thakur	Carlsbad Environmental Monitoring & Research Center	pthakur@cemrc.org
Abraham van Luik	US Department of Energy, Carlsbad Field Office	abraham.vanluik@wipp.ws
Tonya Vitova	Karlsruhe Institute of Technology (KIT), Institute for Nuclear Waste Disposal (INE)	Tonya.Vitova@kit.edu
Lieselotte von Borstel	DBE TECHNOLOGY GmbH (DBE-TEC)	borstel@dbe.de
Stefan Wilhelm	AF-Consult Switzerland Ltd	stefan.wilhelm@afconsult.com
Andrew Wolfsberg	Earth and Environmental Sciences, Los Alamos National Laboratory	awolf@lanl.gov
Ezgi Yalcintas	Karlsruhe Institute of Technology (KIT), Institute for Nuclear Waste Disposal (INE)	ezgi.yalcintas@kit.edu



PART II

1st International workshop on

High Temperature Aqueous Chemistry - HiTAC -

Karlsruhe, Germany, November, 9th 2011

Organisation

Organizers

*Karlsruhe Institute of Technology (KIT)
Institute for Nuclear Waste Disposal (INE)
Karlsruhe, Germany*

Sponsors

Federal Ministry of Economics and Technology (BMWi), Germany

Organizing Committee

*Marcus Altmaier, Christiane Bube, Bernhard Kienzler and Volker Metz
Karlsruhe Institute of Technology (KIT), Institute for Nuclear Waste Disposal (INE)
PO-Box 3640, 76021 Karlsruhe, Germany*

Contact, e-mail: marcus.altmaier@kit.edu, bernhard.kienzler@kit.edu

Acknowledgements

We gratefully acknowledge Elke Bohnert, Elke Lukas, Stefanie Krieger, Andrej Skerencak, Hieronymus Sobiesiak and Denise Wedemeyer (KIT) for their administrative & technical support.

Overview of the HiTAC workshop

Aqueous chemistry and geochemistry has been mostly studied at room temperature. Many relevant processes that define our everyday life take place under these conditions, and it is much more straightforward to perform experimental studies at room temperature without the added complexities in maintaining and controlling the temperature. There are, however, many circumstances where an understanding of the effects of temperature is needed to address scientific questions and it also may be critical to know how various chemical processes will work at elevated temperature. An example of this is the long-term geologic disposal of high level radioactive waste where elevated temperatures due to the thermal output of the waste is expected. As shown in many studies, the room-temperature behavior and chemical models, in most cases, cannot be readily extrapolated to predict behavior at elevated temperature conditions. Different chemical speciation schemes and thermodynamic parameters may lead to distinct changes in overall chemical behavior with increasing temperature. These temperature effects on aqueous systems are best understood by performing dedicated experimental or theoretical studies.

The focus of the HiTAC workshop was the aqueous geochemistry and chemical behavior of radionuclides in systems at elevated temperature that are relevant to the safe disposal of heat producing nuclear waste. The scope of HiTAC, however, was extended beyond the nuclear waste community to provide a broader basis for discussion and exchange with related research fields. The scientific contributions at HiTAC relayed information on many different systems and scenarios, provided an overview of the various experimental approaches used to investigate aqueous chemistry at elevated temperature and reflected several boundary conditions. They ranged from fundamental investigations to applied studies and were not restricted to any particular host rock formation relevant for nuclear waste disposal.

The disposal of high-level waste (HLW) glass or spent nuclear fuel leads to elevated temperatures in the near-field and the surrounding host rock. The temperature evolution in a HLW glass or spent nuclear fuel disposal system depends on the thermal loading of the waste itself, the thermal conductivity of the host rock, the container/canister material and concept, and on the overall design configuration of the repository. For most disposal concepts, a key design goal is to limit the maximum temperature. This maximum temperature is achieved a certain time after the disposal of the waste based on the radioactive decay profile and heat capacity of the host rock. The time-evolution of the temperature and the maximum temperatures reached can have significant impacts on the waste disposal operation, the safety of workers, the design and requirements of the ventilation systems and the thermo-mechanical behavior of the entire disposal area for several centuries. In this context, there can also be significant consequences on the retrievability of the waste.

The performance assessment of a repository for heat generating waste will have well-defined scenarios that correlate to certain periods of time that link to the higher temperatures and repository temperature history. For these scenarios, sufficient knowledge on the processes influenced by elevated temperatures is needed. The aim of HiTAC was not only to provide an international forum to exchange information and discuss scientific results but to also help identify, prioritize and structure research activities on the effects of high temperatures that are especially relevant for aqueous actinide chemistry.

The HiTAC workshop was organized around contributions by invited speakers who provided an overview of their current research on aquatic chemistry of systems at elevated temperatures. The plenary speakers included Pascale Bénézeth (GET, France), Lara Duro (Amphos²¹, Spain), Bernhard Kienzler (KIT-INE, Germany), Dimitrii Kulik (PSI-LES, Switzerland), Linfeng Rao (LBNL, USA) and Andrej Skerencak (KIT-INE, Germany). In addition to the invited speakers, there were a number of contributed talks and posters at HiTAC to permit the presentation of a broad spectrum of topics and facilitate more extensive discussions.

Summary of the HiTAC workshop

The invited talks at HiTAC targeted the overall importance and relevance of key aspects of aqueous chemistry at elevated temperature. All invited speakers were internationally-recognized experts in this field and helped define the overall agenda for the workshop.

B. Kienzler from KIT-INE outlined the relevance of elevated temperature conditions in the context of nuclear waste disposal. Temperature can increase up to 200 °C for certain scenarios and persist above 100 °C for thousands of years depending on repository design and waste inventory. In most cases, however, temperatures should be limited to the lower temperature ranges so that studies at 80 - 90 °C will yield essential information. Predictions that are based on 25 °C investigations are generally not sufficient to reliably describe processes that are expected at elevated temperatures. Considering systematic trends on aqueous complex formation and solid phase stability, however, can provide useful qualitative insights since specific information is often lacking.

P. Bénézeth from the Université Toulouse in France gave an overview of recent studies on fluid-mineral interactions at higher temperatures. Most examples were taken from carbonate sequestration studies and confirmed the importance of including research and investigators beyond the nuclear waste disposal community. It was clear that many relevant chemical processes and experimental approaches used in the research context outlined by *P. Bénézeth* are comparable to problems faced in high level waste disposal research. In this view, increased exchange of information and specific data should be most fruitful and is in the mutual interest of both communities.

Talks by *L. Rao* of Lawrence Berkeley National Laboratories in the USA and *A. Skerencak* from KIT-INE were more focused on actinide chemistry and highlighted recent experimental studies with radionuclides at elevated temperatures. *L. Rao's* comprehensive studies on actinide chemistry at elevated temperatures performed over the last two decades are generally accepted as internationally leading and bridging gaps in the thermodynamic database for nuclear waste disposal. Examples given by *L. Rao* on the hydrolysis of Th(IV), Np(V), U(VI) and Pu(VI) at elevated temperature showed successful studies using several complementary experimental approaches. Hydrolysis of U(VI), Np(V) and Pu(VI) is found to be enhanced by several orders of magnitude as temperature is increased from 10 to 85 °C, which could have a significant effect on the behavior of actinides in the heat-generating waste repository. *A. Skerencak*, presented recent work at KIT-INE on trivalent Curium, which is a well-established chemical analogue for Am(III) and Pu(III) - trivalent actinides that are more important in the actinide source term. Cm(III) has superb spectroscopic properties and can be used to investigate actinide speciation at trace-level concentrations. The examples taken from recent

time-resolved laser fluorescence studies illustrated the applicability of this powerful speciation technique and summarized interesting new data on Cm-sulfate and Cm-nitrate complexation.

Experimental studies performed at elevated temperatures are very time-consuming and technically challenging. It is therefore not realistic to expect a complete set of thermodynamic data that cover all elevated temperature conditions based upon experimental studies alone. The use of estimation methods to derive missing thermodynamic data is a complimentary option to data measurement that permits a more comprehensive treatment of elevated temperature effects. The presentations of *L. Duro* of Amphos²¹, Spain, and *D. Kulik*, Paul-Scherrer Institute, Switzerland, explored the option of deriving a thermodynamic database for elevated temperatures using entropy estimations, and proposed alternative approaches for the geochemical modeling of aqueous systems at moderate temperatures, respectively. It was pointed out that thermodynamic constants and model calculations based on data estimation require experimental validation and often do not provide a sufficient basis for the safety assessment in the context of nuclear waste disposal.

The contributed talks and poster presentations expanded on the information and topics outlined by the invited speakers but also included some additional topics. The question of how to close the most important thermodynamic data gaps and the role of estimation methods in this process were further discussed. The ongoing activities within collaborative research projects that also included elevated temperature effects, e.g. the German THEREDA database project and VESPA, or the European FIRST-Nuclides project, were presented.

Sorption effects cause significant radionuclide retardation under many conditions. Consequently, several poster contributions addressed different aspects of sorption at elevated temperatures. Studies included several different nuclides like Se, Eu(III), Np(V) or U(VI) and considered sorbates like bentonite, anatase, goethite, smectite or natural clays like Opalinus clay. As many different factors influence sorption processes, e.g. the aqueous metal-ion speciation or surface properties such as the point of zero charge, are impacted by temperature, it is difficult to derive comprehensive predictive models. However, based on the general trends observed in the studies reported, it was confirmed that sorption process should also lead to significant radionuclide retardation at elevated temperatures.

Several studies highlighted the need to established strategic experimental data for actinide complexation reactions at higher temperatures. This is critically needed to benchmark and validate of the estimation methods being used. Examples presented at the HiTAC poster session ranged from fundamental studies on Cm(III) hydration, U(VI) hydrolysis reactions, to the complexation of actinides with small organic ligands.

As an example of the high importance in assessing temperature effects on the solubility- limiting solid phases and not limit investigations to the liquid phase, a comprehensive study on Zr(IV)-oxyhydroxide solubility was

presented. As a function of the equilibration time of the batch samples at higher temperatures, a clear impact of temperature on the particle size and hence overall Zr(IV) solubility was observed. The specific condition of spent fuel interactions in saline systems was similarly discussed.

Main conclusions from HiTAC

The presentations and scientific discussions during the HiTAC workshop were summarized in the closing discussion chaired by B. Kienzler of KIT-INE. The focus of the closing discussion was to wrap-up the main outcome of the workshop and point to important topics potentially relevant for future research activities.

It was emphasized that specific experimental studies on high temperature aqueous chemistry are required, as the present knowledge and experimental database is in many cases clearly insufficient. This is especially true for the prediction of actinide chemistry in aqueous systems at elevated temperatures. The present knowledge of high-temperature actinide chemistry is sufficient to give us an understanding of the general trends and in some cases it is possible to make detailed predictions on specific effects, but so far no comprehensive picture and overall predictive model exists. It was also indicated that the often rather intricate experimental investigations can in many cases be expected to be simplified by the fact that many kinetic effects known to influence and complicate studies and data analysis at lower temperatures become less significant at elevated temperatures.

Given the often high demands on experimental techniques and equipment for studies at elevated temperatures, it is clear that studies should, whenever possible, be performed within a larger research context that allows the exchange of technical tools and scientific expertise on an international level. In the specific case of experimental studies on actinides, it is obvious that dedicated facilities are required to handle radionuclides to meet the necessary safety standards. These institutions must have a broad set of experimental techniques available to analyze radionuclides on site since the samples generated in most cases, cannot be transferred to non-nuclear analytical facilities. Strong scientific overlap of research performed by the nuclear waste disposal community with projects and studies from non-nuclear activities exist in many cases, e.g. in the context of geothermal approaches to energy production or geochemical questions connected to carbonate sequestration. Advanced experimental and conceptual approaches can often be transferred and proactive actions and collaborations that exploit these areas of converging interests are encouraged.

Looking at the scope of HiTAC and the different contributions submitted, it should be noted that very few studies were presented on spent nuclear fuel or other potential HLW wasteforms. This however would be very important, as these materials are obviously the first to potentially interact with groundwater at elevated temperatures and the addressing this chemistry and related processes was recognized as a high-priority topic for the future.

Most studies presented at HiTAC were performed either in aqueous solutions or investigated the sorption of radionuclides on mineral surfaces. Only one study was focused on assessing the influence of elevated temperature on the solubility-limiting actinide solid phases. It is known that equilibration at higher temperature will change crucial solid phase characteristics and thus affect solubility limits, actinide retention processes and source term estimations. For example, elevated temperatures can affect the particle size of mineral-oxide crystallites and hence solubility products, lead to changes in solid phase stoichiometry or change crystal water content, influence metal-oxide surfaces and impact the mineral surface characteristics relevant for sorption processes. A more detailed understanding of solid phase behavior therefore will be essential to complement investigations on actinide complexation or actinide sorption in the future.

In order to separate the different effects influencing aquatic chemistry at elevated temperatures, the advantages of combining different experimental approaches as analytical methods was outlined. This is especially important to investigate the intrinsically complex actinide systems with complex speciation schemes and solid phase properties. Here, it is advantageous to use complementary approaches that help separate effects into different thermodynamic quantities and parameters. Coupling spectroscopic investigations to potentiometric and coulometric titrations can yield information on entropy, enthalpy and the free Gibbs energy. The need to address effects on solubility-limiting solid phases and determine the overall radionuclide solubility is similarly important. Systems at elevated ionic-strengths where ion-interaction processes cannot be neglected or estimated for higher temperatures also require special attention since it is important to specifically evaluate the temperature effects e.g. on complex formation constants or thermodynamic solubility, for the ion-interaction processes and activity coefficients at the relevant temperatures.

The availability of complete and consistent thermodynamic databases is needed to model the effect of elevated temperatures on aqueous systems. While there is extensive data on many minerals important to geochemical modeling, the data for actinides and long-lived fission products is rather limited. The books published on actinide thermodynamics within the NEA Thermodynamic Database Series offer expertly evaluated compilations of thermodynamic data for room temperature conditions, but are rather incomplete in their consideration of elevated temperature conditions both in terms of equilibrium data and ion-interaction coefficients. For this reason, there is an important need to improve the thermodynamic database for actinides at elevated temperatures.

The use of estimation methods to close gaps in the thermodynamic database was recognized in HiTAC as a promising approach to quickly improve the present database situation as it is not realistic to close all existing data gaps by performing specific experimental investigations. Different approaches for estimating or extrapolating fundamental thermodynamic data were discussed. There are several examples for the successful

use of thermodynamic data estimations for mineral systems, but the application of these models to actinide species is expected to be challenging, mainly in view of the often highly complex aqueous actinide speciation schemes and ill-defined amorphous solid phases that control actinide solubility. The systematic application of estimation methods established for inactive systems on actinide systems was considered an important step forward if it is supported by experimental validation on some actinide systems. A favorable comprehensive approach would thus include (i) the systematic estimation of thermodynamic data, (ii) calculation of radionuclide solubility limits and aqueous speciation based on the estimated set of thermodynamic data, and (iii) the experimental validation of the calculations. The validation would either confirm the estimated data selections or, when there is insufficient agreement, to identify and prioritize the specific chemical systems that may require closer experimental investigation.

The main outcome of HiTAC that was shared by many of the participants was that increased scientific exchange on this complex topic is needed. This is especially true in view of the large uncertainties in the present understanding of aqueous chemistry at elevated temperatures and the substantial experimental effort required to perform comprehensive and systematic experimental studies. The HiTAC workshop was an important first step in the right direction and successfully brought together scientists working in this broad field with the experts interested in potential applications in an open and scientifically constructive environment. An understanding of the aqueous chemistry at elevated temperatures relevant to many applications inside or outside the nuclear waste disposal community will require more dedicated research efforts in the future and can only profit from constructive and productive interlinking of the scientific community.

PROGRAM

Oral contributions

Introduction

- *M. Altmaier / V. Metz.* Workshop organization comments.
- *H. Geckeis.* Welcome address.

Session 1

- *B. Kienzler.* Elevated Temperatures in a High-Level Waste Repository: Are 25°C Data Sufficient?
- *L. Truche.* Redox reactions induced by hydrogen under deep geological nuclear waste repository
- *P. Bénézeth.* Toward a better understanding of CO₂-fluid-mineral-microorganisms interactions up to high temperature

Session 2

- *L. Rao.* Actinide Complexation in Aqueous Solutions at Elevated Temperatures: Bridging the Gaps in the Thermodynamic Database for Nuclear Waste Repository.
- *A. Skerencak.* TRLFS studies of Cm(III) complexation at elevated Temperatures.

Session 3

- *J. Ganor.* The coupling between dissolution and precipitation.
- *L. Duro.* TDB for elevated temperature conditions using entropy estimations
- *D. Kulik.* Geochemical Modeling of Aqueous Systems at Moderate Temperatures.

Poster presentation

The following posters were presented during the Workshop:

- *H. Moog*. THEREDA.
- *B. Kienzler*. FIRST-Nuclides, Fast / Instant Release of Safety Relevant Radionuclides from Spent Nuclear Fuel.
- *B. Bischofer*. Overview VESPA Project.
- *M. Altmaier, X. Gaona, D. Fellhauer, G. Buckau*. RECOZY intercomparison exercise on redox determination methods – final report on main conclusion and recommendations.
- *D. Fröhlich, S. Ayari, J. Drebert, T. Reich*. Migration of Np(V) in natural clay at elevated temperature.
- *J. Lützenkirchen*. The influence of temperature on sorption: A preliminary assessment for Uranium(VI) sorption to bentonite.
- *K. Schmeide*. Formation of U(VI) lactate and citrate complexes and their sorption onto Opalinus Clay between 7 and 65°C.
- *C. Franzen, N. Jordan, K. Müller, T. Meusel, V. Brendler*. Temperature impact on the sorption of Selenate onto Anatase.
- *M. Kersten, N. Vlasova*. Effect of temperature on selenate adsorption by goethite.
- *Th. Rabung, A. Bauer, F. Claret, T. Schäfer, G. Buckau, Th. Fanghänel*. Influence of temperature on sorption of europium onto smectite: the role of organic contaminants.
- *J. Schott*. Temperature Depending Investigations to the Sorption of Eu(III) on Opalinus Clay
- *P. Lindqvist-Reis, R. Klenze, G. Schubert, Th. Fanghänel*. Octa- and nona- hydrated Cm(III) in aqueous solution up to 200 °C.
- *X. Gaona, M. Grivé, A. Tamayo, A. Skerencak, M. Altmaier, L. Duro*. Assessing temperature effects: methods for the estimation of $S^{\circ m}$ for aqueous actinide species and applicability of the van't Hoff expression.
- *A. Barkleit*. Spectroscopic Characterization of Eu(III) and Am(III) Complexes with Small Organic Molecules at Elevated Temperatures.

- *T. Kobayashi, D. Bach, M. Altmaier, T. Sasaki, H. Moriyama.* Temperature Effect on Solubility and Solid Phase of Zr(IV) Hydroxide.
- *R. Steudtner, K. Müller, T. Meusel, V. Brendler.* Preliminary multi-method spectroscopic approach for the uranium(VI) hydrolysis at temperatures up to 60°C.
- *N. Banik, S. Walz, C. Marquardt, P. Panak.* Complexation studies of Np(V)-Lactate at elevated temperature

ABSTRACTS OF ORAL CONTRIBUTIONS

List of contributions

Elevated Temperatures in a High-Level Waste Repository: Are 25 °C Data Sufficient? <i>B. Kienzler</i>	133
Redox reactions induced by hydrogen under deep geological nuclear waste repository: homogeneous, heterogeneous and surface mediated reactions under hydrothermal conditions <i>L. Truche, G. Berger, A. Albrecht</i>	135
Toward a better understanding of CO ₂ -fluid-mineral-microorganisms interactions up to high temperature <i>P. Bénézeth, O. Pokrovsky, G. Saldi, Q. Gautier, I. Bundeleva, L. Shirokova, A. Stefansson, J.-L. Dandurand, J. Schott</i>	137
Experimental Investigations of Actinide Hydrolysis at Elevated Temperatures <i>L. Rao</i>	139
TRLFS studies of actinides complexation at elevated temperatures <i>A. Skerencak</i>	141
The coupling between dissolution and precipitation <i>J. Ganor, C. Zhu, P. Lu, Z. Zheng</i>	143
TDB for elevated temperature conditions using entropy estimations <i>L. Duro, M. Grivé, E. Colàs, X. Gaona, L. Richard</i>	145
Geochemical Modeling of Aqueous Systems at Moderate Temperatures: Approaches and Tools for Temperature Extrapolations <i>D.A. Kulik</i>	147

Elevated Temperatures in a High-Level Waste Repository: Are 25°C Data Sufficient?

Bernhard Kienzler

*Karlsruhe Institute of Technology, Campus North, Institut für Nukleare Entsorgung (INE)
76344 Eggenstein-Leopoldshafen, Germany
email: Bernhard.kienzler@kit.edu*

INTRODUCTION

The disposal of HLW or spent nuclear fuel gives rise to elevated temperatures in the near-field of radioactive waste and in the surrounding host rock. The temperature evolution in a HLW or spent nuclear fuel disposal depends on the heat production of the waste itself, on the canister concept, on the disposal concept and on the heat conductivity of the host rock. Due to the heat capacity of the host rock, the maximum temperature will be reached some time after the disposal. For most disposal concepts, the design bases on a regulation of the maximum temperature. The evolution of the temperature and the maximum temperatures have significant impact on the operation of the disposal, the safety of workers, the ventilation systems and the thermo-mechanical behaviour of the whole disposal area for several centuries and consequently on the possibility of retrievability. According to the radioactive decay, the thermal power and the resulting temperatures decrease.

For performance assessment of a disposal, it is indispensable to have well-defined scenarios correlated to certain periods of time which are connected to temperatures or temperature histories. For these scenarios, sufficient knowledge on the processes influenced by elevated temperatures is mandatory. The most important scenario corresponds to the normal evolution of the disposal in the host rock when all barriers behave as expected. In this case, penetration of solutions and solution volumes are restricted by diffusion (argillaceous) or by brine migration processes (rocksalt).

In a preliminary safety assessment for a nuclear waste disposal in the Gorleben salt dome, a maximum temperature of 200°C and a minimum operation time span of 40 yrs. are considered. The maximum temperature will be reached after ~100 yrs. After several hundred years, the temperature decreases again and will be in the range of 100°C after about 1000 yrs. After a few thousand years, the temperature approaches the ambient temperature of 35°C of the disposal in 840 m depth. In a disposal in argillaceous or crystalline host rocks, the maximum temperatures at the surfaces of the disposal galleries are limited to ~100°C.

According to the current safety requirements [1], the required lifetime of the waste containers is 500 years and the engineered barriers have to provide for isolation of the wastes until the host rock overtakes this task. This will happen within a few thousand years which is the high temperature period.

PRESENT STATE OF THE ART OF TEMPERATURE EFFECTS

Heat-producing wastes will be stored in thick-walled carbon steel canisters (Pollux concept) in Germany. The influence of increased temperatures on canister material corrosion has been studied for different boundary conditions. The corrosion rate shows only a weak dependence on temperature up to 170°C. Iron corrosion products have been identified and consist simultaneously of Fe(II) and Fe(III) phases, e.g. magnetite and maghemite. Understanding of canister corrosion at elevated temperatures is understood rather well and does not demand research priority.

After penetration of salt solutions into the canisters, the wastes will start to corrode. An important effect on the corrosion rate has the composition of the solution, e.g. NaCl or MgCl₂-rich solutions. It has been shown that temperature has an effect on several parameters of HLW glass dissolution [2]. Most important is the increase of the silicate concentration as function of the temperature. However, HLW glass dissolution did not show drastic deviations from the behaviour at room temperature. Glass corrosion at elevated temperatures does not require a research priority.

Most studies on the temperature dependency of UO₂(s) / spent nuclear fuel corrosion have been conducted solely under oxic or anaerobic conditions. Under significantly reducing conditions to be encountered in a deep geological repository, the temperature dependency of these corrosion processes has not(!) been measured up to now. The influence of temperature on the rate of radionuclide release from grain boundaries, as well as on the rate of UO₂(s) matrix dissolution and the consecutive release of matrix-bound radionuclides has not yet been properly understood [3]. Experiments show that spent fuel corrosion is not a thermally activated process and deviations from room temperature behaviour are constrained.

Spent fuel corrosion is controlled by radiolytic effects. Many reactions involved in radiolysis of aqueous solutions are well known at room temperature. However, kinetic data on the temperature dependency of radiolytic reactions are limited practically to radiolysis of pure H and few trace components in water. Concentration of the hydroxyl radical, OH*, is critical for the evolution of radiolytic chain reaction and consecutive UO₂(s) / spent nuclear fuel corrosion reaction. For instance, the inhibiting effect of H₂ on radiolysis of water is controlled by a reaction with the hydroxyl radical (OH* + H₂ = H).

Modeling of the aqueous chemistry at elevated temperatures requires knowledge of the stability and solubility products of solubility limiting solid phases, the effect of temperature on complex formation constants and finally on ion-interaction parameters for all species involved (SIT, Pitzer). Experimental work on aqueous actinide chemistry at higher temperature is rather limited and does not cover all relevant systems. On the other hand, thermodynamic data for the main components of the solution matrix are often available with adequate precision. At present, there is no reliable thermodynamic database for modelling actinide solubilities and complex formation at elevated temperatures.

In the case of lanthanide/actinide elements, only a few measurements on the temperature dependence of the solubility of solid phases are published. Rao [4] investigated the solubility of Nd(OH)₃ in 0.1 M NaCl solution between 25° and 90°C. Within the scatter of experimental data, no significant temperature effect was found. Giffaut analyzed the solubility of Am(III) in NaCl-NaHCO₃-Na₂CO₃ systems. between 20 and 70°C [5] resulting in variations of less than a factor of 5. For ThO₂(cr) and UO₂(cr), the crystallinity increased by increasing temperatures [6]. The fast transformation into the thermodynamically stable solid phases seems to be a general trend increasing with higher temperatures. The tendency towards formation of metastable solids that often affects experimental work at room temperature is overcome by the much faster kinetics at increased temperature conditions. No temperature dependence of the solubility of UO₂(cr) was found up to 300°C. Also no temperature effect was found for Np(V) solubility. The measured Pu concentration in presence of PuO₂(am,hyd) decreased slightly log[Pu]= -7.7 (25°C), -8.5(60°C) to -8.4(90°C) mainly caused by colloids.

It should be noted, that both the solubility products (of the stable solid phase) and the tendency towards complex formation is determining the solubility for a given element or compound and boundary conditions. If concentration does not change with increasing temperature might not reflect unchanging chemical composition but rather a compensation of different parameter like solubility products and complex formation constants. In this case the speciation and distribution of the aqueous species may change drastically at nearly constant overall nuclide concentration.

Contradicting results of temperature dependent sorption have been published. For Cs⁺ temperature independent sorption was measured, as well as a decreasing sorption with increasing temperature. For the divalent cation Pb a decrease of the Rd and for Ba a constant Rd is reported. For Ni²⁺, Kd increases from

25°C to 80°C by one order of magnitude. In the case of Eu, sorption increases significantly with increasing temperature. The different temperature effects may also be correlated to the substrates and not to the cations.

CONCLUSIONS

For the rocksalt host rock, several aspects have been identified where deeper insight into the temperature dependent mechanisms and reactions is required:

- Model (Pitzer) parameters for description of radionuclides in highly concentrated solutions at elevated temperatures.
- Solubility of radionuclides forming negatively charged OH⁻ complexes in highly concentrated solutions at elevated temperatures.
- Solubility of non oxide/hydroxide solids with radionuclides (such as silicates, carbonates, etc.) at elevated temperatures.
- Elucidation of sorption and sorption mechanisms of radionuclides on solids of different properties at elevated temperatures.

All these investigations require accurate pH measurement over the temperature range which is not state-of-the art, presently.

REFERENCES

- [1] BMU, "Sicherheitsanforderungen an die Endlagerung wärmeentwickelnder radioaktiver Abfälle," ed. Berlin: Bundesministerium für Umwelt Naturschutz und Reaktorsicherheit, 2010, p. 22.
- [2] B. Grambow and R. Muller, "First-order dissolution rate law and the role of surface layers in glass performance assessment," *Journal of Nuclear Materials*, vol. 298, pp. 112-124, Sep 2001.
- [3] B. Grambow, et al., "Long-term stability of spent nuclear fuel waste packages in Gorleben salt repository environments," *Nuclear Technology*, pp. 174-188, 1998.
- [4] L. Rao, et al., "Solubility of Nd(OH)₃(c) in 0.1 M NaCl Aqueous Solution at 25°C and 90°C," *Radiochim. Acta*, vol. 72, pp. 151-155, 1996.
- [5] E. Giffaut, "Influence des ions chlorure sur la chimie des actinides," *Universite de Paris-Sud, Orsay, France*, 1994.
- [6] D. Rai, et al., "Solubility and Solubility Product at 22°C of UO₂(cr) Precipitated From Aqueous U(IV) Solutions," *J. Solution Chem.*, vol. 32, p. 1, 2003.

Redox reactions induced by hydrogen under deep geological nuclear waste repository: homogeneous, heterogeneous and surface mediated reactions under hydrothermal conditions

L. Truche¹, G. Berger², A. Albrecht³

¹Université de Lorraine, G2R; 54506 Vandoeuvre-Lès-Nancy, France
email: Laurent.truche@g2r.uhp-nancy.fr

²CNRS - Université Toulouse, IRAP, 14 av. E Belin, 31400 Toulouse, France

³ANDRA, 1/7 rue Jean Monnet, 92290 Châtenay-Malabry, France

INTRODUCTION

Corrosion of steel canisters, stored in deep geological nuclear waste repository, leads to the generation and accumulation of hydrogen in the surrounding environment. One crucial research interest concerns the role of H₂ as a reducing agent for the aqueous/mineral oxidised species present in the site. We present here an overview of hydrogen abiotic reactivity via three case studies where hydrogen plays the role of an electron donor following three different reaction pathways: i) homogeneous reaction with sulphate reaction, ii) heterogeneous reaction with pyrite reduction into pyrrhotite, and iii) surface mediated reaction with nitrate reduction in the presence of steel. Some considerations and perspectives for further investigations on other hydrogen induced redox reactions are also examined.

DESCRIPTION OF THE WORK AND RESULTS

1) Sulphate reduction via homogeneous reaction

Sulphate reduction experimented in diphasic systems (water+gas) at 250-300°C and under 4 to 16 bar H₂ partial pressure [1] exhibits a high activation energy (131 kJ/mol) and require H₂S initiation and low pH condition as already observed in other published thermal sulphate reduction (TSR) experiments (Fig 1). The corresponding half-life is 210,000 yr at 90°C (thermal peak of the site in the French nuclear waste disposal concept). The condition for the reaction to occur is the speciation of sulphate dominated by non symmetric species (HSO₄⁻ at low pH), and we propose a three step reaction, one for each intermediate-valence sulphur species, the first one requiring H₂S as electron donor rather than H₂.

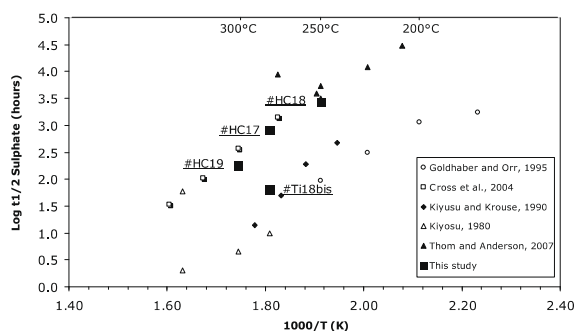


Fig. 1: Arrhenius plot of the inverse of reaction temperature ($1000/T$ with T in Kelvin) against the logarithm of the sulphate half-life and comparison with other published TSR experiments.

2) Pyrite reduction via heterogeneous reaction

On the contrary, pyrite reduction into pyrrhotite by H₂ occurs during a few days at temperature as low as 90°C at pH buffered by calcite [2]. The rate of the reaction could be described by a diffusion-like rate law in the 90-180°C temperature interval. When pH is controlled by calcite, the reaction presents all the characteristics of a coupled dissolution-precipitation mechanism occurring at the pyrite-pyrrhotite interface (Fig 2).

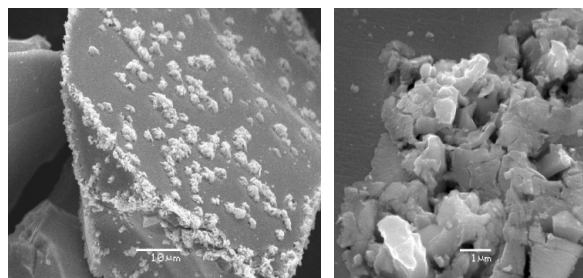


Fig. 2: SEM pictures in secondary electron mode of partially reacted pyrite at 150°C, $P_{H_2} = 15$ bar. Pyrrhotite appears as isolated clumps or islands preferentially located in reactive sites of high excess surface energy. Pyrrhotite exhibits a porous microstructure. Dark grey regions are unaltered pyrite and light grey regions are pyrrhotite

By considering the chemical affinity of the coupled reaction as a function of reaction extent we demonstrate that the spatial coupling is induced by pyrite as substrate for pyrrhotite nucleation and by the role of fluid chemistry at the reaction front. Far from equilibrium with respect to pyrite, the kinetics of sulphide production associated with the reaction is linearly related to the square root of time with an activation energy of 53 kJ/mol. The obtained results suggest that pyrite reduction is a process controlled by the H₂ diffusion across the pyrrhotite pits increasing during reaction progress. Note that under more acidic conditions, pyrite-pyrrhotite equilibrium is reached at lower pyrite dissolution rate.

3) Nitrate reduction via surface mediated reaction

Steels (carbon steel, 316L steel, and Hastelloy C-276) and corrosion by-products (mainly magnetite) provide excellent surfaces for heterogeneous catalysis while also supplying additional electron donors (mainly Fe⁰, Fe²⁺) for nitrate reduction.

Table 1: Comparative summary of results obtained on nitrate reduction in the presence of three different types of steel, carbon steel, 316L steel and Hastelloy C-276.

	Carbon steel	316L stainless steel	Hastelloy C-276
Secondary minerals	Magnetite, goethite, lepidocrocite, siderite	none	none
H₂ effect	H ₂ presence not required	No reaction without H ₂	No reaction without H ₂
pH effect	Strongly dependent upon pH	pH independent in the range 4 -9	pH independent in the range 4 -9
Inhibitor	Not found	Phosphate	Phosphate
Reaction order	2 different rate regime depending on the steel coating by magnetite	0 and 1 depending on nitrate concentration	0
Mechanism	Probably controlled by diffusion process through the magnetite coating	Langmuir Hinshelwood probable with H ₂ and nitrate co-sorption	Langmuir Hinshelwood probable with H ₂ and nitrate co-sorption
Activation Energy	63 kJ/mol	46 kJ/mol	186 kJ/mol

At 90°C, the reaction occurs within hours or a few days, leading to the formation of ammonia associated with a strong increase in pH. A parametric kinetic study (0 < P(H₂) < 10 bar, 0.1 < [NO₃⁻] < 10 mM, 90 < T < 150°C, 4 < pH < 9) reveals that different mechanisms occur depending on the nature of the steel. In the presence of 316L steel and Hastelloy C-276, nitrate reduction requires hydrogen and is independent of pH in the range 4-9. No corrosion of these steels is observed that would indicate a true catalysis process. The reaction is inhibited in the presence of phosphate. A sorption study performed at 90°C on 316L not only demonstrates sorption competition between phosphate and nitrate, but also shows that phosphate and nitrate are strongly sorbed (inner sphere complex) on the 316L steel surface in a wide pH range from 3 to 9. The Langmuir Hinshelwood formalism can be used to fit the kinetic data. On the contrary, nitrate reduction in the presence of carbon steel does not require hydrogen. The reaction rate is strongly dependant upon pH and is not inhibited by phosphate. Magnetite is the main corrosion by-product, and acts itself as catalyst by itself in the presence of hydrogen. The main conclusion is that nitrate reduction by iron metal [3] and carbon steel are very similar. Table 1 presents a summary of the results obtained on H₂-induced nitrate reduction catalysed by the presence of steel

A comparison of the reactions rates and mechanisms with other oxyanions such as selenate or uranate in the presence of hydrogen and metallic materials will provide an integrated overview of abiotic redox processes relevant in nuclear waste repository conditions. These new kinetics data can be applied in mathematical modelling, to evaluate the degree and extent of gas pressure build-up by taking into account the H₂ reactive geochemistry.

Beside the waste storage assessment, this study may also provide relevant conclusions in the understanding of redox processes governing hydrothermal systems.

REFERENCES

1. Truche et al., "Experimental reduction of aqueous sulphate by hydrogen under hydrothermal conditions: implication for the nuclear waste storage" *GCA*, **73**, 4829-4835 (2009).
2. Truche et al., "Kinetics of pyrite to pyrrhotite reduction by hydrogen in calcite buffered solutions between 90 and 180°C: implication for the nuclear waste disposal" *GCA*, **74**, 2894-2914 (2010).
3. Huang et al. "Kinetic of nitrate reduction by iron at near neutral pH" *J. Environ. Eng.* **128** (7), 604-611 (2002).

Toward a better understanding of CO₂-fluid-mineral-microorganisms interactions up to high temperature

Pascale Bénézeth¹, Oleg Pokrovsky¹, Giuseppe Saldi², Quentin Gautier¹, Irina Bundeleva¹, Liudmila Shirokova¹, Andri Stefansson³, Jean-Louis Dandurand¹ and Jacques Schott¹

¹*Géosciences Environnement Toulouse (GET) CNRS-OMP-IRD, 14 avenue Edouard Belin, 31400 Toulouse, France
email: benezeth@get.obs-mip.fr*

²*Lawrence Berkeley National Laboratory, Earth Science Division, 90-R1116, 1 Cyclotron Road, Berkeley, CA 94709-8126, USA*

³*Institute of Earth Sciences, University of Iceland, Sturlugata 7, 101 Reykjavik, Iceland*

INTRODUCTION

Since more than a decade now, research interests has been focusing in developing a fundamental scientific understanding of mitigation schemes to counter the adverse climate change effects associated with fossil fuel utilization, and to assess the feasibility of sequestering large quantities of CO₂ in subsurface aquifers either as trapped CO₂ gas and aqueous species or, ideally, as stable secondary carbonate phases. A significant research effort has focused on geochemical modeling (PHREEQC, EQ3/6, Geochemist's Workbench, to name few), which relies on the application of a molecular understanding of the fluids of interest as well as thermodynamic and kinetics of the reactions involved under conditions of varying solution compositions, temperature and pressure that can be encountered in these geological systems. However, particular pending scientific challenges of these geochemical modelling are the lack of reliable thermodynamic and kinetics data. Very recently, a growing scientific community has contributed to the better understanding of the coupled biological, geochemical, mechanical and hydrodynamical processes that result from the strong disequilibrium induced by injection of large amounts of CO₂ into wellbores and reservoirs and the accompanying modification of the pH of the formation waters [1]. New concepts are now emerging to quantify CO₂ reactive transport in geological reservoirs, using well-controlled laboratory experiments and field observations. Our ultimate goal is to provide robust and comprehensive thermodynamic and kinetic data bases on the CO₂ water-rock interactions in a form facilitating their incorporation in geochemical codes. These codes that might be coupled to reactive transport codes can be used by many research groups to model a wide range of natural systems including (but not limited) geological sequestration of carbon dioxide, geothermal reservoirs and hydrothermal systems, groundwater quality and radionuclide transports.

DESCRIPTION OF THE WORK

In the context of the challenge described above, the primary goal of our research is to focus on the thermodynamic stabilities and the kinetics of dissolution and precipitation of important carbonate-bearing minerals. These studies are performed using state-of-the-

art equipments including high T/P hydrogen electrodes potentiometric cell, batch reactors, and low temperature/high temperature mixed-flow reactors and HAFM (hydrothermal atomic force microscopy) for kinetic studies at macroscopic and atomic scales.

Among these studies, the solubility and stability of various carbonates-bearing minerals have been measured as a function of temperature (from 25 to 250°C) with in situ pH measurements (Hydrogen-Electrode Concentration Cell, HECC). This includes the solubility of dawsonite, siderite and magnesite [2,3,4]. Furthermore, the dissolution rates of various carbonates and the precipitation rates of magnesite have been measured over a wide range of temperature, solution compositions and pCO₂ by using either batch or flow-through cell reactors, HAFM and *in situ* X-ray absorption spectroscopy [e.g., 5-10]. However, a very puzzling problem has been risen from some of the kinetic experiments, which can then have a huge impact on simulations, is the lack of knowledge of metal-carbonate speciation and formation constants, in particular at temperature above *ca* 50°C, high pCO₂ (<50 bars, in our case) and in neutral to alkaline solutions. A combination of potentiometric titration and UV-Vis-IR spectrophotometric measurements are being performed on dilute Mg-CO₂-H₂O aqueous solutions as a function of pH and from 10-100°C [11].

There is a large body of scientific evidence suggesting that biologically mediated processes could potentially affect in-situ carbon mineralization efforts. Toward this goal, biotic experiments are being carried out, at the present time at room temperature [e.g., 12-13].

RESULTS

As an example, the solubility products obtained for siderite and magnesite are reported as a function of the reciprocal of temperature in Fig. 1. From a regression of empirical equations describing the temperature dependence of siderite and magnesite (and dawsonite) solubility constant, their thermodynamic properties have been generated.

Measurements of magnesite growth rates and their activation energy at 100 to 200°C [9] show that rates for magnesite are much lower than those of calcite (by ~6 orders of magnitude lower at 25°C), due to the strong hydration of Mg²⁺ in solution.

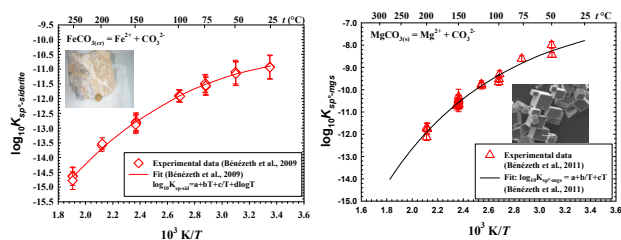


Fig. 1: Effect of ionic strength on $\log \beta_1$ for the complexation of borate with Nd^{3+} (analog for +3 actinides). Pitzer parameters generated as a fit to these data can be used to model this complexation reaction.

Moreover, magnesite crystal growth experiments performed in mixed-flow reactors (80 to 150°C) in presence of three model ligands: oxalate, citrate and EDTA [10] show that the investigated ligands have an inhibitory effect onto magnesite growth, which is positively correlated with the extent of Mg^{2+} complexation by the ligands and to specific interactions of the ligands with the magnesite surface at acute steps.

Various in-situ techniques were used to obtain internally consistent equilibrium constants to high temperatures for $\text{CO}_2(\text{aq})$ ionization and ion-pairs (NaCO_3^+ , MgHCO_3^+ and $\text{MgCO}_3(\text{aq})$). According to IR measurements it is not certain if the complexes are contact ion-pairs as predicted by theoretical calculations. However, a coordination change from 6 to 5 occurs upon CO_3^{2-} addition to Mg^{2+} but not for HCO_3^- addition.

The precipitation experiments in biotic conditions [e.g., 10, 11], as shown for example in Fig. 2, allow quantitative modeling of bacterially-induced $(\text{Ca},\text{Mg})\text{CO}_3$ precipitation and help to distinguish between the effect of cell surface functional groups, surface electrical charge, soluble organic matter and metabolic change of solution pH on the rate and nature of precipitating carbonate solid phases.

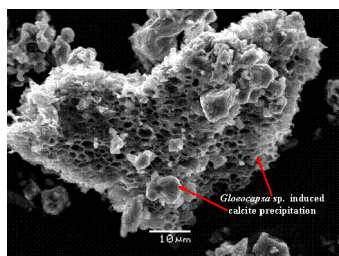


Fig. 2: calcite precipitation by cyanobacteria *Gloeocapsa* sp. [11]

REFERENCES

- Bénézech et al., "CO₂ Geological Sequestration: bio-mechano-hydro-geochemical processes from the pore-scale to the reservoir-scale". Special Issue on CO₂ geological sequestration (eds., P. Bénézech, B. Ménez and C. Noiriél), Chem. Geol., 265, p.1-2 (2009).
- Bénézech et al., "Experimental Dawsonite synthesis and reevaluation of its thermodynamic properties from solubility measurements: Implications for mineral trapping of CO₂" Geochim. Cosmochim. Acta, 71, 4438-4455 (2007).
- Bénézech et al., "The solubility product of siderite (FeCO₃) as a function of temperature" Chem. Geol., 265, 3-12 (2009).
- Bénézech et al., "Experimental determination of the solubility product of magnesite at 50 to 200°C" Chem. Geol., 286, 21-31 (2011).
- Pokrovsky et al., "Calcite, dolomite and magnesite dissolution kinetics in aqueous solutions at acid to circumneutral pH, 25 to 150°C and 1 to 55 atm pCO₂" Chem. Geol., 265, 20-32 (2009).
- Golubev et al., "Siderite dissolution kinetics in acidic aqueous solutions from 20 to 100°C and 0 to 50 atm pCO₂" Chem. Geol., 265, 13-19 (2009).
- Testemale et al., "An X-ray absorption spectroscopy study of the dissolution of siderite at 300 bars between 50°C and 100°C" Chem. Geol., 259, 8-16 (2009).
- Saldi et al., "An experimental study of magnesite dissolution rate at neutral to alkaline conditions..." Geochim. Cosmochim. Acta, 74, 6344-6356 (2010).
- Saldi et al., "Magnesite growth rates as a function of temperature and saturation state" Geochim. Cosmochim. Acta, 73, 5646-5657 (2009).
- Gautier et al., "Effects of organic ligands on magnesite precipitation rates" Geochim. Cosmochim. Acta, 73, A419 (2009)
- Stefansson et al "The stability and structure of Mg²⁺ bicarbonate and carbonate ion pairs – An experimental and theoretical study" Abstract of the Goldschmidt Conference in Prague (2011).
- Bundeleva et al., "Experimental modeling of calcium carbonate precipitation in the presence of phototrophic anaerobic bacteria *Rhodovulum* sp." Geophys. Resea. Abstracts, 12, EGU2010-9521 (2010).
- Shirokova et al., "Impact of cyanobacteria *Gloeocapsa* sp. On calcium carbonate precipitations rates" Geochim. Cosmochim. Acta, 72, A863 (2008).

Experimental Investigations of Actinide Hydrolysis at Elevated Temperatures

Linfeng Rao

Lawrence Berkeley National Laboratory, USA,
LRao@lbl.gov

INTRODUCTION

One of the strategies for the safe management of nuclear wastes is to store the high-level nuclear wastes (HLW) in underground geological repositories. According to the estimated inventory of the proposed Yucca Mountain (YM) repository, some radionuclides, including ^{238}U , ^{235}U , ^{234}U , ^{233}U , ^{239}Pu , ^{237}Np , ^{241}Am , ^{129}I , ^{99}Tc , ^{79}Se and ^{36}Cl , are considered to be the most important contributors to dose at different times after the closure of the repository [1]. Among these, uranium is the most abundant and neptunium is one of the few most soluble radionuclides that might be mobilized from the degraded waste forms and carried out of the repository. This could happen if the engineered barrier systems (waste packages and drip shields) gradually deteriorate and eventually lose the integrity [2,3]. The migration of actinides, particularly uranium, neptunium and plutonium, in the postclosure chemical environment of nuclear waste repositories is of great concern to long-term repository performance.

The postclosure chemical environment is expected to be at near neutral pH, slightly oxidizing, and at elevated temperatures [2]. For example, the projected temperature in the vicinity of the waste form in the YM Repository is around 80-100°C one thousand years after the closure of the repository [2] (Figure 1). Therefore, predictions of the migration behavior of actinides in the repository cannot be made without taking into consideration the effect of temperature on the complexation/hydrolysis.

Until recently, there had been very few thermodynamic data on the complexation/hydrolysis of actinides at temperatures above 20-25°C [4,5,6,7,8] so that gaps exist in the thermodynamic database available for the performance assessment of nuclear waste repositories. Consequently, the chemistry model currently used for the proposed YM repository relies on the reaction paths calculated at 25°C [2,9,10]. As a result, the dissolved concentration limits calculated by the model used for the performance assessment of the repository inherently have high uncertainties, which could lead to decisions that are too conservative with unnecessarily large and costly safety margins. For example, a recently revised estimation of the solubility limits of ^{237}Np and other nuclides could easily reduce the total annual dose by a factor of more than five [2,10].

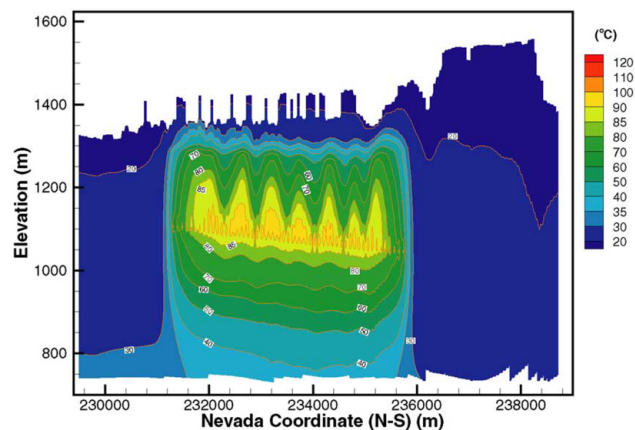


Fig. 1: Temperature profile at 1,000 years along NS#2 cross section of the proposed Yucca Mountain Repository (with ventilation) from the Mountain-Scale Thermal-Hydrologic Model [2].

DESCRIPTION OF THE WORK

To help achieve more accurate predictions of the transport behavior of actinides in the HLW repository, bridge the gap in the thermodynamic data on actinide complexation at elevated temperatures, and improve our fundamental understanding of the thermodynamic principles governing the release of key radionuclides from the waste packages, systematic studies have recently been conducted on the complexation/hydrolysis of actinides at elevated temperatures. This presentation describes the studies of the hydrolysis of U(VI), Np(V) and Pu(VI) at 10 – 85°C.

Potentiometric titrations were conducted to determine the equilibrium constants of the hydrolysis of U(VI), Np(V) and Pu(VI). Special titration apparatus was used for the titrations at different temperatures to avoid the interference of condensed water that could accumulate underneath the cap of the titration cell. The titration cell was protected with inert gas (argon) to avoid the interference of carbon dioxide, which was extremely important for the potentiometric titrations of Np(V) because the titrations were conducted into the neutral to basic regions.

Calorimetric titrations were conducted with an ITC 4200 microcalorimeter to determine the enthalpy of hydrolysis. Optical absorption and luminescence spectroscopic techniques were used to corroborate the potentiometric data and obtain further information on the hydrolyzed species.

RESULTS

Data from these studies indicate that, the hydrolysis of U(VI), Np(V) and Pu(VI) is enhanced by a few orders of magnitude from 10 to 85°C [11-13] (Figure 2). The effect of temperature is discussed in terms of the enhanced ionization of water at higher temperatures. In fact, the ionic product of water increases by almost three orders of magnitude when the temperature is increased from 0 to 100°C.

The data, while bridging the gaps in the chemical thermodynamic database for nuclear waste repository, help to make more accurate predictions of actinide migration in the environment where the temperature could remain significantly higher than 25°C for a long time after the closure of the repository.

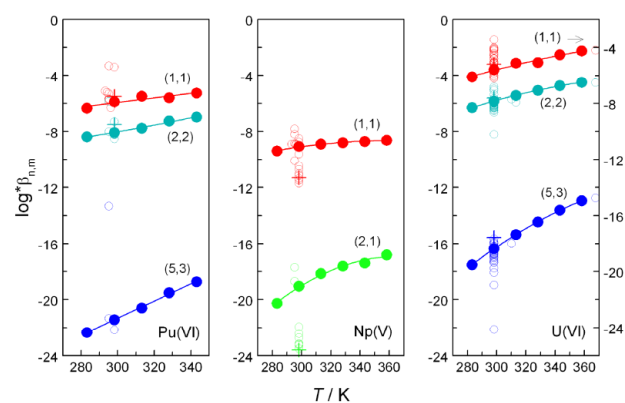


Fig. 2: Hydrolysis constants of Pu(VI), Np(V) and U(VI) at variable temperatures [11-13].

REFERENCES

1. OCRWM report, "Solicitation for Submission of Project Proposals from National Laboratories and the U.S. Geological Survey", OCRWM OSTO, January 19, 2005.
2. OCRWM report, "Yucca Mountain Science and Engineering Report Rev.1", DOE/RW-0539-1, Office of Civilian Radioactive Waste Management: North Las Vegas, NV. 2002.
3. BSC report, "Total System Performance Assessment-License Application Methods and Approach", TDR-WIS-PA-000006REV 00. Las Vegas, Nevada: Bechtel SAIC Company. ACC:MOL.20020923.0175.
4. I. Grenthe, J. Fuger, JR. J. M. Konings, R. J. Lemire, A. B. Muller, C. Nguyen-Trung, H. Wanner, "Chemical Thermodynamics of Uranium"; Wanner, H.; Forest, I., Ed.; Elsevier Science Publishers B.V.: Amsterdam, 1992.
5. R. J. Lemire, J. Fuger, H. Nitsche, P. Potter, M. H. Rand, J. Rydberg, K. Spahiu, J. C. Sullivan, W. J. Ullman, P. Vitorge, H. Wanner, "Chemical thermodynamics of neptunium and plutonium" (edited by OECD Nuclear Energy Agency, Data Bank), Amsterdam: Elsevier Science Publishers B.V. 2001.

6. R. Guillaumont, T. Fanghanel, J. Fuger, I. Grenthe, V. Neck, D. A. Palmer, M. H. Rand, "Update on the Chemical Thermodynamics of Uranium, Neptunium, Plutonium, Americium and Technetium"; Mompean, F. J.; Illemassene, M.; Domenech-Orti, C.; Ben Said, K. Ed.; Elsevier B.V.: Amsterdam, 2003.

7. W. Hummel, G. Anderegg, I. Puigdomenech, L. Rao, O. Tochiyama; "Chemical Thermodynamics of Compounds and Complexes of: U, Np, Pu, Am, Tc, Zr, Ni and Se with Selected Organic Ligands", Nuclear Energy Agency Data Bank, OECD, Ed., North Holland Elsevier Science Publishers B.V., Amsterdam, The Netherlands, 2005.

8. L. Rao, "Thermodynamics of actinide complexation in solution at elevated temperatures: Application of variable-temperature titration calorimetry", *Chem. Soc. Rev.*, 36, 881-892 (2007).

9. BSC report, "Technical Basis Document No.7: In-Package Environment and Waste Form Degradation and Solubility", Rev. 1, Bechtel SAIC Company, LLC, July 2004.

10. OCRWMS report, "Dissolved Concentration Limits of Radioactive Elements", ANL-WIS-MD-000010, Rev. 03, CRWMS M & O Technical Documents, November 2004.

11. P. Zanonato, P. Di Bernardo, A. Bismondo, G. Liu, X. Chen, L. Rao, "Hydrolysis of Uranium(VI) at variable temperatures (10 - 85 °C)", *J. Am. Chem. Soc.*, 126, 5515-5522 (2004).

12. L. Rao, T. G. Srinivasan, A. Yu. Garnov, P. Zanonato, P. Di Bernardo, A. Bismondo, "Hydrolysis of Neptunium(V) at Variable temperatures (10 - 85 °C)", *Geochim. Cosmochim. Acta*, 68, 4821-4830 (2004).

13. L. Rao, G. Tian, P. Di Bernardo, P. Zanonato, "Hydrolysis of plutonium(VI) at variable temperatures (283 - 343 K)", *Chem. Eur. J.*, 17, 10985-10993 (2011).

TRLFS studies of actinides complexation at elevated temperatures

Andrej Skerencak

Karlsruhe Institute of Technology, Institut für Nukleare Entsorgung, Karlsruhe, Germany
email: andrej.skerencak@kit.edu

INTRODUCTION

One of the worldwide discussed strategies for the safe disposal of high level radioactive waste is the storage in deep geological formation. Due to the very long half lives of the actinides, such a repository must effectively isolate the stored waste from the ecosphere for more than 10^5 - 10^6 years. In order to model the migration of the actinides in the aquifer of the host rock formation, detailed thermodynamic data of the geochemical processes which are important for their mobilization (e.g. solubility, complex formation) and retardation (e.g. sorption processes) are crucial.

A broad set of data for various actinides in their important oxidation states and for many chemical reactions are available in the literature and in thermodynamic databases [1,2]. However, the major part of this data is valid only for 25°C. Due to the heat production of radioactive waste, the temperature in the close vicinity of the repository (near-field) may reach up to 200°C, depending on the stored nuclides, the host rock formation and the geometry of the repository. Such increased temperatures will have a distinct impact on the geochemistry and the migration behaviour of the actinides in the near field. Hence, in order to give a comprehensive long term safety assessment of a nuclear waste repository thermodynamic data is needed at 25°C as well as at increased temperatures.

DESCRIPTION OF THE WORK

In the present work the complexation of Cm(III) with NO_3^- and SO_4^{2-} is studied in the temperature range from 25 to 200°C by time resolved laser fluorescence spectroscopy. Although nitrate does not play an important role in natural systems, it is chosen as a model ligand for the first studies of complexation of trivalent actinides with inorganic ligands at such high temperatures. Nitrate is a relatively weak ligand at 25°C, but Breen and Horrocks showed that it forms “inner sphere” complexes with trivalent lanthanides [3]. The sulphate ion on the other hand is one of the anionic components of natural groundwaters, of pore waters of natural clay rocks and of brines from rock salt formations [4].

TRLFS is a versatile tool for the non-invasive investigation of the solution chemistry of Cm(III). Details on this technique are given elsewhere [5]. Due to its formidable spectroscopic properties (e.g. high quantum yield), Cm(III) is chosen as a representative for trivalent actinides. The high sensitivity of TRLFS allows studies at submicromolar concentration levels of

Cm(III), which is well below the solubility limit of trivalent actinides in natural ground waters. This method enables the direct derivation of the molar fractions of the individual species from the emission spectra without disturbing the chemical equilibrium.

The experiments are performed in a custom build high temperature and high pressure cell (Figure 1). The hot region is composed of Ti with 0.2 wt% Pd, which has a high resistance towards corrosion. Four silica windows are embedded into the central body for optical coupling of the laser beam to the sample solution via an optical waveguide.

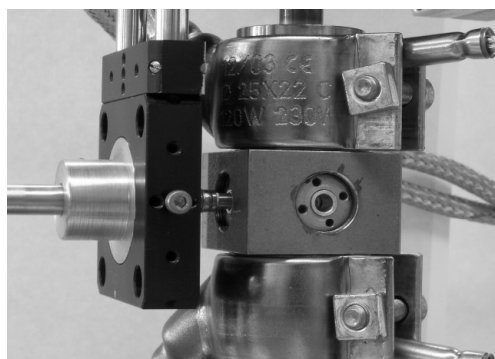


Fig. 1: High temperature and high pressure cell

RESULTS

The results for the nitrate as well as the sulphate system show a strong shift of the chemical equilibrium towards the complexed species at increased temperature (Fig. 2).

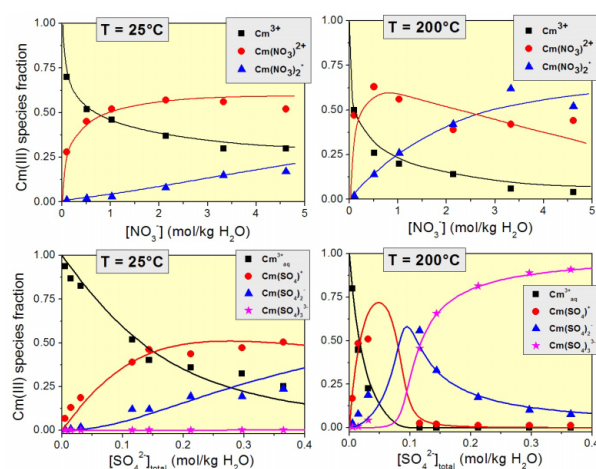


Fig. 2: Speciation of the Cm(III) nitrate and sulphate system at 25 and 200°C.

This temperature dependency of the solution speciation is reflected in the stability constants of the two complexation reactions. For this, the thermodynamic

stability constants ($\log K_n^0$) are extrapolated from the conditional values ($\log K_n'$) with the SIT approach [1]. The determined $\log K_n^0(T)$ values of both systems increase by several orders of magnitude in the studied temperature range.

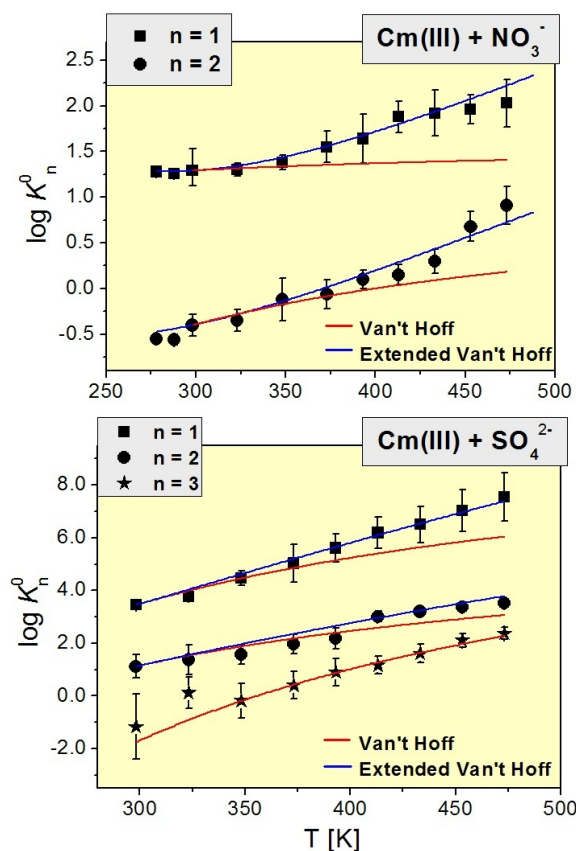


Fig. 3: Fitting of the $\log K_n^0(T)$ data of the Cm(III) nitrate and sulphate system with eq 1 and eq 2.

The temperature dependency of the thermodynamic stability constants of both studied systems is very well fitted with the integrated van't Hoff equation up to 90°C.

$$\log K_n^0(T) = \log K_n^0(T_0) + \frac{\Delta_r H^0(T_0)}{R \cdot \ln(10)} \left(\frac{1}{T_0} - \frac{1}{T} \right) \quad \text{eq1}$$

The fitting of the data over the entire temperature range requires an extended van't Hoff equation accounting for the heat capacity of reaction ($\Delta_r C_{p,m}^0$).

$$\log K_n^0(T) = \log K_n^0(T_0) + \frac{\Delta_r H^0(T_0)}{R \cdot \ln(10)} \left(\frac{1}{T_0} - \frac{1}{T} \right) + \frac{\Delta_r C_{p,m}^0(T_0)}{R \cdot \ln(10)} \left(\frac{T_0}{T} - 1 + \ln \frac{T}{T_0} \right) \quad \text{eq2}$$

The fitting of the $\log K_n^0(T)$ values for both systems is displayed in figure 3.

However, the temperature dependency of $\log K_3^0(\text{Cm}(\text{SO}_4)_3^{3-})$ is well described with the integrated van't Hoff equation over the entire temperature range, regarding the relative large error of the data at lower temperatures.

The present work shows that the estimation of temperature effects on the near field geochemistry of trivalent actinides is a difficult task since little experimental data is available at high temperatures. Furthermore, species which can be neglected at ambient temperatures could play an important role at increased temperatures. Thus, the present results are of major importance for the geochemical modeling of the migration behaviour of trivalent actinides under near field conditions of a nuclear waste repository.

REFERENCES

1. R. Guillaumont, T. Fanghanel, J. Fuger, I. Grenthe, V. Neck, D. A. Palmer, M. H. Rand, "Update on the Chemical Thermodynamics of Uranium, Neptunium, Plutonium, Americium and Technetium"; Mompean, F. J.; Illemassene, M.; Domenech-Orti, C.; Ben Said, K. Ed.; Elsevier B.V.: Amsterdam, 2003.
2. W. Hummel, U. Berner, E. Curti, F.J. Pearson, T. Thoenen, *Nagra/PSI Chemical Thermodynamic Data Base 01/01*, 2001
3. Breen, P.J.; Horrocks, W. D., *Europium(III) luminescence excitation spectroscopy. Inner-sphere complexation of europium(III) by chloride, thiocyanate, and nitrate ions*, *Inorg. Chem.* **22**, 536-540 (1983).
4. Gaucher, E., Robelin, C., Matray, J.M., Négrel, G., Gros, Y., Heitz, J.F., Vinsot, A., Rebours, H., Cassagnabère, A., Bouchet, A., *ANDRA underground research laboratory: interpretation of the mineralogical and geochemical data acquired in the Callovian-Oxfordian formation by investigative drilling*, *Physics and Chemistry of the Earth*, **29**, (2004), 55-77.
5. Edelstein, N. M., Klenze, R., Fanghanel, Th., Hubert, S.: Optical properties of Cm(III) in crystals and solutions and their application to Cm(III) speciation. *Coord. Chem. Rev.* **250**, 948-973 (2006).

The coupling between dissolution and precipitation

Jiwchar Ganor¹, Chen Zhu², Peng Lu², and Zuoping Zheng²

¹*Department of Geological and Environmental Sciences, Ben-Gurion University of the Negev, Beer-Sheva 84105, Israel.*

²*Department of Geological Sciences, Indiana University, Bloomington, IN 47405, USA*

To explore how dissolution and precipitation reactions are coupled in batch reactor, experimental systems at elevated temperatures were modeled (Zhu et al., 2010). For the model, the data of single point batch experiments of albite dissolution and sanidine precipitation of Alekseyev et al. (1997) was examined. Modeling results show that a quasi-steady state was reached, with constant ratio between dissolution rate and precipitation rate. The values of this ratio are a function of the overall reaction stoichiometry. At the quasi-steady state, dissolution reactions proceeded at rates that are orders of magnitude slower than the rates measured at far-from-equilibrium. The quasi-steady state is determined by the relative rate constants, and strongly influenced by the function of Gibbs free energy of reaction (ΔG_r) in the rate laws and by changes in reactive surface area. Following the nucleation of the sanidine, the reactive surface area of the albite decreased due to coating. The results of the present study suggest that kinetic of dissolution must be studied together with that of secondary mineral(s) precipitation.

REFERENCES

1. Alekseyev, V. A., Medvedeva, L. S., Prisyagina, N. I., Meshalkin, S. S., and Balabin, A. I., 1997. Change in the dissolution rates of alkali feldspars as a result of secondary mineral precipitation and approach to. *Geochimica et Cosmochimica Acta* 61, 1125-1142.
2. Zhu, C., Lu, P., Zheng, Z., and Ganor, J., 2010. Coupled alkali feldspar dissolution and secondary mineral precipitation in batch systems: 4. Numerical modeling of kinetic reaction paths. *Geochimica et Cosmochimica Acta* 74, 3963-3983.

TDB for elevated temperature conditions using entropy estimations

Lara Duro¹, Mireia Grivé¹, Eli Colàs¹, Xavi Gaona² and Laurent Richard¹

¹*Amphos 21, P. Garcia Faria 49-51, 1.1, Barcelona, Spain
email: lara.duro@amphos21.com*

²*KIT-INE, Hermann-von-Helmholtz-Platz 1 76344 Eggenstein-Leopoldshafen. Germany*

INTRODUCTION

Temperature variations are expected to significantly affect radionuclide behaviour in the near and far-field of a HLNW repository, therefore requiring the appropriate evaluation of its possible effects within Performance Assessment exercises. One of the concerns of the authorities refers to the systematic lack of enthalpy data for radionuclides, which makes difficult the proper assessment of the effect of temperature variations on radionuclide behaviour.

This thermodynamic data gap is a consequence of the inherent difficulties associated with the determination of experimental data for the temperature effect, therefore requiring the use of estimation methodologies, which are commonly based on empirical observations.

Several methods are available in the literature to estimate entropies of formation of aqueous species and entropies of reaction at 298.15K. These methods use correlations between entropies of analogous complexes and a combination of crystallographic radii, molar volumes and mass, electrical charge, etc. For solid compounds, the scarce information available for amorphous phases, which are of relevance relevant from a solubility point of view according to the Ostwald's rule, makes more difficult and less reliable the use of correlation methods. The work presented has been partly developed within the framework of development of ThermoChimie, the ANDRA thermodynamic database of ANDRA, in order to fill in enthalpy gaps for relevant aqueous species and solid compounds and therefore properly assess temperature effects in PA exercises

DESCRIPTION OF THE WORK

A very extensive literature review has been conducted on methods for estimation of temperature effects (entropy and in some cases enthalpy estimations) of aqueous species and solid compounds. From the different methods, a comparison has been conducted in order to frame the level of consistency among the methods as well as the level of reliability in case of availability of experimental data.

In the case of the solid compounds, the literature review has been focused on oxide solids. No methods for estimating temperature effects for amorphous solid phases, which are the ones normally selected as exerting the solubility control for the systems under study, are

available in the literature. The approach followed in this case is presented in the following section.

Aqueous complexes

Although with a rather limited theoretical basis, we have observed that all the available experimental entropies for lanthanide and actinide aqueous complexes provide entropy of formation values that follow a defined parabolic trend when represented versus the charge of the complex. This correlation was proposed by Langmuir and co-workers, (1980) although limited to U and Th complexes. Figure 1 plots all entropy data selected in the ThermoChimie database for An and Ln from experimental studies, together with the model curve resulting from the fitting of these data to a fourth degree polynomial function (analogous to the one proposed by Langmuir). The dashed lines in Figure 1, corresponding to an entropy uncertainty of $\pm 126 \text{ J}\cdot\text{K}^{-1}\cdot\text{mol}^{-1}$, includes all the available experimental data, therefore providing clear boundaries for the entropy estimates.

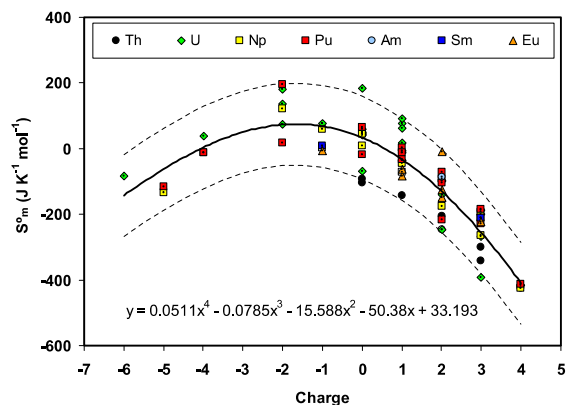


Fig. 1: Experimental data available for some actinide and lanthanide aqueous complexes (symbols) and fitting of the available experimental data to a 4th degree polynomial (curve)

Solids

The methods for estimating entropies for solids that have been reviewed in the present work include:

- those based on the Latimer approach, that is, apparent entropy contribution of a given anion related to the charge of the cation in the salt: Latimer (1952), Naumov (1971), Mills (1974),

Langmuir (1978), Lemire (1984) Grenthe and Fuger (1992);

- those based on additivity rules or entropies of structural analogs which are modified to take explicit account of atomic mass, ionic size and charge, and/or the standard molal volumes of the minerals (Helgeson, 1978)
- those applied for solid and molten salts based on the linear dependence of the entropy with the radii of the cation in the compound. Limited to mono- and divalent cations of alkaline, alkaline-earth and transition metals (Rickard, 1978)
- those based on analogies and Latimer contributions (Lemire and Tremaine, 1980)
- others (Rand and Fuger, 2000)

The method selected for application was the one based on Latimer (1952), due, among others, to the following reasons: i) it provides accurate estimations for a large number of (crystalline) phases; ii) it is simple to apply given that most of the ionic contributions are available in the literature; iii) it is extensive and easily extended to other elements and ligands not considered in the initial source, given that the calculation of missing ion contributions is relatively easy; iv) it is self consistent and reliable in the light of the extensive application by many authors to different compounds to the ones included by Langmuir original work. Some of its limitations refer to the lack of application to amorphous solids and that it has been so far applied only to binary compounds. In our work we have extended its application to ternary compounds and also to amorphous solid phases.

The test for validity for amorphous phases has been conducted by means of its application to hydrated phases not considered in the original work. In figure 2 the comparison between the application of the Latimer approach to oxide hydrates and the experimental data available is shown. The level of coincidence is very high, obtaining an average deviation between predictions and experimental data of 14 kJ·mol⁻¹ and a maximum deviation of 40 kJ·mol⁻¹. This test was taken as an indication of the reliability of the application of Latimer approach to amorphous compounds presenting different hydration waters. The values estimated for some of the solids of interest are shown in the following table.

Species	S ^o _m [J·K ⁻¹ ·mol ⁻¹]	Δ _f H ^o [kJ·mol ⁻¹]
ThO ₂ ·2H ₂ O	147.0	-1778.2
UO ₂ ·2H ₂ O	165.3	-1635.8
NpO ₂ ·2H ₂ O	162.1	-1611.3
PuO ₂ ·2H ₂ O	150.7	-1611.6
Pu(OH) ₄ (am)	150.7	-1647.6

The applied approaches provide an interesting way to frame the effect of temperature on the stability of aqueous species and solid phases until 90°C, although

the lack of experimental data on solubility of non-crystalline solid phases at different temperatures makes difficult an actual comparison of the estimations. A good characterization of solid phases before and after the experiments conducted at temperatures different from 25°C is required to validate the approaches.

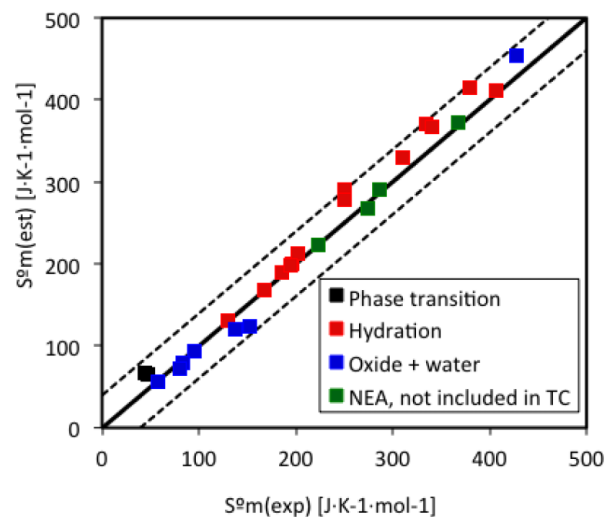


Fig. 2: Comparison between experimental entropy of formation (symbols) of water containing solids and entropy of formation calculated by applying the Latimer approach. (TC stands for ThermoChimie)

REFERENCES

- HELGESON, H.C. et al. "Summary and critique of the thermodynamic properties of rock-forming minerals" *American Journal of Sciences*, **278A**, 1-220 (1978).
- LANGMUIR, D., et al. "The mobility of thorium in natural waters at low temperature" *Geochimica et Cosmochimica Acta*, **44A**, 1753-1766 (1980).
- LATIMER, W.M. "Oxidation potentials" Second edition, Prentice-Hall Inc. Englewood Cliffs, NJ, USA (1952).
- LEMIRE, R.J. et al. "Uranium and Plutonium equilibria in aqueous solutions to 200°" *Journal of Chemical Engineering Data*, **25**, 361-370 (1980).
- RAND, M.H., et al. "The thermodynamic properties of the transuranium halides. Part I: Neptunium and Plutonium Halides" Report EUR 17332 EN (2000).
- RICHTER, J. et al. "Estimation of the molar entropies of solid salts and their melts basing on the linear dependence of the cation radius entropy" *Berichte der Bunsen-Gesellschaft. Phys. Chem.* **83**, 1023-1026 (1979).

Geochemical Modeling of Aqueous Systems at Moderate Temperatures: Approaches and Tools for Temperature Extrapolations

Dmitrii A. Kulik

¹Laboratory for Waste Management, Paul Scherrer Institut, 5232 Villigen PSI, Switzerland
email: dmitrii.kulik@psi.ch

INTRODUCTION

Computer-aided thermodynamic modelling is relevant in geochemical and safety studies of nuclear waste repositories. A modelling result cannot be better than the underlying thermodynamic data base (TDB). Most TDBs are application-specific in regard to temperature T and pressure P ranges, as well as the selection of chemical elements, aqueous species, and solid phases. For instance, Nagra-PSI TDB [1] is officially limited to $T_0 = 298.15$ K and $P_0 = 1$ bar due to knowledge gaps and scarcity of experimental data on aqueous speciation and solubility of some actinides and fission products at elevated T and P .

In a typical scenario of nuclear waste repository evolution, a T raise from ambient (38 °C) up to 90 – 160 °C due to radioactive decay is foreseen within 1000 years [2]. To cover these conditions by modelling, it is desirable to extend the TDB applicability to about 200 °C. The approximation of thermodynamic data and parameters of solution mixing models in a wide T , P ranges has been a priority in hydrothermal geochemistry and petrology over 50 years. This research resulted in extensive TDBs such as SUPCRT [3-5] and HP [6] covering gases/fluids, minerals and aqueous species of major elements, heavy and rare metals and metalloids. Some of the data and extrapolation methods, supported by software tools, can be useful in nuclear-waste-related TDBs for operational extensions to moderate T (150-200 °C), even if only the species formation constant at $T_0 = 25$ °C is available.

The aim of this contribution is to summarize ‘simple and cheap’ approaches to T extrapolation of standard molar stability constants for aqueous complexes and secondary minerals, supported by code tools implemented e.g. in the GEM-Selektor code [7] and its built-in TDB. Some open issues, potential biases and pitfalls will also be highlighted, including T approximations for surface complexation/ ion exchange equilibrium constants.

TEMPERATURE APPROXIMATIONS

For T correction of standard Gibbs energy per mole G_{298}^0 of gases and condensed compounds, i.e. calculation of increments $g_T^0 - G_{298}^0$, the integration of heat capacity function $Cp^0(T)$ at known absolute entropy S_{298}^0 is commonly in use [8], coded into many modeling packages. The $Cp^0(T)$ function is represented in TDBs via polynomial coefficients fitted to the data in a given T interval, outside of which, calculated Cp_T^0

values may be very inaccurate. For aqueous ions and complexes, the *de facto* standard for T correction of (partial molal) g_T^0 function is the revised HKF EoS [4] supported by the SUPCRT92 code and TDB [5]. g_T^0 values for all components in all phases comprise a direct input for GEM solvers of chemical equilibria [7].

The equilibrium constant K_0 of any reaction can be corrected from T_0 to T after performing T approximation for g_T^0 value of each component of reaction, as e.g. the SUPCRT92 code does. A comprehensive review of T approximation methods for solids, aqueous species and their formation reactions [9] is recommended.

In speciation models such as MINEQL or EQ3/6, the thermodynamic data for ‘master species’ (aqueous ions) are not used at all. Any ‘product’ species (gas, mineral, aqueous or surface complex) must be defined via the formation reaction from ‘master species’ and its K_T^0 . Respectively, the TDB contains (encoded) reactions, with K_{298}^0 , $\Delta_r H_{298}^0$ or $\Delta_r S_{298}^0$ values to be used in the Van’t Hoff (2-term) approximation for K_T^0 , or with empirical coefficients of the $K^0(T)$ polynomial function.

If properties defining the T trend of K_T^0 are available, they can be combined with standard thermodynamic data for all but one component of the reaction to retrieve properties (G_{298}^0 , H_{298}^0 , S_{298}^0) of that ‘new’ component [10]. As implemented in the ReacDC module of GEM-Selektor code [7], the G_T^0 value for this ‘new’ component can be obtained from G_T^0 values of other components and K_T^0 of this reaction, and directly used in calculation of the equilibrium state at T of interest. This ‘hybrid’ structure of TDB is especially convenient for extensions with more complexes or minerals, for which only properties of the reaction with other compounds are known [11].

TEMPERATURE EXTRAPOLATIONS

In any geochemically plausible system, solids, aqueous or surface complexes have to be considered, for which the data required for T corrections is insufficient. For aqueous species of actinides, HKF EoS coefficients are available only for Am^{3+} and its complexes [12]; ions and some hydroxocomplexes of U^{III} , U^{IV} , U^V and U^{VI} [5]; and Th^{4+} ion [5]. Solubility products of many actinide hydroxides, phosphates, and silicates are only known at 25 °C. Is it possible then to obtain T extrapolations up to 150-200 °C with reasonable uncertainty?

Some useful techniques are mentioned in Tables 1 to 4.

Table 1. Solid compounds [9].

Method	Predicts	Comment
Kopp; <u>KAS</u> ; Helgeson; Isocoulombic reactions	Cp°_T	<u>Kubashevsky</u> , <u>Alcock & Spencer</u>
Latimer, Langmuir; Helgeson +Magnetic contributions	S°_{298}	Ionic contributions Constituent oxides For actinides, REE

Table 2. Aqueous ions and complexes [9].

Method	Predicts	Comment
Criss-Cobble; Shock-Helgeson (Parcor *) Isocoulombic reactions	$Cp^{\circ}_T S^{\circ}_T$	Correlation $T < 600$ K
Latimer; Couture-Laidler; David; Helgeson	S°_{298}	Estimation

Table 3. Effects of reactions.

Method	Predicts	Comment
Pronsprep(OH) * [5,13] Marshall-Franck * [9] Modified <u>RB</u> * [9]	$\Delta_r Cp^{\circ}_T$, $\Delta_r S^{\circ}_T$	Correlation Estimation <u>Ryzhenko-Bryzgalin</u>
3-term extrapolation* 2-term extrapolation* 1-term $\Delta_r H^{\circ} = 0^*$ 1-term $\Delta_r S^{\circ} = 0^*$	K°_T	Constant $\Delta_r Cp^{\circ}$ $\Delta_r Cp^{\circ} = 0$; const. $\Delta_r H^{\circ}$ $\Delta_r Cp^{\circ} = 0$; const. $\Delta_r G^{\circ}$ $\Delta_r Cp^{\circ} = 0$; const. K°
Isoelectric 2-term* Isocoulombic 1-term*	K°_T	Reliable at $\Delta_r Cp^{\circ} = 0$ also at $\Delta_r S^{\circ} = 0$

*Implemented in ReacDC module of GEM-Selektor [7].

Table 4. Effects of adsorption reactions [15].

Method	Predicts	Comment
Constant $\Delta_r S^{\circ}_H$	$pH_{PZC,T}$	(Hydr)oxides to 300 °C
Isoelectric 0-term	K_C, K_A	Electrolyte adsorption
Isocoulomb. 1-term	$K_{X,T}$	Ion exchange
Ion dehydration numbers	$\Delta_r S^{\circ}_{298}$	T trend of K°_M for adsorption**

Isocoulombic or isoelectric reactions have on both sides equal species charges or equal sums of like charges, respectively [9,11,14]. It is remarkable that such reactions can be used for T extrapolations in a variety of cases. A dissolution or complexation reaction can be turned into one of such forms by combining with another reaction, for which an accurate T approximation is available. This is much facilitated by using appropriate software tools [7,10], as shown in examples for secondary minerals, aqueous and surface complexes. So far, the potential of this approach in extending the range of TDB applicability to moderate temperatures appears under-explored.

As emphasized in [16], the development of geochemical TDBs is an on-going process. So far, much of the 'data' e.g. in SUPCRT TDB are, in fact, values obtained using various kinds of empirical correlations or estimations. Therefore, long-lasting efforts to acquire new high-quality experimental measurements at elevated temperatures (especially for actinides) are essential to reduce uncertainties and to gain more confidence in estimation methods, in particular, those related to moderate T approximations for aqueous- and surface complexation.

REFERENCES

- HUMMEL W. et al. *Nagra/PSI chemical thermodynamic data base 01/01*. UPubl.com, 1-600 (2002)
- NAGRA *Technical Report* 02-05, section 5.3.2 (2002)
- HELGESON H.C. et al. *Amer.J.Sci.* v. 278-A, 1-229 (1978)
- HELGESON H.C. et al. *Amer.J.Sci.* v. 281, 1249-1516 (1981)
- SHOCK E.L. et al. *Geoch.Cosmoch.Acta* v. 61, 907-950 (1997)
- HOLLAND T.J.B, POWELL R. *J.Metamorph.Petrol.* v. 29, 333-383 (2011)
- GEM-Selektor package, <http://gems.web.psi.ch> (2011)
- ANDERSON G. *Thermodynamics of Natural Systems*, Cambridge, 1- 648 (2005)
- PUIGDOMENECH I. et al. Chapter X in *Modelling in aquatic chemistry*, OECD NEA, 427-493 (1997)
- PEARSON F.J. et al. *PMATCHC. PSI Technical Report* TM-44-01-07, 1-50 (2001)
- KULIK D.A. In: *The use of thermodynamic databases in performance assessment*. OECD NEA, 125-137 (2002)
- MURPHY W.M., SHOCK E.L. *RiMG* v.38, 221-253 (1999)
- SVERJENSKY D.A. et al. *Geoch.Cosmoch.Acta* v. 61, 1359-1412 (1997)
- GU Y. et al. *Geoch.Cosmoch.Acta* v.58, 3545-3560 (1994)
- KULIK D.A. *Interf.Sci.Technol.* v.11, 171-250 (2006)
- OELKERS E. et al. *RiMG*, v.70, 1-46 (2009)

Partial financial support by Nagra, Wettingen, is gratefully acknowledged.

OUTLOOK

POSTER ABSTRACTS

List of contributions

Fast / Instant release of safety relevant radionuclides from spent nuclear fuel (FIRST-Nuclides) <i>B. Kienzler, V. Metz, V. Montoya</i>	153
Recosy Intercomparison exercise on redox determination methods – final report on main conclusions and recommendations <i>M. Altmaier, X. Gaona, D. Fellhauer, G. Buckau</i>	155
VESPA: Collaborative project on the chemical behavior of long-lived fission and activation products in the near field of a nuclear waste repository <i>B. Bischofer, M. Altmaier, D. Bosbach, V. Brendler, H. Curtius, H. Geckeis, N. Jordan, A. Muñoz</i>	157
Migration of Np(V) in natural clay at elevated temperatures <i>D. R. Fröhlich, S. Amayri, J. Drebert, T. Reich</i>	159
The influence of temperature on sorption: A preliminary assessment for Uranium(VI) sorption to bentonite <i>J. Lützenkirchen, P. Wersin</i>	161
Temperature Impact on the Sorption of Selenate onto Anatase <i>C. Franzen, N. Jordan, K. Müller, T. Meusel, V. Brendler</i>	163
Effect of Temperature on Selenate Adsorption by Goethite <i>M. Kersten, N. Vlasova</i>	165
Influence of temperature on the sorption of Europium into Smectite: The role of organic contaminants <i>A. Bauer, T. Rabung, F. Claret, T. Schäfer, G. Buckau, T. Fanghänel</i>	167
Octa- and Nonahydrated Cm(III) in Aqueous Solution from 20 to 200 °C <i>P. Lindqvist-Reis, R. Klenze, T. Fanghänel</i>	169
Assessing temperature effects: methods for the estimation of S_m^0 for aqueous actinide species and applicability of the van't Hoff expression <i>X. Gaona, M. Grive, A. Tamayo, A. Skerencak, M. Altmaier, L. Duro</i>	171
Spectroscopic Characterization of Eu(III) and Am(III) Complexes with Small Organic Molecules at Elevated Temperatures <i>A. Barkleit, M. Acker, G. Geipel, S. Taut, G. Bernhard</i>	173
Temperature Effect on Solubility and Solid Phase of Zr(IV) Hydroxide <i>T. Kobayashi, D. Bach, M. Altmaier, T. Sasaki, H. Moriyama</i>	175
Preliminary multi-method spectroscopic approach for the uranium(VI) hydrolysis at temperatures up to 60 °C <i>R. Steudner, K. Müller, T. Meusel, V. Brendler</i>	177

Complexation studies of Np(V)-Lactate at elevated temperatures

N. L. Banik, S. Walz, C. M. Marquardt, P. Panak, A. Skerencak 179

FAST / INSTANT RELEASE OF SAFETY RELEVANT RADIONUCLIDES FROM SPENT NUCLEAR FUEL (FIRST-Nuclides)Bernhard Kienzler¹, Volker Metz¹, Vanessa Montoya²

¹ *Karlsruhe Institute of Technology, Institut für Nukleare Entsorgung, Karlsruhe, Germany*
email: bernhard.kienzler@kit.edu

² *Amphos 21, Barcelona, Spain*

INTRODUCTION

The EURATOM FP7 Collaborative Project “Fast / Instant Release of Safety Relevant Radionuclides from Spent Nuclear Fuel (CP FIRST-Nuclides)” contributes to the progress towards implementing of geological disposal in line with the Vision Report and the Strategic Research Agenda (SRA) of the “Implementing Geological Disposal – Technology Platform (IGD-TP)”. The key topic “waste forms and their behaviour“ where the FIRST-Nuclides project is included, deals with understanding the behaviour of various wastes in geological repositories, in particular, high burn-up spent uranium oxide (UO₂) fuels. This waste type represents the source for the release of radionuclides after loss of the disposed canister integrity. For safety analysis, the time-dependent release of radionuclides from spent high burn-up UO₂ fuel is required. The first release consists of radionuclides (1) in gaseous form, and (2) those radionuclides showing a high solubility in groundwater.

Some important nuclides undergo only marginal retention on their way to the biosphere. In present safety analyses, these radionuclides have a significant contribution to dose to man. The basis for the calculated significant dose contribution is a simplified description of the release function. It is expected that a realistic release function results in lower peak dose rates, and thus contributes to acceptance of nuclear waste disposal.

The CP is accepted under EC FP7-Fission-2011 ”Research activities in support of implementation of geological disposal”. It started in January 2012 and has a duration of 36 months.

OBJECTIVES OF FIRST-Nuclides

With respect to the fast / instant release of radionuclides (RN) from spent nuclear fuel elements under deep underground repository conditions, a series of questions are still open. These questions concern key input data to safety analysis, such as “instant release fraction (IRF)” values of iodine, chlorine, carbon and selenium that are still largely unknown. The elements I, C, Cl and Se tend to form anionic species. Such anions are hardly chemically retained in the repository barrier system and may thus significantly contribute to the dose to man. Moreover, ¹⁴C may be present as carbide reacting with water forming mobile hydrophilic organic species.

Consortium

The project is implemented by a consortium with 10 partners from 7 EURATOM Signatory States (KIT (DE), AMPHOS21(ES), FZ JÜLICH(DE), PSI(CH), SCK·CEN(BE), CNRS(FR), CTM(ES), AEKI(HU), STUDSVIK(SE), and the EC Joint Research Center Institute for Transuranium Elements. The project is coordinated by KIT. The Coordination Team consists of KIT and AMPHOS21 which are responsible for project management, knowledge management, documentation, dissemination and training. Workpackage leaders head the individual workpackages and are members of the Executive Group.

Associated Groups (AG) participate in the project at their own costs with specific research and technological development (RTD) contributions or particular information exchange functions. Several organisations from France, Finland, USA (3) and UK contribute in this way. A group of implementation and regulatory oriented organizations are participating as an “End-User Group”. This group has a number of functions, such as: i) ensuring that end-user interests are reflected in the project work, ii) reporting, dissemination and communication, iii) providing for review of the project work and scientific-technical outcome, and iv) participating in assessment and discussion of the project outcome with respect to the potential impact on the Safety Case.

STRUCTURE OF THE COLLABORATIVE PROJECT

The CP is organized in several workpackages (WP). WP 1: Samples and tools. This WP deals with the selection, characterization and preparation of materials and set-up of tools.

Limited irradiated fuel material is available where the initial enrichment and irradiation history, etc. is known and where data can be used and published without restrictions. As a first step, fuel characterisation data are collected, revealing several categories of information: (i) essential information representing the minimum data required and information that should be available for the fuel chosen for the study, (ii) parameters and data which are not directly measured, but are derived from calculations, and (iii) supplemental information referring to characteristics that may be needed depending on the studies to be performed. Fission gas release (FGR)

is determined and samples prepared for investigations of structural defects.

WP 2 “Gas release and rim and grain boundary diffusion” and WP 3 “Dissolution based release” cover the experimental determination of fission gases release, rim and grain boundary diffusion processes and the dissolution based fast/instant radionuclide release. These investigations include the determination of the chemical form of released radionuclides, fission gases, ^{135}Cs , ^{129}I , ^{14}C compounds, ^{79}Se , ^{99}Tc and ^{126}Sn . Moreover, the gap and grain boundary inventories are determined and the dependence of the fast/instant release on i) the UO_2 fuel and the respective manufacturing process, ii) the evolution of higher burn-up and burn-up history, iii) the linear power and fuel temperature history, ramping processes, and iv) storage time are assessed.

WP 3 aims at the quantification of the fast/instant radionuclide release by leaching experiments in the aquatic phase considering the fuel characteristics, burn-up and burn-up history, and the characteristics of the samples under investigations. Differences are expected with respect to the presence or absence of cladding, to the application of fuel fragments from different radial positions of fuel pellets and to the specific fuel, and burn-up characteristics (see WP 1). The instantly released elements, including their isotopic composition and chemical form, if possible, are measured in the gas phase and in the leaching solution. The investigations are complemented by micro-scale investigations on the oxidation state and coordination environments of the relevant radionuclides as well as on the crystallographic structure by using synchrotron radiation techniques.

WP 4 “Modelling” deals with modelling of migration/retention processes of fission products in the spent fuel structure. A series of codes have been developed which integrate neutronics, burn-up, fuel and fuel rod mechanical and thermal-hydraulic calculations.

The modelling work within FIRST-Nuclides helps to clarify which geometric scales dominate the fast/instant release. Special attention is attributed to model the fission product migration along the grain boundaries, the effects of fractures in the pellets and of holes/fractures in the cladding. Emphasis is given to provide more realistic relationships between FGR and release of iodine, caesium and other radionuclides in the relevant burn-up ranges by modelling the release of gaseous and non-gaseous fission products. Other modelling aims concern the speciation of ^{14}C and rare fission / activation products after cooling to disposal conditions, the migration of gaseous and non-gaseous fission products in the microstructures of spent fuel pellets (grains, grain boundaries, gas bubbles or pores), the development of improved models to predict the FGR and release of non gaseous fission products on the fuel rod scale.

Modelling also supports the experimental set-up/designs by assessing concentration/activity limits for the elements under investigation. It also contributes to the up-scaling from the analytical and modelling micro-scale to the experimental bulk observations and to the release on a fuel-rod scale.

WP 5 is responsible for the knowledge management, the state-of-the-art report, the general reporting, keeping the documentation up-date, and all dissemination and training measures. The state-of-the-art report addresses the specific topics of the respective workpackages. It compares previously investigated samples with material used in the present project; it describes the experimental determination procedures of fission gases release on the basis of published and grey literature as well as results from rim and grain boundary diffusion experiments.

The project aims on making available all results generated to any interested party. The dissemination of scientific-technical results through reviewed publications is encouraged. Reflecting previous experiences, the persons involved in driving the scientific-technical program have a keen interest in publishing their results in prominent peer reviewed journals.

ACKNOWLEDGEMENT

The research leading to these results has received funding from the European Atomic Energy Community's Seventh Framework Programme (FP7/2007-2011) under grant agreement No. 295722 (FIRST-Nuclides).

CONTACTS

bernhard.kienzler@KIT.EDU
Vanessa.Montoya@amphos21.com

Recosy Intercomparison exercise on redox determination methods – final report on main conclusions and recommendations

M. Altmaier¹, X. Gaona¹, D. Fellhauer^{1,2}, G. Buckau^{1,2}

¹Karlsruhe Institute of Technology, Institut für Nukleare Entsorgung, P.O. Box 3640, 76021 Karlsruhe, Germany

²EC Joint Research Centre, Institute for Transuranium Elements, P.O. Box 2340, 76125 Karlsruhe, Germany

Redox processes play an important role in defining the aqueous chemistry of redox sensitive actinide elements like plutonium, neptunium and uranium. In order to assess the chemical behavior of these elements in the context of nuclear waste disposal but also for more general studies in actinide chemistry, it is necessary to predict and quantify the impact of redox conditions on the solution chemistry. The reliable measurement of redox potentials in solution therefore is a matter of highest importance for many scientific applications and research fields.

In this contribution, the outcome of the ReCosy Intercomparison Exercise (ICE) on redox determination methods is presented. The ICE exercise was conducted within the EURATOM FP7 Collaborative Project “Redox phenomena controlling systems” (CP ReCosy) and was hosted by the “Institut für Nukleare Entsorgung” (“Institute for Nuclear Waste Disposal”), Karlsruhe Institute of Technology (KIT-INE). More than 40 scientists working on different topics related to redox chemistry from 20 ReCosy partner organisations and associated groups contributed to ReCosy ICE, thus providing a broad scientific basis for ICE. The objectives of the ReCosy ICE were to compare different redox determination methods in order to

- (i) identify critical redox determination issues,
- (ii) provide the basis for more confidence in redox determinations for the individual groups, and
- (iii) identify future activities that could contribute to further progress in the confidence in determination of the redox state of nuclear waste disposal Safety Case relevant systems and conditions.

The intercomparison was based upon different redox determination methods, i.e. static electrodes (platinum, gold glassy carbon, single/combined electrodes), dynamic electrochemical measurements, amperometric measurements, optodes (optical fibres with oxygen sensitive tips) and thermodynamic calculations based on chemical composition and physicochemical properties (such as pH, ionic strength and temperature). For this purpose, a wide set of samples was used with three different types of origin and properties, namely

- (a) simple samples with well defined composition,
- (b) natural samples under near-natural conditions,
- (c) samples with microbial cultures.

Following the joint evaluation and critical discussion of ICE, the final report on ReCosy ICE has been published in 2010 as a joint effort of all ReCosy ICE participants. The final outcome of ReCosy ICE is available as a report from the authors and can be downloaded via the ReCosy website www.recosy.eu or at:

<http://digbib.ubka.uni-karlsruhe.de/volltexte/1000021898>.

The main conclusion of ReCosy ICE is that the redox state of an aqueous system can be determined by the existing experimental techniques, although the degree of confidence strongly depends of the kind of aqueous system investigated and the degree of optimisation of the experimental equipment and handling protocols. In how far the available experimental accuracy and precision is sufficient to adequately characterise the sample must be assessed in each single case and cannot be generalised. As observed in the ReCosy ICE, some samples show clusters of readings from different groups and electrodes used. These samples are artificial, with high redox buffer content, with pH buffered and in the pH neutral to acidic range. Natural samples show very large differences between the different groups, electrodes and handling protocols. A predictive capability based on any of such measurements alone is considered rather uncertain. The ReCosy ICE has not yet provided the basis for identification of different processes responsible for the large drift and large differences in redox readings.

Based upon the outcome of ReCosy ICE and the joint data evaluation and interpretation, the partners of ReCosy ICE have agreed on several recommendations. ReCosy ICE was using the presently available experimental and conceptual approaches to compare and evaluate various aspects related to redox measurement and redox data interpretation, aiming at defining the current state-of-the-art. In this respect, ReCosy ICE has compiled a list of recommendations regarding redox measurements. Important outcomes are:

- It is strongly recommended to use a combination of several experimental approaches to identify and assess systematic errors as there is no single “best method” to determine the redox state of a given system. This is especially true for the analysis of (intrinsically highly complex) real systems. Ideally, it is recommended to use different sensor materials and complement potentiometric measurements with

thermodynamic model calculations based upon the distribution of redox couples.

- The use of a “quality assurance” protocol for Eh measurements is advisable.
- The use of non-conventional approaches (optodes, amperometry, ...) can help to clarify the redox state and could also be used to complement conventional measurements whenever possible.
- The problems arising from electronics of the instrumentation are generally minor compared to “chemical” interferences affecting redox measurements.
- It is recommended to consider that dilution experiments with redox buffers indicate that there is a “critical minimum concentration” of redox active species to allow measurement of meaningful pe values with combined electrodes.

Further recommendations concerning sampling and handling, better equilibration of samples, stirring or non-stirring during measurements, drift and surface effects on the sensor, pe-pH measurements and thermodynamic modelling of redox processes have been derived and are reported in the final ReCosy ICE report.

In addition, several topics have been identified within ReCosy ICE beyond the present state-of-the-art that may provide significant input for future research activities related to redox state determination. The main arguments again concern the central question of how the redox state of a system is defined, and what consequences result for redox state determinations? Individual questions related to this overall context are concerning:

- New approaches to identify and quantify the reasons for the observed long-term drift on measurements in a comprehensive multi-step approach.
- Better understanding of the alteration processes at the electrode surface, caused by sorption of ions, colloids or organics on the sensor material, or partial oxidation (PtO formation) and consecutive surface coating of the sensor.
- Work towards the further optimisation of cleaning protocols for electrode surfaces.
- Improve alternative techniques to complement conventional potentiometric measurements. None of the non-conventional techniques used in ReCosy ICE at present can be used for routine analysis under reducing conditions.

- Systematic assessment of temperature effects or ionic strength effects on redox related processes and redox measurements.
- Development of advanced tools for long-term redox monitoring, relevant for the robust (experimental) assessment of main performance indicators in post-closure scenarios.

For further information on ReCosy ICE, please visit the project web page www.recosy.eu or contact marcus.altmaier@kit.edu.

Acknowledgement: The research leading to these results has received funding from the European Union's European Atomic Energy Community's (Euratom) Seventh Framework Programme FP7/2007-2011 under grant agreement no. FP7-212287 (ReCosy Project).

VESPA: Collaborative project on the chemical behavior of long-lived fission and activation products in the near field of a nuclear waste repository

B. Bischofer¹, M. Altmaier², D. Bosbach³, V. Brendler⁴,
H. Curtius³, H. Geckeis², N. Jordan⁴, A. Muñoz¹

¹*Gesellschaft für Anlagen- und Reaktorsicherheit (GRS) mbH, Braunschweig, Deutschland*
email: Barbara.Bischofer@grs.de

²*Institut für Nukleare Entsorgung, Karlsruher Institut für Technologie (KIT-INE), Karlsruhe, Deutschland*

³*Institut für Energie- und Klimaforschung, IEK-6: Nukleare Entsorgung und Reaktorsicherheit, Forschungszentrum Jülich, Deutschland*

⁴*Institut für Radiochemie, Helmholtz-Zentrum Dresden-Rossendorf (HZDR), Dresden, Deutschland*

INTRODUCTION

This poster presents the collaborative project VESPA with its main objectives and the research to be carried out by the single four project partners. VESPA was started in July 2010 and is designed for three years.

DESCRIPTION OF THE COLLABORATIVE PROJECT VESPA

Long term safety analyses are an essential element of the safety assessment of potential repositories for nuclear waste. For the analysis of the safety case, various scenarios are modelled, in order to predict radionuclide mobilization over geological timescales. Reliable predictions of radionuclide solubility and retention processes are required. But due to limited information on related geochemical key processes, in many long term safety calculations it is assumed that anionic fission products such as ¹⁴C, ⁷⁹Se, ¹²⁹I, and ⁹⁹Tc do not adsorb at all, do not form insoluble solid phases and thus are highly mobile. As a consequence, these elements contribute often significantly to the calculated dose.

As an answer to this situation, the key objective of the project VESPA is to establish an experimental and conceptual basis for a better understanding of the chemical behavior of the anionic fission and activation products ¹⁴C, ⁷⁹Se, ¹²⁹I, ⁹⁹Tc and ¹³⁵Cs. With the results of VESPA conservative assumptions for the named long-lived radionuclides in long term safety analyses shall be reduced. Therefore different experimental investigations by the four involved research institutions are carried out aiming to improve the model like description and quantitative modelling of radionuclides significantly. Research will be carried out concerning sorption and precipitation of anionic radionuclides under conditions found in the near field of nuclear waste repositories established in salt and clay formations in order to identify and quantify important retention mechanisms. Investigations on solubility and complex building of long-lived fission products are done in order to derive thermodynamic data for modelling. Experiments are carried out in a temperature range from 25°C to 90°C.

The intercomparison was based upon different redox determination methods, i.e. static electrodes (platinum, gold glassy carbon, single/combined electrodes), dynamic electrochemical measurements, amperometric measurements, optodes (optical fibres with oxygen sensitive tips) and thermodynamic calculations based on chemical composition and physico-chemical properties (such as pH, ionic strength and temperature). For this purpose, a wide set of samples was used with three different types of origin and properties, namely

ACKNOWLEDGEMENTS

The research receives funding from the German Federal Ministry of Economics and Technology (BMWi), grant agreement n° 02 E 10770 (GRS), 02 E 10780 (FZJ-IEF-6), 02 E 10790 (HZDR) und 02 E 10800 (KIT-INE).

Migration of Np(V) in natural clay at elevated temperatures

Daniel R. Fröhlich, Samer Amayri, Jakob Drebert, Tobias Reich

Institute of Nuclear Chemistry, Johannes Gutenberg-Universität Mainz, 55099 Mainz, Germany
email: froehlich@uni-mainz.de, treich@uni-mainz.de

INTRODUCTION

Natural clay rocks are considered as possible host rock formation for high-level nuclear waste repositories in different European countries (e.g. Belgium, France, Germany, Switzerland). For the planning of such a repository, it is necessary to investigate the interactions between the potential host rock and the different radionuclides that are important with respect to the long-term storage of the waste material. Besides long-lived fission products, especially the transuranium elements (Np, Pu, Am, Cm) have to be studied in detail. In the case of neptunium the long-lived ^{237}Np (2.1×10^6 a) will contribute significantly to the radiotoxicity of the waste.

Sorption and diffusion are the most important mechanisms regulating transport and retardation of actinides in clay. While most migration studies are performed under ambient conditions, less is known about the sorption and diffusion behaviour of actinides at elevated temperatures that could occur due to a significant heating of the environment of the storage place. An increase in temperature might change the physical and chemical properties of the clay and influence the interaction processes with radionuclides.

The aim of our study was to investigate the interaction between Np(V) and natural clay at room temperature (RT) and 60 °C and to compare the results of diffusion and batch sorption experiments. Therefore, Opalinus Clay (OPA) from Mont Terri, Switzerland, was used as a representative for a natural clay rock.

DESCRIPTION OF THE WORK

Three cylinders of OPA ($d \approx 25.5$ mm, $h \approx 11$ mm) were prepared from the OPA bore core BLT 14. Two samples were used in the diffusion experiments; the third one was pulverized and sieved to a particle size of less than 150 μm . This powder was used in two batch sorption experiments with 8 μM Np(V) under ambient air conditions in OPA pore water (pH 7.6, I 0.4 M) at RT and 60 °C, respectively. In the sorption experiments, the solid-to-liquid (S/L) ratio was varied between 4 and 20 g/L. The OPA suspensions were preconditioned in the pore water for 72 h, then aliquots of the Np(V) stock solution (≈ 20 mM) were added. After a contact time of 72 h, the solid and liquid phases were separated by centrifugation (108,800 g) and the amount of Np(V) in the supernatant solution was analyzed by γ -ray spectroscopy to obtain the related distribution coefficients (K_d).

The diffusion experiments were performed as described in [1]. After sandwiching the cylinder between to filter plates, the clay was inserted into a diffusion cell. Both the filters and the cell were made from stainless steel. The samples were preconditioned by circulating pore water along both sides for at least two months. The set-up is shown in detail in [2]. The clay was then characterized by through-diffusion of tritiated water (HTO). After out-diffusion of HTO, Np(V) was added to one reservoir (total concentration 8 μM). The time for in-diffusion of Np was about one month. One day before the end of this period, $^{22}\text{Na}^+$ was added to the reservoir containing Np to determine the diffusion and distribution coefficients for sodium as well. The cell was opened and the clay was removed in slides of 10-30 μm from the core using the abrasive peeling method [3]. After measuring the ^{237}Np and ^{22}Na activities in each slide via γ -ray spectroscopy, the effective diffusion (D_e) and distribution coefficients (K_d) as well as the rock capacity factor (α) were calculated using Mathematica 8. A detailed description of the theoretical background of the data evaluation can be found in [4].

RESULTS

Fig. 1 shows the result of the batch experiments performed at RT and 60 °C. It becomes clear that sorption increases continuously with increasing temperature and S/L ratio. The corresponding average K_d -values amount to 34 ± 10 L/kg at room temperature and 157 ± 52 L/kg at 60 °C, indicating that the sorption of Np(V) on OPA is an endothermic process.

The characterization of the diffusion samples with HTO delivered similar porosities of 0.20 ± 0.01 and 0.19 ± 0.01 , respectively. D_e increased with increasing temperature from 1.97 ± 0.14 to $3.13 \pm 0.22 \times 10^{-11}$ m^2/s . Figures 2 and 3 show the diffusion profiles of Np(V) in OPA at room temperature and 60 °C together with the fit curves. The resulting coefficients are summarized in Tab. 1 together with the results for Na^+ . The results show that diffusion of Na^+ is not significantly affected by the temperature. The shapes and positions of the bacterial titration curves in 2 and 4 M NaClO_4 are in agreement, within experimental uncertainty (Figure 1), indicating that the effect of ionic strength on proton adsorption/desorption to the bacterial surface is negligible over this range of ionic strength.

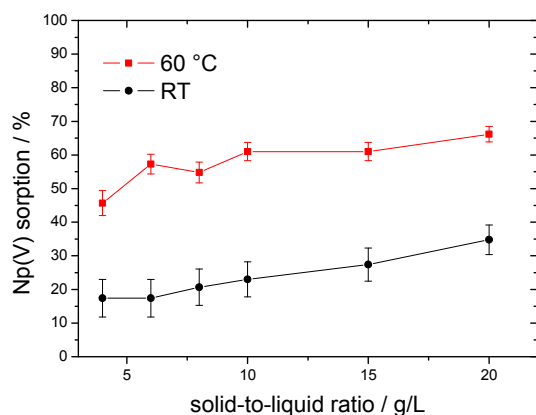


Fig. 1: Sorption of 8 μM Np(V) on OPA in dependence of S/L ratio and temperature in OPA pore water (pH 7.6, I 0.4 M) under ambient air conditions.

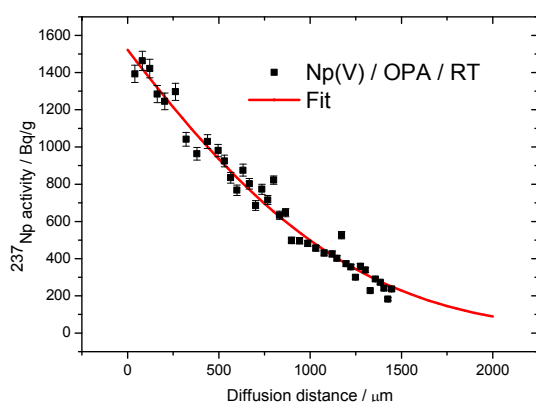


Fig. 2: Diffusion of 8 μM Np(V) in OPA under ambient air conditions in OPA pore water (pH 7.6, I 0.4 M) at RT.

Further, previous titrations of non-halophilic gram-positive and gram-negative bacteria show a similar extent of buffering in these pC_{H^+} ranges indicating that the halophilic bacteria used in this study exhibits similar protonation/deprotonation behavior as common non-halophilic soil bacteria. Therefore, it can be concluded that the interaction mechanisms between Np(V) and OPA during sorption and diffusion are significantly different pointing out that the processes that determine the endothermic behaviour in batch experiments are almost not relevant in diffusion experiments. With respect to the safety assessment of a nuclear waste repository, the usage of sorption data would lead to an overestimation of Np(V) uptake by OPA at 60 °C, while room temperature data seem to be sufficient for conservative estimations.

Further diffusion experiments including analysis of Np speciation in the OPA core are needed to gain a better understanding of the relevant interaction mechanisms during the migration process.

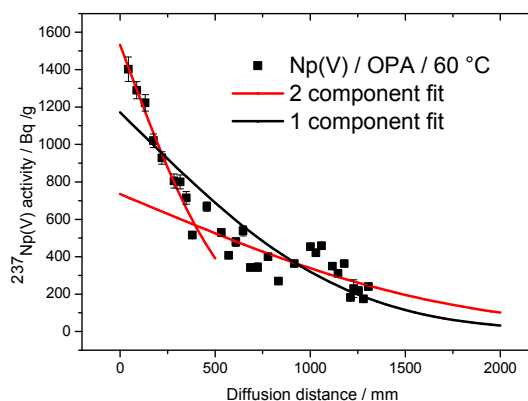


Fig. 3: Diffusion of 8 μM Np(V) in OPA under ambient air conditions in OPA pore water (pH 7.6, I 0.4 M) at 60 °C.

Tab. 1: Fit-results of Np(V) and Na^+ diffusion in OPA (error in brackets).

Np(V)	α	$D_e / \text{m}^2/\text{s}$	$K_d / \text{L}/\text{kg}$
RT	110 (3)	$2.3 (2) \times 10^{-11}$	46 (3)
60 °C (1 comp.)	148 (2)	$1.0 (1) \times 10^{-11}$	19 (1)
60 °C (2 comp.)	169 (2)	$2.1 (2) \times 10^{-12}$	29 (2)
	134 (2)	$9.7 (7) \times 10^{-12}$	14 (1)
Na^+	α	$D_e / \text{m}^2/\text{s}$	$K_d / 10^{-3} \text{L}/\text{kg}$
RT	0.44 (1)	$2.5 (4) \times 10^{-11}$	97 (8)
60 °C	0.40 (1)	$3.5 (7) \times 10^{-11}$	91 (7)

ACKNOWLEDGEMENT

This work was financed by the Federal Ministry of Economics and Technology (BMWi) under contract No. 02E10166. Daniel Fröhlich has been supported by a fellowship of DFG-GRK 826. We are grateful to Dr. Christian Marquardt (INE, KIT) for providing the OPA samples.

REFERENCES

1. T. Wu et al., "Neptunium(V) sorption and diffusion in Opalinus Clay" *Environ. Sci. Technol.*, **43**, 6567-6571 (2009).
2. L. R. Van Loon et al., "Diffusion of HTO, $^{36}\text{Cl}^-$ and $^{125}\text{I}^-$ in Opalinus Clay samples from Mont Terri - Effect of confining pressure" *J. Contam. Hydrol.*, **61**, 73-83 (2003).
3. L. R. Van Loon et al., "High-resolution abrasive method for determining diffusion profiles of sorbing radionuclides in dense argillaceous rocks" *Appl. Radiat. Isot.*, **63**, 11-21 (2005).
4. A. E. Yaroshchuk et al., "Improved interpretation of in-diffusion measurements with confined swelling clays" *J. Contam. Hydrol.*, **97**, 67-74 (2008)

**The influence of temperature on sorption:
A preliminary assessment for Uranium(VI) sorption to bentonite**

Johannes Lützenkirchen¹, Paul Wersin²

¹*Institut für nukleare Entsorgung, Karlsruher Institut für Technologie, Hermann-von-Helmholtz-Platz 1,
76344 Eggenstein-Leopoldshafen, Germany
Johannes.Luetzenkirchen@KIT.edu*

²Gruner Ltd, Gellertstrasse 55, 4020 Basel, Switzerland

INTRODUCTION

Sorption data used in PA are usually derived at 298.15 K. However, a SF/HLW repository may remain “hot” for extended periods of time. For example, in the current Swiss SF/HLW waste concept temperatures are expected to reach up to 90 °C after about 1000 years, and remain at temperatures as high as 50 °C up to 10000 years after closure. Sorption parameters may be significantly altered under these conditions with regard to the usually involved temperature of 25 °C common for most laboratory adsorption studies. The present contribution provides a preliminary assessment as to how temperature may affect the sorption behaviour of Uranium(VI) onto bentonite in a temperature range that may be relevant for PA (though U(VI) probably is not relevant due to expected reducing conditions). Adsorption processes are affected through aqueous speciation and potentially by solubility. Increased temperature tends to favor complex formation in solution and increase solubility. Complications arise, when temperature changes cause phase transformations. Surface related properties have been studied in some detail with respect to temperature changes. Thus, it is well established that variable charge properties of minerals are affected by temperature changes through variation of points of zero charge and absolute surface charge densities: The increase in temperature yields a decrease in point of zero charge. It also results in an increase in absolute proton related surface charge. It is also known that an increase in temperature yields an increase in cation adsorption at intermediate and low pH, while studies on anion adsorption appear to indicate that an increase in temperature yields a decrease in anion sorption at high pH. Both tendencies can be understood from the change of the point of zero charge with temperature. The electrostatic contributions to the free energy of adsorption would favor cation adsorption and decrease anion adsorption with increasing temperature. However, exceptions to this general rule may occur.

DESCRIPTION OF THE WORK

The objective of this exercise was to obtain a tentative prediction of the temperature dependence for U(VI) adsorption to bentonite from data available in the literature. In the first step we extracted surface complexation parameters from Pabalan et al. [1] and

simulated U(VI) adsorption data set for a relevant solid concentration of bentonite (4.5 kg/l) at total uranium concentration (TOTU) of 1 μM. The simulation results were subsequently fitted to the existing two site non-electrostatic acid/base model for bentonite. Ion exchange was not considered, because the adsorption of U(VI) is very strong at low pH. In absence of better data, the thermodynamic parameters for Cd on hematite and rutile from Fokking [2] are model independent. We further use the fact that the difference in reaction enthalpy for Cd and H for rutile and hematite was nearly constant. This information can be used for the bentonite along with proton adsorption enthalpies obtained from equations by Kulik [3] and can be applied to the 2-pK bentonite surface complexation. With these values it is possible to calculate the reaction enthalpy for U(VI) adsorption to bentonite (table 1).

Table 1. Summary of estimated thermodynamic parameters at 298.15 K.

Property	Site 1	Site 2
Reaction	$S_1OH + H^+ = S_1OH_2^+$	$S_2OH + H^+ = S_2OH_2^+$
Log Stability constant	4.5	6.0
Enthalpy in kJ/mole	-6.1	-8.2
Reaction	$S_1OH = S_1O^- + H^+$	$S_2OH = S_2O^- + H^+$
Log Stability constant	-7.9	-10.5
Enthalpy in kJ/mole	6.4	10.0
Reaction	$S_1OH + UO_2^{2+} = S_1OUO_2^+ + H^+$	$2S_2OH + UO_2^{2+} = (S_2O)_2UO_2 + 2H^+$
Log Stability constant	1.7	-3.6
Enthalpy in kJ/mole	+22.6	+19.0

The procedure includes some obvious uncertainties, involving assumptions (e.g. bentonite and montmorillonite parameters are merged), simplifications (e.g. reduced aqueous speciation) and inconsistencies (e.g. reaction enthalpies for Cd adsorption on two oxides are simply applied to U(VI) adsorption to bentonite). All calculations are performed using MINTEQA2 [4].

RESULTS

Figures 1 and 2 show the predicted adsorption behaviour of U(VI) to bentonite. At low pH uranyl shows the typical cation-like behaviour, where adsorption increases with increasing pH (Fig. 1).

In the intermediate range at all temperatures nearly 100 % U(VI) is adsorbed and no effect of temperature is observed.

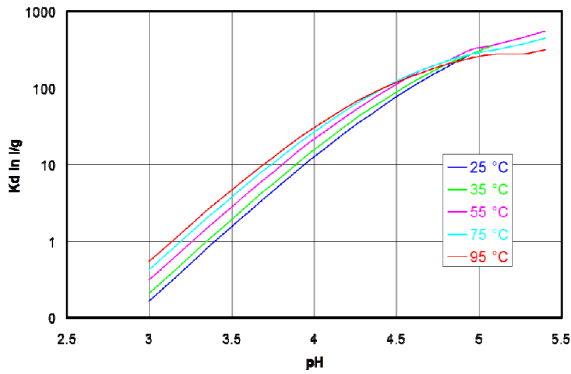


Fig. 1: Predicted K_d values for U(VI) adsorption onto bentonite at low pH (Figure 2).

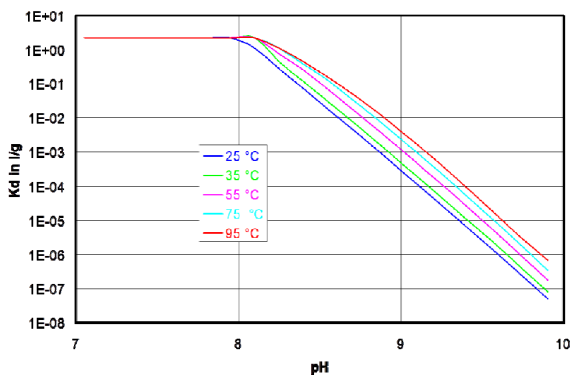


Fig. 2: Predicted K_d values for U(VI) adsorption onto bentonite at low pH.

Finally at still higher pH, the adsorption of Uranyl decreases with increasing pH, because of its aqueous solution speciation. Again the higher temperature still involves higher adsorption, although one would expect anionic behavior in this case, for which literature usually suggests a decrease in adsorption with increasing temperature. However, in the model only cationic species are involved in adsorption reactions and the predicted temperature dependence arises only from the basic charging model and the temperature dependent speciation.

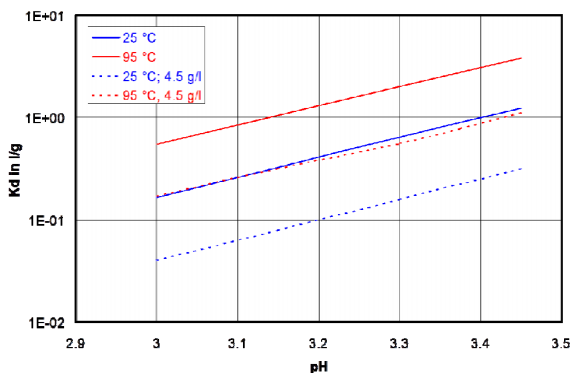


Fig. 3: Predicted K_d values for U(VI) adsorption on bentonite at low pH at two different temperatures and two different solid concentrations.

The discussed uncertainties strongly suggest that a larger experimental basis of results is required to apply simulations procedures as those discussed in this contribution with sufficient accuracy. In particular we note that anion-like behavior that might be relevant for U(VI) at higher pH cannot obviously not be simulated based on the thermodynamic adsorption data used in the present approach.

REFERENCES

1. Pabalan, R.T., Turner, D.T., Bertetti, F. P., Prikryl, J. D.: Uranium (VI) Sorption to selected mineral surfaces, in Adsorption of metals by geomedia (ed. E.A. Jenne), Academic Press, 1998.
2. Fokking, L.G.J.: Ion adsorption on oxides: surface charge and cadmium binding on rutile and hematite. Ph.D. thesis, 1987, Wageningen, the Netherlands.
3. Kulik, D.A.: Thermodynamic properties of surface species at the mineral water interface under hydrothermal conditions: A Gibbs energy minimisation single-site 2pKa triple-layer model of rutile in NaCl electrolyte to 250 °C, *Geochimica et Cosmochimica Acta* 64, 3161 (2000).
4. Allison, J.D., Brown, D.S., and Novo-Gradac, K.J.: Minteqa2/Prodefa2, A Geochemical Assessment Model for Environmental Systems: Version 3.0 US EPA, Athens, GA, 1991, users manual. Version 4 (2000) with an updated and commented database was used.

Temperature Impact on the Sorption of Selenate onto Anatase

Carola Franzen, Norbert Jordan, Katharina Müller, Tilmann Meusel, Vinzenz Brendler

*Helmholtz-Zentrum Dresden-Rossendorf, Institute of Radiochemistry,
P.O. Box 510119, D-01314 Dresden, Germany
email: c.franzen@hzdr.de*

INTRODUCTION

The radioactive isotope Selenium-79 is a long-lived fission product found in nuclear waste. Due to its long half live of $3.27 \cdot 10^5$ years [1] it is expected to be one of the most contributing isotopes concerning safety assessments of nuclear waste underground repositories. The control of the mobility and bioavailability of selenium is therefore of great importance for a safe disposal of radioactive waste.

One major process controlling selenium mobility and bioavailability is the adsorption onto mineral surfaces of both the geological and engineered barrier. In the past, many studies on selenium retention onto several mineral surfaces were performed; primarily regarding the selenium oxyanions (SeO_4^{2-} and SeO_3^{2-}). Most of these studies were conducted at 25°C. However, high level and long-lived radioactive waste is well-known to increase the temperature in the vicinity of the waste disposal site for at least 10,000 years. Thus, it is important to understand to what extent the retention of selenium is influenced at elevated temperatures. So far, only a few sorption studies at higher temperatures [2-6], are available. They showed a lowering of Se sorption with increasing temperature.

The present study focuses on the impact of temperature on the sorption of selenate (SeO_4^{2-}) onto anatase (TiO_2). Because of its abundance in rocks and its well-known crystal structure, anatase represents an ideal model system for the study of sorption behaviour of Se onto transition metal oxide phases. The sorption of selenate onto anatase at different temperatures (25°C – 60°C) was investigated both with batch experiments and ATR FT-IR spectroscopy. In order to explain possible differences in sorption at higher temperatures, the surface of the anatase was investigated.

DESCRIPTION OF THE WORK

For batch experiments samples were prepared by diluting 20 mg of anatase in 40 ml NaCl ($I = 0.1$ M) getting a solid-to-solution ratio of 0.5 g L^{-1} . The initial Se(VI) concentration was $10^{-5} \text{ mol L}^{-1}$. The suspensions were equilibrated for 48 hours in a thermostatically controlled head-over-head shaker. The pH values (pH 3.5 – pH 7) of the suspensions at different temperatures (25°C, 40°C, 60°C) were adjusted by addition of either HCl or NaOH. Prior, the pH-electrodes were calibrated at every temperature using buffer solutions. All preparations were conducted in N_2 -

atmosphere. After thermostatically controlled centrifugation during two hours at 12,000 g, the remaining selenium concentration in the supernatant was determined by ICP-MS.

The selenate sorption reactions onto anatase were investigated by ATR FT-IR spectroscopy, in comparison to a recent study at 25°C [7]. For the in situ sorption experiments a flow set-up with integrated temperature monitoring of the solutions and the ATR crystal was used.

The impact of temperature (25°C and 60°C) on the variable surface charge of anatase (pH 3.5-11) was evaluated by a zeta potential measurement using laser Doppler electrophoresis. Anatase samples were prepared like described for the batch experiments, but in ambient air, since no difference was observed in a recent study [7].

RESULTS

The sorption of Se(VI) onto anatase as a function of pH is similar at 25°C and 60°C, i.e. a decrease of the sorption with increasing pH (figure 1). However, the sorption capacity of anatase towards Se(VI) is lowered at a higher temperature. Furthermore, the pH value above which no Se(VI) sorption occurs is shifted to lower pH values.

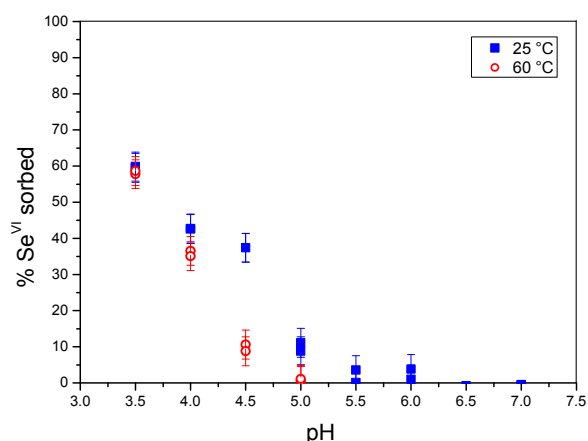


Fig. 1: Se(VI) sorption edges onto anatase at 25°C and 60°C [$[\text{Se(VI)}]_{\text{ini}} = 10^{-5} \text{ mol L}^{-1}$, $m/v = 0.5 \text{ g L}^{-1}$, $I = 0.1 \text{ M NaCl}$].

As shown in figure 2, the isoelectric point of anatase was located at pH 6.3 at 25°C. At higher temperatures the pH_{IEP} was shifted towards lower pH with a value of

5.5 at 60°C; being in good agreement with data from literature where the pH_{PZC} of different oxides and hydroxides were experimentally determined and calculated at different temperatures [5,8]. In addition, the absolute values of the zeta potential were lowered at higher temperatures. Both findings were in good agreement with the batch experiments.

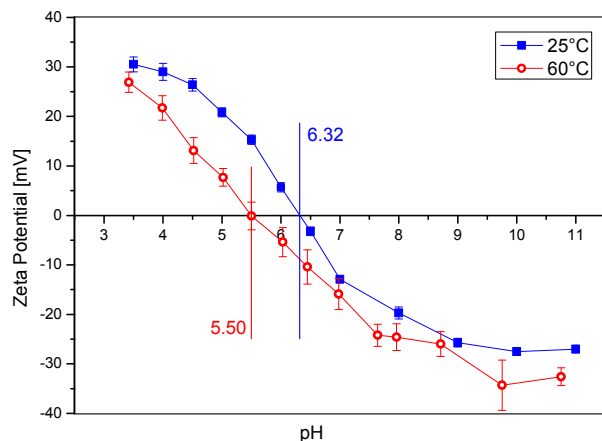


Fig. 2: Zeta potential of the neat surface of anatase at 25°C and 60°C ($m/v = 0.5 \text{ g L}^{-1}$, $I = 0.1 \text{ M NaCl}$).

ATR FT-IR spectroscopy showed a significant blue shift of the asymmetric $\nu_3(\text{Se-O})$ stretching mode of the sorbed Se(VI) onto anatase (880 cm^{-1}) compared to the ν_3 mode of the free SeO_4^{2-} species in solution (885 cm^{-1}), indicating the formation of outer-sphere complexes on the anatase surface (7).

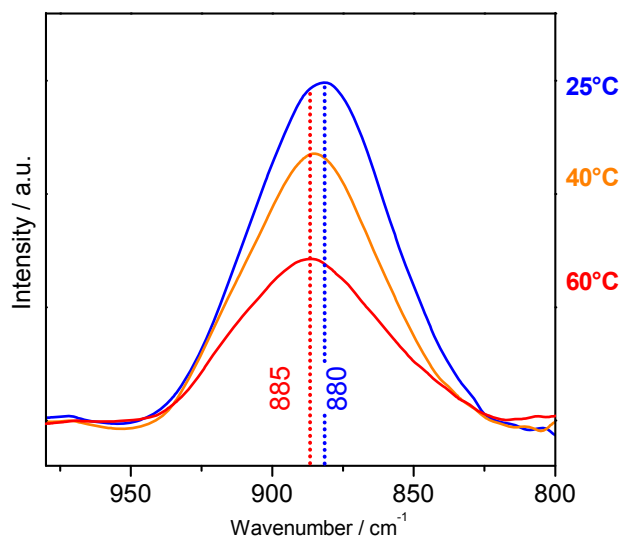


Fig. 3: IR spectra of the Se(VI) sorption onto anatase ($\text{Se(VI)} = 500 \mu\text{M}$; $\text{pH} = 3.5$, $I = 0.1 \text{ M NaCl}$).

At higher temperatures, ATR FT-IR measurements show a reduction of the band intensity of the $\nu_3(\text{Se-O})$ mode, providing evidence for an overall decrease of selenium(VI) sorption capacity onto anatase (Fig. 3). This is in agreement with macroscopic batch experiments. However, since only a very small blue shift (885 cm^{-1}) of the $\nu_3(\text{Se-O})$ mode, but no splitting of the band was observed, no significant structural changes on the sorbed selenium(VI) surface complexes are predicted at higher temperature.

ACKNOWLEDGMENTS

This work is part of the VESPA project, funded by BMWi through contract 02E10790.

REFERENCES

1. JOERG et al., "Preparation of radiochemically pure Se-79 and highly precise determination of its half-life." *Appl. Radiat. Isot.*, **68**, 3339-2351 (2010).
2. Balistrieri et al., "Selenium adsorption by goethite." *Soil Sci. Soc. Am. J.* **51**, 1145-1151 (1987).
3. Parida et al., "Studies on ferric oxide hydroxides .III. Adsorption of selenite (SeO_3^{2-}) on different forms of iron oxyhydroxides." *J. Colloid and Interface Sci.* **185**, 355-362 (1997).
4. Parida et al., "Studies on Indian ocean manganese nodules .III. Adsorption of aqueous selenite on ferromanganese nodules." *J. Colloid Interface Sci.* **187**, 375-380 (1997).
5. Vlasova et al., "Effect of temperature on selenite adsorption by goethite." In: Wanty, Seal (eds.) *Water-Rock Interaction 2*. Balkema Publ., Leiden, 1017-1021(2004).
6. Zhang et al., "Sorption behavior of nano-TiO₂ for the removal of selenium ions from aqueous solution." *J. Hazard. Mat.* **170**, 1197-1203 (2009).
7. JORDAN et al., "Sorption of selenium(VI) onto anatase: Macroscopic and microscopic characterization." *Geochim. Cosmochim. Acta* **75**, 1519-1530 (2011).
8. KULIK, "Thermodynamic properties of surface species at the mineral-water interface under hydrothermal conditions:..." *Geochim. Cosmochim. Acta* **64**, 3161-3179 (2000).

Effect of Temperature on Selenate Adsorption by Goethite

Michael Kersten¹, Nataliya Vlasova¹

¹First Geosciences Institute, Johannes Gutenberg-University Mainz, Germany 55099
email: kersten@uni-mainz.de

INTRODUCTION

Despite a growing number of studies on surface complexation modeling, and although a major source of oxyanions are hydrothermal waters, not much is known yet about the effect of temperature on oxyanion adsorption. Data for silicate and arsenite have recently been reported from our laboratory [1,2]. Selenate is known to form both inner- and outer-sphere surface complexes. This continuum of adsorption mechanisms is strongly affected by both pH and ionic strength, but, as we will show here for the first time, also by temperature.

EXPERIMENTS

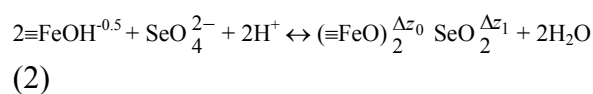
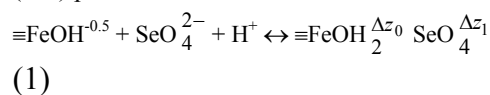
The sorbent goethite phase was precipitated from ferric nitrate solution under highly alkaline conditions, aged at elevated temperature (90 °C) for at least one week, and ultimately dialyzed in cellulose tubing with deionized boiled water at room temperature during a further week. BET surface area of the thus produced goethite was as low as 20 m² g⁻¹ indicating well crystallized material. All experiments were carried out in plastic vessels under bubbling argon to minimize silica and carbonate contamination, which may severely interfere with oxyanion adsorption. For the batch titration and adsorption experiments, suspensions with final goethite concentrations of 1 g L⁻¹ were prepared. Background electrolyte concentrations of 0.01, 0.05, and 0.1 M were fixed using nearly inert NaNO₃. In each of the 50 mL polypropylene bottles, 30 mL of suspension was filled with argon in the headspace, and heated in a water bath to the desired temperature of between 20°C to 75°C in steps of 25°C. Selenate was added at 10, 50, and 100 μM final concentrations. The dissolved adsorbate concentrations in centrifuged and additionally membrane-filtered (0.2 μm) solutions were analyzed by HG-AAS.

RESULTS

Adsorption model parameterization was carried out using the speciation code ECOSAT coupled to the optimization code FIT [3]. For all batch systems, the pH_{PZC} is continuously decreasing from the starting value at 10°C to a 1.2 pH unit lower value at the maximum 75°C [1]. Input of the surface charge parameters was made in the “goethite-BS” mode, i.e. by applying the Basic Stern option as the electrostatic model (BSM). Site density for the multi-site surface ion complexation (MUSIC) model was assumed at 3.45 nm⁻² for the singly coordinated groups, and 2.7 nm⁻² for one

third part of the μ₃-hydroxo groups according to a recommendation by Hiemstra & Van Riemsdijk [4]. The logK_H value for the protonation of both sites is set equal to the pH_{PZC} = 9.1 determined from both batch titration and electroacoustic measurement results [1]. The presence of background electrolyte in the outer Stern layer was considered by fixed intrinsic equilibrium reaction constants for an outer-sphere surface complexation logK_{Na} = logK_{NO3} - logK_H = -1 [4]. Stern layer capacitance C₁ = 0.97 F m⁻² for columbic term correction to obtain the intrinsic constants in the BSM option was derived from non-linear regression of proton surface charge data [1]. The charge distribution (CD-MUSIC) model was used to fit the oxyanion adsorption data. It can distinguish not only between inner- and outer-sphere complexation, but also between bidentate and monodentate complexes [4]. The net charge introduced in the Stern layer region can be formulated as Δz₀ = n₀ + n_{H0} for the inner, and Δz₁ = n₁ for the outer Stern layer, respectively, in which n₀ and n₁ represent the ion charge proportion allocated to the respective plane, and n_{H0} is the additional proton(s) introduced in the inner plane.

The % adsorption vs. pH curves reveal distinct adsorption edges below the goethite pH_{PZC} value. Based on the hypothesis of a mono-dentate outer-sphere and a bi-dentate inner-sphere surface complex formation, the adsorption reactions may be formulated in terms of the CD-MUSIC approach with these charge distribution (CD) parameters:



The outer-sphere surface complexation reaction (1) compares with that of the background electrolyte nitrate anion, but the difference is that the sum of the charge distribution (CD) values for the bivalent oxyanion is not entirely located in the outer plane (i.e., Δz₁ < -2). For reaction (1), the CD values were rather fixed with Δz₀ = 0.67 at the 0-plane (with n_{H0} = 1), and Δz₁ = -1.67 at the outer plane. This choice implies an outer-sphere surface complexation with a slightly higher affinity towards the surface than that for the nearly inert nitrate background electrolyte. For the bidentate inner-sphere surface complexation reaction (2) where two moles of water are desorbed, the CD parameters were set at Δz₀ = 1 (n_{H0} = 2) and Δz₁ = -1, as suggested for a bidentate surface complex of a bivalent oxyanion [4]. These CD

parameters were fixed to fit the whole range of experimental data of pH, ionic strength, and temperature with only variation in the $\log K$ values of reactions (1) and (2). Fitting with ECOSAT-FIT ultimately led to a unique set of surface complexation constants reproducing the entire data set ($n > 500$) with $r^2 \geq 0.97$.

Generally, the higher the temperature, the less amount of selenate is adsorbed on the goethite surface at the same total Se concentration. The effect is similar to that of increasing ionic strength. This indicates an influence by the temperature dependent electrostatic properties of the goethite surface. The decrease of surface acidity (pH_{PZC}) with temperature results in a lower screening of the negative charge of the surface complex, i.e., more repulsion will occur at a higher temperature. This leads to a shift in the selenate adsorption edge by about 0.2 units per 10 °C towards the more acidic region. Consequently, the pH value at which the proportion of both inner- and outer-spheric surface species is equal (i.e., the point at which their curves crosses) decreases with increasing temperature. Opposite to the effect of ionic strength, the higher the temperature, the higher is now the proportion of the outer-sphere complexes at the same selenate surface loading and pH value (Figure 1). This indicates a strong weakening of the overall adsorption affinity for selenate with increasing temperature.

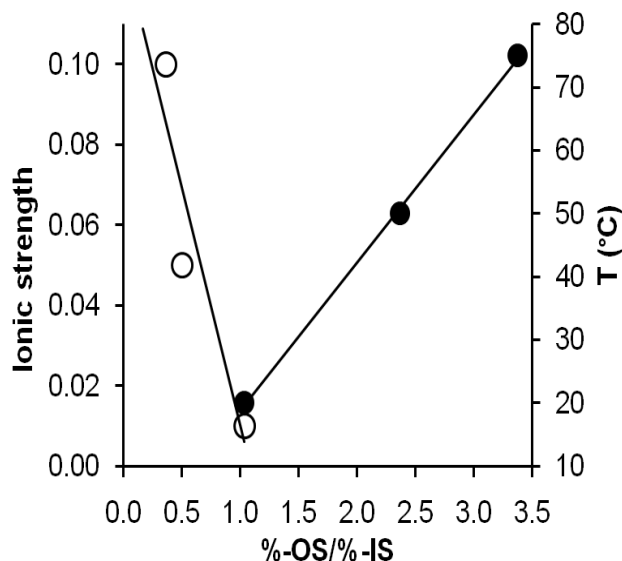


Fig. 1: Ratio of outer-spheric (%-OS) to inner-spheric (%-IS) SeO_4 surface complex formation in dependence of background electrolyte ionic strength (left curve, open dots) and temperature (right curve, black dots) at a $\text{pH} = 4$ ($10 \mu\text{M Se}$, 1.0 g L^{-1} goethite suspension).

The fitted intrinsic $\log K_T$ constants of both adsorption reactions change linearly with inverse temperature ($1000/T$ when using the Kelvin scale). The linear fit to

the $\log K_{\text{OS},T}$ vs. $1000/T$ data pairs for the outer-sphere complexation reaction (1) nearly parallels those of the surface protonation reaction. Such a correlation appears reasonable because of the direct influence of the temperature dependent electrostatic surface properties on binding of the outer-sphere surface complex as discussed above. However, there is no such simple relationship for the inner-sphere surface complexation reaction (2), because the slope for the linear fit to the respective $\log K_{\text{IS},T}$ data deviates significantly from that for the surface protonation reaction. With the reasonable assumption of zero heat capacity and hence constant $\Delta_r S$ within the temperature range, the temperature behaviour of the equilibrium constants can be well represented by the common van't Hoff two-term equation. The limited experimental temperature range does not allow derivation of a reliable value for the heat capacity by a three-term extrapolation. Using the values for $\log K_T$ determined in the temperature range, a linear least square fit yield values for the reaction enthalpy. From the general relationship $\Delta_r G_{298}^0 = 2.3 \cdot R \cdot 298 \cdot \text{p}K_{298} = \Delta_r H_{298}^0 - 298 \cdot \Delta_r S^0$, the standard energy and ultimately the standard entropy of the selenate adsorption reactions were determined. Note, however, that the entropy term is of the same order as the uncertainty in the enthalpy of reaction. The thus derived data can readily be applied in aqueous equilibrium speciation codes, which allow for implementation of adsorption enthalpy constants with the 1-pK BSM and CD-MUSIC option like ECOSAT, Visual-MINTEQ, or GEMS (<http://gems.web.psi.ch/>).

REFERENCES

1. M. KERSTEN, N. VLASOVA, "Arsenite adsorption on goethite at elevated temperatures" *Appl. Geochem.*, **24**, Page 32-43 (2009).
2. M. KERSTEN, N. VLASOVA, "Silicate adsorption by goethite at elevated temperatures" *Chem. Geol.*, **262**, Page 372-379 (2009).
3. M.G. KEIZER, W.H. VAN RIEMSDIJK, "ECOSAT – A Computer Program for the Calculation of Speciation and Transport in Soil-Water Systems, Version 4.8" Wageningen University, The Netherlands (1999).
4. T. HIEMSTRA, W.H. VAN RIEMSDIJK, "A surface structural approach to ion adsorption: The charge distribution (CD) model" *J. Colloid Interf. Sci.*, **179**, Page 488-508 (1996).

Influence of temperature on the sorption of Europium into Smectite: The role of organic contaminants

A. Bauer¹, T. Rabung¹, F. Claret², T. Schäfer¹, G. Buckau³, T. Fanghänel³

¹ Institut für Nukleare Entsorgung, Karlsruhe Institute of Technology, Hermann-von-Helmholtz-Platz 1, 76344 Eggenstein-Leopoldshafen, Germany

email: thomas.rabung@kit.edu

² BRGM, Environment and Process Division 3, Avenue Claude Guillemin, F-45060 Orleans Cedex 2, France

³ European Commission, JRC, Institute for Transuranium Elements, P.O. Box 2340, 76125 Karlsruhe, Germany

INTRODUCTION

In the near field environment of a spent fuel or vitrified high level waste repository the temperature in the bentonite buffer will remain elevated for a long time period (> 70-90°C for 1000 years). To analyze the effect of temperature on the sorption, the sorption process of Eu(III) at 25°, 60° and 80°C was investigated. To examine the sorption process and the influence of organic contaminants, wet chemistry and time-resolved laser fluorescence spectroscopy (TRLFS) was used.

DESCRIPTION OF THE WORK

The Eu(III) sorption were measured at 20°, 60° and 80°C as a function of pH in 0.1 M KClO₄. All experiments were performed in a glove box under Argon atmosphere. After the addition of Eu(III) to the solution and the pH adjustment the 60° and 80°C samples were stored in an oven with an Argon atmosphere. The pH was adjusted by adding analytical grade KOH or HClO₄. Various chemical and spectroscopic tests showed no difference in the behaviour of Eu(III) when added before or after raising the solution temperature. The experiments were performed in high density polyethylene (HDPE) 20 ml Zinsser bottles (Zinsser Analytics, Frankfurt/M.) and 3 ml quartz cuvettes with a solid/solution ratio of 0.25 g/L. According to the manufacturer the HDPE bottles are made of 100 % pure HDPE and contain no traces of impurities. All the solutions were prepared with deionised water (Milli-Q Reagent Water System from Millipore) with a resistivity of > 18 MΩ · cm⁻¹. To avoid carbonate complexation of the metal ion CO₂ free water and KOH solution was used. The initial DOC concentration of the Millipore Water was found to be 0.08 mg/L.

The Eu(III) stock solution used was a ICP/DCP standard solution (Alpha) containing 1 g/L of Eu. The Eu(III) concentration was fixed to 3.3 × 10⁻⁶ mol/L. Clay samples were equilibrated in 0.1 M NaClO₄ at pH 6.7 for one week in the dark. Kinetic tests were performed during a period between 0.1 h and 9600 hours (400 days). Equilibrium was reached within 24 hours at 25°C and within 1 hour at 80°C. Nevertheless batch samples were shaken periodically for at least two days.

RESULTS

The sorption mechanism of Eu(III) on smectite was studied by TRLFS. Single component spectra with mono-exponential decay behaviour are found for all temperatures for both reaction vessels at pH < 5. Fluorescence emission lifetimes were measured to be 110 μs corresponding to the free Eu(III) aquo ion (Fig. 1) indicating outer-sphere complexation [1].

Near-field chemical conditions: Anoxic corrosion will result in strongly reducing conditions that are at or even below the lower stability limit of H₂O on an Eh-pH diagram (see below). In fact, f_{O₂} is so low that H₂O is unstable in the WIPP and H₂O is reduced to H₂ by low-C steels.

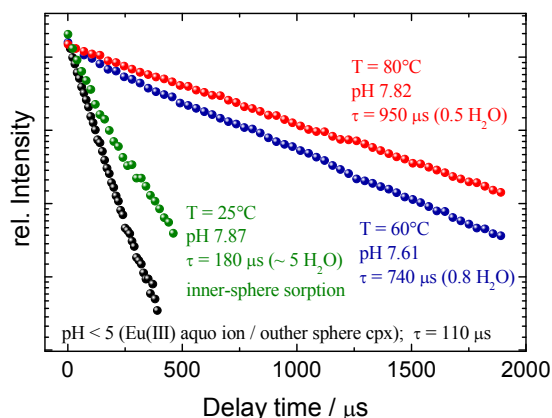


Fig. 1: Fluorescence emission lifetimes of Eu(III) sorbed onto smectite at different temperatures in HDPE Zinsser bottles. At pH < 5 only the Eu(III) aquo ion was detected at any temperature. With increasing pH and temperature a different evolution of the fluorescence emission lifetimes was observed.

At higher pH values and higher temperatures a different evolution for the different types of reaction vessels was observed. At 25°C (pH > 6) fluorescence emission lifetime of 180-200 μs was found for the two types of reaction vessels, corresponding to 5 water molecules in the first coordination sphere (Fig. 1). At 60° and 80°C (pH > 5) the fluorescence emission lifetime increased significantly in the Zinsser bottles up to 700-950 μs indicating almost a complete loss of water in the first coordination sphere of europium (Fig. 1). In the quartz

cuvettes under the same conditions, a fluorescence emission lifetime of 190-200 μs was measured (Fig. 2). The influence of the reaction vessel was verified by heating Eu(III) at 80°C for 48 hours in HDPE Zinsser bottles at a pH value of 6 without smectite. Under these conditions a fluorescence emission lifetime of 833 μs was found similar to the experiments with smectite (Fig. 2). DOC measurements of the solutions as a function of pH showed that up to 6.5 mg/L organic material can be leached out of the HDPE Zinsser bottle (Fig. 3) at 60° and 80°C. DOC measurements of experiments at 25°C and of smectites in quartz cuvettes (25-80°C) showed no increase of organic material in solution.

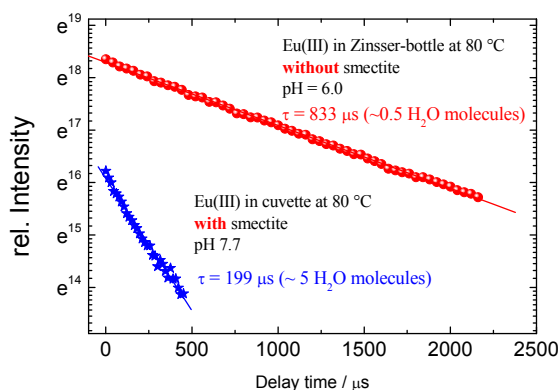


Fig. 2: Comparison of the fluorescence emission lifetime of Eu(III) after an experiment in a HDPE Zinsser bottle without smectite and an experiment performed in a quartz cuvette with smectite at 80°C.

Because of the increase in layer charge and the fluorescence emission lifetimes of 700-950 μs (for the experiments in the Zinsser bottles) indicating a complete loss of the water coordination sphere, the first working hypothesis was that Eu(III) is incorporated into the crystal structure via dissolution/recrystallisation processes. We thought that this process might be responsible for the long fluorescence emission lifetimes. In comparing the results from the HDPE Zinsser bottles with the results from the quartz cuvettes it became evident that a third component coming from the Zinsser bottles might be responsible for this difference. DOC measurements of the solutions without clay clearly showed that organic material is released from the Zinsser bottles. In the tests we made (e.g. Fig. 2; pH 6) secondary Eu(III) phases are implausible because we were always at least one order of magnitude below the solubility limit of Eu(III) compounds. EQ3/6 calculations also indicated that we were in nearly all experiments undersaturated with respect to any probable phase.

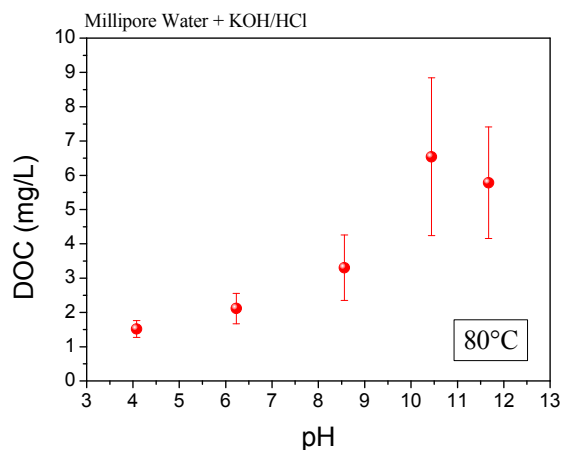


Fig. 3: Evolution of the DOC as function of pH in a HDPE Zinsser bottle at 80°C after 48 hour reaction time. Error bars correspond to the standard deviation of triplicates.

The experiments clearly demonstrate that at elevated temperatures organic material with strong complexing properties towards (at least) trivalent lanthanides and actinides can be leached out from sample containers and affecting strongly the metal ion speciation [2].

The possibility of affecting experimental results by releasing organic material at elevated temperatures has to be checked out in all further experiments where organic surfaces are involved in.

REFERENCES

1. Stumpf, T., Bauer, A., Coppin, F., Fanghanel, T., Kim, J.I., "Inner-sphere, outer-sphere and ternary surface complexes: a TRLFS study of the sorption process of Eu(III) onto smectite and kaolinite", *Radiochimica Acta*, **90**(6), page 345-349 (2002)
2. Bauer, A., Rabung, T., Claret, F., Schäfer, T., Buckau, G., Fanghanel, T., "Influence of temperature on sorption of europium onto smectite: The role of organic contaminants", *Applied Clay Sci.*, **30**, page 1-10 (2005)

Octa- and Nonahydrated Cm(III) in Aqueous Solution from 20 to 200 °C

Patric Lindqvist-Reis¹, Reinhardt Klenze¹, Thomas Fanghänel²¹Institute for Nuclear Waste Disposal, Karlsruhe Institute of Technology, P.O. Box 3640, 76021, Karlsruhe, Germany
patric.lindqvist@kit.edu²European Commission, Joint Research Centre, Institute for Transuranium Elements, Karlsruhe, Germany

INTRODUCTION

Structure and thermodynamic data of actinide (An) ions in aqueous solution at elevated temperatures is scarce in the literature. Nevertheless, such information is essential, for example, for predicting actinide transport in the near-field environment to a nuclear waste repository. Depending on the waste load and the type of geo-engineered barrier, the temperature at the canister surface may indeed reach 200 °C due to the radioactive decay. Despite the lack of data at high temperatures, a primary step is to obtain a detailed picture about the local structure of the hydrated actinide ions at room temperature.

EXAFS has been used to obtain bond distances and coordination numbers and for several An³⁺ aqua ions.¹⁻³ The results showed fairly consistently the An–O bonds to decrease with increasing Z, while the hydration numbers were scattered between nine and ten. Due to their similar structure chemistry to the trivalent lanthanides, the early An³⁺ ions are expected to be nine-coordinated in aqueous solution while a “smooth” transition from nine- to eight-coordinated ions is believed to occur between Cm³⁺ and Es³⁺.¹ We showed using time-resolved laser fluorescence spectroscopy (TRLFS) that the ⁶D_{7/2} → ⁸S_{7/2} spectrum of Cm³⁺(aq) was composed of two emitting species, A and B, assigned to [Cm(H₂O)₉]³⁺ and [Cm(H₂O)₈]³⁺, respectively, and that the A:B intensity ratio decreased with increasing temperature due to a temperature-dependent equilibrium.⁴



Similar results were found in a recent molecular dynamics study.⁵ This paper summarizes key results of the TRLFS study⁴ and provides some new, unpublished data.⁶

RESULTS

Laser-induced excitation at 397 nm of Cm³⁺(aq) gives rise to a slightly asymmetric emission band at ~594 nm (Fig. 1). The asymmetry, which appears at the band's blue side, increases with temperature from 20 to 200 °C due to the transitions from thermally populated crystal-field levels of the first excited state (⁶D_{7/2}) to the ground

state (⁸S_{7/2}). In addition, the emission intensity decreases markedly with increasing temperature. Note that the total splitting of the excited state is appreciably larger than that of the ground state.

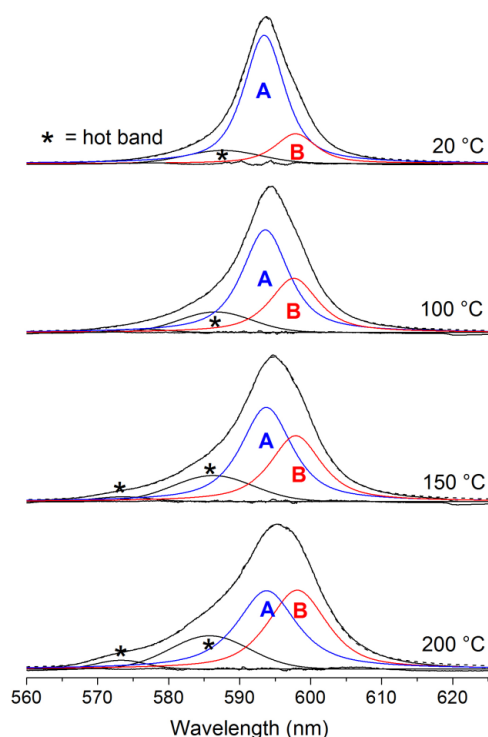


Fig. 1: Curve-fitted and intensity-normalized emission spectra of Cm³⁺(aq) at 20, 100, 150, and 200 °C. Spectra are deconvoluted into A and B species and their combined hot bands (“*”). Experimental data are shown with black solid lines, fits to the data with black dashed lines, and the fitted component bands are shown with black solid lines (hot bands), blue (A) and red (B) lines.

Typically, in Cm³⁺ aqua complexes the excited state splitting is in the range of 300–700 cm⁻¹, while that of the ground state is 10–20 cm⁻¹, although 35 cm⁻¹ was reported for an octahydrated complex.⁷ Also, a shoulder develops at the red side of the band with increasing temperature. The main band and the shoulder are attributed to the nona (A) and octahydrated species (B), respectively. The A:B ratio is given by the equilibrium constant *K*(*T*) defined by eq 1. The assignment is rational spectroscopically and thermodynamically. Spectroscopic analysis of crystalline compounds showed that the crystal-field in [Cm(H₂O)₈]³⁺ is stronger than that in [Cm(H₂O)₉]³⁺ owing to the slightly contracted coordination shell of the former.⁴ Therefore,

an increase of the crystal-field splitting explains the redshift of the spectrum at elevated temperature, and a stronger crystal field of the octaqua ion than the nonaqua ion is also in accord with prior studies on crystalline reference compounds.⁴

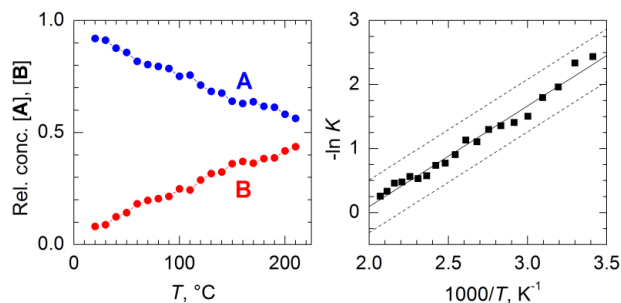


Fig. 2: (left) Relative concentration of species A and B vs temperature. (right) Van't Hoff linear representation $-\ln K$ versus $1/T$.

Spectroscopic information of the A and B species and their mole ratios as a function of temperature was gained by peak deconvolution of the spectra into four component bands, which accounted for the main electronic transitions of A and B and for the asymmetry at the band's blue side. The fitting results at four selected temperatures are shown in Fig. 1. Plotting the A/B mole ratios against temperature gave a near linear conversion of A to B with temperature, with A:B ratios of about 9:1 at 20 °C and 6:4 at 200 °C (Fig. 2a). By using a Van't Hoff plot we obtained ΔH , ΔS , ΔG , and $K(T)$, values of which are given in Tab. 1, which also lists the corresponding values of $\text{Ce}^{3+}(\text{aq})$ obtained from absorption spectra,⁸ and $K(298)$ of $\text{Cm}^{3+}(\text{aq})$ from molecular dynamics simulations.⁵

To investigate the temperature influence on the ${}^6\text{D}_{7/2}$ crystal field levels of $\text{Cm}^{3+}(\text{aq})$, we recorded ${}^8\text{S}_{7/2} \rightarrow {}^6\text{D}_{7/2}$ excitation spectra at 20 and 200 °C while monitoring the corresponding emission spectrum. Clearly, the spectrum at 200 °C is broader than that at 20 °C, most likely due to an increase of the splitting of the ${}^6\text{D}_{7/2}$ crystal field levels. Again, this is consistent with a stronger crystal field of the $[\text{Cm}(\text{H}_2\text{O})_8]^{3+}$ ion than that of $[\text{Cm}(\text{H}_2\text{O})_9]^{3+}$.⁴ A stronger field of the former is presumably due to a more compact coordination shell than of the latter.

To conclude, emission/excitation spectra of $\text{Cm}^{3+}(\text{aq})$ show a slight redshift with increasing temperature from 20 to 200 °C. We explain this shift by an increase of the mole fraction of octahydrated ions on the expense of the nonhydrated ions. ΔH , ΔS , ΔG , and $K(T)$ for the reaction $[\text{Cm}(\text{H}_2\text{O})_9]^{3+} \rightarrow [\text{Cm}(\text{H}_2\text{O})_8]^{3+} + \text{H}_2\text{O}$ were obtained.

Tab. 1: ΔH^0 , ΔS^0 , and $K(298)$ associated with the forward reaction of $[\text{M}(\text{H}_2\text{O})_9]^{3+} \rightleftharpoons [\text{M}(\text{H}_2\text{O})_8]^{3+} + \text{H}_2\text{O}$

	$\text{Ce}^{3+}(\text{aq})^a$	$\text{Cm}^{3+}(\text{aq})^b$	$\text{Cm}^{3+}(\text{aq})$
$\Delta H^0(\text{kJ mol}^{-1})$	13	13.1 ± 0.4	
$\Delta S^0(\text{J mol}^{-1}\text{K}^{-1})$	33	25.4 ± 1.2	
$K(298)$	0.28	0.11 ± 0.02	0.05^c

^a Ref. 8, ^b Ref. 4, ^c Ref. 5.

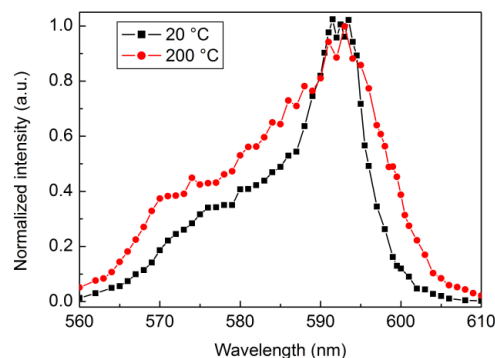


Fig. 3: Excitation spectra of $\text{Cm}^{3+}(\text{aq})$ at 20 and 200 °C.

REFERENCES

- Lindqvist-Reis et al., "The Structures and Optical Spectra of Hydrated Transplutonium Ions in the Solid State and in Solution" *Angew. Chem. Int. Ed.*, **46**, 919-922 (2007).
- Apostolidis et al., " $[\text{An}(\text{H}_2\text{O})_9](\text{CF}_3\text{SO}_3)_3$ (An = U–Cm, Cf): Exploring Their Stability, Structural Chemistry, and Magnetic Behavior by Experiment and Theory" *Angew. Chem. Int. Ed.*, **49**, 6343-6347 (2010).
- Galbis et al., "Solving the Hydration Structure of the Heaviest Actinide Aqua Ion Known: The Californium(III) Case" *Angew. Chem. Int. Ed.*, **49**, 3811-3815 (2010).
- Lindqvist-Reis et al., "Hydration of Cm^{3+} in Aqueous Solution from 20 to 200 °C. A Time-Resolved Laser Fluorescence Spectroscopy Study" *J. Phys. Chem. B*, **109**, 3077-3083 (2005).
- Hagberg et al., "A Quantum Chemical and Molecular Dynamics Study of the Coordination of $\text{Cm}(\text{III})$ in Water" *J. Am. Chem. Soc.*, **129**, 14136-14137 (2007).
- Details for the TRLFS setup are given in ref. 4.
- Lindqvist-Reis et al., "Large Ground-State and Excited-State Crystal Field Splitting of 8-fold-Coordinate Cm^{3+} in $[\text{Y}(\text{H}_2\text{O})_8]\text{Cl}_3 \cdot 15\text{-crown-5}$ " *J. Phys. Chem. B*, **110**, 5279-5285 (2006).
- Miyakawa et al., "An electrostatic approach to the structure of hydrated lanthanoid ions. $[\text{M}(\text{OH}_2)_9]^{3+}$ versus $[\text{M}(\text{OH}_2)_8]^{3+}$ " *J. Chem. Soc. Faraday Trans. 1*, **84**, 1517-1529 (1988).

Assessing temperature effects: methods for the estimation of S_m^0 for aqueous actinide species and applicability of the van't Hoff expression

X. Gaona^{1,2}, M. Grive¹, A. Tamayo¹, A. Skerencak², M. Altmaier², L. Duro¹

¹*Amphos 21, Passeig de Garcia i Fària 49-51, 08019 Barcelona, Spain
xavier.gaona@kit.edu*

²*Institut für Nukleare Entsorgung, Karlsruhe Institute of Technology, Karlsruhe, Germany*

INTRODUCTION

Temperature is one of the parameters that will vary during the different phases of the operation of a High Level Nuclear Waste repository. Elevated temperature conditions (up to 200°C, depending on repository concept) will affect radionuclide behaviour in the near-field of a HLW repository. This necessitates dedicated research efforts on the aqueous chemistry and thermodynamics at higher temperatures as basis for reliable long-term safety predictions. In spite of this, only a very few enthalpy data are available from experimental studies for aqueous species and solid compounds of actinides [1]. With respect to aqueous species, several estimation approaches have been developed in the past to fill in these thermodynamic gaps, most of them dealing with empirical correlations of entropy with charge, molar volumes, mass and ionic radii of the species involved [2-6, among others – see also 7].

DESCRIPTION OF THE WORK

Experimental enthalpy and entropy data reviewed and selected in the NEA-TDB [1] for aqueous actinide species were used in this work to further develop an empirical approach for the estimation of S_m^0 . Considering $\Delta_r G_m^0$ from [1], enthalpies were internally calculated ($\Delta_r G_m^0 = \Delta_r H_m^0 - T \Delta_r S_m^0$) and the temperature dependence of the equilibrium constant determined assuming constant enthalpy of reaction (van't Hoff expression). In a first step, the purely electrostatic correlation applied in [3] to U(VI) and Th(IV) was extended to all actinides, redox states and inorganic ligands considered in [1] (Fig. 1). This approach allows explaining all experimental S_m^0 data for aqueous species with $-6 \leq Z \leq +4$ with an uncertainty of $\pm 125 \text{ J}\cdot\text{K}^{-1}\cdot\text{mol}^{-1}$ ($\pm 1.2 \text{ log K}$ -units when extrapolating log K^0 to 90°C). For simple aquo-ions, the incorporation of size (as Z_M / r_M) in the empirical equation resulted in a significant decrease in the uncertainty to $\pm 40 \text{ J}\cdot\text{K}^{-1}\cdot\text{mol}^{-1}$ ($\pm 0.4 \text{ log K}$ -units at 90°C). The difficulty in formulating this empirical correlation for complex species where water of the coordination sphere has been substituted by other ligands was addressed by looking for additional experimental parameters with a known charge and size dependence. In this framework, the case of ion interaction coefficients (according to the SIT theory) was evaluated and will be also presented.

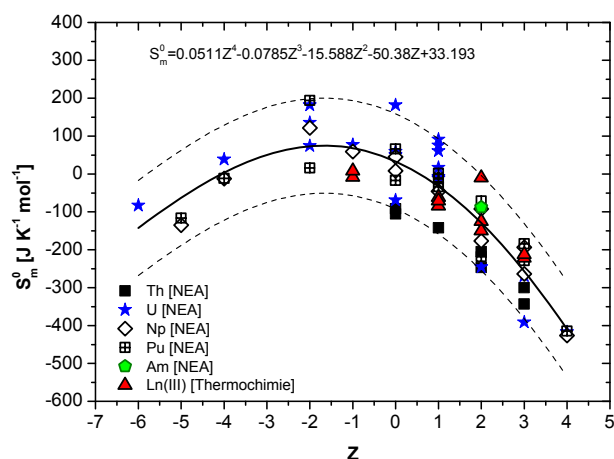


Fig. 1: Empirical correlation of S_m^0 with the charge (Z) of the aqueous species, according with data selected (from experimental studies) in the NEA and Thermochemie for actinides and lanthanides, respectively.

REFERENCES

- Guillaumont, R. et al., "Chemical Thermodynamics 5. Update on the Chemical Thermodynamics of Uranium, Neptunium, Plutonium, Americium and Technetium" NEA OECD, Elsevier (2003).
- Cobble, J.W. "Empirical considerations of entropy. II. The entropies of inorganic complex ions" *The Journal of Chemical Physics*, **21**, 1446-1450 (1953).
- Langmuir, D. "Techniques of estimating thermodynamic properties for some aqueous complexes of geochemical interest", in: *Chemical Modeling in Aqueous Systems: Speciation, sorption, solubility, and kinetics* (Jenne, E.A., ed.), ACS Symp. Ser. 93, American Chemical Society, Washington D.C., pp. 353-387 (1979).
- Baes, C.F. et al. "The thermodynamics of cation hydrolysis" *American Journal of Science*, **281**, 935-962 (1981).
- Lemire, R.J. et al. "The solubility of U, Np, Pu, Th and Tc in a geological disposal vault for used nuclear fuel" Atomic Energy of Canada Limited, AECL-10009 (1989).

6. Sverjensky, D.A. et al. "Prediction of the thermodynamic properties of aqueous metal complexes to 1000°C and 5kb" *Geochimica et Cosmochimica Acta*, **61**, 1359-1412 (1997).

7. Grenthe, I. et al. (eds.) "Modelling in aquatic chemistry" Nuclear Energy Agency, OECD, Paris, 724 pp (1997).

Spectroscopic Characterization of Eu(III) and Am(III) Complexes with Small Organic Molecules at Elevated Temperatures

Astrid Barkleit^{1,2}, Margret Acker³, Gerhard Geipel¹, Steffen Taut³, Gert Bernhard^{1,2}

¹*Helmholtz-Zentrum Dresden-Rossendorf, Institute of Radiochemistry, P.O. Box 510119, 01314 Dresden, Germany
Email: a.barkleit@hzdr.de*

²*Technische Universität Dresden, Department of Chemistry and Food Chemistry, Division of Radiochemistry, 01062 Dresden, Germany*

³*Technische Universität Dresden, Central Radionuclide Laboratory, 01062 Dresden, Germany*

INTRODUCTION

The knowledge of thermodynamic data of actinide complexes with organic ligands is fundamental for the risk assessment of both potential nuclear waste repositories and contaminated soils or aquatic systems in the environment. Argillaceous rocks which are potential host rocks for nuclear waste repositories can contain dissolved organic matter like formate, citrate or lactate. Such small organic molecules can like the ubiquitous humic acid influence the migration behaviour of radionuclides. For the latter, different substituted benzoic acids mimic the main functionalities and are often used as model compounds for humic substances. The understanding of the complex behaviour of radionuclides with such natural organic matter and the thermodynamic quantification of the interaction is of great importance to simulate and predict their migration behaviour in the environment. Additionally, it is crucial to study the complex behaviour of radionuclides at elevated temperatures, because especially in the near field of nuclear waste disposals higher temperatures are prevailing.

We investigated the complex behaviour of Am(III) and the inactive analogue lanthanide Eu(III) with lactate and salicylate at ambient and elevated temperatures with time-resolved laser-induced fluorescence spectroscopy (TRLFS). From the spectra we determined conditional complex stability constants at different temperatures and the resulting thermodynamic data (reaction enthalpy $\Delta_R H$, reaction entropy $\Delta_R S$).

DESCRIPTION OF THE WORK

For spectrophotometric TRLFS titration at different temperatures between 25 and 70 °C 2.5 mL of $5 \cdot 10^{-6}$ M Am³⁺ or Eu³⁺ at pH 5.0 or 6.0 and 0.1 M NaClO₄ were titrated with aliquots (5, 10 or 20 μ L) of ligand solution ($5 \cdot 10^{-3}$ M to 1 M, pH 5.0 or 6.0, 0.1 M NaClO₄). 20 to 30 titration steps up to a ligand concentration of 0.1 M were performed; every mixture was allowed to equilibrate for at least 15 min. At the beginning and after every titration step both a static and a time-resolved fluorescence spectrum was measured.

The TRLFS measurements for Am(III) were carried out with a pulsed Nd:YAG-MOPO laser system from Spectra Physics (Mountain View, USA), combined with

a delay generator from Spectrum One, a Spectrograph M270 and an ICCD camera system from Horiba-Jobin Yvon. The excitation wavelength was varied between 503 and 508 nm. TRLFS spectra for Eu(III) were recorded using a pulsed flash lamp pumped Nd:YAG-OPO laser system from Continuum (Santa Clara, CA, U.S.A.), combined with a spectrograph and an ICCD camera (Andor iStar) from Lot-Oriel. The excitation wavelength was 394 or 395 nm. The temperature was adjusted using a stirred temperature-controlled cuvette holder (Flash 300TM, Quantum Northwest, U.S.A.).

RESULTS

The Am(III) aquo ion shows at pH 3-6 and between 25 and 65 °C a luminescence emission maximum at 691 nm (the ⁵D₁-⁷F₁ transition) and a luminescence lifetime of 23.2-23.8 ns, corresponding to a number of 9 coordinating water molecules in the first coordination shell [1]. Complexation with lactate causes a red shift of the luminescence maximum of about 5 nm. The luminescence lifetime is prolonged up to 37 ns which corresponds to a number of 5-6 remaining water molecules, indicating an exchange of about 3-4 water molecules with coordination sites of ligand molecules which implies the formation of 1:1, 1:2 and possibly 1:3 complexes. The stability constants of the 1:1 complex remain nearly similar with rising temperature within the error bars (see Figure 1). Thermodynamic data were determined with the van't Hoff plot to be $\Delta_R H = 6.0 \pm 6.6$ kJ·mol⁻¹ and $\Delta_R S = 62 \pm 20$ J mol⁻¹·K⁻¹ implying a temperature independent entropy-driven reaction.

The luminescence spectra of Eu(III) show the typical changes with ligand addition which indicate a complexation: (i) the intensity of the hypersensitive ⁵D₀-⁷F₂ transition at about 615 nm increases strongly, (ii) the symmetry-forbidden ⁵D₀-⁷F₀ transition appears, and (iii) the luminescence lifetime prolongs from 110 μ s (Eu³⁺(aq)) up to 225 μ s for the lactate system and 300 μ s for the salicylate system. This corresponds to a number of 4 (lactate) and 3 (salicylate) remaining water molecules in the first coordination shell of Eu(III) [2]. For both ligands the formation of 1:1, 1:2 and 1:3 metal-to-ligand complexes with Eu³⁺ could be identified. The complex stability constants were determined for different temperatures between 25 and 70 °C. The stability constants of the Eu(III) lactate

complexes are all nearly temperature independent (see Figure 1) like it was observed for the Am(Lac)²⁺ complex, and the reaction enthalpies are around zero within the error bars ($\Delta_R H_{1,1} = 6.7 \pm 9.2$ kJ·mol⁻¹, $\Delta_R H_{1,2} = 3.3 \pm 1.3$ kJ·mol⁻¹, $\Delta_R H_{1,3} = -2.1 \pm 1.6$ kJ·mol⁻¹). The Eu(Lac)₃ complex seems to be slightly exotherm. Similar observations were made in a recent study [3]. For the Eu(III) salicylate system the temperature dependent behaviour of the complex formation is different. The complex stability constant of the 1:1 complex Eu(Sal)²⁺ is also nearly temperature independent (see Figure 2), and the reaction enthalpy is around zero ($\Delta_R H_{1,1} = -2.1 \pm 4.9$ kJ·mol⁻¹) which is in accordance with literature [4]. The formation of the 1:2 complex is with $\Delta_R H_{1,2} = 12.7 \pm 4.8$ kJ·mol⁻¹ endothermic (similar to the literature value [4]), and the 1:3 complex is with $\Delta_R H_{1,3} = 23.7 \pm 4.9$ kJ·mol⁻¹ even stronger endothermic. This complex has not been observed until now, possibly because former studies were carried out only at room temperature and this complex occurs only at elevated temperatures in observable amounts.

This study shows that the temperature dependent complex behaviour of trivalent lanthanides and actinides with small organic molecules varies with different ligand. Both, exothermic or endothermic reaction can be observed; sometimes the complex formation reaction can be also temperature independent.

FIGURES

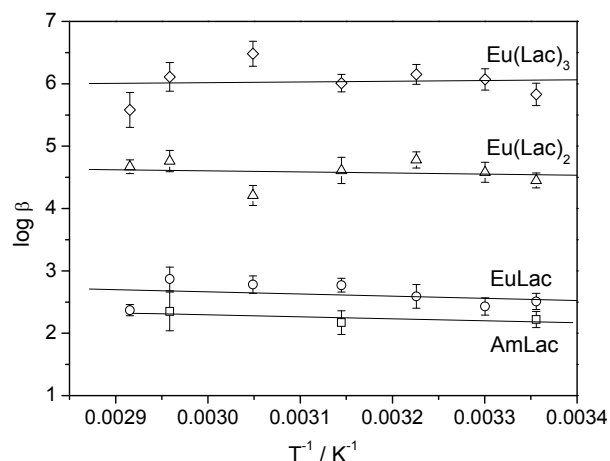


Fig. 1: Van't Hoff plot of the Eu(III)/Am(III) lactate complex formation.

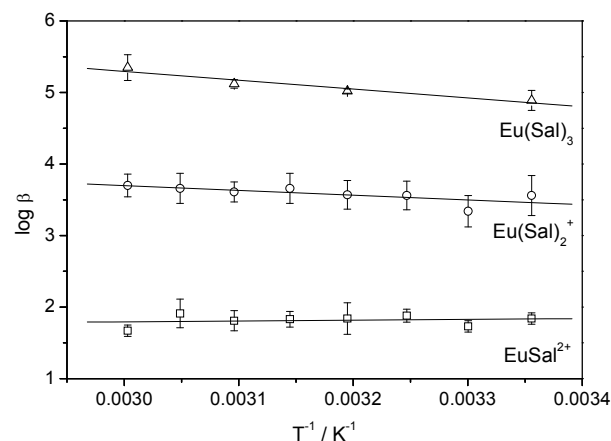


Fig. 2: Van't-Hoff plot of the Eu(III) salicylate complex formation.

REFERENCES

1. T. Kimura et al., "Luminescence study on determination of the inner-sphere hydration number of Am(III) and Nd(III)" *J. Alloys Compd.*, **271**, 867-871 (1998).
2. W.D. Horrocks et al., "Lanthanide ion probes of structure in biology - laser-induced luminescence decay constants provide a direct measure of the number of metal-coordinated water-molecules" *J. Am. Chem. Soc.*, **101**, 334-340 (1979).
3. G.X. Tian et al., "Complexation of Lactate with Neodymium(III) and Europium(III) at Variable Temperatures: Studies by Potentiometry, Microcalorimetry, Optical Absorption, and Luminescence" *Inorg. Chem.*, **49**, 10598-10605 (2010).
4. Y. Hasegawa et al., "Effects of phenyl groups on thermodynamic parameters of lanthanoid(III) complexation with aromatic carboxylic-acids" *Bull. Chem. Soc. Jpn.*, **63**, 2169-2172 (1990).

Temperature Effect on Solubility and Solid Phase of Zr(IV) Hydroxide

T. Kobayashi^{1,2}, D. Bach¹, M. Altmaier¹, T. Sasaki², H. Moriyama³

¹ Karlsruhe Institute of Technology, Institute für Nukleare Entsorgung, P. O. Box 3640, 76021 Karlsruhe, Germany, taishi.kobayashi@kit.edu

² Department of Nuclear Engineering, Kyoto University, Yoshida-honmachi, Sakyo-ku 606-8501, Kyoto, Japan

³ Research Reactor Institute, Kyoto University, Kumatori-cho, Sennan-gun 590-0494, Osaka, Japan

INTRODUCTION

For the safety assessment of nuclear waste repositories, it is important to understand and predict the solubility of radionuclides. Since high level waste repositories will operate under elevated temperature conditions over a considerable time-span, the effect of temperature on solid phase stability, complex formation reactions, redox equilibria, and activity coefficients, which control the radionuclide solubility limit, needs to be investigated.

In the current study, the temperature effect on the solubility of Zr(IV) hydroxide and solid phase characteristics is focused. At room temperature, it has been reported that the strong hydrolysis reaction of Zr(IV) leads to mononuclear, polynuclear, and colloidal hydrolysis species in aqueous systems [1]. The solubility of amorphous Zr(IV) hydroxide is defined as sum of these species, which are equilibrated with the amorphous hydroxide solid phase [1]. On the other hand, at elevated temperature, a transformation of the amorphous solid phase to more crystalline solid phase can be expected [2,3]. The Zr(IV) solubility at elevated temperature needs to be assessed taking such solid phase transformation into account.

In this study, Zr(IV) sample solutions were kept in an oven at 50°C, 70°C and 90°C for several days. After cooling down the samples, solubility, size distribution of the soluble species, and solid phase were investigated. The changes in solubility caused by high temperature conditions are discussed with the identification of related changes in the solubility limiting solid phase.

EXPERIMENTAL

The sample solutions were prepared from oversaturation approach. A stock solution of Zr(IV) perchlorate was prepared from ZrCl₄(Aldrich, 99.9%) to obtain 0.01 mol/dm³ (M) initial Zr sample solutions. The ionic strength (*I*) was fixed at *I* = 0.5 by adding appropriate amount of NaClO₄, and the hydrogen ion concentration (pH_c) adjusted within the pH_c range of 0-6 by addition of NaOH. The sample solutions were then kept in an oven controlled at 50°C, 70°C and 90°C. After the given periods, sample solutions were taken out from the oven and slowly cooled down to room temperature. The pH_c was then measured and the Zr concentrations were determined by ICP-MS (HP4500, Hewlett Packard) after filtration with various pore-sized membranes (Microcon NMWL 3k - 100 kDa filter, Millipore).

The solid samples were treated in a similar manner in 0.5 M NaCl to avoid potential problems caused by the disintegration of perchlorate salt in the measurement. The precipitates were separated by centrifugation and dried at room temperature. XRD (D8 ADVANCE, Bruker) and TEM (200 kV FEI Tecnai G2 F20 X-Twin) were used to investigate the crystallinity and particle size of the solid phase.

RESULTS

1. Solubility after heating at 90°C, 70°C and 50°C

Figure 1 shows the solubility (3kD filtration) after heating at 90°C compared with the reference solubility data of Zr(OH)₄(am) and ZrO₂(cr) at room temperature [4,5]. The solubility after heating at 90°C significantly decreased within several days, and the values after 18 days are rather close to the solubility of ZrO₂(cr), suggesting the transformation of solubility limiting solid phase. At pH_c 0.87 after 18 days, the solubility after the filtration with larger pore-sized filters showed higher values. This indicates the existence of Zr colloidal species in the solution even after heating at 90°C.

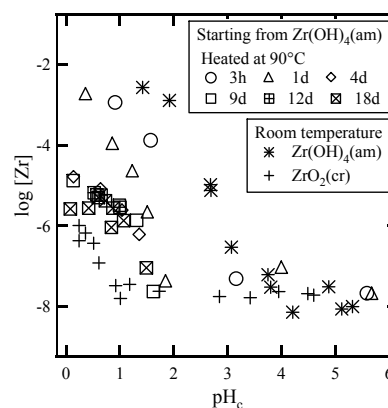


Fig. 1 Zr(IV) solubility after heating at 90°C compared with Zr(OH)₄(am) and ZrO₂(cr) at room temperature.

Similar trends were observed in the solubility after heating at 50°C and 70°C. Size distributions obtained by the filtration using different pore-sized filters also suggested the existence of Zr colloidal species in the solutions.

Similar to the previous studies, where the size distribution of the colloidal species was treated with the Flory-Schulz distribution [4], the simple polymer model was also used to exclude the contribution of colloidal species to the solubility in the present study. Provided that a “monomeric” unit connects linearly with a certain

probability (P) to form a “polymer”, the total number, $N(l_1, l_2)$, of monomeric units comprising the chain molecules in the range l_1 to l_2 in size is given by

$$N(l_1, l_2) = N_0 \frac{1}{P} \left(\frac{1-P}{\ln P} \right)^2 \left\{ P^{(l_2/l_0)} \left(\left(\frac{l_2}{l_0} \right) \ln P - 1 \right) - P^{(l_1/l_0)} \left(\left(\frac{l_1}{l_0} \right) \ln P - 1 \right) \right\} \quad (1)$$

where N_0 is the total number of unit molecules present in solution. The fractional ratio of mononuclear species N_1 to N_0 is given by

$$N_1/N_0 = (1-P)^2 \quad (2)$$

The size of a monomeric unit was taken to be 0.5 nm, assuming a cubic structure [4] and the P values were obtained from the analysis of size distribution data. Calculating the solubility of mononuclear species from obtained P values, solubility product at each temperature was determined in the least square analysis. In the analysis, the hydrolysis constants of mononuclear species were treated as fixed parameters [4].

2. Solid phase after heated at 90°C and 70°C

The XRD spectra of the solid phase after heating at 90°C for 34 days showed several sharp peaks corresponding to that of $ZrO_2(\text{cr})$. The result of TEM analysis (Fig. 2) shows agglomeration of solid particles and growth in size.

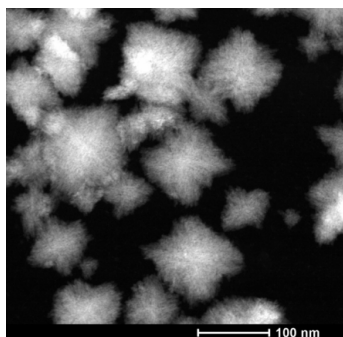


Fig. 2 TEM image of Zr(IV) solid phase at pH 1.9 after heating at 90°C.

The average size of the agglomerated solid particle is about 80 nm, while the particle size of initial amorphous solid is about 2 nm. In the TEM image of the solid phase heating at 90°C, each agglomeration exhibits the same crystal orientation, supports the result of XRD, and indicating clearly that the initial amorphous solid phase transferred to the large crystalline Zr oxide. On the other hand, no agglomeration was observed in the solid phase after heating at 70°C for 5 days.

Figure 3 shows a relationship between solubility product values and particle size of the solid phase. Because of the larger molar surface area of the smaller particle, the solubility is considered to be higher than

that of larger particle [6]. As shown in Fig.3, the trend for Zr solid phase observed in the present study agrees with the theoretical curve based on the Schindler effect.

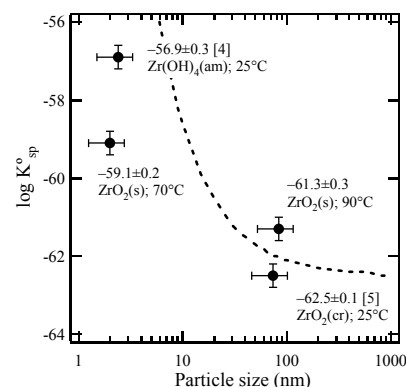


Fig. 3 Effect of particle size on solubility product of Zr oxides. The broken line represents calculated line for particle size effect.

CONCLUSION

$Zr(OH)_4(\text{am})$ solubility after equilibration at 50°C, 70°C, 90°C and subsequent cooling to RT are decisively lower than the values at 25°C. At 90°C, increased crystallization and the agglomeration of the solid phase particles up to 80 nm were observed. Solubility product values were calculated using a simple polymer model and the values correlated to predictions from “particle size” model. This work clearly supports the predicted trend to more crystalline and hence more stable / less soluble solid phases forming under elevated temperature conditions.

REFERENCES

1. Brwon P. et al., *Chemical Thermodynamics of Zirconium*, Elsevier, Amsterdam (2005).
2. Keramidis V. and White W. “Raman scattering study of the crystallization and phase transformations of ZrO_2 ” *J. Am. Ceram. Soc.*, **57**, 22-24 (1974).
3. Štefanič G. et al., “Influence of pH on the hydrothermal crystallization kinetics and crystal structure of ZrO_2 ”, *Thermochim. Acta*, **303**, 31-39 (1997).
4. Sasaki T. et al., “Solubility measurement of zirconium(IV) hydrous oxide”, *Radiochim. Acta*, **94**, 489-494 (2006).
5. Kobayashi T. et al., “Solubility of Zirconium(IV) Hydrous Oxides”, *J. Nucl. Sci. Technol.*, **44**, 90-94 (2007).
6. Schindler, P., “Heterogeneous Equilibria Involving Oxides, Hydroxides, Carbonates, and Hydroxide Carbonates”, *Adv. Chem. Ser.*, **67**, 196-221 (1967).

Preliminary multi-method spectroscopic approach for the uranium(VI) hydrolysis at temperatures up to 60°C

R. Steudner, K. Müller, T. Meusel, V. Brendler

*Helmholtz-Zentrum Dresden-Rossendorf e.V., Institute of Radiochemistry, Germany**Email: r.steudtner@hzdr.de; k.mueller@hzdr.de***INTRODUCTION**

For the safety assessment of high-level nuclear waste repositories in deep geologic formations, the understanding of actinide migration behaviour is one of the most important issues. In recent decades, the solution chemistry, e.g. hydrolysis [1], complexation with inorganic ligands [1], but also the interactions of the actinides at interfaces with the geo- and biosphere have been intensely investigated [2]. However, because of the experimental difficulties, only few studies have been performed at temperatures outside the range 20 – 30 °C which hampers the prediction of actinide reactive transport in the environment of heat generating high-level nuclear waste repositories. The speciation of (radioactive) metal ions in solution will be affected by the thermal conditions, since the properties of water, e.g. density, dielectric constant, viscosity, ion product, are altered with temperature and pressure [3,4]. The formation and distribution of U(VI) hydrolysis species is predicted to depend strongly on the temperature. In particular the stability of U(VI) polynuclear hydroxo complexes, which are dominant species at 25°C may change. According to experimental studies of other metal ions, namely Al(III) and La(III), the nuclearity of polynuclear complexes decreases upon increasing temperature [5,6]. At 25°C several spectroscopic techniques, namely UV-vis, TRLFS, EXAFS and vibrational spectroscopy have been applied for identification and structural characterization of U(VI) hydroxo species [7-10]. At elevated temperatures, TRLFS was used for the determination of luminescent characteristics of single hydroxo species as a function of the temperature [11,12]. But, approaches to examine alterations in the thermodynamic data itself are rare.

In this study, we investigate the U(VI) hydrolysis reactions up to 60°C using a multi-methodical approach by application of TRLFS and ATR FT-IR spectroscopy. The spectral data is compared to computed speciation patterns based on state-of-the-art thermodynamic models.

DESCRIPTION OF THE WORK

The luminescence of U(VI) was measured after excitation with laser pulses at 266 nm (Minilite laser system, Continuum) and an averaged pulse energy of 300 µJ. The emitted fluorescence light was detected using a spectrograph (iHR 550, HORIBA Jobin Yvon) and an ICCD camera (HORIBA Jobin Yvon). The TRLFS spectra were recorded from 450.0 to 649.9 nm by accumulating 50 laser pulses using a gate time of 20

µs. For the time-resolved measurements 101 spectra were recorded during a delay time of maximum 100 µs. The first time step started 50 ns after the excitation pulse.

ATR-FTIR spectra of aqueous solutions were measured on a Bruker Vertex 80/v vacuum spectrometer. The used ATR accessory (DURA SamplIR II, Smiths) is a horizontal diamond crystal with nine internal reflections. For adequate subtraction of the background a flow cell was used which allows an exchange of the sample solution with minimal external interference of the equilibrated system which was found to be an indispensable prerequisite for the detection of low absorption changes.

RESULTS

In Fig. 1 the luminescence spectra between 400 and 650 nm of aqueous U(VI) solutions at 25 °C (left) and 60 °C (right) are shown. The U(VI) concentration was constant at 0.1 mM, and pH ranged from 2 to 5 (from bottom to top). In the strong acidic pH range the free UO_2^{2+} cation dominated the U(VI) speciation. At the elevated temperature the luminescence spectra (\leq pH 3.0) are characterized by the typical emission bands at 487.8, 508.7, 532.2 and 558.9 nm for the free UO_2^{2+} [8]. With increasing pH value to pH 5 the luminescence spectra at 25°C and 60°C are different. At 60°C the luminescence spectra are strong influenced by the formation of a U(VI) hydroxo complex. The respective peak maxima at 497.8, 518.0, 542.2 and 568.1 are attributed to U(VI) dimer hydroxo complex [8]. At pH 5 the luminescence spectra (25°C and 60°C) are dominated by the U(VI) trimer hydroxo complex.

In Fig. 2 the infrared spectra between 1050 and 850 cm^{-1} of aqueous U(VI) solutions at 25 °C (left) and 60 °C (right) are shown. The U(VI) concentration was constant at 10 mM, and pH ranged from 3.5 to 5 (from bottom to top). The strong infrared absorption is related to the asymmetric stretching vibration (ν_3) of the UO_2^{2+} . At 25°C the transition of three distinct band positions at 961, 943 and 922 cm^{-1} is detected as a function of pH. They can be assigned to the free UO_2^{2+} cation, predominantly at lower pH (\leq pH 3.5), the dimer hydroxo complex dominating at pH 4, and the trimer hydroxo complex ($\text{pH} \geq 4.5$) [13]. At 60°C the course of U(VI) hydrolysis is considerably changed. Although all three species were redetected, the transition between them seems to be faster and hydrolysis starts at lower pH compared to 25 °C. Additionally, the solubility seems to be reduced at higher temperature, because the

formation of a U(VI) precipitate with absorption maximum at 948 cm⁻¹ is detected in the spectrum at pH 4.5. In contrast, at 25 °C precipitation in freshly prepared 10 mM occurs only at pH > 5. At the reduced concentration level of 0.1 mM U(VI) in TRLFS experiments the formation of colloidal species was not observed.

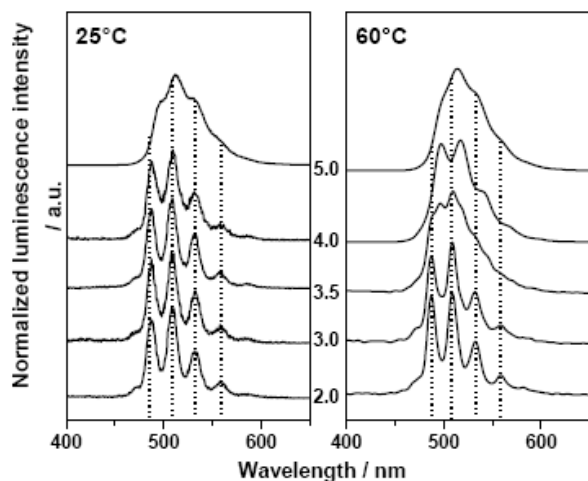


Fig. 1 TRLF spectra of aqueous 0.1 mM U(VI) solutions (0.1 M NClO_4 , air) in the pH range from 2.0 to 5.0 (from bottom to top) at 25°C (left) and 60°C (right).

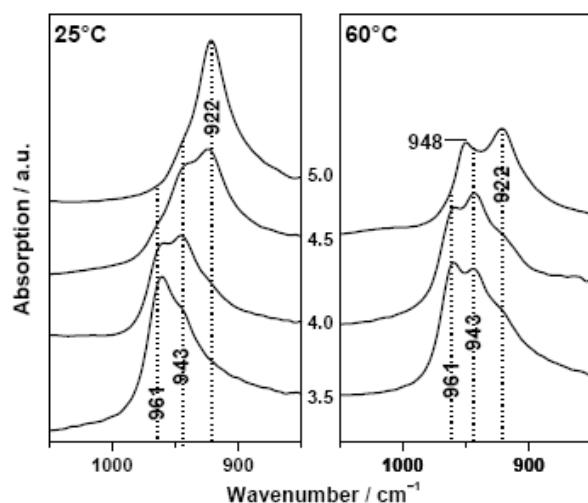


Fig. 2 ATR FT-IR spectra of aqueous 10 mM U(VI) solutions (0.1 NaCl, air) in the pH range from 3.5 to 5.0 (from bottom to top) at 25°C (left) and 60°C (right)

In summary, the obtained spectral data constitute a reference to a modified speciation in diluted millimolar U(VI) aqueous solutions at different temperatures. The formation of U(VI) hydroxo complexes shifts to lower pH at 60 °C. No indication for decrease in nuclearity of the polynuclear complexes was observed in the investigated concentration range (0.1 – 10 mM).

REFERENCES

- Guillaumont, R. et al., *Update on the chemical thermodynamics of uranium, neptunium, plutonium, americium and technetium. Chemical Thermodynamics Vol. 5*, OECD Nuclear Energy Agency, Elsevier (2003).
- Brendler, V. et al., RES3T-Rosendorf expert system for surface and sorption thermodynamics, *Journal of Contaminant Hydrology* 281-291 (2003).
- Marshall, W.L. et al., UO_2 product of water substance, 0 - 1000°C, 1-10,000 bars - New international formulation and its background, *Journal of Physical and Chemical Reference Data* 2, 295-304 (1981).
- Fernandez, D.P. et al., A formulation for the static permittivity of water and steam at temperatures from 238 K to 873 K at pressures up to 1200 MPa, including derivatives and Debye-Huckel coefficients, *Journal of Physical and Chemical Reference Data* 4, 1125-1166 (1997).
- Mesmer, R.E. et al., Acidity measurements at elevated temperatures. 5. Aluminum ion hydrolysis, *Inorg. Chem.* 10, 2290-2296 (1971).
- Ciavatta, L. et al., The hydrolysis of the La(III) ion in aqueous perchlorate solution at 60°C, *Polyhedron* 6, 1283-1290 (1987).
- Meinrath, G., Uranium(VI) speciation by spectroscopy, *J. Radioanal. Nucl. Chem.* 1-2, 119-126 (1997).
- Moulin, C. et al., Time-resolved laser-induced fluorescence as a unique tool for low-level uranium speciation, *Appl. Spectrosc.* 4, 528-535 (1998).
- Müller, K. et al., Aqueous uranium(VI) hydrolysis species characterized by attenuated total reflection Fourier-transform infrared spectroscopy, *Inorg. Chem.* 21, 10127-10134 (2008).
- Tsushima, S. et al., Stoichiometry and structure of uranyl(VI) hydroxo dimer and trimer complexes in aqueous solution, *Inorg. Chem.* 25, 10819-10826 (2007).
- Eliet, V. et al., Time-resolved laser-induced fluorescence of uranium(VI) hydroxo-complexes at different temperatures, *Appl. Spectrosc.* 1, 99-105 (2000).
- Kirishima, A. et al., Speciation study on uranium(VI) hydrolysis at high temperatures and pressures, *Journal of Alloys and Compounds* 1-2, 277-282 (2004).
- Quilès, F. et al., Infrared and Raman spectra of uranyl(VI) oxo-hydroxo complexes in acid aqueous solutions: a chemometric study, *Vib. Spectrosc.* 2, 231-241 (2000).

Complexation studies of Np(V)-Lactate at elevated temperatures

N. L. Banik, S. Walz, C. M. Marquardt, P. Panak, A. Skerencak

Karlsruhe Institute of Technology (KIT), Institute for Nuclear Waste Disposal (INE),
D-76344 Eggenstein-Leopoldshafen, Karlsruhe, Germany
email: nidhu.banik@kit.edu

INTRODUCTION

For the safety assessment of high-level nuclear wastes (HLW) in deep geological repositories are essential to understand the fate of HLW after some thousands years. Due to radioactive decay, temperatures in the near-field nuclear waste repository are likely to be increased in a post closure repository during thousands of years. Clay organics and small organic molecules (Lactate, Propionate, and Acetate) exist in clay rock pore water like in Opalinus Clay (OPA, Switzerland) and the Callovo-Oxfordian argillite (COx, France) [1]. Clay rocks are considered as potential host rock for deep geological disposal of nuclear waste. Carboxylic acids containing organic ligands exist in the nuclear wastes and are of importance in the nuclear waste repository, to form complexes with actinides and lanthanides. Actinide like neptunium-237 (Np) has longer half life and in its pentavalent state is the most stable and soluble and highly environmental importance element for nuclear waste in deep repository. The understanding of the complexation of actinides under near field conditions at elevated temperatures and their thermodynamic data is required for the safety assessments of a nuclear waste repository. A few thermodynamic data on the complexation of NpO_2^+ and other actinides at elevated temperatures are available. Therefore we studied here the complexation NpO_2^+ with lactate (Lac) at elevated temperatures (20-85 °C).

All chemicals are of p.a. quality or better and are obtained from Merck (Darmstadt, Germany) or Riedel de Haen (Seelze, Germany). All of the experiments are conducted using de-ionized, "MilliQ" water ($\rho = 18 \text{ M}\Omega\text{-m}$), ^{237}Np , is used from laboratory stock solutions. The activity of ^{237}Np is measured by liquid scintillation counting (LSC) using the scintillation cocktail Ultima Gold XR (Packard). A stock solution of lactic acid (i.e., 2-hydroxypropanoic acid) is prepared by appropriate dilutions of the 85% DL-lactic acid solution (Alfa Aesar). The ionic strength of all working solutions is maintained at range of 0.5-1.0 M (NaCl) at 25 °C. The pHc measurements [2] have been performed at different ionic strength and temperatures of the sample solution. NpO_2^+ -Lac complexation at elevated temperature (20-85 °C) is characterized by absorption spectroscopy with a high-resolution UV-Vis/NIR spectrometer Cary 5 (Varian). The spectra are analysed using Grams/A1 (7.02 version) software. All complexation experiments are conducted according to titration procedures with initial NpO_2^+ concentration in the range of $5.0 \cdot 10^{-5} \text{ M}$. Multiple titration's with different concentrations lactate

has been performed. In each titration, appropriate aliquots of the titrant (0.5 M lactate) are added to the NpO_2^+ and mixed thoroughly with stirrer (for 1-2 min) before the spectrum has been collected.

RESULTS AND DISCUSSION

The absorption spectra of representative spectrophotometric titrations at 20-85°C are shown in Fig. 1 at ionic strength (NaCl), $I=1.0 \text{ m}$. The absorption bands are shifted from 980 nm (NpO_2^+) to 984 nm (NpO_2Lac) confirming the complexation. A significant change in spectra is observed at higher temperatures (e.g., 85°C). The observation suggested a weak NpO_2Lac complex formed and here slightly stronger complex has been found at elevated temperatures. The species distribution has been calculated by peak deconvolution [3] of the absorption spectra and indicates the formation of 1:1 complex NpO_2Lac .

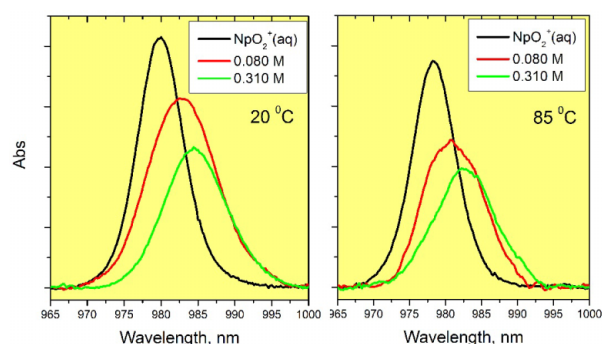


Fig 1: Absorption spectra of neptunium-lactate complex at 20°C and 85°C (pH 3, Ionic strength, NaCl = 1.0 m), $[\text{NpO}_2^+]_{\text{initial}} = 5.0 \cdot 10^{-5} \text{ M}$, $[\text{Lac}] = 0-0.310 \text{ M}$.

Complexation of NpO_2^+ with lactate at elevated temperature has been studied. Only one complex NpO_2Lac (aq) (1:1) has been observed by spectrophotometry in the temperature range of 20-85°C. Preliminary results show that the complexation of NpO_2Lac is weak but slightly enhanced with increasing temperatures ($\log K = 2.0$ (20°C), 2.34 (85 °C)). Similar results were also found by Eberle et al., [4] for the complexation of NpO_2Lac at room temperature with zero ionic strength ($\log K^\circ = 1.75 \pm 0.02$). Thermodynamic data ($\log K$, ΔG , ΔH , ΔS) from all present experiments in according to the specific ion interaction theory (SIT) [5] will be calculated and delivered in near future.

ACKNOWLEDGEMENTS

This work was financed by The Federal Ministry of Economics and Technology (Germany) under Contract No. 02E10961

REFERENCES

- [1] A. Courdouan et al., *Appl. Geochem.*, 22, 2926 - 2939, (2007).
- [2] M. Altmaier et al., *Geochimica et Cosmochimica Acta.*, 67, 3595 - 3601 (2003).
- [3] A. Skerencak et al., *Radiochim. Acta.*, 97, 385-393 (2009).
- [4] S. H. Eberle et al., *J. Inorg. Nucl. Chem.*, 31, 1523-1527, (1969)
- [5] R. Guillaumont et al., OECD, NEA-TDB: Chemical Thermodynamics Vol. 5, (2003).

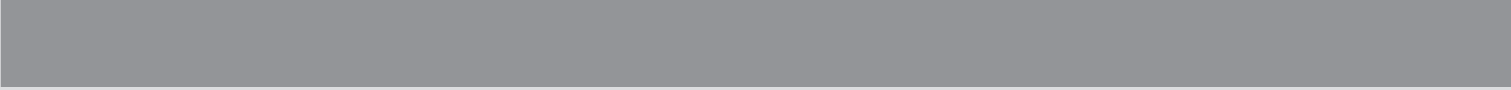
WORKSHOP PARTICIPANTS

Margret Acker	TU Dresden, Sachgebiet Strahlenschutz	margret.acker@tu-dresden.de
Marcus Altmaier	Karlsruhe Institute of Technology (KIT), Institute for Nuclear Waste Disposal (INE)	marcus.altmaier@kit.edu
Samer Amayri	Johannes Gutenberg-Universität Mainz, Institute of Nuclear Chemistry	amayri@uni-mainz.de
Nidhu Banik	Karlsruhe Institute of Technology (KIT), Institute for Nuclear Waste Disposal (INE)	nidhu.banik@kit.edu
Astrid Barkleit	TU Dresden, Sachgebiet Strahlenschutz	a.barkleit@hzdr.de
Pascale Bénézeth	Université Toulouse, France	benezeth@lmtg.obs-mip.fr
Barbara Bischofer	GRS Braunschweig, Germany	Barbara.bischofer@grs.de
Felix Brandt	Forschungszentrum Jülich, Germany	f.brandt@fz-juelich.de
Ingo Böttcher	Federal Office for Radiation Protection (BfS)	iboettcher@bfs.de
Muriel Bouby	Karlsruhe Institute of Technology (KIT), Institute for Nuclear Waste Disposal (INE)	muriel.bouby@kit.edu
Vinzenz Brendler	Helmholtz-Zentrum Dresden-Rossendorf, Institute of Radiochemistry	v.brendler@hzdr.de
Gunnar Buckau	EC Joint Research Centre, Institute for Transuranium Elements (ITU)	gunnar.buckau@ec.europa.eu
Christiane Bube	Karlsruhe Institute of Technology (KIT), Institute for Nuclear Waste Disposal (INE)	christiane.bube@kit.edu
Paul Carbol	EC Joint Research Centre, Institute for Transuranium Elements (ITU)	paul.carbol@ec.europa.eu
Benoith Cochepin	ANDRA, France	benoit.cochepin@andra.fr
Lara Duro	AMPHOS XI, Spain	lara.duro@amphos21.com
Sascha Eidner	University of Potsdam, Institute of Chemistry (Physical Chemistry)	eidner@chem.uni-potsdam.de
David Fellhauer	EC Joint Research Centre, Institute for Transuranium Elements (ITU)	david.fellhauer@ec.europa.eu
Nicolas Finck	Karlsruhe Institute of Technology (KIT), Institute for Nuclear Waste Disposal (INE)	nicolas.finck@kit.edu
Heidmarie Fischer	Gesellschaft für Anlagen- und Reaktorsicherheit (GRS mbH)	heidmarie.fischer@grs.de
Carola Franzen	Helmholtz-Zentrum Dresden-Rossendorf, Germany	c.franzen@hzdr.de
Daniel Fröhlich	Universität Mainz, Germany	froehlich@uni-mainz.de

Jiwchar Ganor	Ben-Gurion University of the Negev, Dept. of Geological and Environmental Sciences	ganor@bgumail.bgu.ac.il
Xavier Gaona	Karlsruhe Institute of Technology (KIT), Institute for Nuclear Waste Disposal (INE)	xavier.gaona@kit.edu
Horst Geckeis	Karlsruhe Institute of Technology (KIT), Institute for Nuclear Waste Disposal (INE)	horst.geckeis@kit.edu
Bastian Graupner	ENSI, Switzerland	Bastian.Graupner@ensi.ch
Ernesto Gonzáles-Robles	Karlsruhe Institute of Technology (KIT), Institute for Nuclear Waste Disposal (INE)	ernesto.gonzalez-robles@kit.edu
Alix Günther	Helmholtz-Zentrum Dresden-Rossendorf, Institute of Radiochemistry	a.guenther@hzdr.de
Ralf Kautenburger	Universität des Saarlandes	r.kautenburger@mx.uni-saarland.de
Michael Kersten	Universität Mainz, Germany	kersten@uni-mainz.de
Bernhard Kienzler	Karlsruhe Institute of Technology (KIT), Institute for Nuclear Waste Disposal (INE)	bernhard.kienzler@kit.edu
Reinhardt Klenze	Karlsruhe Institute of Technology (KIT), Institute for Nuclear Waste Disposal (INE)	reinhardt.klenze@kit.edu
Taishi Kobayashi	Karlsruhe Institute of Technology (KIT), Institute for Nuclear Waste Disposal (INE)	taishi.kobayashi@kit.edu
Raymond Kowe	Nuclear Decommissioning Authority (NDA)	raymond.kowe@nda.gov.uk
Dmitrii Kulik	Paul-Scherrer Institut (PSI)	dmitrii.kulik@psi.ch
Christi Leigh	Sandia National Laboratory, Carlsbad Office	cdleigh@sandia.gov
Johannes Lützenkirchen	Karlsruhe Institute of Technology (KIT), Institute for Nuclear Waste Disposal (INE)	johannes.luetzenkirchen@kit.edu
Patric Lindqvist-Reis	Karlsruhe Institute of Technology (KIT), Institute for Nuclear Waste Disposal (INE)	patric.lindqvist@kit.edu
Christian Marquardt	Karlsruhe Institute of Technology (KIT), Institute for Nuclear Waste Disposal (INE)	christian.marquardt@kit.edu
Maria Marques-Fernandez	Paul-Scherrer Institut, Switzerland	Maria.Marques@psi.ch
Volker Metz	Karlsruhe Institute of Technology (KIT), Institute for Nuclear Waste Disposal (INE)	volker.metz@kit.edu
Jens Mibus	NAGRA, Switzerland	Jens.Mibus@nagra.ch
Henry Moll	Helmholtz-Zentrum Dresden-Rossendorf, Institute of Radiochemistry	h.moll@hzdr.de
Helge Moog	Gesellschaft für Anlagen- und Reaktorsicherheit (GRS mbH)	helge.moog@grs.de
Christina Möser	Universität des Saarlandes	c.moeser@mx.uni-saarland.de
Claude Musikas	Agence de l'OCDE pour l'Énergie Nucléaire (OECD-NEA)	musikas.claude@neuf.fr

Katharina Müller	Helmholtz-Zentrum Dresden-Rossendorf, Germany	k.mueller@hzdr.de
Stefan Neumeier	Forschungszentrum Jülich, Germany	s.neumeier@fz-juelich.de
Petra Panak	Heidelberg University, Physikalisch- Chemisches Institut	petra.panak@kit.edu
Ignasi Puigdomenech	Svensk Kärnbrenslantering, Sweden	Ignasi@skb.se
Thomas Rabung	Karlsruhe Institute of Technology (KIT), Institute for Nuclear Waste Disposal (INE)	thomas.rabung@kit.edu
Linfeng Rao	Lawrence Berkeley National Laboratory	lrao@lbl.gov
Donald T. Reed	Los Alamos National Laboratory, Carlsbad Operations	dreed@lanl.gov
Beate Riebe	Leibniz-University Hannover, Institute for Radioecology and Radiation Protection	riebe@irs.uni-hannover.de
Greg Roselle	Sandia National Laboratory, Carlsbad Office	gtrosel@sandia.gov
Yoav Rosenberg	Ben-Gurion University of the Negev, Dept. of Geological and Environmental Sciences	yoavoved@gmail.com
Sonia Salah	Belgian Nuclear Research Center	ssalah@sckcen.be
Jonas Sander	Universität des Saarlandes	r.kautenburger@mx.uni-saarland.de
Thorsten Schäfer	Karlsruhe Institute of Technology (KIT), Institute for Nuclear Waste Disposal (INE)	thorsten.schaefer@kit.edu
Katja Schmeide	Helmholtz-Zentrum Dresden-Rossendorf, Institute of Radiochemistry	k.schmeide@hzdr.de
Juliane Schott	Helmholtz-Zentrum Dresden-Rossendorf, Institute of Radiochemistry	j.schott@hzdr.de
Holger Seher	Gesellschaft für Anlagen- und Reaktorsicherheit (GRS mbH)	holger.seher@grs.de
Andrej Skerencak	Karlsruhe Institute of Technology (KIT), Institute for Nuclear Waste Disposal (INE)	andrej.skerencak@kit.edu
Robin Steudtner	Helmholtz-Zentrum Dresden-Rossendorf, Germany	r.steudtner@hzdr.de
Silvia Stumpf	Project Management Agency Karlsruhe (KIT-PTKA)	silvia.stumpf@kit.edu
Juliet Swanson	Los Alamos National Laboratory (LANL), Carlsbad Office	jsswanson@lanl.gov
Steffen Taut	TU Dresden, Sachgebiet Strahlenschutz	steffen.taut@tu-dresden.de
Punam Thakur	Carlsbad Environmental Monitoring & Research Center	pthakur@cemrc.org
Laurent Truche	Université Henri Poincaré Nancy, France	laurent.truche@g2r.uhp-nancy.fr
Tonya Vitova	Karlsruhe Institute of Technology (KIT), Institute for Nuclear Waste Disposal (INE)	Tonya.Vitova@kit.edu

Wolfgang Voigt	TU BA Freiberg, Germany	Wolfgang.Voigt@chemie.tu-freiberg.de
Gabriela von Goerne	Bundesministerium Umwelt, Naturschutz, Reaktorsicherheit, Germany	gabriela.vongoerne@bmu.bund.de
Stefan Wilhelm	AF-Consult Switzerland Ltd	stefan.wilhelm@afconsult.com



ISSN 1869-9669
ISBN 978-3-86644-912-1

